DIFFERENTIAL SKELETAL MUSCLE ENERGY EXPENDITURE IN LEAN VS. OBESITY-PRONE RATS

A dissertation submitted

to Kent State University in partial

fulfillment of the requirements for the

degree of Doctor of Philosophy

By

Chaitanya K. Gavini

December 2015

Dissertation written by

Chaitanya K. Gavini

B.Tech., Jawaharlal Nehru Technological University, India, 2008

Approved by

Dr. Colleen M. Novak, Chair, Doctoral Dissertation Committee

Dr. John Y.L Chiang, Members, Doctoral Dissertation Committee

Dr. John D. Johnson

Dr. Dianne Lorton

Dr. John Gunstad

Accepted by

Dr. Ernest Freeman, Director, School of Biomedical Sciences

Dr. James L. Blank, Dean, College of Arts and Sciences

TABLE OF CONTENTS

Page

Appendix 1: List of Figures

Page

Appendix 2: List of Tables

Page

Appendix 3: List of Abbreviations

Acetyl-CoA carboxylase……ACC

Activity energy expenditure……..……AEE

Adrenocorticotropic hormone……..……...……ACTH

Agouti-related peptide…….……AgRP

AMP-activated protein kinase……...……AMPK

Analysis of covariance……..……ANCOVA

Arcuate nucleus…….……ARC

Ascorbic acid……..……..……AA

ATP-sensitive potassium channels……..……..K^+_{ATP}

Body mass index……...……..BMI

Brown adipose tissue……..BAT

Carnitine palmitoyltransferase-1……...……CPT1

Central nervous system……...……CNS

Cocaine- and amphetamine-regulated transcript……..……CART

Corticotrophin-releasing hormone…….……CRH

Dihydroxybenzylamine……..……DHBA

Dorsomedial hypothalamus……...……...……DMH

Energy expenditure…….…….…… EE

Epididymal white adipose tissue…….……..……..EWAT

Extensor digitorum longus……..……EDL

Fatty acid synthase……...……..…….FAS

Fatty acid translocase……..……..FAT/CD36

Gastrocnemius……...……Gastroc

Glucose transporter 4……...……..……GLUT4

Gluteal white adipose tissue……...……GWAT

Glyceraldehyde 3-phosphate dehydrogenase…….……..……GAPDH

High-capacity runners…….…….……..HCR

Inguinal white adipose tissue…….…..…….IWAT

Lateral gastrocnemius……..……Lat.gastroc

Lateral hypothalamus……...…….LH

Long-chain fatty acids……...…….LCFAs

Low-capacity runners……..……...LCR

Medial gastrocnemius……...…….Med.gastroc

Medial hypothalamus…….……..MH

Mediator of RNA polymerase II transcription subunit 1……...……..MED1

Melanocortin 3 receptor……..……MC3R

Melanocortin 4 receptor……..……MC4R

Melanocortin 5 receptor……..……MC5R

Melanocortin……...…….MC

Melanotan II……..……MTII

Mesenteric white adipose tissue…….……MWAT

Neuropeptide Y……..……NPY

Non-exercise activity thermogenesis……...……NEAT

Non-shivering thermogenesis…….NST

Norepinephrine turnover…….NETO

Norepinephrine……NE

Oxygen consumption……...……...……VO_2

Paraventricular hypothalamus……..……...PVH

Perchloric acid…….……...PCA

Peroxisomal proliferator activator γ coactivator 1-α…….……...…….PGC-1α

Peroxisome proliferator activated receptor α……..……...…….PPARα

Peroxisome proliferator activated receptor γ……..…..……..PPARγ

Peroxisome proliferator activated receptor δ……...…….……..PPARδ

Phosphoenolpyruvate carboxykinase……...…….…….PEPCK

Phospholamban…….……..PLB

Proopiomelanocortin…….…….POMC

Quadriceps……...……..Quad

Reactive oxygen species…….ROS

Respiratory exchange ratio…..……..……...……....RER

Respiratory quotient…….……RQ

Retroperitoneal white adipose tissue……...…….……..RWAT

Sarcolipin…….…….……..SLN

Sarcoplasmic/endoplasmic reticulum Ca2+-ATPase……SERCA

Steroidogenic factor 1……...……..SF-1

Sympathetic nervous system…….…….…….SNS

Uncoupling protein 3……UCP3

Uncoupling proteins 1……..……UCP1

Uncoupling proteins 2……UCP2

Ventromedial hypothalamus…….……VMH

White adipose tissue……..……WAT

α-melanocyte stimulating hormone……...…….α-MSH

α-methyl-*p*-tyrosine……...……..aMPT

β_2-adrenergic receptor……..β_2-AR

β_3-adrenergic receptor……..β_3-AR

β-adrenergic receptor…….…….……..β-AR

ACKNOWLEDGEMENTS

I would like to express my deep sense of gratitude to my advisor Dr. Colleen Novak, for her transcendent suggestions and constant support to make my work a useful and knowledge enhancing experience. I am grateful for the time she spent on me teaching basics of neuroscience and helping me improve my writing skills. I cannot thank her enough for giving me the freedom and opportunity to work on my own, pursuing my research interests.

My heart felt indebtedness to my committee members, Dr. Brent Bruot, Dr. John Chiang, Dr. John Johnson, and Dr. Dianne Lorton for their valuable insights regarding my work here at Kent State University. I am very much thankful to Dr. Haifei Shi, Dr. Timothy Bartness, and Dr. Christopher Ehlen for their help and co-operation during initial trials of my work. My special thanks go to all the staff of School of Biomedical Sciences and Department of Biological Sciences for making this journey a memorable one.

For generous assistance in my project work, I would like to acknowledge my friends and lab mates Charu Shukla, Mark Smyers, Sromona Mukherjee, and Tariq Almundarij for their help and constructive criticism during our meetings both on and off-work. I would like to specially thank Lydia Heemstra for helping me and other lab mates by keeping everything organized and maintaining an effective work environment.

I am very much indebted to my parents Venkateswara Rao and Sujatha Gavini, and my sister and her husband, Snigdha and Ramakrishna, for their moral support and encouragement to achieve higher goals. I have no words to express my gratitude and still I am very thankful to my parents who have shown me this world and for every support they gave me.

CHAPTER 1: Introduction

1.1 Obesity

Obesity, along with its related innumerable health problems, is increasing worldwide, decreasing quality of life and increasing mortality (Allison, Fontaine, Manson, Stevens, & VanItallie, 1999; Heo, Allison, Faith, Zhu, & Fontaine, 2003; Jensen, 2000; K.M. Flegal, 2002; K.R. Fontaine, 2003; Taegtmeyer, 2003). Obesity, declared to be disease by the American Medical Association in their 2013 annual meeting, generates a large portion of medical and health care costs, crossing $100 billion mark, particularly in the United States where two-thirds of the population is either overweight or obese (Ogden, Carroll, Kit, & Flegal, 2014; Tsai, Williamson, & Glick, 2011). Obesity goes hand in hand with many fatal co-morbidities including cardiovascular diseases and metabolic syndrome that can then result in other disorders (Haslam, 2005; Sheehan & Jensen, 2000). Related to this, metabolic flexibility refers to a capacity to utilize lipid and carbohydrate fuels and to transit between them, depending on the individual's energy needs (Kelley, He, Menshikova, & Ritov, 2002). The condition wherein there is a failure in this transition is termed metabolic inflexibility, which can lead to diabetes and obesity in affected individuals. This flexibility is difficult to achieve in individuals with low fat oxidation, low energy expenditure (EE), and low sympathetic activity, and this explains the tendency of those individuals to gain weight (Galgani & Ravussin, 2008).

Obesity, being a complex disease, is affected by genetic predisposition along with a multitude of factors that contribute to an individual's likelihood of becoming obese. Factors that predispose an individual to be obese or resistant to obesity in an obesogenic environment are not fully explained. While the preponderance of data points to the interaction between genetic predisposition and obesogenic environment as a cause for obesity in the current environment, a significant fraction of people remain lean posing the question what is different about them?

1.2 Physical activity, energy expenditure, and obesity

Obesity is an outcome of disruption in energy balance homeostasis, which is strongly influenced by both genetic and environmental factors including a sedentary lifestyle (sitting or lying down for most part of the day (Sedentary Behaviour Research, 2012)) and a western diet (D.W. Brown, 2004; Klein, 2004). The decline in daily physical activity levels is related to increased prevalence of obesity (Church et al., 2011). Both sedentary lifestyle and being physically inactive increase risk of metabolic syndrome and metabolic inflexibility, diabetes, and other cardiovascular diseases (George, Rosenkranz, & Kolt, 2013; Hu, 2001; Warren et al., 2010) leading to the phrase "sitting is the new smoking" (George et al., 2013). On average, physically inactive people have a life span that is 5 years shorter than that of physically active people (Pedersen, 2011). It is well known that physical inactivity and poor physical fitness, independently of body mass index (BMI), are associated with an increased risk of cardiovascular diseases, type 2 diabetes, and mortality (Pedersen, (2009b)). This suggests that the health

consequences of physical inactivity and abdominal adiposity are similar and that physical inactivity could be a key factor in the development of abdominal adiposity.

The World Health Organization recommends a minimum of 150 minutes per week of moderate to vigorous physical activity a healthy adult which improves their metabolic profile and life expectancy (D.W. Brown, 2004; Moore et al., 2012; Teske, Billington, Kuskowski, & Kotz, 2012). A sedentary lifestyle can decrease EE and other related mechanisms (Hamilton, 2008) affecting body weight and health (D.W. Brown, 2004; Klein, 2004). The levels of physical activity or tendency to be physically active varies greatly between individuals and this variation is biologically regulated and is mostly inherited (Garland et al., 2011; Novak & Levine, 2007). Little is known regarding the molecular or physiological mechanisms underlying differences in physical activity, although the links between physical activity levels and obesity propensity are evident (Levine, Eberhardt, & Jensen, 1999; Levine et al., 2005). Genetic studies on obesity have identified a broad range of genes that are involved in obesity or are known to promote the obese phenotype by altering individual's energetics. Some of these genes are involved in changing EE by affecting their activity energy expenditure (Novak CM, 2009; Novak et al., 2010). The underlying mechanisms of this alteration are unknown, however.

Non-exercise activity thermogenesis (NEAT) is defined as the energy expended during the day by an individual outside of volitional exercise, sleeping, eating, and/or sport activities (Levine, 2002; Levine et al., 2005). EE associated with both voluntary exercise and NEAT are vital contributors to both weight maintenance and weight loss

(Levine et al., 1999). NEAT accounts for the bulk of activity-associated EE in most individuals and is involved in body weight maintenance (Levine & Kotz, 2005). The ability to increase NEAT during overfeeding prevents fat gain in non-obese individuals, demonstrating the influence of NEAT on body weight regulation (Levine et al., 1999). Compared to the obese or overweight subjects, lean subjects tend to spend more time standing rather than sitting (Levine et al., 1999; Levine et al., 2005). Even relatively small amounts of weight loss can have beneficial effects on health and metabolic disorders (G. A. Bray, Ryan, & Harsha, 2003; LaMonte, Blair, & Church, 2005). Altogether, these studies show that NEAT varies considerably between individuals and can explain to some extent the variance among individual propensity to be lean or obese. Even though NEAT plays an important role in overall EE, little is known about the molecular and neural mechanisms that are involved in the variance among individuals. Thus, there is a need to understand the mechanisms involved in altering EE which influence weight gain and obesity propensity.

1.3 Animal model for leanness and obesity

The use of animal models to study mechanisms that underlie obesity – genetic, physiological, epigenetic, and environmental – as well as potential treatment strategies, have provided abundant of information related to obesity and its associated co-morbidities. Most animal models of obesity are small rodents (rats or mice), but as is the case with most mammals, when maintained in closed enclosures with free access to food, obesity develops (Lutz & Woods, 2012). The most commonly used animal models of obesity are probably the leptin-deficient ob/ob mouse, the leptin receptor deficient db/db

mouse and its rat counterpart the Zucker rat, the melanocortin 4 receptor-deficient animals, and models of diet-induced obesity (Lutz & Woods, 2012). Approximately 20 different genes have been implicated in monogenic causes of obesity; however, they account for a fewer than 5% of all severe obesity cases (Ranadive & Vaisse, 2008). This suggests the importance of polygenic mechanisms in the development of obesity. Diet-induced obese animals are believed to better mimic the state of common obesity in humans than most of the genetically modified models and may be the best choice for testing prospective therapeutics (Lutz & Woods, 2012). Transgenic models or models with spontaneous mutations may be used in the evaluation of a prospective therapies to determine whether they engage a specific target or pathway in vivo or to explore the role of specific molecular targets and pathways in the physiology of food intake and their potential role in obesity (Lutz & Woods, 2012).

Physical activity levels vary widely between individuals in both humans and rodents, and daily physical activity level is an inherited trait (Joosen, Gielen, Vlietinck, & Westerterp, 2005; Levine & Kotz, 2005; Levine et al., 2005). A key trait that predicts high physical activity is intrinsic aerobic capacity; this holds true for both humans and rodents where high aerobic capacity strongly predicts a favorable metabolic profile (Aspenes et al., 2011; M. S. Bray, 2000; Koch & Britton, 2001; Kodama et al., 2009; Novak CM, 2009; Zhan et al., 1999). Aerobic capacity, even in the absence of exercise, consistently predicts health and longevity (Kokkinos P, 2008; Myers J, 2002). To answer the question why some fraction of people remains lean in this obesogenic environment, I investigated a rat model that reproduces human leanness to greater degree. Rats that have

been selectively bred for high endurance capacity (HCR) are more physically active than their counterparts with low endurance capacity (LCR). The HCR have a low risk of obesity, have high EE and physical activity (independent of differences in body weight), and live significantly longer than LCR (Koch, Britton, & Wisloff, 2012). LCR are prone to obesity and other metabolic and cardiovascular disorders, and gain more weight on either a regular or a high-fat diet (Novak et al., 2010). Therefore, HCR and LCR act as animal models for leanness and obesity, respectively (Koch LG, 2008; Koch et al., 2011; Noland RC, 2007). As these rats show significantly different activity levels and EE, they make an ideal model to study the differences in skeletal muscle energetics and their influence on weight gain or loss. These rats, bred for their endurance capacity, more accurately represent a complex trait like obesity compared to traditional obese and non-obese models which fail to effectively model the polygenic nature of obesity and metabolic diseases. Therefore, the use of HCR and LCR will help to identify obesity-associated differences in skeletal muscle molecular and neural mechanisms which contribute to obesity prevalence in a metabolically diverse human population.

Table 1: Comparison between lean HCR and obesity-prone LCR rats

	High capacity runners (HCR)	**Low capacity runners (LCR)**
Aerobic Capacity	High intrinsic aerobic capacity	Low intrinsic aerobic capacity
Physical activity	High	Low
Economy of activity	Low	High
Body composition	Lean	Obese
Life span	Long-lived	Relatively short life span
Metabolic profile	Healthy metabolic profile	Prone to metabolic and cardiovascular diseases
Insulin resistance	Sensitive	Resistant
Effect of high-fat diet	Gain less weight	Gain more weight

1.4 Hypothalamic regulation of energy balance

Energy balance is achieved when energy intake equals energy output (energy expenditure, thermogenesis). Based on more than five decades of research on the regulation of food intake and energy expenditure in rodents and humans, but most importantly triggered by the discovery of leptin in early 90's, the current model for the complex neuroendocrine regulation of energy balance has emerged. Based on this model, afferent signals continuously inform central nervous circuits about acute and chronic changes in energy homeostasis, which in turn integrate this information and respond with efferent signals to immediately initiate the appropriate adaptive changes and reestablish energy balance (Berthoud, 2003; Seeley & Woods, 2003; York & Bouchard, 2000).

The central nervous system (CNS) controls energy intake and EE, and the hypothalamus plays a critical role in this. The hypothalamus is comprised of interconnected yet anatomically distinct nuclei that respond to changes in energy status by regulating the expression of specific homeostasis-related neuropeptides and neurotransmitters (Chari, Lam, & Lam, 2010). Circulating hormones like ghrelin, leptin, and insulin, depending on their concentrations, suppress or increase energy intake and expenditure by acting on the brain (Figure 1). Glucose, fatty acids, and amino acids also serve as indicators of energy state by acting on the brain and modulating food intake and EE (Lopaschuk, Ussher, & Jaswal, 2010). Studies over the last decade identified roles of various hypothalamic nuclei on food intake through actions mediated by orexigenic and anorexigenic hypothalamic peptides. Even though the hypothalamus has been the main focus of study for these orexigenic and anorexigenic peptides, hypothalamic nuclei

interact with other homeostatic systems, such as hindbrain nuclei and non-homeostatic systems to regulate food intake and EE (Grill, 2006); many of these interactions remain to be elucidated in detail.

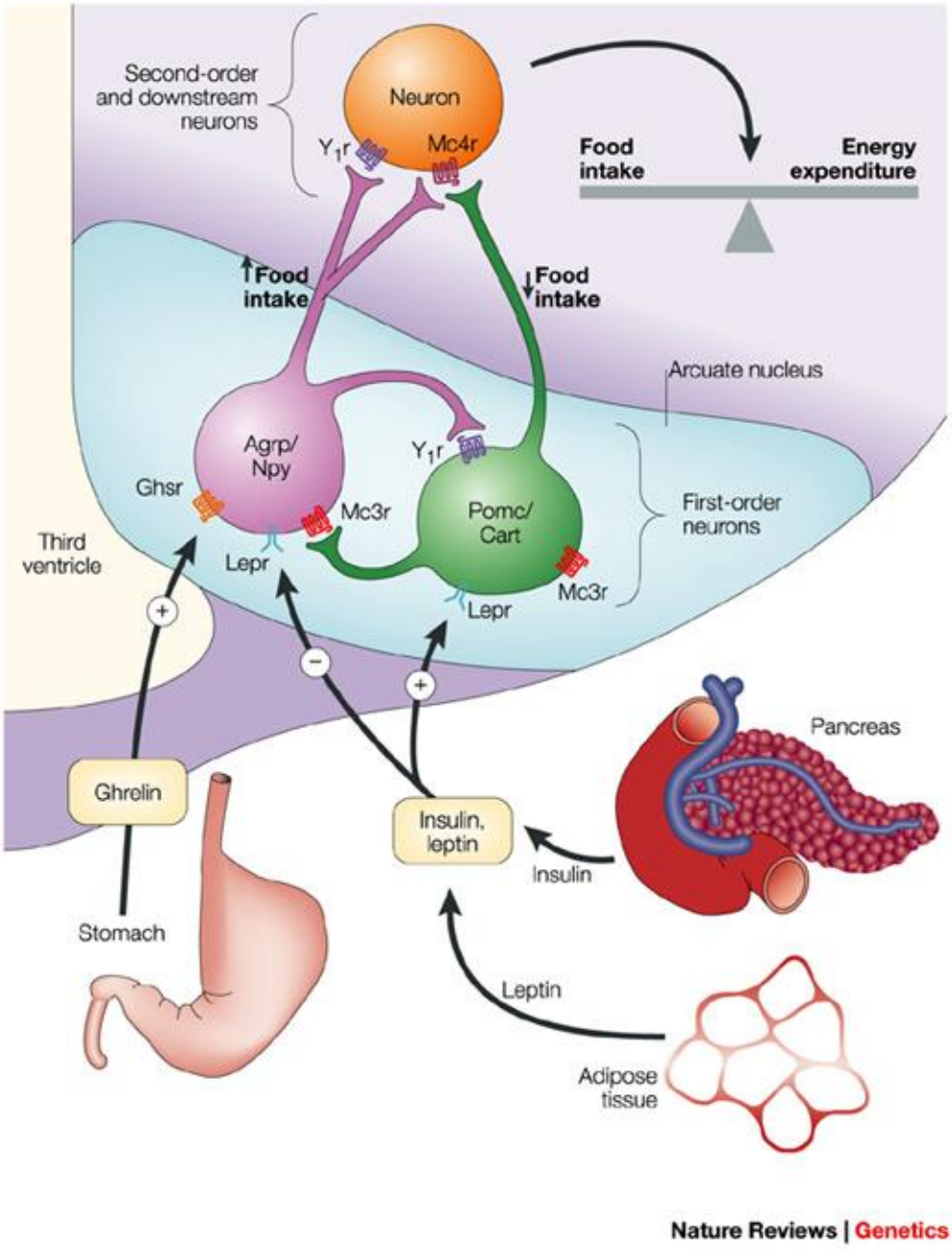

Figure 1: Neurons in hypothalamus that process peripheral metabolic and feeding signals and inhibit each other. (Barsh & Schwartz, 2002)

The arcuate nucleus (ARC) at the base of the hypothalamus is believed to be the primary hypothalamic sensor nucleus for the regulation of energy and glucose homeostasis (Chari et al., 2010). Related to the regulation of energy balance, there are two distinct neurons in the ARC that process peripheral metabolic and feeding signals. The first set of neurons, called anorexigenic-peptide-expressing neurons, synthesizes proopiomelanocortin (POMC) and cocaine- and amphetamine-regulated transcript (CART). POMC is cleaved into smaller peptides including adrenocorticotropic hormone (ACTH) and α-melanocyte stimulating hormone (α-MSH). These act to reduce appetite and food intake and, to certain extent, increase EE. The second set of neurons express orexigenic peptides like neuropeptides Y (NPY) and agouti-related peptide (AgRP). They increase food intake and reduce EE. These two sets of neurons inhibit each other, and the opposing signals of these orexigenic and anorexigenic neuronal subsets are important in the regulation of energy homeostasis. These neuronal populations project to other hypothalamic nuclei including the paraventricular hypothalamus (PVH or PVN), dorsomedial hypothalamus (DMH), lateral hypothalamus (LH), and ventromedial hypothalamus (VMH or VMN) (Hakansson, Brown, Ghilardi, Skoda, & Meister, 1998). Apart from sensing circulating hormones, these neuronal subsets also detect and respond to changes in metabolic fuels (Figure).

The PVH, situated on either side of the 3rd ventricle is involved in maintenance of energy homeostasis via modulating metabolism and appetite (J. W. Hill, 2012) and produces peptides corticotropin- and thyrotropin-releasing hormones that modulate energy balance, including physical activity and food intake (Sutton, Koob, Le Moal,

Rivier, & Vale, 1982; Valassi, Scacchi, & Cavagnini, 2008). The PVH is normally associated with satiety suggested from PVH lesion studies (Weingarten, Chang, & McDonald, 1985) as well as the effects of the PVH neuropeptides. The PVH receives a strong input from POMC and AgRP neurons and regulates a variety of neuroendocrine, behavioral, and autonomic functions (Cowley et al., 1999; Sohn et al., 2013).

The DMH plays a key role in central regulation of metabolism. It has classically been implicated in the control of several functions, such as ingestive behavior, carbohydrate metabolism, reproduction, thermogenesis (Bernardis & Bellinger, 1998) and stress-induced and circadian corticosterone secretion (Kalsbeek et al., 1996). The DMH is composed of cells and fibers containing neuropeptide Y (NPY), and the nutritional status (starvation-refeeding) is reflected in NPY levels in the DMH (Bernardis & Bellinger, 1998). The DMH is involved in the final common pathway of corticotrophin-releasing hormone (CRH) secretion by the PVN, sympathetic nervous system outflow to the adrenal gland, and brown adipose tissue (BAT) thermogenesis (Bernardis & Bellinger, 1998). The DMH is also part of a "fear circuit" regulating cardiovascular responses to stress such as myocardial blood flow and the tachycardia associated with the defense reaction (Bernardis & Bellinger, 1998). Although exhibiting reduced ponderal and linear growth and hypophagia and hypodipsia, the rat with DMH lesions has normal body composition, anabolic hormone levels, and intermediary metabolism, and responds normally to numerous endocrine, nutritional, intra- and extracellular thirst and body weight-regulatory challenges (Bernardis & Bellinger, 1998). These rats shows normal efficiency of food utilization, but have an attenuated response to

the feeding-stimulatory effect of insulin with lesion-induced abnormalities including hyperprolactinemia and a disrupted circadian corticosterone rhythm (Bernardis & Bellinger, 1998).

Neurons in the LH are the largest in the hypothalamus, and are topographically well organized (Bernardis & Bellinger, 1993). The LH belongs to the parasympathetic area of the hypothalamus, and connects with all major parts of the brain and the major hypothalamic nuclei (Bernardis & Bellinger, 1993). Lesions to the LH inhibit feeding, reducing body weight, though rats with LH lesions regulate their body weight in a primary manner and not because of destruction of a "feeding center". In the early stages of the syndrome, catabolism and running activity are enhanced, and so is the activity of the sympathetic nervous system (SNS) as shown by increased norepinephrine excretion that normalizes later on (Bernardis & Bellinger, 1993). The LH promotes glucose utilization and insulin release and affects neuroendocrine secretions (Bernardis & Bellinger, 1993). Stimulation studies show a profound role of the LH in glucose metabolism (glycolysis, glycogenesis, gluconeogenesis), the mechanism being cholinergic which does not appear to be a key player in lipolysis (Bernardis & Bellinger, 1993). Orexin-expressing cells are located in the lateral, dorsal, and perifornical regions of the LH (Muroya et al., 2004). Orexin stimulates feeding, regulates appetite, arousal, and wakefulness (Beck, Kozak, Moar, & Mercer, 2006; Kotz, Teske, Levine, & Wang, 2002). Microinjections of orexin into the ARC, PVH, and LH stimulate feeding and intra PVH microinjections of orexin increases physical activity and weight loss in rats (Dube, Kalra, & Kalra, 1999; Novak & Levine, 2009).

Studies on rats starting in the 1940's and 50's used electrolytic lesions to demonstrate that lesioning the VMH produced hyperphagia and massive obesity, while lesions to the LH produced aphagia and weight loss (Anand & Brobeck, 1951; Hetherington AW, 1940). This formed the basis for the dual-center model, whereby the VMH acts as the 'satiety center' and the LH acts as the 'feeding center' (King, 2006). According to this model, the interplay between the two regions would then be responsible for determining energy intake (Elmquist, Elias, & Saper, 1999). Although the lesion studies did conclusively demonstrate a central role for the hypothalamus in energy homeostasis, the dual-center model was much criticized. Gold (Gold, 1973) stated that lesions which extended beyond the borders of VMH, damaging ventral noradrenergic bundle or PVH, were responsible for the observed hyperphagia and obesity. He also pointed out that VMH-lesioned rats became obese even after pair-feeding them at normal levels of food intake, demonstrating that "VMH obesity" was not completely secondary to hyperphagia. Thus, anatomical studies using knockout and pair-fed rats indicate that VMH lesion-induced obesity alters metabolism, likely through altered regulation of the autonomic nervous system, parasympathetic as well as sympathetic (King, 2006).

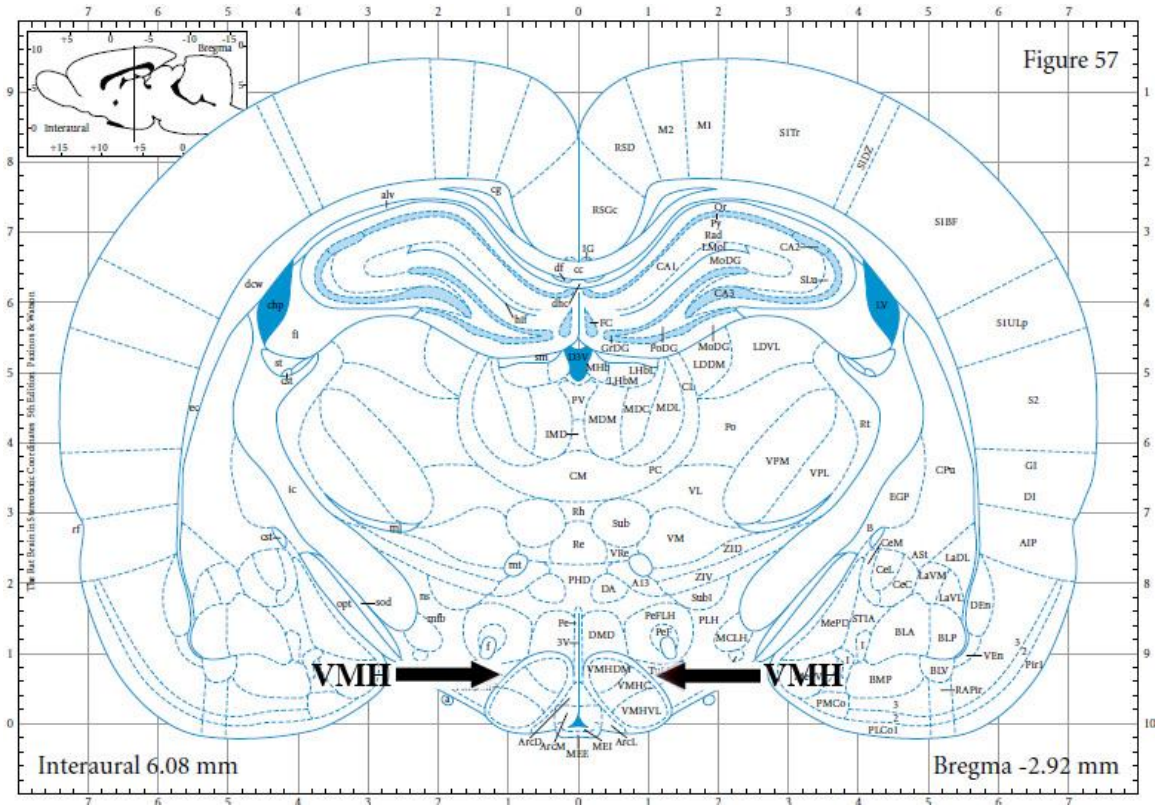

Figure 2: Illustration of a coronal section of a rat brain showing ventromedial hypothalamus (VMH). *The rat brain in stereotaxic coordinates* (Watson).

Today, the VMH is conceptualized as a part of a pathway regulating energy balance through its actions on peripheral glucose and lipid allocation, modulating respiratory quotient (RQ or RER) and high-fat diet-induced thermogenesis (Kim et al., 2011; Miyaki et al., 2011; Takahashi & Shimazu, 1981; Toda et al., 2009). With regards to the role of the VMH in energy balance, the best studied neuropeptides are melanocortins. The central melanocortin (MC) system plays a vital role in controlling energy balance, increasing EE, decreasing appetite, and modulating peripheral lipid metabolism (Butler, 2006; Nogueiras et al., 2007). The neuropeptide α-MSH is derived from the precursor polypeptide POMC and is an endogenous MC receptor agonist that reduces food intake and increases EE when it acts on MC3, MC4, and MC5 receptors (MC3R, MC4R, and MC5R). AgRP is an endogenous inverse agonist to both MC3R and MC4R (A. S. Chen et al., 2000; Fan, Boston, Kesterson, Hruby, & Cone, 1997; Huszar et al., 1997; Ollmann et al., 1997). POMC and AgRP neurons project from the arcuate nucleus to the VMH which express both MC3 and MC4 α-MSH (i.e., MC) receptors (Bagnol et al., 1999; Elias et al., 1998; Gantz et al., 1993; Haskell-Luevano et al., 1999). Loss-of-function mutations in MC4R are associated with hyperphagia and severe early-onset obesity, supporting the key role for the MC system in energy homeostasis in rodents and humans (Huszar et al., 1997; Razquin, Marti, & Martinez, 2011; Santini et al., 2009). Mutations in MC3R and MC4R have been associated with decreased EE partly through decreased physical activity in mice and rats (Cauchi et al., 2009; Chagnon et al., 1997; A. S. Chen et al., 2000; Mul et al., 2012). Although characterized as similar to MC3R and MC4R and found in the brain and other tissues, MC5R is less studied with respect to energy balance (Fathi, Iben, & Parker, 1995; Griffon et al., 1994).

Central MC controls peripheral glucose and lipid metabolism as well as thermogenesis in BAT (Nogueiras et al., 2007; Obici et al., 2001; Voss-Andreae et al., 2007), demonstrating neuroendocrine control over peripheral cell metabolism, likely through regulation of the SNS (Rahmouni, Haynes, Morgan, & Mark, 2003). There has been a gradual shift in studies the on central regulation of metabolism from adipose and hepatic tissue towards regulation of muscle metabolism. Peripheral signals regarding the energy status of the individual alter the functioning of the hypothalamic nuclei which in turn regulate energy partitioning in muscle, possibly via a sympathetic relay (Belgardt & Bruning, 2010; Braun & Marks, 2011). Injection of leptin or orexin-A into the VMH increases glucose uptake and glycogen synthesis in skeletal muscle via the SNS, and this is dependent on MC signaling, as shown by studies using Melanotan II (MTII), a potent activator of MC3R, MC4R, and MC5R (Shiuchi et al., 2009; Toda et al., 2009). To summarize, the present-day view of VMH in altering energy balance includes its role in modulating peripheral fuel partitioning through several systems including MC.

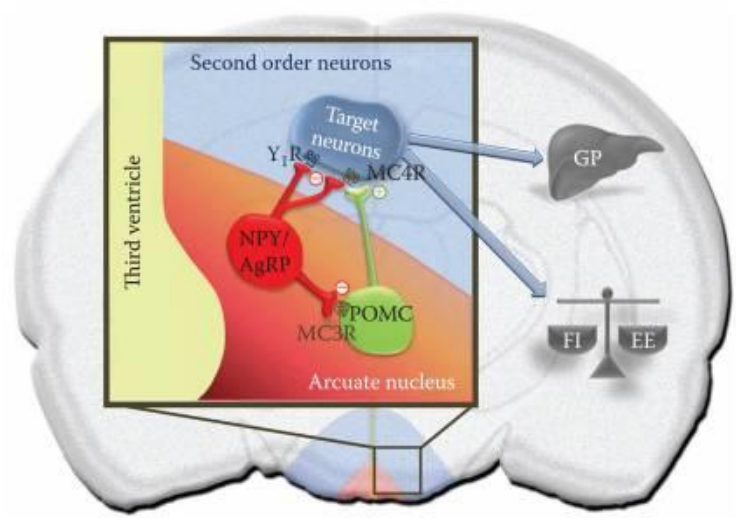

Figure 3: The hypothalamic melanocortin system and the regulation of energy and glucose homeostasis. The hypothalamic ARC is a critical mediator of energy and glucose homeostasis. Two groups of ARC neurons ("first-order" neurons), the NPY and AgRP coexpressing neurons and the POMC expressing neurons, are proposed to play a major part in mediating these regulatory effects. Projections from the ARC neurons reach adjacent hypothalamic nuclei ("second-order" neurons) including the PVH. The melanocortin signaling progressing along these nuclei and to downstream brain areas is mediated by α-MSH, a cleavage product of POMC, which binds the melanocortin receptor MC4R. Inhibition of this "melanocortin tone" is mediated by (1) synaptic inhibition of POMC neurons by NPY/AgRP neurons (via MC3R) and of target second-order neurons by neuropeptide Y1 receptor (Y_1R) and (2) AgRP acting as an endogenous antagonist on MC4R. Insulin and leptin carry out their anorectic effects via inhibiting NPY/AgRP neurons and stimulating POMC neurons, while ghrelin activates NPY/AgRP neurons to promote feeding behavior. Nutrients such as LCFAs have been shown to downregulate the expression of AgRP to mediate the hypothalamic anorectic signal. GP, glucose production; FI, food intake; EE, energy expenditure (Chari et al., 2010).

1.5 Obesity and skeletal muscle energy expenditure

The prevalence of obesity is rising despite treatment strategies aimed at reducing energy intake. Although, programs focusing on energy intake have some impact on short-term energy balance, the bigger problem still persists and cannot be tackled by dietary treatments alone. Present-day programs designed to increase EE are generating mixed results, suggesting the need for new strategies, for example strategies to modulate adaptive thermogenesis, a regulated production of heat in response to environmental changes in temperature and diet, modulating metabolic efficiency (van den Berg, van Marken Lichtenbelt, Willems van Dijk, & Schrauwen, 2011). In humans, in addition to the putative role of the thermogenic BAT, skeletal muscle has been demonstrated to significantly contribute to adaptive thermogenesis (van den Berg et al., 2011). The capacity of skeletal muscle to contribute to whole-body EE can be related to the fact that muscle is composed of approximately 40% of the total body mass and accounts for approximately 20–30% of the total resting oxygen uptake (Zurlo F, 1990). Skeletal muscle is an endocrine organ which by secretion of hormone-like factors (myokines) may influence metabolism in tissues and organs (Pedersen, 2011). Furthermore, the contribution of muscle mitochondrial proton leak to resting metabolic rate can be as large as 20–50% (Rolfe & Brown, 1997) and in combination with heart accounts for 100% of increased energy consumption during exercise (Gallagher et al., 1998), demonstrating the large potential of skeletal muscle to increase oxygen uptake and energy use. The contribution of the skeletal muscle to diet-induced adaptive thermogenesis ranges between 35 and 67% (van Baak, 2008); also, up to 50% of adrenalin-induced thermogenesis was demonstrated to originate at the skeletal muscle level (Astrup, Bulow,

Madsen, & Christensen, 1985). Mitochondrial uncoupling, the process whereby substrate oxidation is uncoupled from ATP production and directed towards heat loss, is postulated to be an excellent target to elevate whole-body EE (Conley, Jubrias, Amara, & Marcinek, 2007). This is mostly due to the high oxidative capacity of muscle which allows for significant uncoupling-related EE. The other mechanisms that contribute to skeletal muscle adaptive thermogenesis may also provide potential targets, although the scaling possibilities are limited in comparison with uncoupling (van den Berg et al., 2011).

Skeletal muscle is heterogeneous and composed of slow and fast-twitch fiber types. Which differ in the composition of contractile proteins, oxidative capacity, and substrate preference for ATP production. Slow-twitch fibers display low fatigability, high oxidative capacity, and a preference for fatty acids as substrate for ATP production. Fast-twitch fibers have a higher fatigability, higher strength of contraction, lower oxidative capacity, and a preference for glucose as a substrate for ATP production through anaerobic glycolysis (Bassel-Duby & Olson, 2006; Schiaffino & Reggiani, 2011). Endurance or aerobic exercise increases mechanical and metabolic demand on skeletal muscle, resulting in a switch from a fast-twitch to a slow-twitch fiber type (Baskin, Winders, & Olson, 2015). Conversely, in obesity and diabetes, characterized by excess caloric intake without increased metabolic demand, a slow-to fast fiber type switch occurs in muscle, which decreases oxidative capacity (Mootha et al., 2003). Insulin resistance, a hallmark of metabolic syndrome and diabetes, correlates with a higher composition of fast-twitch muscle fibers (Simoneau, Colberg, Thaete, & Kelley, 1995). Resistance training also impacts skeletal muscle metabolism by increasing muscle mass

and enhancing the oxidative and glycolytic capacity of fast-twitch fibers (LeBrasseur, Walsh, & Arany, 2011). Diabetic patients on a regimen of resistance training have improved insulin sensitivity (Zanuso, Jimenez, Pugliese, Corigliano, & Balducci, 2010), and obese patients subjected to resistance training develop increased lean mass and a higher resting metabolic rate (Willis & Houmard, 2012). Exercise impacts systemic glucose and lipid homeostasis and alters muscle fiber type composition, which is regulated at the level of transcription (Baskin et al., 2015).

1.6 A functional model of hypothalamic control of peripheral metabolism

The hypothalamus regulates muscle glucose metabolism and insulin sensitivity (Shiuchi et al., 2009). For example, electrical stimulation of the VMH increases glucose uptake in certain peripheral tissues, including skeletal muscle, BAT, and heart of rats (Shiuchi et al., 2009). Intravenous (i.v.) or intracerebroventricular (i.c.v.) administration of leptin also induces an acute increase in both whole-body glucose turnover and glucose uptake by the same peripheral tissues in mice without any substantial change in plasma insulin or glucose level. Administration of leptin into the medial hypothalamus (MH) increases glucose uptake in skeletal muscle, heart, and BAT via sympathetic nerves in a manner that apparently is dependent on β-adrenergic receptor (β-AR) stimulation. In support of this, injection of leptin into the MH results in the stimulation of fatty acid oxidation in skeletal muscle through the activation of sympathetic nerves and of α2 subunit-containing AMP kinase (α2AMPK) in skeletal muscle (Minokoshi et al., 2002).

One tissue that is targeted by the sympathetic nervous system in this process is skeletal muscle. Central administration of fatty acid synthase (FAS) inhibitors in both obese and lean mice rapidly activates fatty acid oxidation in skeletal muscle (Cha, Hu, Chohnan, & Lane, 2005). Skeletal muscle is the most abundant fatty-acid metabolizing tissue in most animals. Because fatty acids are the major physiological fuel for muscle, an increase in the rate of fatty acid oxidation in this tissue would be expected to have a major impact on whole-body EE. Moreover, evidence supports the assertion that skeletal muscle fatty acid metabolism is modulated by the CNS, and that the signal transmitted from CNS to muscle is mediated through the SNS via α-adrenergic receptors in skeletal muscle (Cha et al., 2005). This statement gets support from the study made by Cha et al (2005), where, α receptor blockade prevented the FAS inhibitor-induced increase of skeletal muscle uncoupling protein 3 (UCP3), whole-body fatty acid oxidation, and decreased skeletal muscle malonyl-CoA.

A possible explanation for the increase of energy expenditure induced by intra-hypothalamic FAS inhibition is increased thermogenesis caused by upregulation of skeletal muscle UCP3. UCP3 is thought to dissipate the proton gradient across the inner mitochondrial membrane, producing heat rather than ATP. This thermogenic response may contribute to whole-body EE. Because UCP3 is expressed primarily in skeletal muscle, which is a major energy-consuming tissue in most animals, up-regulation of skeletal muscle UCP3 is a likely candidate for the FAS inhibitor-induced increase in EE. Fatty acids most likely fuel this thermogenic response. There is a positive correlation between upregulation of UCP3 induced by central administration of FAS inhibitors and

the increase in fatty acid oxidation by skeletal muscle (Cha et al., 2005). This increase is the result of decreased malonyl-CoA concentration caused by the phosphorylation-induced inactivation of acetyl CoA carboxylase (ACC) (Figure 4) (Cha et al., 2005). The decrease in malonyl-CoA levels in skeletal muscle normally leads to activation of carnitine palmitoyltransferase-1 (CPT1) in skeletal muscle, allowing translocation of fatty acids into the β-oxidation compartment of mitochondria. Skeletal muscle has little-to-no FAS, so malonyl-CoA cannot be used for fatty acid synthesis but is used primarily in the regulation of CPT1b, the muscle-specific CPT1, in combination with the outer-mitochondrial tethered ACC2. Therefore, there is evidence for malonyl-CoA as a signaling intermediate in altering whole-body energy expenditure by acting at the level of skeletal muscle (Figure 4).

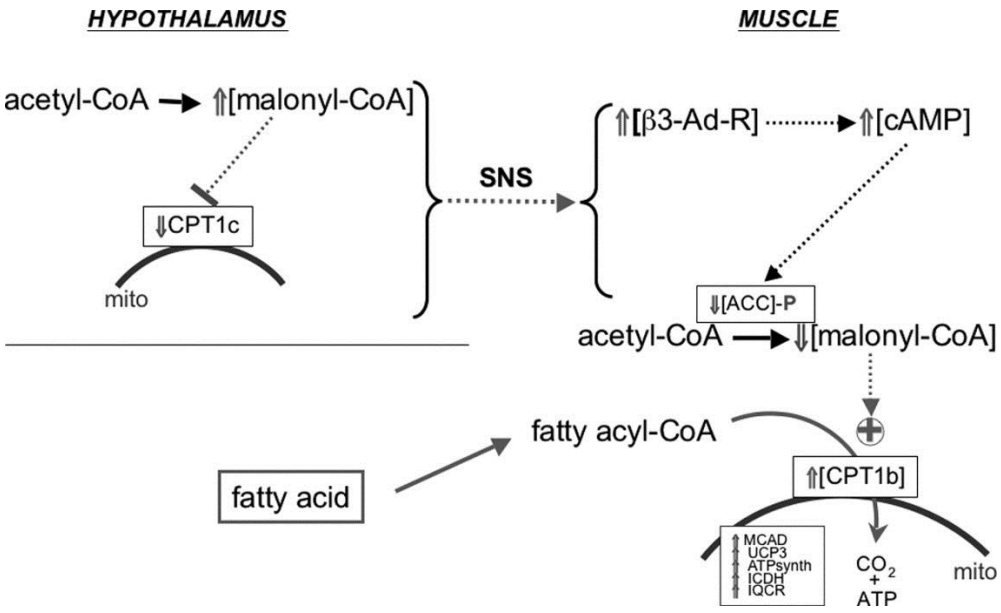

Figure 4: Proposed model for transmission of the malonyl-CoA signal from the hypothalamus to skeletal muscle. β3-Ad-R, β3-adrenergic receptor; ATPsynth, ATP synthase; ICDH, isocitrate dehydrogenase; Mito, mitochondria (Cha, Rodgers, Puigserver, Chohnan, & Lane, 2006).

Cha et al (2005) demonstrated how central sensing of lipids affects skeletal muscle fuel use and altered skeletal muscle energetics. Central administration of FAS inhibitors up-regulates the expression of the transcriptional coactivators peroxisomal proliferator activator γ coactivator 1α (PGC-1α) and of peroxisome proliferator activated receptor α (PPARα) in skeletal muscle (Cha et al., 2006). The role of these coactivators in skeletal muscle is to activate β-oxidation and thermogenesis, as shown by ectopic expression of PGC-1α in muscle cell line, which activates fatty acid oxidation and induces expression of UCP3 and PPARα (Cha et al., 2006). PGC-1α is known to activate the transcription of genes that promote adaptive thermogenesis in both brown adipose tissue and skeletal muscle, and it stimulates mitochondrial biogenesis (Cha et al., 2006). PGC-1α is a transcriptional coactivator that interacts with transcription factors like peroxisome proliferator activated receptor γ (PPARγ), PPARα, and thyroid hormone receptor by binding to the promoters of target genes which encodes proteins that carry out its metabolic effects. These findings reinforce the importance of these transcriptional regulators in the control of energy homeostasis which may mediate the effects of the CNS on skeletal muscle through the SNS.

The studies described above support a model in which malonyl-CoA signaling in the brain, initiated by the central administration of a FAS inhibitor, is rapidly communicated to skeletal muscle via the SNS; in muscle, fatty acid oxidation and the expression of the genes related to this process are up-regulated (Cha et al., 2005). The malonyl-CoA signal appears to be transmitted by the SNS because the β-blocker, propranolol, and the α-blocker, phentolamine, prevent the centrally administered FAS

inhibitor's effects on skeletal muscle gene expression, for example inhibiting the rise of UCP3 expression (Cha et al., 2005). There is a correlation between these gene expression patterns and increases in effectors of the β-adrenergic signaling system in muscle (namely norepinephrine and cAMP, the expression of the β-adrenergic receptor, and the phosphorylation of ACC) (Cha et al., 2005). Actions of these centrally administered FAS inhibitors resemble the effects of leptin, which also acts through the hypothalamic-SNS axis (Cha et al., 2006). Both FAS inhibitors and leptin trigger the expression of the genes encoding a group of enzymes involved in mitochondrial fatty acid oxidation and oxidative phosphorylation in skeletal muscle (Figure 4).

In addition to above mentioned systems, there are other brain systems in the hypothalamus, for instance orexin, that effect SNS and skeletal muscle. The orexin-containing neurons are activated during motivated behaviors and active waking and they regulate sympathetic tone, metabolic rate, and blood glucose concentration as well as food intake, wakefulness, and reward seeking (Shiuchi et al., 2009). Furthermore, orexin transgenic mice were recently found to exhibit enhanced insulin sensitivity with regard to whole-body glucose metabolism. Effects of orexin-A on skeletal muscle appear to be mediated through β-adrenergic rather than α-adrenergic pathway. Stimulation of sympathetic nerves and subsequent β2-AR signaling results in activation of the insulin signaling pathway in skeletal muscle (Shiuchi et al., 2009). Insulin delivery to skeletal muscle cells via blood vessels plays a key role in whole-body glucose disposal. Both β2-ARs in blood vessels and insulin stimulate vascular relaxation. (Shiuchi et al., 2009). Orexin-A injection into the VMH induced greater effect on glucose uptake in red type of

skeletal muscles (e.g., soleus) than in white type of muscles (e.g., quadriceps). Red type muscles have many mitochondria, a key organelle for thermogenesis (Shiuchi et al., 2009). It is also possible that the orexin-VMH-SNS axis regulates muscle glucose metabolism during fasting. Although the activity of sympathetic nerves in tissues such as BAT decreases markedly in response to fasting, that in skeletal muscle does not (Shiuchi et al., 2009). The β2-adrenergic receptor in both myocytes and nonmyocyte cells of skeletal muscle is involved in this regulation. Collectively, these data suggest that the VMH modulates skeletal muscle energetics and associated thermogenesis via multiple pathways, one of which is modulated by hypothalamic peptides including orexin.

At present, pharmacological, genetic, and physiological evidence clearly demonstrates that discrete sets of hypothalamic neurons modulate peripheral lipid metabolism by integrating the signaling effects of hormones (such as leptin and ghrelin) and neuropeptidergic systems (such as melanocortins and NPY). It is very likely that other peripheral signals and central neuropeptides may also control peripheral lipid metabolism. There is lot of attention lately on the role of BAT in EE, but skeletal muscle can be a better target organ, as it is larger tissue in animals, burns more calories, and is more relevant to whole body insulin sensitivity. But first, it is necessary to elucidate which nuclei and neuropeptides in the brain are important for the regulation of peripheral metabolism. It is also necessary to look at the tissues like skeletal muscle that can be a good target system for pharmacological interventions that are aimed at changing EE to treat over-weight and obesity which lead us to the designing and development of efficient drugs for the treatment of obesity and its related disorders.

1.7 Uncoupling proteins, metabolism, and obesity

The uncoupling proteins 1, 2, and 3 (UCP1, UCP2, and UCP3) are members of the super family of anion carrier proteins located in the inner membrane of mitochondria. UCP1 is found only in brown fat mitochondria of mammals (Fisler & Warden, 2006). Studies beginning in the 1960s, identified the function of UCP1 in providing heat and decreasing energy efficiency through dissipation of the proton electrochemical gradient across the inner mitochondrial membrane of brown adipose tissue without the generation of ATP (Nicholls, 2001). Thus, the function of UCP1 was known before the gene was cloned. On the other hand, UCP2 (Fleury et al., 1997) and UCP3 (Boss et al., 1997; Vidal-Puig, Solanes, Grujic, Flier, & Lowell, 1997), were identified in 1997 by reverse cloning (i.e., by 'mining' databases of expressed sequence tags or from similarity to UCP1 in cDNA libraries). UCP2 and UCP3 have 59% and 57% identity, respectively, with UCP1, and 73% identity with each other (Krauss, Zhang, & Lowell, 2005). These uncoupling proteins have several hypothesized functions including thermogenesis in certain tissues, protection from reactive oxygen species (ROS), mediation of insulin secretion, neuroprotection, and export of fatty acids. Several of these functions are either directly or indirectly linked to the etiology of the metabolic syndrome. The major protein involved in the process of mitochondrial uncoupling is UCP1, which is primarily associated with BAT (Ribeiro MO, 2010). Homologues of UCP1 include UCP2 and UCP3; UCP2 has been demonstrated to be expressed in a variety of tissues, but UCP3 expression is mainly limited to the skeletal muscle (Azzu, Jastroch, Divakaruni, & Brand, 2010).

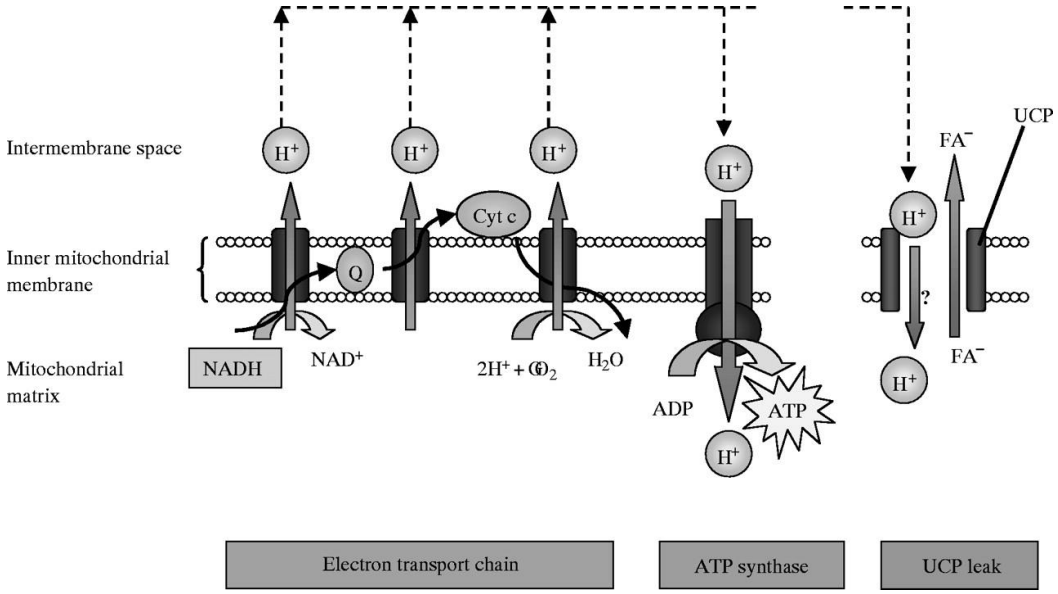

Figure 5: Action of the electron transport chain leading to the build-up of a proton gradient across the inner mitochondrial membrane. Protons can cross the inner mitochondrial membrane *via* the F_0F_1 complex, thereby providing energy for the conversion of ADP to ATP. Alternatively, the proton gradient can be reduced by uncoupling proteins (UCP), either by direct transport of protons from the intermembrane space to the matrix or by transport of fatty acid anions in the opposite direction. Cyt c, cytochrome *c*. Q, coenzyme Q (Schrauwen & Hesselink, 2002).

Energy wastage and protection from obesity were initially suggested to be significant functions of UCP2 and UCP3 due to their homology to UCP1 and their distribution in tissues, such as in white adipose tissue and muscle, which could dissipate energy. Gene expression of UCP2 and UCP3 increases during fasting (Cadenas S, 1999), however, the opposite of what would be expected for a thermogenic compound. Also, neither UCP2 nor UCP3 knockout mice are obese (Arsenijevic et al., 2000; Gong et al., 2000), providing evidence against these proteins contributing to whole-body thermogenesis. Transgenic mice over-expressing a UCP2/UCP3 construct, however, are leaner than wild type mice (Fuller, Warden, Barry, & Fuller, 2000; Horvath, Diano, Miyamoto, et al., 2003) and those overexpressing only UCP3 in skeletal muscle are leaner despite hyperphagia (Clapham et al., 2000). However, even though uncoupling in over-expression studies does not reflect the native function of the protein in the cell, they cannot negate UCP2 or UCP3's whole-body thermogenic function and protection against obesity.

Evidence suggests that, under specific conditions, these UCP homologues can have a thermogenic function. UCP2 mRNA was positively associated with higher temperatures within certain areas of the brain, suggesting that UCP2 could function as a thermogenic protein in the microenvironment of the brain (Horvath, Diano, & Barnstable, 2003; Horvath et al., 1999). In UCP3 knockout mice, the thermogenic response to the drug MDMA (ecstasy) is significantly reduced, suggesting that UCP3 in muscle can affect whole body thermogenesis in this non-physiological condition (Mills, Banks, Sprague, & Finkel, 2003). The contribution of higher rates of skeletal muscle

mitochondrial uncoupling to thermogenesis has been demonstrated in mouse models (Li et al., 2000). Evidence for beneficial effects of skeletal muscle uncoupling comes from UCP1 muscle-specific overexpressing mice that have a higher degree of whole-body EE and skeletal muscle mitochondrial uncoupling, and are protected against high-fat diet induced obesity as well as glucose intolerance (van den Berg et al., 2011). Similarly, UCP3 overexpression protects mice from high-fat diet-induced obesity and insulin resistance (C. S. Choi et al., 2007). Stimuli such as cold and leptin administration increase skeletal muscle uncoupling and total EE (Rousset et al., 2004). UCP3 mRNA expression in skeletal muscle is upregulated after thyroid hormone treatment which is known to increase thermogenesis both in rodents (Gong, He, & Reitman, 1999) and humans (Schrauwen et al., 2000). Skeletal muscle expression of UCP3 is rapidly upregulated after cold exposure with levels reaching peak after 1 day, but prolonged exposure leads to a reduction in UCP3 mRNA expression (B. Lin, Coughlin, & Pilch, 1998). Mice overexpressing UCP3 eat considerably more than their wild type littermates, but do not become obese, suggesting that metabolic rate is increased in these animals (Clapham et al., 2000). This implies that UCP3 plays role in uncoupling oxidative phosphorylation, dissipating energy as heat. In conclusion, muscle mitochondrial uncoupling lowers body weight and plays a key role in adaptive thermogenesis. In addition, because of the large potential physiological impact of elevating EE in skeletal muscle, increasing skeletal muscle mitochondrial uncoupling may be an effective treatment against obesity.

UCP3 has been proposed to be a transporter of fatty acid anions out of mitochondria (Himms-Hagen & Harper, 2001) analogous to UCP1 in BAT. The fatty acid cycling model, proposed for UCP1 in 1996 (Garlid, Orosz, Modriansky, Vassanelli, & Jezek, 1996), suggests that UCP3, by transporting fatty acids out of mitochondria, protects the mitochondria from the toxic effects of fatty acid anions or peroxides (Schrauwen & Hesselink, 2004) (Figure 6). The hypothesis is attractive in that it is consistent with observations that UCP3 expression is correlated with improved fatty acid oxidation when fatty acid supplies are high, for example with fasting or a high-fat diet (Krauss et al., 2005). Also, muscle UCP3 protein levels are increased when rats are fed a diet high in long-chain triglycerides but not a diet high in medium-chain triglycerides which are oxidized via a different pathway (Schrauwen et al., 2003), again linking fatty acid oxidation with UCP3. Results from UCP3 knockout mice are not consistent, however, some showing reduced rates of fatty acid oxidation and others finding no effect (Krauss et al., 2005). Thus, the proposal that UCP3 protects against fatty acid toxicity in the mitochondria remains to be confirmed.

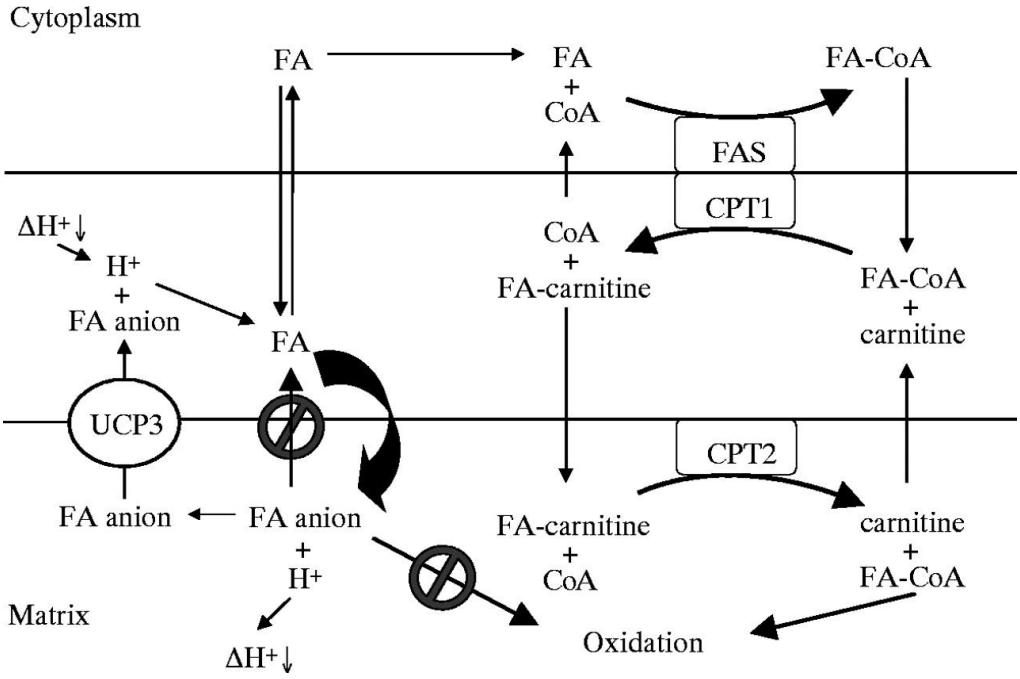

Figure 6: Hypothesis for the function of uncoupling protein-3 (UCP3): fatty acid anions are transported out of the mitochondrial matrix to prevent accumulation of fatty acid anions inside the matrix. FA, fatty acid; CoA, coenzyme A; FAS, fatty acyl-CoA synthetase; CPT1, carnitine palmitoyl transferase-1; CPT2, carnitine palmitoyl transferase-2;ΔH^+, proton gradient (Schrauwen & Hesselink, 2002).

UCP2 and UCP3 expression levels are elevated during fasting (Samec, Seydoux, & Dulloo, 1999) as well as in other states including feeding of high-fat diets, where circulating fatty acid levels are elevated and there is a shift from carbohydrate to lipid oxidation (Fisler & Warden, 2006). Up-regulation of UCP expression depends on strain and tissue type: a high-fat diet increased UCP3 mRNA expression in skeletal muscle of C57BL/6J mice (Gong et al., 1999) and rats (Kusunoki et al., 2005) but increases UCP2 expression only slightly in white adipose tissue of AKR mice and not at all in C57BL/6J mice (Gong et al., 1999) or in rats (Kusunoki et al., 2005). The up-regulation of UCP3 protein by a high-fat diet also occurs in human skeletal muscle (Hesselink et al., 2003). Similarly, within the brain, a high-fat, ketogenic diet increases UCP2 mRNA and protein levels and reduces ROS production (Sullivan, Rippy, et al., 2004; Sullivan, Springer, Hall, & Scheff, 2004). Conversely, substitution of a low-fat diet to immature rats reduces UCP2 levels and increases ROS production and seizure-induced excitotoxicity (Sullivan, Dube, Dorenbos, Steward, & Baram, 2003). Thus, a ketogenic diet may be neuroprotective by diminishing ROS production through activation of UCP2 in the brain (Sullivan, Rippy, et al., 2004). Indeed, UCP2 up-regulation in the brain is proposed as the mechanism by which a ketogenic diet reduces pediatric seizures (Fisler & Warden, 2006).

Features of the metabolic syndrome include central adiposity, increased plasma triglycerides and free fatty acids, insulin resistance, hyperglycemia, increased inflammation and hypertension, leading to increased risk of type-2 diabetes, atherosclerosis, and stroke. Several of these features are influenced by UCP2 and/or UCP3 (Fisler & Warden, 2006). Genetic association of natural polymorphisms with

phenotypes in humans provides an independent method to determine the *in vivo* functions of UCP2 and UCP3. Thus, one can demonstrate the influence of UCP2 on type-2 diabetes or BMI in an association study even without proving the underlying biochemical reaction carried out by these proteins (Fisler & Warden, 2006). Indeed, genetic studies can be used to guide biochemical investigations towards understanding the biochemistry of UCP2 and UCP3 (Fisler & Warden, 2006).

A review of human genetic studies examining expression of UCP2 or UCP3 and the propensity to obesity suggested that some obesity related phenotypes are significantly associated with these UCPs. A UCP2 insertion/deletion variant was associated with BMI in 4 studies, and polymorphisms of UCP3 were associated with BMI in 2 studies (Schonfeld-Warden & Warden, 2001). These authors concluded that since the UCP2 insertion/deletion variant association with BMI was observed in a variety of ethnic groups, the variant itself underlies the association with BMI (Schonfeld-Warden & Warden, 2001). Population studies showed that a common polymorphism in the UCP2 promoter, -866G/A, was associated with a reduced risk of obesity in Caucasian Europeans (Esterbauer et al., 2001; Krempler et al., 2002). However, the data suggesting an effect of UCPs on obesity remains uncertain, with papers reporting no linkage or association with UCP2 or UCP3 alleles, while another reports an association of UCP3 alleles with measures of body composition in women (Fisler & Warden, 2006).

Insulin resistance in type-2 diabetes and obesity involves muscle, liver, and adipocytes. UCP2 knockout mice show increased insulin sensitivity and are protected

against dietary fat-induced insulin resistance (Joseph et al., 2002). Conversely, data from *in vitro* studies in L6 muscle cells suggest that UCP3 functions to facilitate fatty acid oxidation and minimize mitochondrial ROS production, perhaps thereby reducing muscle insulin resistance (MacLellan et al., 2005). Higher expression of UCP2 in white adipose tissue and skeletal muscle are associated with reduced risk of developing obesity (Schrauwen & Hesselink, 2002). The data presently available suggest that UCP2 up-regulation has opposing effects on different components of type-2 diabetes. Increased UCP2 results in β-cell dysfunction, impaired insulin sensitivity, and earlier, more severe diabetes, but may protect from diabetic neuropathy (Fisler & Warden, 2006). Thus, UCP2 is proposed as a diabetes gene (Marx, 2002). Increased UCP3 may, on the other hand, reduce muscle insulin resistance (Fisler & Warden, 2006).

1.8 ATP-sensitive potassium channels (K^+_{ATP}), metabolism, and obesity

ATP-sensitive potassium (K^+_{ATP}) channels, a family of weak inward rectifiers inhibited by intracellular ATP that couple cellular energy metabolism to membrane electrical activity, have perhaps been the most widely explored K^+ channels in terms of therapeutic potential (S. J. Ashcroft & Ashcroft, 1990). Various types of ion channels are involved in the regulation of electrical activity in the pancreatic β-cell, and of these, the K^+_{ATP} channel plays a critical role; these are also found in the sarcolemmal, mitochondrial, and nuclear membranes (sarc, mito, and nuclear K^+_{ATP}). In pancreatic β-cells opening the K^+ channels leads to membrane hyperpolarization and consequently suppression of insulin secretion (Shieh, Coghlan, Sullivan, & Gopalakrishnan, 2000). The K^+_{ATP} channels predominantly determine the resting potential of β-cell and couple

cellular metabolism to electrical activity (F. M. Ashcroft & Rorsman, 1989; Dukes & Philipson, 1996). When plasma glucose is elevated, increases in intracellular ATP/ADP ratio lead to closure of K^+_{ATP} channels and membrane depolarization that, in turn, leads to the activation of voltage-dependent Ca^{2+} channel, a rise in intracellular Ca^{2+}, and insulin secretion.

The subunit composition of K^+_{ATP} channels is tissue specific and is regulated by tissue energetics. The molecular structure of sarc K^+_{ATP} channels has been clarified by cloning members of the inwardly rectifying K^+ channel subfamily Kir6.0 (Kir6.1 and Kir6.2) and the receptors for sulfonylureas (SUR1, SUR2A and SUR2B) (Inagaki et al., 1995; Seino, 1999). Evidence indicates that an integrated sarc K^+_{ATP} molecule is an octameric complex composed of four Kir subunits and four SUR subunits. The Kir subunits have two transmembrane domains and form the pore. The SUR subunits belong to members of the ATP-binding cassette (ABC) protein superfamily. They have three transmembrane domains and two nucleotide-binding domains (NBD1 and NBD2) on the cytoplasmic side (Seino & Miki, 2003). The SUR functions as regulatory subunit (Aguilar-Bryan et al., 1998), conferring sensitivities of the channel to regulators like sulfonylureas, MgADP and some channel openers (Enkvetchakul, Loussouarn, Makhina, & Nichols, 2001). The subunit composition of sarc K^+_{ATP} channels is tissue specific: in the pancreatic β-cell, K^+_{ATP} consists of SUR1 and Kir6.2 subunits; in the cardiac and skeletal myocytes, it is composed with SUR2A and Kir6.2; in vascular smooth muscle cells, with SUR2B and Kir6.1, and in non-vascular smooth muscle cells, with SUR2B and Kir6.2 (Seino & Miki, 2003).

Cell energy metabolism regulates the expression of K^+_{ATP} channels present in sarcolemma, mitochondria, and the nuclear membrane; alteration of cell metabolism leads to changes in channel number (Zhuo, Huang, Liu, & Liang, 2005). High glucose uptake leads to significant decrease in kir6.2 mRNA expression level in pancreatic islets. This effect is reversed by exposure to low glucose (Moritz, Leech, Ferrer, & Habener, 2001). Diabetes (Ren, Xu, & Wang, 2003) and hormones like glucocorticoids (Hernandez-Sanchez, Ito, Ferrer, Reitman, & LeRoith, 1999) and estrogen (Ranki, Budas, Crawford, & Jovanovic, 2001), which alter cell metabolism, can regulate K_{ATP} gene expression. K_{ATP} gene transcription responds dynamically to cell energy metabolism. Some of the products of energy metabolism like ATP and ADP can directly regulate the channel activity.

Sarc K^+_{ATP} can prevent intracellular Ca^{2+} overloading into cells which would result in reduction in contraction and energy sparing, demonstrated in the case of kir6.2 knockout mice (Suzuki et al., 2001). Mito K^+_{ATP} protect mitochondria from disturbances like over-production of free radicals, imbalance in trans-membrane ion transport by controlling mitochondrial Ca^{2+} ion concentration, and matrix swelling. Opening of mito K^+_{ATP} restores membrane potential, allowing extrusion of H^+ ions, creating a more favorable electrochemical gradient for ATP synthesis (Szewczyk, 1996; Y. Wang & Ashraf, 1999; Xu, Wang, Ayub, & Ashraf, 2001). But Garlid (2000) proposed that opening of mito K^+_{ATP} induces matrix swelling which maintains architecture and permeability of mitochondrial membranes (Garlid, 2000). Matrix swelling can activate

fatty acid oxidation, respiration, and ATP production (Halestrap, 1989). In case in energy crisis, depletion of intracellular ATP and consequently Ca^{2+} inflow will activate some of the K^{+}_{ATP} channels, which then results in the opening of all the K^{+}_{ATP} channels to initiate a coordinated metabolic response, with sarc K^{+}_{ATP} decreasing cell excitability and reducing energy cost, mito K^{+}_{ATP} channels maintaining the homeostasis of intra-mitochondrial environment and keeping the production of ATP to provide constant energy supply, and nuclear K^{+}_{ATP} regulating genes that are related with energy metabolism (Zhuo et al., 2005).

The homeostatic role of K^{+}_{ATP} channels has been demonstrated by using KCNJ11 gene (encodes Kir6.2)-deficient mice to demonstrate the effects of the skeletal muscle-specific ablation of K^{+}_{ATP} activity (Alekseev et al., 2010). These mice showed a higher rate of oxygen consumption under sedentary conditions, reflecting increased EE and heat production, and did not show any deficit in food intake or blood energy substrates (Alekseev et al., 2010). Data from a different study using a low-level exercise regimen revealed that the K^{+}_{ATP} deficiency amplifies energy use through an extra cost of physical activity, primarily determined by physical activity performance (Ghanassia, Brun, Mercier, & Raynaud, 2007), resembling animal models overexpressing mitochondrial uncoupling proteins in skeletal muscle (Li et al., 2000). By modulating exercise thermogenesis and NEAT (Alekseev et al., 2010), sarc K^{+}_{ATP} channels could also contribute to heat production during acute cold exposure through muscle shivering. The enhanced energy use in K^{+}_{ATP} channel-deficient skeletal muscles, resulting in limited body weight gain and compromised physical endurance (Alekseev et al., 2010),

implicates K^+_{ATP} as an important energy-sparing system that defines muscle thermogenic response through optimization of energy use.

1.9 Mediator of RNA polymerase II transcription subunit 1 (MED1)

Mediator, a large multisubunit protein complex consisting of nearly 30 subunits, plays an essential role in the transcription of all RNA polymerase II-transcribed genes in eukaryotic cells (W. Chen & Roeder, 2011) thus serving as a bridge between DNA-bound activators and the general transcription machinery to facilitate formation and/or function of the preinitiation complex (W. Chen, Zhang, Birsoy, & Roeder, 2010). In particular, in vitro studies have established ligand-dependent Mediator coactivator functions that involve ligand-dependent binding of Mediator, through the MED1 subunit, to nuclear receptor AF2 domains. A subsequent study showed that MED1 is essential for PPARγ–mediated differentiation of mouse embryonic fibroblasts to adipocytes and for associated PPARγ-dependent transcription events (Ge et al., 2002), and an earlier study of a liver-specific MED1 knockout mouse demonstrated a role for MED1 in PPARα-mediated oxidation of fatty acids (Jia et al., 2004). As a major site for the regulation of fatty acid and glucose metabolism, skeletal muscle plays a significant role in the control of obesity, diabetes, and cardiovascular disease; nuclear receptors (Desvergne, Michalik, & Wahli, 2006; Smith & Muscat, 2005) and coregulators (Feige & Auwerx, 2007; J. Lin, Handschin, & Spiegelman, 2005) play key roles as the critical regulators of transcriptional programs that govern the processes of normal muscle maintenance and function.

Muscle-specific MED1 knockout (MED1 MKO) mice exhibit enhanced insulin sensitivity and improved glucose tolerance and are resistant to high-fat diet-induced obesity despite a similar food intake to control mice, possibly through increased EE (W. Chen et al., 2010). Med1 MKO mice also exhibit increased mitochondrial density and increased expression of genes specific to type I and type IIA fibers in white muscle, indicating a switch toward slow fibers, as well as increased expression of BAT-specific genes involved in energy expenditure through uncoupled respiration (W. Chen et al., 2010). These results strongly suggest that MED1 acts in the muscle to regulate glucose and energy metabolism as observed in Med1 MKO where around 140 genes were upregulated in skeletal muscle (W. Chen et al., 2010). Of these, more than half are involved in metabolic pathways particularly involved in EE and may account, at least in part, for the enhanced glucose tolerance and insulin sensitivity of the knockout mice as well as the associated protection from high-fat diet-induced obesity (W. Chen et al., 2010). This study indicates a strong suppressive function of MED1 on energy expenditure pathways in muscle and also has significant implications for therapeutic approaches to metabolic and muscle diseases.

1.10 AMP-activated protein kinase (AMPK)

AMP-activated protein kinase (AMPK) is a heterotrimeric complex consisting α subunit (catalytic), β, and γ (regulatory subunits). Activation of this kinase into pAMPK is through AMP and occurs by three independent mechanisms: 1) allosteric activation of the phosphorylated enzyme; 2) promotion of phosphorylation of Thr-172 by an upstream kinase; 3) inhibition of dephosphorylation of Thr-172 by protein phosphatases (Hardie,

Hawley, & Scott, 2006). All these three mechanisms make the AMPK system very effective because a small change in the concentration of AMP can induce a large change in the kinase activity of the complex. ATP inhibits the activation of AMPK by antagonizing binding of AMP. Almost all eukaryotic cells express enzyme adenylate kinase which converts ADP to AMP and ATP. This makes AMP to ATP ratio a better indicator of cellular energy status than ADP to ATP ratio, and AMPK a better sensor for the cellular energy levels (Hardie et al., 2006).

In skeletal muscle, the degree of activation of AMPK is dependent of the metabolic stress caused by contraction. The response to metabolic stresses, such as energy depletion, is probably the key role for AMPK in single celled eukaryotes but it is now becoming clear that during the course of evolution of multicellular organisms, hormones and cytokines have acquired the ability to regulate AMPK system. It is activated by the adipokine, leptin in skeletal muscle and by adiponectin in skeletal muscle and liver (Minokoshi et al., 2002; Tomas et al., 2002; Yamauchi et al., 2002). This increases EE in muscle by increasing fatty acid oxidation and up-regulating mitochondrial biogenesis. Conversely, leptin inhibits AMPK in the hypothalamus, consistent with the ability of the adipokine to inhibit food intake, which suggests that hypothalamic AMPK also has a key role in the regulation of body weight and whole body energy balance (Minokoshi et al., 2002).

The first targets of AMPK to be identified were acetyl-CoA carboxylase (ACC) and HMG-CoA reductase, activation of AMPK (i.e., pAMPK) caused inhibition of fatty

acid and cholesterol synthesis in hepatocytes (Corton, Gillespie, Hawley, & Hardie, 1995; Henin, Vincent, Gruber, & Van den Berghe, 1995). AMPK activation also inhibits muscle glycogen synthesis via phosphorylation of glycogen synthase (Jorgensen et al., 2004). In skeletal muscle it stimulates glucose uptake both via translocation of the glucose transporter 4 (GLUT4) to the plasma membrane and by increasing its expression (Holmes, Kurth-Kraczek, & Winder, 1999; Kurth-Kraczek, Hirshman, Goodyear, & Winder, 1999; Merrill, Kurth, Hardie, & Winder, 1997). By phosphorylating ACC, AMPK lowers malonyl-CoA, relieving the inhibition of uptake of fatty acids into mitochondria via the carnitine carrier system, and thus stimulating fatty acid oxidation and up-regulating mitochondrial biogenesis (Merrill et al., 1997; Winder et al., 2000).

1.11 Peroxisome proliferator-activated receptors (PPARs)

Peroxisome proliferator-activated receptors (PPARs) are ligand-activated transcription factors involved in the transcriptional regulation of key metabolic pathways including lipid metabolism, adipogenesis, and insulin sensitivity. As these nuclear receptors are activated by extracellular signals and control multiple gene targets of metabolism, PPARs can be viewed as a system that control multiple inputs and outputs involved in energy balance. They are of three isotypes: PPARα, PPARδ, and PPARγ. Their activation is initiated by specific ligand binding to the ligand-binding domain which is specific to isotype. Each of the three PPAR subtypes is expressed in a distinct, tissue-specific pattern. PPARα is highly expressed in liver, heart, kidney, skeletal muscle, and BAT, tissues that are metabolically very active. PPARγ is most-highly expressed in white and brown adipose tissue, large intestine, and spleen. In contrast to PPARα and

PPARγ, which are abundantly expressed in just a few tissues, PPARδ is expressed in virtually all tissues at comparable levels (Berger, Akiyama, & Meinke, 2005).

PPARα plays an important role in regulating the β-oxidation of fatty acids, a major source of cellular energy. PPARα target genes include multiple proteins essential for fatty acid uptake, intracellular transport, and β-oxidation, including fatty acid transport protein, fatty acid translocase, long-chain fatty acid acetyl-coenzyme A synthase, and CPT1 (Evans, Barish, & Wang, 2004). PPARα activation induces expression of lipase, which hydrolyzes triglyceride rich lipoproteins, the major source of circulating fatty acids. Fasting potently induces PPARα expression, which underlines the importance of this transcription factor in energy balance (Kersten et al., 1999).

PPARγ also regulates genes involved in lipid metabolism, including lipoprotein lipase, acyl-coenzyme A synthetase, and aP2, and glucose control such as the GLUT4 and phosphoenolpyruvate carboxykinase (PEPCK) (Lehrke & Lazar, 2005; Spiegelman, Hu, Kim, & Brun, 1997). PPARγ regulates signaling molecules like leptin that are secreted from adipose and affect glucose utilization and/or production in other tissues (Kliewer, Xu, Lambert, & Willson, 2001). PPARγ agonists reduce serum concentrations of both esterified and nonesterified fatty acids, presumably by promoting their uptake and storage in adipocytes (Kliewer et al., 2001). PPARγ is expressed at low levels, in both skeletal muscle and liver. Thus, PPARγ agonists may have direct effects on glucose utilization or production in both of these tissues (Kliewer et al., 2001). In liver, PPARγ

agonist treatment results in decreased expression of phosphoenolpyruvate carboxykinase, which encodes the rate-limiting step in hepatic gluconeogenesis (Kliewer et al., 2001).

Selective overexpression of a constitutively active form of PPARδ in mouse adipose tissue induces significant weight loss and protects against obesity and dyslipidemia induced by a high-fat diet (Y. X. Wang et al., 2003). This PPARδ effect correlated with activation of genes involved in fatty acid oxidation and adaptive thermogenesis. Importantly, PPARδ did not have an effect on genes involved in lipid storage and thus appears to be involved primarily in energy consumption in adipose tissue. This enhancement of fatty acid oxidation also was found in genetically altered mice that overexpress PPARδ in skeletal muscle. In the presence of a PPARδ agonist, the mouse skeletal muscle fibers reportedly switch from type II "glycolytic/fast twitch" to type I "oxidative/slow twitch." (Y. X. Wang et al., 2004) This change explains why these PPARδ overexpressed mice can run twice the distance of control mice. The muscle fiber type switch also confers resistance to obesity.

1.12 Peroxisome proliferator-activated receptor gamma coactivator 1-α (PGC1-α)

The transcriptional coactivator PGC1-α is highly expressed and interacts with nuclear receptor PPARγ in oxidative tissues like BAT, heart, and slow-twitch skeletal muscle where it regulates mitochondrial function and metabolism (Finck & Kelly, 2006). PGC1 co-activators affect biological processes that regulate cellular responses to meet energy demands according to their environment by increasing mitochondrial biogenesis, cellular respiration, and energy substrate uptake and utilization. The expression and

activity of PGC1-α is linked to a number of upstream signaling pathways which include beta adrenergic/cAMP pathway and AMPK, particularly in BAT and skeletal muscle (Finck & Kelly, 2006).

Forced expression of PGC-1α at high physiologic levels in mice resulted in an increased proportion of oxidative or type I muscle fibers coincident with an increase in the expression of mitochondrial markers, red muscle coloration, increased expression of contractile protein characteristic of type I fibers, and resistance to electrically stimulated fatigue (J. Lin et al., 2002). These results indicated that PGC-1α is sufficient to drive the slow-twitch skeletal muscle program. Recent evidence also implicates PGC-1α in the regulation of muscle glucose metabolism. Studies demonstrate that PGC-1α robustly activates expression of GLUT4 in skeletal muscle cells in culture and represses glucose oxidation in muscle cell lines by activating the expression of the gene encoding pyruvate dehydrogenase kinase 4 (Michael et al., 2001; Wende, Huss, Schaeffer, Giguere, & Kelly, 2005). These results suggest that PGC-1α controls muscle fuel selection by increasing fatty acid oxidation while temporarily shutting down glucose oxidation — a gene regulatory equivalent of the fatty acid-glucose cycle (Finck & Kelly, 2006).

1.13 Fatty acid synthase (FAS)

Fatty acid synthase (FAS) is a key enzyme in fatty acid synthesis from acetyl CoA, which is expressed at high levels in liver and adipose tissue, but at low levels in other tissues including skeletal muscle (Weiss et al., 1986). FAS catalyzes the last step in fatty acid biosynthetic pathway and is believed to be a determinant of the maximal

capacity of a tissue, and in particular to synthesize fatty acids by de novo lipogenesis (Aye & Izaguirre, 1991). Liver-specific FAS knockout mice possess a similar phenotype to control animals when fed normal chow, and did not show protection against the development of fatty liver but rather exacerbated it under specific nutritional conditions (Chakravarthy et al., 2005). Indeed, when fed a low-fat/high-carbohydrate diet for 4 weeks, these mice developed hepatic steatosis due to a reduction in β-oxidation, increased hepatic malonyl-CoA concentrations, and a significant decrease in blood ketone bodies (Chakravarthy et al., 2005). In fact, this mouse model led to the novel and interesting concept that "new fat" synthesized via FAS activity would specifically activate nuclear receptors like PPARα and would in turn lead to enhanced β-oxidation.

1.14 Fatty acid translocase (FAT/CD36)

Long-chain fatty acids (LCFAs) cross the plasma membrane via a protein-mediated mechanism involving one or more LCFA-binding proteins. Among these, FAT/CD36 has been identified as key LCFA transporter in the heart and skeletal muscle, where it is regulated acutely and chronically by insulin (Bonen, Tandon, Glatz, Luiken, & Heigenhauser, 2006). FAT/CD36 is expressed ubiquitously to varying extents among metabolically active tissues such as the heart, skeletal muscle, liver, and adipose tissue where, along with CPT1, it regulates fatty acid transport and oxidation in the mitochondria (Bonen et al., 2006; Holloway, Bonen, & Spriet, 2009). In skeletal muscle, FAT/CD36 expression and/or its subcellular distribution is altered in obesity and type-2 diabetes (Bonen et al., 2006; Love-Gregory & Abumrad, 2011). FAT/CD36 response to metabolic disturbances can differ in muscle and adipose tissue. Unlike muscle

FAT/CD36, adipose tissue FAT/CD36 expression was not altered in an animal model of type-1 diabetes and in contrast, in the insulin-resistant obese rats, adipose tissue, but not muscle, FAT/CD36 expression was increased (Bonen et al., 2006).

1.15 Sarcoplasmic/endoplasmic reticulum Ca^{2+}-ATPase (SERCA)

A thermogenic system has evolved for the specific purpose of protecting a tissue or organism from the cold in the myocytes (Kozak & Young, 2012). This system is based on the cycling of Ca^{2+} by the sarcoplasmic/endoplasmic reticulum Ca^{2+}-ATPase (SERCA)—a pump that transfers Ca^{2+} into the sarcoplasmic reticulum upon ATP hydrolysis and there by generating heat (Kozak & Young, 2012). The SERCA pump is encoded by a highly conserved multigene family whose function is to transport Ca^{2+} ions and regulate intracellular calcium homeostasis. Their presence is ubiquitous and they are the only mechanism to maintain SR/ER calcium stores in muscle and non-muscle cells (Periasamy & Kalyanasundaram, 2007). The SERCA pump regulates the cytosolic calcium level tightly and controls many cellular functions, from muscle contraction to cell signaling responsible for growth and differentiation (Periasamy & Kalyanasundaram, 2007).

The diversity of SERCA pump isoforms and pump expression level imparts tissue- and cell specific Ca^{2+} transport capacity. Furthermore, this diversity can be better understood in skeletal muscle, where the SERCA1 isoform with faster kinetics is expressed several-fold higher in fast-twitch skeletal muscle, whereas SERCA2a is expressed at a lower level in cardiac and slow-twitch skeletal muscle (Periasamy &

Kalyanasundaram, 2007). The differences in the function of individual SERCA pump isoforms can be further amplified by their cellular environment and the presence of SERCA regulatory proteins (inhibitors) phospholamban (PLB) and sarcolipin (SLN) which provide additional regulation of SERCA pump activity and contribute to Ca^{2+} homeostasis in cardiac and skeletal muscle (Periasamy & Kalyanasundaram, 2007).

In humans, this muscle-based thermogenic Ca^{2+} cycling is also the basis of a pathological condition, malignant hyperthermia, caused by a mutation of the ryanodine receptor that results in uncontrolled leakage of Ca2+ into the cytoplasm, causing heat generation as Ca^{2+} passes down its concentration gradient (similar to uncoupling protein-associated heat generation) (Kozak & Young, 2012). Stimulation of Ca^{2+} cycling, uncoupled to muscle contraction, with ATP hydrolysis by SERCA activity is therefore a powerful thermogenic mechanism. SLN induces non-shivering thermogenesis (NST) by regulation of SERCA in skeletal muscle to maintain core body temperature when mice are exposed to cold, even in the absence of BAT and shivering thermogenesis, and protects these mice from developing diet-induced obesity, suggesting this thermogenesis system has a role in energy balance and has potential as a target to induce fat burning to treat obesity (Bal et al., 2012).

1.16 Summary

The alterations in the peripheral energy homeostatic mechanisms leading to phenotypic differences may have a central origin. The hypothalamus, particularly the VMH, along with the central MC system, plays an important role in determining fuel

partitioning and usage in peripheral tissues. Activation of MC receptors in the hypothalamus increases EE by increasing SNS activity and may engage molecular mediators of energy homeostasis in the periphery, including in skeletal muscle. Although numerous studies show the importance of the VMH, central MC, and SNS in obesity resistance, there is lack of an effective model to describe function of VMH-central MC-SNS-skeletal muscle pathway and its potential relevance in promoting the lean phenotype.

CHAPTER 2

As described in the introduction in Chapter 1, lean HCR have high total daily EE, high physical activity, and are less prone to metabolic disorders, whereas their counterparts, LCR, are prone to metabolic and cardiovascular diseases and have low total daily EE and low physical activity. This high EE in HCR is consistent even when matched by body weight suggesting these HCR have low economy of activity. I wanted to see which component of EE was altered in these HCR/LCR rats. I took the approach of partitioning EE data into resting and non-resting EE to test the hypothesis that there is higher activity-related EE in HCR, and that this high activity EE is due to heightened daily activity plus low economy of activity in HCR, implying that there may be excess calories used by skeletal muscle during activity. I proposed that this high activity EE and low economy of activity arises through differential skeletal muscle thermogenesis and enhanced expression of molecular and neural intermediates in lean (HCR) vs. obesity-prone rats (LCR). One strategy to compare EE between phenotypes that differ in bodyweight and composition is to compare EE by obtaining animals that overlap in body weight or lean mass. Here, I used female HCR and LCR rats, as the male HCR and LCR have minimal overlap in body weight and composition between the groups.

I tested the hypothesis that the lean HCR have heightened activity-related EE and low economy of activity due to increased sympathetic drive to peripheral tissues which in

turn increase mediators of EE. I quantified EE using indirect calorimetry and used norepinephrine turnover to determine the level of sympathetic drive to peripheral tissues. Quantitative RT-PCR and western blotting were performed to evaluate the mRNA and protein expression of mediators of energy balance.

2.1 Methods

Animals

Adult female HCR/LCR rats (selection generation 25, N=13/group; 10-12 months of age and overlapping in body weights) were obtained from the University of Michigan. Each rat was housed individually on a 12:12 light:dark cycle with lights on at 0700 EST. Rats received rodent chow (5P00 MRH 3000, T.R. Last Co. Inc) and water *ad libitum.* All studies were conducted according to the rules and approval of the Kent State University IACUC.

Body composition

I measured body composition using EchoMRI-700 (Echo Medical Systems, Houston, TX) to determine the fat and lean mass (in grams) of each rat the day before test. This did not interfere with temperature transponder function (see transponder implantation below).

Measurement of total energy expenditure (TEE) and its components

After body composition determination, adult female HCR and LCR rats were measured for total EE and 24-hr physical activity using small-animal indirect calorimetry

(4-chamber Oxymax FAST system, Columbus Instruments, Columbus, OH). Rats were acclimated to the calorimetry chamber (7.5 in x 12 in x 9 in) and room for 24-48 hrs prior to testing; this is sufficient to avoid novelty-induced increases in physical activity. On the day of calorimetry, rats were weighed and placed in the chamber with food and water; the chamber was then sealed. The calorimeter was calibrated using primary gas standards. Air was pumped into the chamber at 1.9-3.1 lpm, depending on the weight of the rat, and chamber air was sampled at 0.4 lpm. Measurement of gas exchange took place every 30 sec throughout the 24-hr period except for a 3.5-min room-air reference and settle period after each 60-sample interval. Physical activity data were collected using infrared beam-break counts, collected every 10 sec uninterrupted throughout the 24-hr period, in the X and Z axes; the first hour of data was not included in the analysis. Data collected from 1200 (EST) on day 1 through 1200 on day 2 were analyzed. EE data (VO_2, VCO_2, RER, kcal/hr) were averaged, and physical activity data were expressed as mean beam breaks per minute. Body weight and food intake data indicate that rats were in homeostatic energy balance during EE measurements and body weight did not change significantly (within and between groups) compared to home-cage days.

Next, I separated the non-resting EE and resting EE components of total EE data described above using Columbus Instruments software (CLAX). Using the data set described above, resting EE was defined as the lowest level of EE, excluding the lowest 5 episodes (i.e., short sequences of consecutive data points) to eliminate potential error due to variation in gas exchange values that can occur during the switch from sample to reference air measurement. This same method was used to define resting EE during the

treadmill test (see below). Because each rat had two separate resting EE values calculated within a short period of time (one for 24-hr EE, one before treadmill walking), we compared the two values for each rat to validate our method. The two resting EE measurements were very similar (data in Results). Non-resting EE is defined as (TEE) – (resting EE).

As previously reported (Gavini et al., 2014; Novak CM, 2009), resting and physical activity EE were directly assessed by measuring gas exchange once every 10 sec during a treadmill activity test. At least one day after a 15-min treadmill acclimation period, rats were placed in the treadmill and allowed to acclimate without food for 2 hrs. Over the course of this 2-hr period, rats showed a predictable pattern of behavior: physical activity and EE rise markedly then fall gradually, reaching a steady state. After the 2-hr resting period, the treadmill was started at 7 m/min for 30 min, during which time steady-state activity EE data were collected. Rats that did not show adequate resting or activity (walking backward on the treadmill, sitting on the treadmill or shocker) were measured at a later date.

All EE data from HCR/LCR rats were analyzed using *t*-tests, ANOVA, and analysis of covariance (ANCOVA). Because our previous studies suggested the hypothesis that EE was elevated in HCR, we compared resting and non-resting EE between weight-matched or lean-mass-matched HCR and LCR using a 1-tailed paired *t*-test. An unpaired 1-tailed *t*-test was used to compare treadmill gas exchange values between groups based on our previous results. Lastly, total EE, resting EE, and non-

resting EE were analyzed using analysis of covariance (ANCOVA) with either body mass or lean mass as the covariate; interaction terms were removed from the analysis if not significant. While lean mass is regarded as the best covariate for analyzing resting EE or total EE (Tschop et al., 2012) activity EE is better evaluated using body weight (Schoeller & Jefford, 2002). Thus resting and non-resting EE were analyzed using each lean mass and body weight as covariates in separate analyses to allow full comparison.

Transponder implantation

Adult female HCR/LCR (n=7/group, a subset of actual group mentioned above) rats were anesthetized using isoflurane. A short incision was made on both hind legs. Sterile temperature transponders IPTT-300 (Bio Medic Data Systems, Inc.) were implanted adjacent to the gastrocnemius (gastroc) muscle group of both hind limbs to measure the heat generated by skeletal muscle during activity. Care was taken to place the transponders so as not to disrupt locomotor function. Rats were allowed to recover for a week before the graded treadmill test was performed. Implant placement was examined during tissue harvest and data from inaccurately placed transponders were omitted from final analyses.

Graded treadmill test

To determine skeletal muscle heat dissipation during controlled physical activity, we measured the temperatures of the gastroc muscle group using a graded treadmill exercise test. The rats were acclimated to the treadmill for 10 minutes in the days prior to the test as well as immediately before the test. Gastroc temperatures in each leg were

recorded at baseline and at set intervals during a 5-level graded treadmill test. Starting at 7 m/min, 0^0 incline, temperature was measured at 2, 5, and 10 minutes, 15 minutes (9 m/min at 0^0 incline), 20 minutes (9 m/min, 10^0 incline), 25 minutes (11 m/min, 10^0 incline), and 30 minutes (11 m/min, 20^0 incline). The test was stopped at end of 35 minutes; however some LCR were not able to complete all 5 levels of activity.

Muscle gene expression

Skeletal muscle (gastroc and quadriceps (quad)) was collected from adult female HCR/LCR rats (from a separate group, generation 25, N = 8 or 7/group) after euthanasia by rapid decapitation without anesthetic agents after several weeks without exercise. Muscle samples were homogenized and total mRNA was extracted using an Ambion ribopure kit following manufacturer's instructions. The purity of mRNA was measured using NANODROP (ND-1000) (Nanodrop technologies) and A260/280 ratio to be ranging from 1.8 – 2.1.This mRNA was used to prepare cDNA using an Applied Biosystems kit and thermal cycling at 25^0C for 10 minutes, 48^0C for 30 minutes, 95^0 C for 5 minutes and holding at 4^0C. The cDNA was used for quantifying the expression of uncoupling proteins 2 and 3 (UCP2, UCP3), ATP-dependent potassium channel (K^+_{ATP} subunits Kir6.1, Kir6.2), Mediator of RNA polymerase II transcription subunit 1 (MED1), and glyceraldehyde 3-phosphate dehydrogenase (GAPDH, used as a control). The relative expression was calculated using comparative Ct method (ΔCt). Data are expressed as a percent expression using the HCR as the reference value (defined as 100%), and groups were compared using a 2-tailed t-test.

Western blotting

UCP2, UCP3, and the K^{+}_{ATP} subunits Kir 6.1 and Kir 6.2 and MED1 were examined in skeletal muscle (gastroc and quad) from adult female HCR/LCR rats (same group of generation 25 rats used for muscle gene expression, N = 5 or 4/group), using actin as a loading control for protein expression. Skeletal muscle samples were homogenized with ice-cold RIPA buffer (Thermo Scientific) containing a protease inhibitor cocktail (Roche Diagnostics). The supernatant from the homogenization and subsequent centrifugation was used for the analysis. Equal quantities of supernatant and sample buffer (150mM tris-HCl pH 6.8, Trizma-base for pH, 6% SDS, 30% glycerol, 0.03% pyronin-Y, DTT) were mixed and tubes were heated at 90^{0}C for 3 minutes. Samples containing equal quantity of protein were loaded on to a gradient gel (4-15%) (Bio Rad) and electrophoresed using SDS running buffer (0.384M glycine, 0.05M Trizma bas, 0.1% SDS) at constant voltage (150V) for 30 minutes. The gel was blotted on to a PVDF membrane using semi-wet blotting apparatus and Otter et al. transfer buffer (49.6mM Trizma base, 384mM glycine, 17.5% methanol, 0.01% SDS) (Otter, King, & Witman, 1987) at constant current (400mAmp). The blot was incubated overnight in a blocking solution of 5% milk (Blotto) in 1xPBST (Phosphate buffered saline; 84mM sodium hydrogen phosphate, 16mM sodium dihydrogen phosphate, 100mM sodium chloride, tween20), then rinsed using 1xPBST. Primary antibodies for UCP2, UCP3, actin, MED1 (Abcam Inc. ab67241, ab3477, ab1801, ab60950 respectively), and for Kir 6.1, Kir 6.2 (Santa Cruz Biotechnology, Inc. sc-11224 and sc-11230 respectively) were diluted in blocking solution at ratio of 1:1000 (Kir 6.2, Kir 6.1, and MED1 at 1:500) and incubated with the blot overnight. Secondary antibodies were diluted in blocking solution

in the ratio 1:5000 and incubated for 1 hour at room temperature. After washing, the blots were developed using a chemiluminiscence detector using an Amersham kit (GE Healthcare, UK). The expression levels relative to actin were plotted as a percent of the reference value (with HCR as 100%), and groups were compared using a 2-tialed t-test.

Norepinephrine turnover (NETO)

Adult male HCR/LCR rats (generation 30, N= 13 HCR, 12 LCR) were used to assess sympathetic drive to skeletal muscle (including quad, lateral and medial gastroc, and soleus) and BAT. They were individually housed on a 12:12 light:dark cycle with *ad libitum* access to standard rodent chow and water and acclimated to daily handling for a week. Level of sympathetic drive to peripheral tissues was determined by norepinephrine (NE) turnover (NETO) method using α-methyl-*p*-tyrosine (aMPT) (Gavini et al., 2014; Shi, Bowers, & Bartness, 2004). aMPT is a competitive inhibitor of tyrosine hydroxylase, the rate limiting enzyme in catecholamines biosynthesis. After aMPT administration, the endogenous tissue levels of NE decline at a rate proportional to the initial NE concentrations. The rats were divided into 2 sub-groups per group (aMPT, control). On the day of study, rats receiving aMPT were injected with aMPT (125 mg aMPT/kg of BW, 25 mg/ml) and with a booster dose at same concentration 2 hours later. All rats were euthanized by rapid decapitation between 1200 and 1500, 4 hours after first aMPT injection. Tissues were rapidly dissected and snap-frozen in liquid nitrogen.

Briefly, tissue was thawed and homogenized in a solution containing dihydroxybenzylamine (DHBA, internal standard) in 0.2M perchloric acid (PCA) with 1

mg/ml ascorbic acid (AA). Following centrifugation for 15 min at 7,500 *g* at 4°C, catecholamines were extracted from the homogenate with alumina and were eluted into the PCA/AA. The catecholamines were assayed using an HPLC system with electrochemical detection (Coulochem III), MDTM mobile phase and reverse phase MD 150x3.2 column. NETO in quad, lateral and medial gastroc, soleus, and BAT were calculated using the following formula (Gavini et al., 2014; Shi et al., 2004):

$k = (\lg[NE]0 - \lg[NE]4)/(0.434 \times 4)$

$K = k[NE]0$

k is the constant rate of NE efflux (also known as fractional turnover rate),

[NE]0 is the initial NE concentration or from 0-hr group (control),

[NE]4 is the final NE concentration or from 4-hr group (aMPT), and

K = NETO.

Difference in NETO of HCR and LCR tissues were compared using 1-tailed, unpaired t-test for each tissue.

2.2 Results

Rats of the lean, high-activity phenotype have higher total EE and non-resting EE, but not consistently high resting EE.

As shown in Figures 7, 8, and 9, female HCR have significantly higher total EE when rats were matched for either body weight (Figure 7) or for lean mass (Figure 8), or when analyzed as a group (Figure 9). To parse the components of total EE (i.e., resting EE + non-resting EE), I first validated our method to estimate resting EE from the 24-hr calorimetry dataset using the 2 hr treadmill test described above (Novak CM, 2009). The

two methods of calculating resting EE did not significantly differ (t = -0.64; p = 0.53), supporting the validity and accuracy of our resting EE calculation from total EE data. After matching for body weight, total energy cost of activity (treadmill walking) was higher in HCR (3.09±0.10 kcal/hr) compared to the LCR (2.88±0.08 kcal/hr).

Resting EE over the 24-hr test did not differ between female HCR and LCR, neither as a group (without matching; Figure 9) or when matched for lean mass (Figure 8). Non-resting EE was significantly higher in female HCR in every analysis performed—after matching for either lean mass or body weight, or without matching (Figures 7, 8, and 9). The heightened non-resting EE in the lean, high-capacity phenotype (HCR) was not secondary to a higher workload as fat mass and/or total mass were higher in the LCR in each analysis. Physical activity, both horizontal and ambulatory activity, was also higher in female HCR than LCR in every analysis performed (Figures 7, 8, and 9). ANCOVA analyses of EE data from female HCR/LCR revealed that body weight or lean mass were the dominant determinants of resting EE, as resting EE was consistently higher in rats with greater body weight or lean mass (Figure 10). Lastly, non-resting EE increased with higher body weight or lean mass, and HCR consistently had higher non-resting EE compared to LCR, even after body weight or composition were considered using ANCOVA (Figure 10).

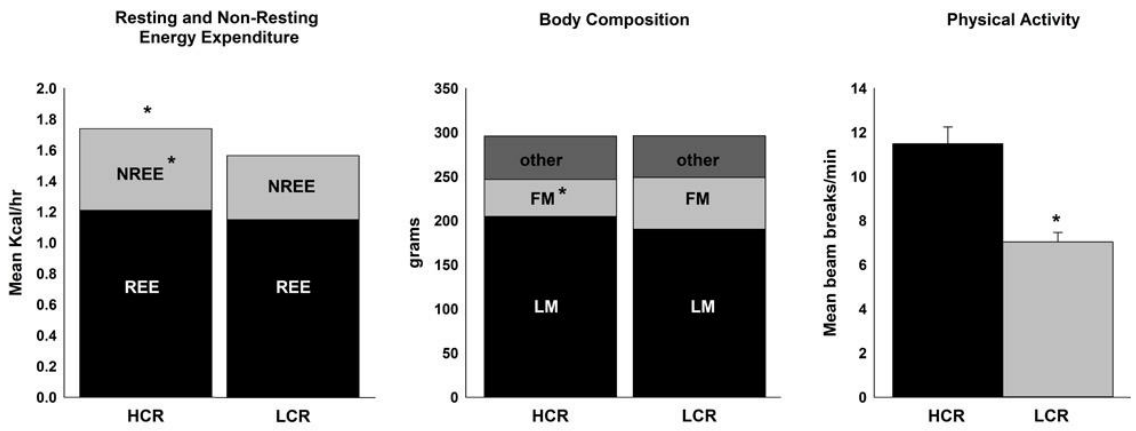

Figure 7: Lean high-capacity rats have higher total energy expenditure and physical activity when matched by body weight. High-capacity runners (HCR) have heightened total energy expenditure (TEE) and non-resting energy expenditure (NREE), but not resting energy expenditure (REE), when matched for body weight. Daily physical activity was higher in HCR when matched for body weight. HCR and low-capacity runners (LCR) show significant differences in fat mass (FM) but not in lean mass (LM) when weight matched.*$p<0.05$ (HCR≠LCR). All data are means ± SEM. (N = 8/group)

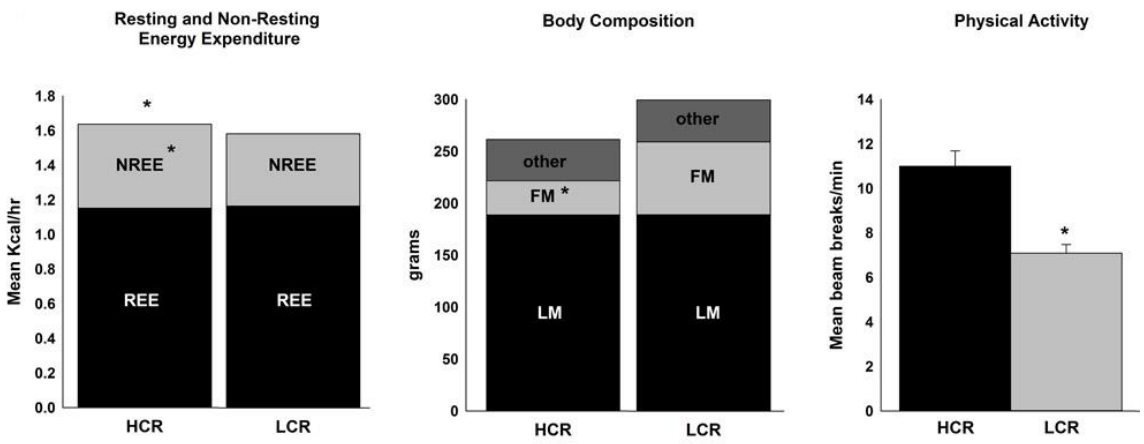

Figure 8: Lean high-capacity rats have higher total energy expenditure and physical activity when matched by lean mass. High-capacity runners (HCR) have heightened total energy expenditure (TEE) and non-resting energy expenditure (NREE), but not resting energy expenditure (REE), when matched for lean mass (LM). Daily physical activity was higher in HCR when matched for LM. HCR and low-capacity runners (LCR) show significant differences in fat mass (FM) and body weight when matched for LM.*$p<0.05$ (HCR≠LCR). All data are means ± SEM. (N = 8/group)

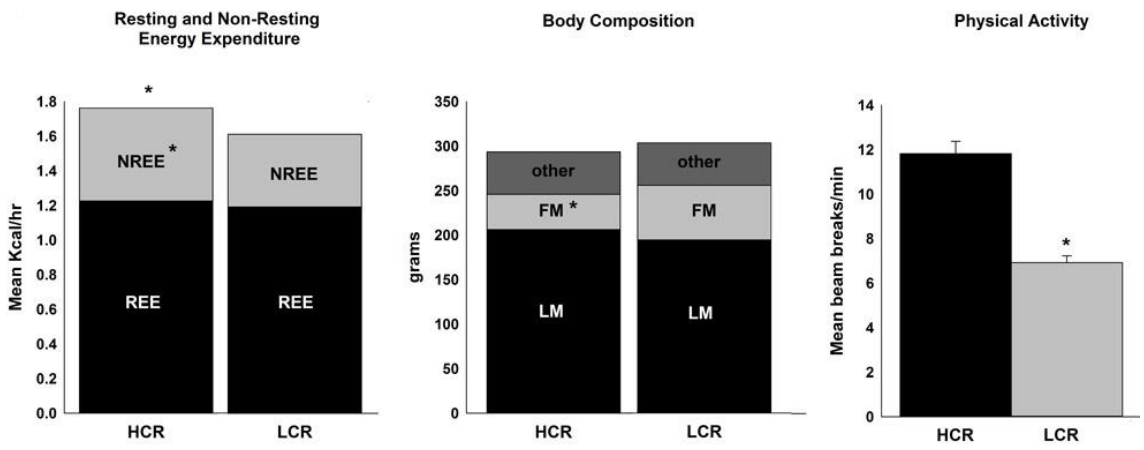

Figure 9: Lean high-capacity rats have higher total energy expenditure and physical activity. High-capacity runners (HCR) have heightened total energy expenditure (TEE) and non-resting energy expenditure (NREE), but not resting energy expenditure (REE), when analyzed by group. Daily physical activity was higher in HCR when analyzed by group. HCR and low-capacity runners (LCR) show significant differences in fat mass (FM) but not in lean mass (LM) or body weight when analyzed by group.*$p<0.05$ (HCR≠LCR). All data are means ± SEM. (N=13/group)

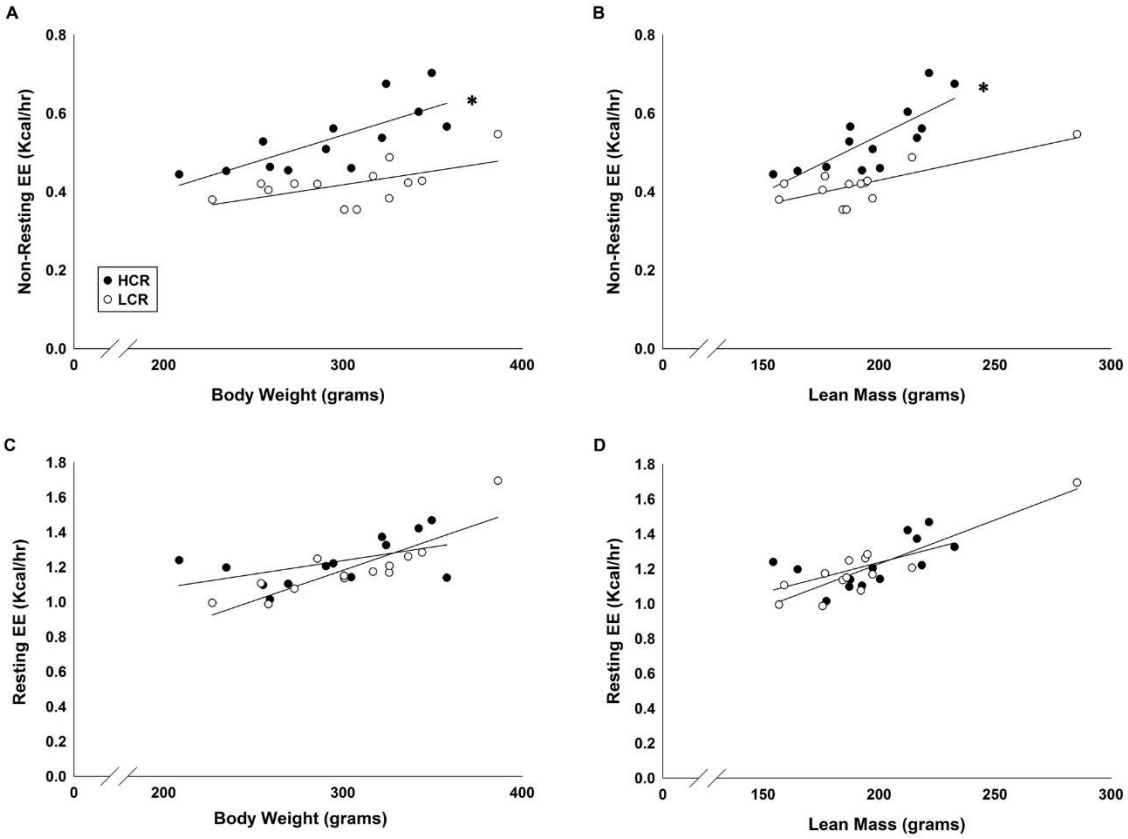

Figure 10: Body weight or lean mass are the dominant determinants of energy expenditure. In all rats, non-resting energy expenditure (NREE) increased along with body weight (A) and lean mass (B); NREE was significantly higher in the lean phenotype (high-capacity runners, HCR) compared to low-capacity runners (LCR), even after lean mass and body weight were factored out. Resting EE (REE) also increased with body weight (C) and lean mass (D), but did not significantly differ between female HCR and LCR. (N = 13/group) *$p<0.05$, HCR>LCR.

Table 2: Physical activity and body composition in rats of the lean (HCR) and obesity-prone (LCR) phenotype

		Body weight (g)	Lean mass (g)	Fat mass (g)	Total counts	Ambulatory counts
All rats	**HCR**	293.4 ± 12.8	206.27 ± 7.92	*39.39 ± 4.29	*11.82 ± 0.55	*4.93 ± 0.35
	LCR	303.3 ± 12.0	194.26 ± 8.32	61.32± 6.16	6.92 ± 0.31	2.7 ± 0.23
Matched by body weight	**HCR**	295.99 ± 11.5	*204.96 ± 6.91	*41.85 ± 5.58	*11.49 ± 0.75	*4.86 ± 0.5
	LCR	296.06 ± 11.9	190.33 ± 5.73	58.66 ± 6.7	7.04 ± 0.43	2.9 ± 0.34
Matched by lean mass	**HCR**	*264.74 ± 11.44	188.95 ± 6.3	*32.77 ± 3.97	*10.99 ± 0.69	*4.44 ± 0.42
	LCR	307.89 ± 12.13	189.12 ± 6.11	70.2 ± 7.74	7.09 ± 0.38	2.94 ± 0.33

HCR, High-capacity runners; LCR, Low-capacity runners. *$p<0.05$, HCR≠LCR

High activity energy expenditure is accompanied by skeletal muscle energy dissipation as heat.

Our analysis of EE clearly implicated non-resting EE (composed primarily of activity EE), more than resting EE, as the predominant contributor to the heightened total EE seen in the lean phenotype. This, along with previous data showing decreased economy of activity in HCR (Novak CM, 2009), strongly implicates differential skeletal muscle energy use as an underlying cause of differences in non-resting EE and, therefore, total EE. The question remained as to how the HCR dispose of these additional calories. Here, I tested the hypothesis that HCR ultimately expend calories through heat dissipation in skeletal muscle. This hypothesis was tested by measuring gastroc temperature during a graded exercise treadmill test equalizing workload between rats (matched by body weight). HCR showed significantly higher gastroc temperatures, and their maximal rise in temperature was significantly higher in HCR compared to LCR (Figure 11), demonstrating that HCR have heightened skeletal muscle heat dissipation compared to LCR.

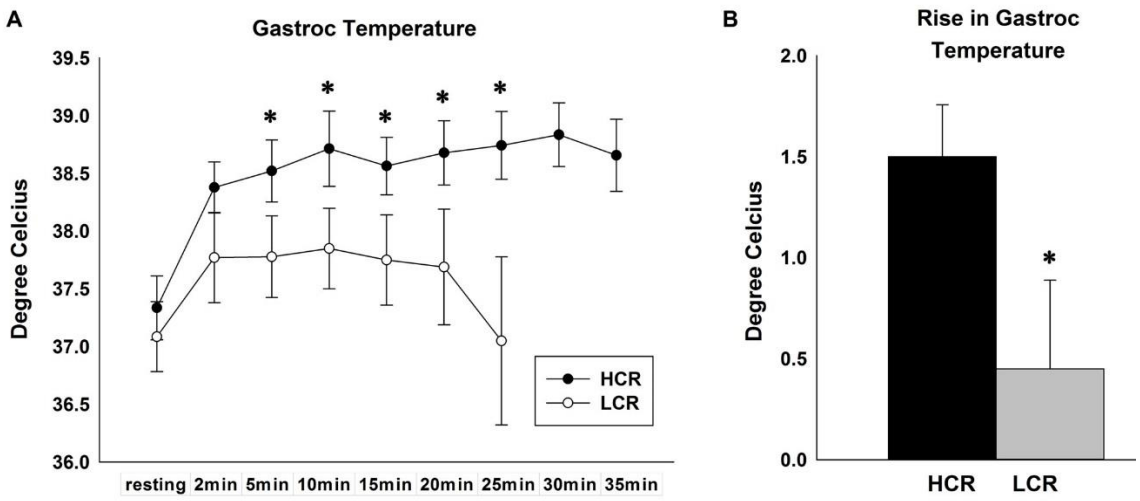

Figure 11: High-capacity runners (HCR) have heightened muscle heat dissipation during physical activity. (A) Mean gastrocnemius (gastroc) temperature during a graded treadmill exercise test. HCR show higher gastroc temperatures throughout the test period compared to low-capacity runners (LCR) with exception of resting. (B) Maximal rise in gastroc temperature was significantly higher in HCR compared to LCR during the graded treadmill test. *$p<0.05$ (HCR>LCR). All data are means ± SEM. (N=7/group)

Lean, high-activity rats have higher expression of mRNA and proteins involved in energy expenditure, and lower expression of energy conserving processes in both quadriceps and gastrocnemius.

To determine the source of the calorie use and heat dissipation in HCR skeletal muscle, we examined mRNA and protein expression of molecular endpoints known to alter energy use in quad and gastroc of HCR and LCR; for energy conservation, MED1 and K^+_{ATP} (subunits Kir6.1, Kir6.2); for energy expenditure, we examined UCP2 and UCP3. The mRNA content of UCP2 and UCP3 were found to be higher in HCR compared to LCR; that of potassium channel subunits Kir6.1 and 6.2, as well as MED1, were higher in LCR compared to HCR (Figure 12). Protein expression levels of proteins involved in energy expenditure (UCP2, 3) were found to be higher in HCR compared to LCR in both quad and gastroc. Protein expression levels of MED1 were higher in LCR compared to HCR in both quad and gastroc (Figure 13). No differences were found in protein levels of K^+_{ATP} subunits Kir6.1 and 6.2 in the quad.

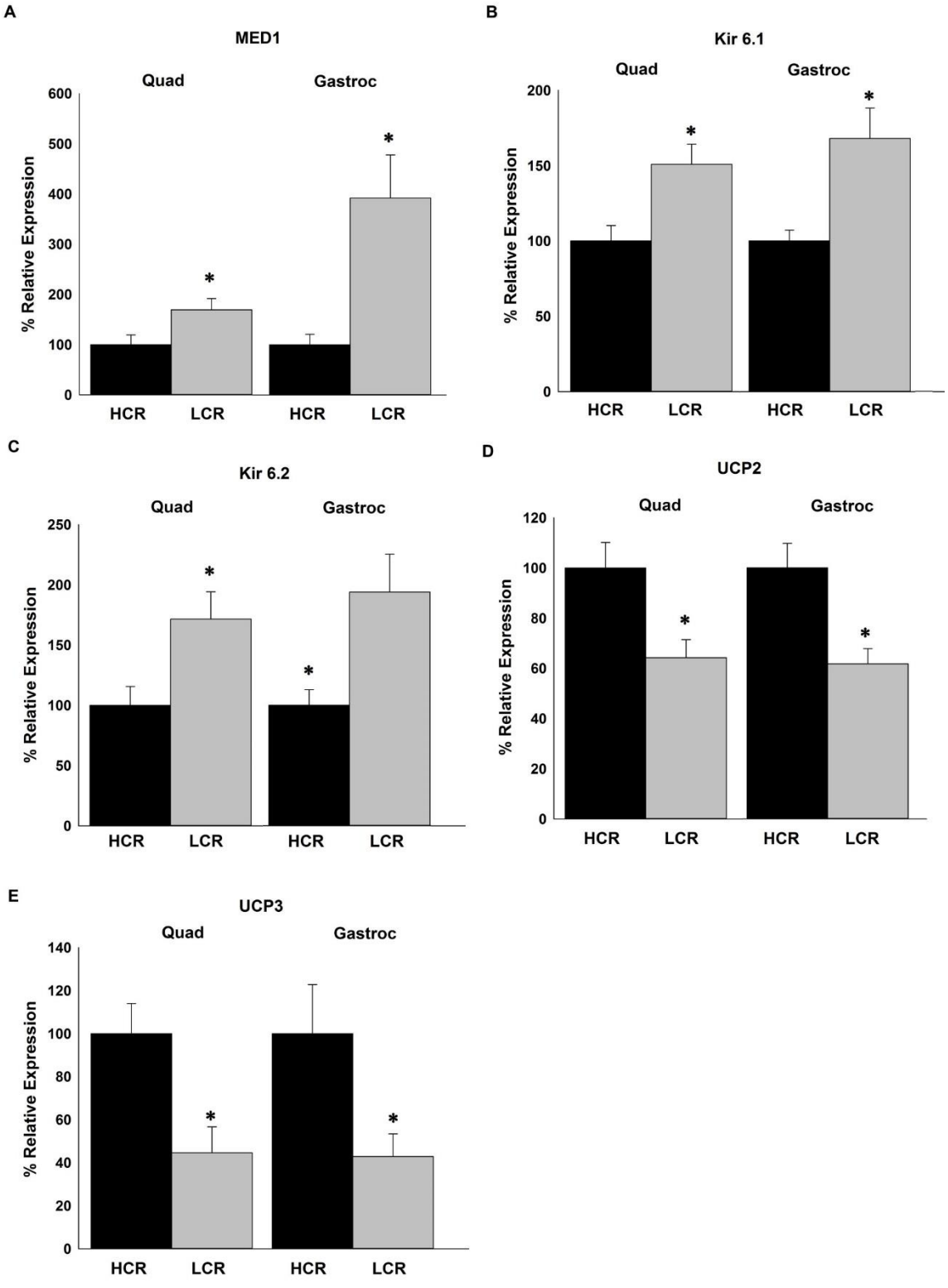
A
MED1
Quad
Gastroc
% Relative Expression
600
500
400
300
200
100
0
*
*
HCR
LCR
HCR
LCR
B
Kir 6.1
Quad
Gastroc
% Relative Expression
200
150
100
50
0
*
*
HCR
LCR
HCR
LCR
C
Kir 6.2
Quad
Gastroc
% Relative Expression
250
200
150
100
50
0
*
*
HCR
LCR
HCR
LCR
D
UCP2
Quad
Gastroc
% Relative Expression
120
100
80
60
40
20
0
*
*
HCR
LCR
HCR
LCR
E
UCP3
Quad
Gastroc
% Relative Expression
140
120
100
80
60
40
20
0
*
*
HCR
LCR
HCR
LCR

Figure 12: Lean high-capacity rats have higher mRNA expression of mediators of energy expenditure than energy conservation. Compared to low-capacity runners (LCR), high-capacity runners (HCR) have lower mRNA expression of molecular mediators of energy conservaiton in skeletal muscle [quadriceps (quad) and gastrocnemius (gastroc)], including (A) Mediator of RNA polymerase II transcription subunit 1(MED1), and subunits of the ATP-gated K^+ channels (K^+_{ATP}) Kir6.1 (B) and Kir6.2 (C); (D, E) Uncoupling protein 2 and 3 (UCP2, UCP3) mRNA expression was significantly higher in skeletal muscle of HCR compared to LCR. *$p<0.05$ (HCR>LCR for UCP2, UCP3; and HCR<LCR for Kir6.1, Kir6.2, and MED1). All data are means ± SEM. (N=8/group)

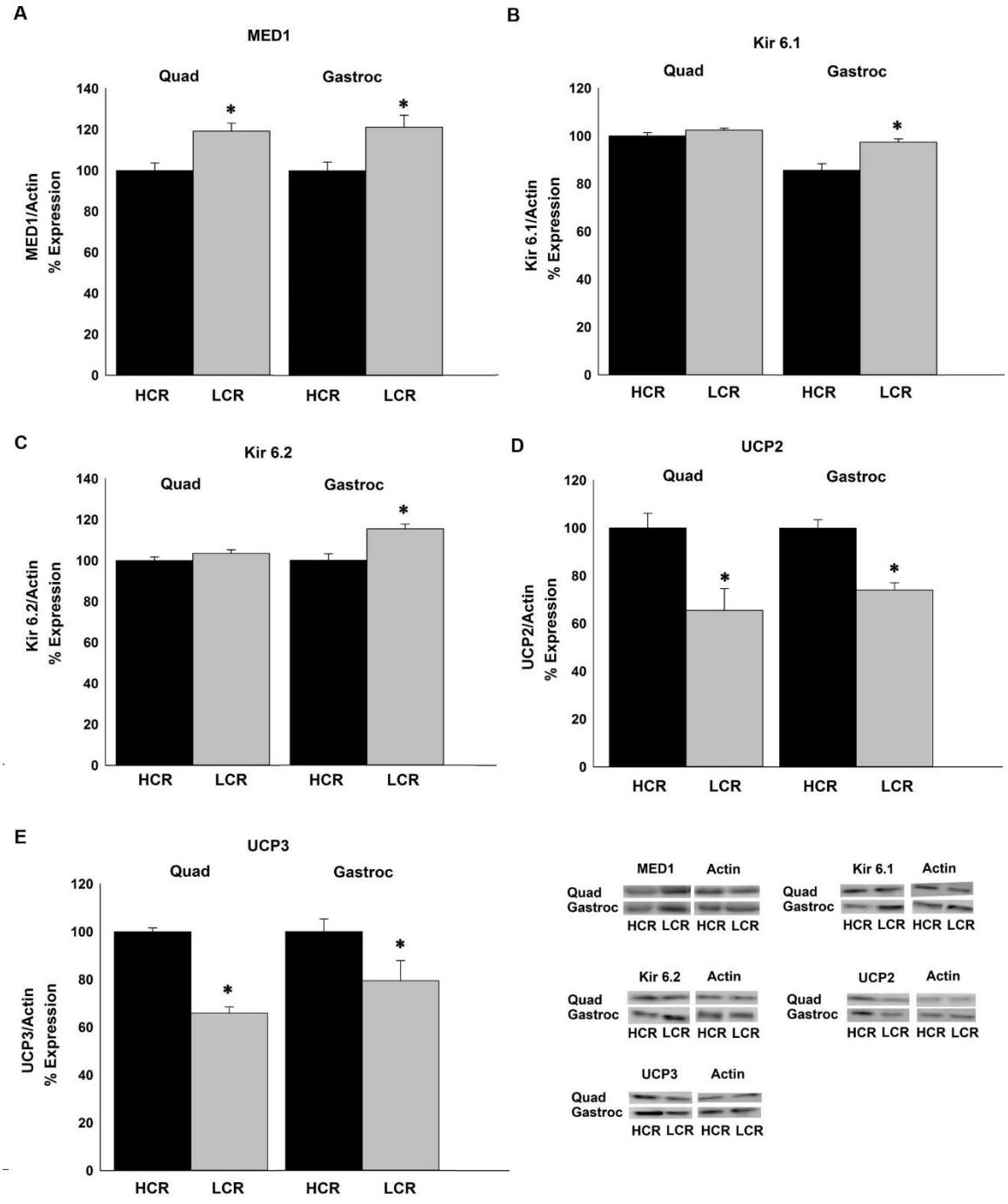
A
MED1
Quad
Gastroc
MED1/Actin
% Expression
HCR
LCR
B
Kir 6.1
Kir 6.1/Actin
% Expression
C
Kir 6.2
Kir 6.2/Actin
% Expression
D
UCP2
UCP2/Actin
% Expression
E
UCP3
UCP3/Actin
% Expression
MED1
Actin
Kir 6.1
Kir 6.2
UCP2
UCP3

Figure 13: Lean high-capacity rats have higher protein expression of mediators of energy expenditure than energy conservation. Compared to low-capacity runners (LCR), high-capacity runners (HCR) have lower protein expression of molecular mediators of energy conservaiton in skeletal muscle [quadriceps (quad) and gastrocnemius (gastroc)], including (A) Mediator of RNA polymerase II transcription subunit 1(MED1), and subunits of the ATP-gated K^+ channels (K^+_{ATP}) Kir6.1 (B) and Kir6.2 (C). Compared to HCR, Kir6.1 and Kir6.2 protein levels were higher in LCR gastroc, but not quad. (D, E) Uncoupling protein 2 and 3 (UCP2, UCP3) protein levels were significantly higher in skeletal muscle of HCR compared to LCR. *$p<0.05$ (HCR>LCR for UCP2, UCP3; and HCR<LCR for Kir6.1, Kir6.2, and MED1). All data are means ± SEM. (N=5/group)

Lean rats have elevated sympathetic drive to skeletal muscle.

As illustrated in Figure 14, compared to LCR, HCR had higher NETO in several skeletal muscle groups, including medial (D) and lateral gastroc (C), quad (A), and soleus (B), indicating higher sympathetic drive to skeletal muscle, potentially modulating their economy of activity. Higher NETO was also found in interscapular BAT in HCR compared to LCR (E).

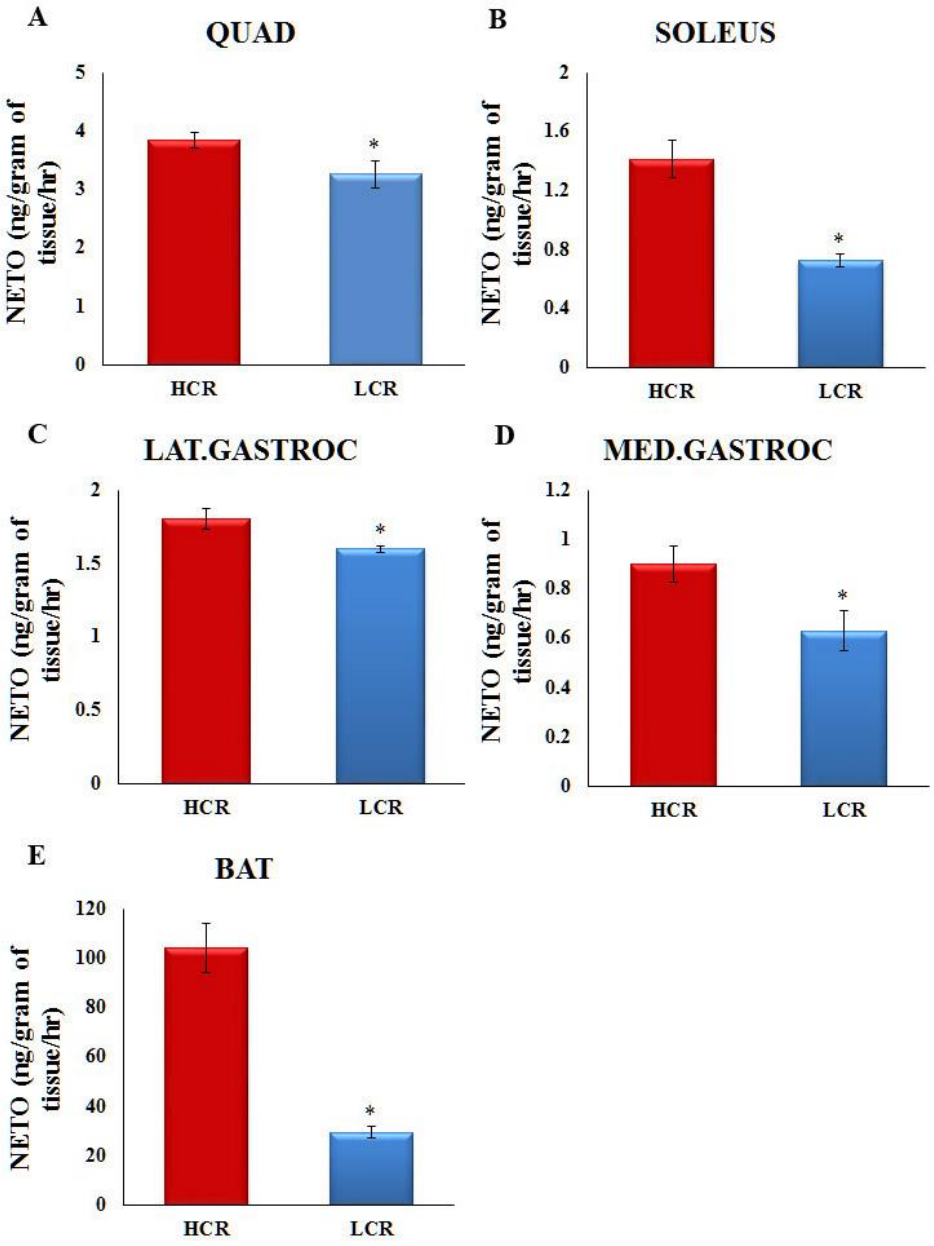

Figure 14: Lean rats have heightened sympathetic drive to peripheral metabolic tissues. Compared to low-capacity runners (LCR), high-capacity runners (HCR) have elevated sympathetic drive indicated by higher norepinephrine turnover (NETO) in skeletal muscle groups: (A) quadriceps (Quad), (B) soleus, (C) lateral gastrocnemius (lat.gastroc) (D) medial gastrocnemius (med.gastroc), and (E) brown adipose tissue (BAT). *$p<0.05$ (HCR>LCR). All data are means ± SEM. (N= 7 HCR, 6 LCR)

2.3 Discussion

It is known that lean people and lean animals have higher daily physical activity levels (Johannsen, Welk, Sharp, & Flakoll, 2008; Levine et al., 2005; Novak CM, 2009; Novak & Levine, 2007) and that this is a biologically regulated trait (Joosen et al., 2005; Levine & Kotz, 2005). It was not known, however, whether or not this physical activity energy expenditure, or NEAT, meaningfully contributes to total EE. Here, I use a rat model of a lean phenotype to demonstrate that lean rats show heightened total EE, and that this is primarily due to elevated non-resting EE. Taken together with previous studies (Novak CM, 2009; Novak et al., 2010), I have shown that the amplified NEAT characteristic of this lean phenotype is predominantly due to increased daily activity levels combined with increased fuel cost of that activity (Gavini et al., 2014). The increased calorie use may be secondary to heightened function of muscle UCPs, combined with decreased function of K^{+}_{ATP} and MED1, potentially driven by sympathetic outflow to skeletal muscle.

Relative to female LCR, female rats of the lean, high-capacity phenotype (HCR) did not show significantly elevated resting EE. Instead, the lean, high-capacity rats consistently displayed significantly heightened non-resting EE (Figures 7, 8, and 9). This persisted when the groups were matched for body weight or lean mass, or without matching (Figures 7, 8, and 9; Table 2). This was consistent with ANCOVA analyses, which demonstrated that non-resting EE was consistently higher in female HCR, even after body weight and lean mass were considered as covariates, without any detectable difference in resting EE (Figure 10). Overall, this gives little support for the hypothesis

that there is a meaningful deficiency in resting metabolic rate in the obese. Rather, my results support the assertion that non-resting EE, including physical activity EE, is consistently elevated in the lean phenotype associated with high aerobic capacity even after individual differences in body mass and composition are taken into account. This is in line with elevated activity EE observed in other models of leanness (Kotz, Teske, & Billington, 2008).

It is conceivable that economy of activity is differentially modulated in HCR than in LCR, potentially by sympathetic outflow, resulting in greater variance in activity EE in HCR. The difference in non-resting EE persists even when body weight and composition are nearly identical (Figures 7, 8, and 9), indicating that lower daily physical activity levels in LCR are not due to the any difficulty in locomotion incurred by greater body mass, but are inherent to the obesity-prone, low aerobic capacity phenotype. This reflects what many studies have established regarding leanness in humans, namely the link between high aerobic capacity, high physical activity and NEAT, and favorable metabolic health (Ekelund et al., 2005; Levine et al., 1999; Novak et al., 2010; Simmons et al., 2008).

NEAT (i.e., activity EE) is the component of total EE that consistency differs between lean and obesity-prone individuals, and this is elevated in obesity-resistant rats through higher levels of physical activity combined with decreased fuel economy of activity (Levine & Kotz, 2005; Novak et al., 2010) (Figures 7, 8, and 9; Table 2). Skeletal muscle is the major contributor to activity EE, and also significantly impacts resting EE

(Zurlo F, 1990). Therefore, the logical next step was to investigate cellular and molecular mechanisms that differentially regulate NEAT in skeletal muscle of these phenotypes. Specifically, what is the fate of the "extra" calories being burned during NEAT in HCR (Novak et al., 2010)? In an attempt to answer this question, I hypothesized that excess calories used during the less-economical NEAT in the lean, high-capacity phenotype are being dissipated as heat, analogous to the fuel inefficiency that occurs during BAT thermogenesis (Kozak, 2010; Rothwell & Stock, 1979). Hind-limb gastroc muscle temperature was significantly higher in HCR than LCR during physical activity of equivalent workload (treadmill speed and incline, similar body weight (Figure 11)). This supports the hypothesis that the "wasted" calories utilized for non-resting EE are being used by muscle, specifically for NEAT, and at least some of the energy is being dissipated as heat. This is consistent with the work of others demonstrating relatively inefficient coupling in HCR mitochondria specifically in HCR skeletal muscle (Lessard et al., 2009; Lessard et al., 2011; Naples et al., 2010; Stephenson, Stepto, Koch, Britton, & Hawley, 2012b; Tweedie et al., 2011). This is also consistent with reports that, relative to LCR, HCR have enhanced muscle glucose uptake, glucose and lipid oxidation, and higher muscle glycogen (Rivas et al., 2011). Obesity-related differences in walking or running economy in humans is a matter of some contention. Studies in both athletes and non-athletes, however, support the idea that those with higher VO_{2max} (i.e., aerobic capacity) have lower economy of activity (Lucia, Hoyos, Perez, Santalla, & Chicharro, 2002; Sawyer et al., 2010). This relative inefficiency may be a trade-off for enhanced aerobic capacity.

I predicted that the lean vs. obesity-prone phenotypes would exhibit differential expression of molecular mediators of energy consumption in myocytes. I examined K^+_{ATP} channels, which are important in determining the metabolic state of the cell by maintaining potential gradient for ATP synthesis (Alekseev et al., 2010; Nichols, 2006). Given that mice deficient in of K^+_{ATP} channels are lean and have lower fuel economy of activity (Alekseev et al., 2010), similar to HCR, I predicted that lean, high-NEAT HCR would show low expression of K^+_{ATP} channels in skeletal muscle compared to obesity-prone LCR. Consistent with the hypothesis, Kir6.2, the predominant subtype of the K^+_{ATP} channel in muscle (Aguilar-Bryan et al., 1998), showed dampened levels of expression in gastroc of HCR (Figures 12 and 13). In addition, a component of mediator cofactor complex, MED1, also showed lower levels of expression in the muscle of HCR than LCR, particularly in gastroc (Figures 12 and 13). This component of mediator cofactor complex is associated with several nuclear receptors involved in the transcription of genes involved in fatty acid oxidation (Kodera et al., 2000; Yuan, Ito, Fondell, Fu, & Roeder, 1998), and is hypothesized to mediate myocyte fuel conservation (W. Chen et al., 2010). Low levels of both MED1 and K^+_{ATP} channels are consistent with the compromised economy of activity and increased heat generation of HCR muscle, likely through altered control of fatty acid oxidation (Alekseev et al., 2010); assessments of channel function are needed to directly test this hypothesis, however.

Similar to BAT, skeletal myocytes express uncoupling proteins (UCP2 and 3). UCPs play an important role in uncoupling ATP generation and in proton leak across mitochondrial membranes, opposing the function of K^+_{ATP} channels in the cell. Here, I

find that lean rats have consistently heightened expression of both UCP2 and UCP3 in skeletal muscle (both quad and gastroc) compared to the obesity-prone LCR (Figures 12 and 13), consistent with what has been reported by others in rats (Lessard et al., 2009; Lessard et al., 2011; Stephenson et al., 2012b). There is no consensus on the role of UCPs, especially UCP 3, in skeletal muscle, though they are hypothesized to facilitate fatty acid translocation or mitigation of ROS (Harper et al., 2001; Samec, Seydoux, & Dulloo, 1998). It is unknown whether the uncoupling affects efficiency or thermogenesis. Altogether, the data support a theoretical model in which the myocytes of the lean phenotype have increased use of metabolic fuels, particularly fatty acids, through heightened UCP function along with reduced ability to conserve fuel through MED1 and K^{+}_{ATP} channels.

My findings using a contrasting genetic model system support a role for differential activity-related skeletal muscle thermogenesis in maintaining leanness, and identify potential molecular mechanisms underlying this; the data also identify a potential source of these differences. It is possible that the central nervous system modulates muscle fuel efficiency through the SNS in a fashion analogous to what has been documented in other systems such as BAT (Cannon & Nedergaard, 2004). As illustrated in Figure, compared to LCR, HCR were found to have significantly higher skeletal muscle NETO, an indicator of SNS drive (Bartness, Vaughan, & Song, 2010). It is possible that muscle fuel uptake and utilization is modulated through the SNS, controlled by central nervous system effectors (Nogueiras et al., 2007; Shiuchi et al., 2009), possibly including brain orexigenic and anorexigenic peptides that are known to act in the

paraventricular nucleus to affect muscle uncoupling protein levels (Kotz, Wang, Levine, & Billington, 2002; Kotz, Wang, Briggs, Levine, & Billington, 2000; C. Wang, Billington, Levine, & Kotz, 2000). Brain melanocortins have been found to impact muscle lipid mobilization and glucose uptake (Nogueiras et al., 2007; Tanaka et al., 2007; Toda et al., 2009) and the lean and obesity-prone rats show differences in central melanocortins (Shukla, Britton, Koch, & Novak, 2012), a system recognized to modulate SNS drive (Sohn et al., 2013). Taken together with previous evidence, these data are consistent with a model in which brain systems (e.g., melanocortins) modulate SNS outflow and myocyte beta adrenoreceptors to increase myocyte glucose and fatty acid uptake and utilization, amplifying energy expenditure of activity (i.e., NEAT) (Miyaki et al., 2011; Shiuchi et al., 2009; Tanaka et al., 2007; Toda et al., 2009) which will be discussed in the next chapters. Similar to skeletal muscle, I also found that NETO was higher in brown adipose tissue of HCR compared to LCR. Effects of BAT thermogenesis on EE would not be expected to preferentially affect non-resting EE, however. The data described here support a theoretical model where the modulation of metabolic fuel use of skeletal myocytes, potentially through enhanced SNS drive, results in increased or decreased fuel efficiency during locomotion. This hypothesis will be tested further in the subsequent studies.

CHAPTER 3

The preponderance of data supports the assertion that the hypothalamus, particularly the ventromedial hypothalamus (VMH), plays an important role in modulating energy homeostasis, thermoregulation, food intake, peripheral metabolic fuel allocation, RER, and high-fat diet-induced thermogenesis via the modulation of SNS. As explained above, the MC system is a well-studied system that impacts the control of feeding, body weight, and thermogenesis. Melanocortins are also associated with increased EE and physical activity. Decreased expression and loss-of-function mutations in MCR are associated with increased calorie intake, decreased EE, and severe early-onset obesity in humans and rodents. Skeletal muscle, a major fuel-burning tissue, is often neglected as a target for obesity treatments. Based on these studies on the VMH and central MC, I propose the existence of an axis between VMH and skeletal muscle, modeled on the hypothalamic control of BAT via the SNS.

To test this hypothetical model, I examined the ability of VMH MC receptor activation to increase activity-related thermogenesis and EE, as well as SNS drive to muscle. I also measured the expression of molecular mediators of EE in other peripheral metabolically active tissues like BAT, liver, and white adipose tissue (WAT) along with skeletal muscle. BAT remains the primary target for studies on enhancing EE through central regulatory mechanisms such as activation of MC receptors. Heightened mRNA

and protein expression of EE mediators in BAT explains the majority of MC receptor-induced increase in EE via SNS. Liver and WAT are important for providing fuel to other tissues, both during activity and resting, and receive a significant autonomic relay. Integrating the changes in these metabolically active tissues after intra-VMH MC receptor activation will help determine the scope of the influence of central MC on peripheral metabolism and in generation of lean and obese phenotypes.

3.1 Methods

3.1.1 Study 1: Examine the effects of VMH MC receptor activation on activity-related EE. I predicted that activation of VMH neurons with a MCR agonist will alter skeletal muscle energetics and thus activity-related EE. I also predicted that activation of MCR in the VMH will increase EE, and decrease RER, switching fuel use to fats. I will focus primarily on changes in EE as well as changes in heat dissipation at the level of skeletal muscle, after activation of VMH MC receptors.

Design

Preliminary study: A dose-response study was conducted using Sprague-Dawley rats to determine optimal concentration of MTII (10, 20, 50, and 100pmoles) required to induce VMH MC receptor activation-induced changes in temperature and calorimetric parameters.

3.1.1.1 Study 1a: Measure changes in EE and other calorimetric parameters (RER) upon VMH MC receptor activation with MTII in freely moving and activity-controlled rats. (N=12)

Day -10 – 0: Arrival of animals, separation, and housing.

Day 1 – 4: Stereotaxic surgeries to implant guide cannula aimed at VMH.

Day 5 – 11: Recovery.

Day 11: Divided into groups (MTII or vehicle), total 3 cohorts (4/cohort, two from each group), making sure each of them goes into both treatments at some point.

Day 12: Acclimation of animals to calorimetry chamber and test cages.

Day 13: 0900 – 1300 - Measured EE and other calorimetric parameters using Oxymax FAST system (Columbus Instruments, Columbus, Ohio) of cohort 1 for 4 hrs post-injection with MTII (20pmoles/200nl) or vehicle. (based on preliminary study).

Day 13: 1400 – 1800 – Repeated for cohort 2.

Day 14: 0900 – 1300 – Repeated for cohort 3. Removed the animals from calorimetry chamber and return to the animal facility.

Day 17 - 19: Repeated day 12-14 by changing the treatment.

Day 22: Acclimated cohorts 1, 2, and 3 in calorimetry chamber for treadmill run (controlled activity). Trained rats to run on a treadmill.

Day 23: Each cohort was subdivided into MTII- or vehicle-treatment groups. Rats were injected with MTII (20pmoles/200nl) or aCSF and allowed to run on a treadmill 105 - 120 minutes after injection for 30 minutes and changes in EE and other calorimetric parameters were measured.

Day 24: Repeated the same with remaining rats. Removed the rats from the chamber after completion of run.

Day 27 – 29: Repeated day 22 – 24 by changing treatment (no treadmill training necessary).

3.1.1.2 Study 1b: Measure skeletal muscle heat dissipation after VMH MC receptor activation with MTII in these rats during light phase in their regular cages and during a graded treadmill test. (N=8)

Day -10 – 0: Arrival of animals, separation, and housing.

Day 1 – 4: Stereotaxic surgeries to implant guide cannula aimed at VMH and transponder implants adjacent to gastroc in both hind limbs and adjacent to BAT.

Day 5 – 11: Recovery.

Day 12: Divided into MTII- and vehicle-treatment groups. Injection of MTII (20pmoles/200nl) or vehicle (aCSF) and measured heat dissipation at the level of skeletal muscle and BAT every 15 minutes for 4 hrs post-injection.

Day 17: Repeated day 12 by changing treatment (day 12 MTII group gets vehicle on day 17).

Day 21: Trained rats to walk on treadmill.

Day 22: Rats were divided into two groups (MTII- or vehicle-treatment groups). Rats were injected with MTII (20pmoles/200nl) or aCSF; 105 – 120 minutes post-injection, rats were allowed to walk on a treadmill at varying intensities for 30-40 minutes. Gastroc temperatures were measured at regular intervals.

Day 23: Repeated the same with remaining rats.

Day 27-28: Repeated the process by changing the treatment.

3.1.2 Study 2: Examine the effects of VMH MC receptor activation on the SNS and how this pathway alters skeletal muscle energetics. I predicted that activation of MC receptors in the VMH will increase sympathetic drive to peripheral tissues. I also predicted that this higher sympathetic drive will increase fuel utilization and molecular mediators of EE.

Design

3.1.2.1 Study 2a: Measure the level of sympathetic drive to peripheral tissues after VMH MC receptor activation with MTII.

Day -7 – 0: Arrival of animals, separation, housing and acclimate. (n=24)

Day 1 – 4: Stereotaxic surgeries to implant guide cannula aimed at VMH

Day 5 – 11: Recovery

Day 11: Divided into groups depending on treatment.

Day 12: Day of study

t hrs: Euthanized zero time point group (to obtain baseline tissue NE content) (n=8) and injected remaining with aMPT (125 mg aMPT/kg BW). (n=16, 8/group)

t+0.5hrs: Injected with either MTII (20pmoles/200nl) or aCSF (200nl) depending on the group (n=8/group).

t+2hrs: Injected all remaining animals with second dose of aMPT (125 mg aMPT/kg BW). (n=16, 8/group)

t+4hrs: Euthanized the rats and harvest tissue.

3.1.2.2 Study 2b: Measure the expression of molecular mediators of EE in peripheral tissues after VMH MC receptor activation with MTII.

Day -7 – 0: Arrival of animals, separation, housing and acclimate. (n=18)

Day 1 – 4: Stereotaxic surgeries to implant guide cannula aimed at VMH

Day 5 – 11: Recovery

Day 11: Divided into groups depending on treatment.

Day 12: Day of study

t hrs: Injected with either MTII (20pmoles/200nl) or aCSF (200nl) depending on the group (n=9/group).

t+4hrs: Euthanized the rats and harvest tissue.

Animals

Male Sprague-Dawley (SD) rats (N=62; 8 weeks, ~ 250g) were obtained from Harlan labs. Each rat was housed individually on a 12:12 light:dark cycle with lights on at 0700 EST. Rats received rodent chow (5P00 MRH 3000, T.R. Last Co. Inc.) and water *ad libitum*. All studies were conducted according to the Guide for the Care and Use of Laboratory Animals ("National Research Council (US) Committee for the Update of the Guide for the Care and Use of Laboratory Animals," 2011) and approval of the Kent State University IACUC.

Stereotaxic surgeries

After the rats were acclimated to the housing conditions, stereotaxic surgeries were performed to chronically implant guide cannulae (PlasticsOne) aimed at VMH. The rats were anesthetized using isoflurane and mounted on a stereotaxic apparatus. The following coordinates obtained from "*The rat brain in stereotaxic coordinates"* (Watson), were used for VMH: anterior-posterior, -2.5mm; medial-lateral, +0.5mm; dorsal-ventral, -6mm (from dura); and an injection needle with 3mm projection (final dorsal-ventral, -9mm (from dura)). The guide cannulae were attached to the skull using a sterile wound clip and dental cement. The rats were then allowed to recover with periodic monitoring before the start of the study.

Site checks

After the completion of all data collection, placement of the cannula was determined at the end of the study by histologically examining its anatomical placement. The brains were removed and fixed in 10% phosphate buffered formalin and then placed in 10% phosphate buffered formalin with 30% sucrose. Brains were sectioned at 50 μm using a cryostat and mounted onto slides (Fisher Superfrost Plus); slides were dehydrated, stained using cresyl violet, and the injection sites were determined using a microscope. Only rats whose guide cannulae were within 250μm of the VMH were used for data analysis.

Transponder implantation

A group of male Sprague-Dawley rats (n=10, a subset of actual group mentioned above) received transponder implants during the stereotaxic surgery. A short incision was made on both hind legs and near the interscapular region. Sterile temperature transponders IPTT-300 (Bio Medic Data Systems, Inc.) were implanted on interscapular BAT and also adjacent to the gastrocnemius (gastroc) muscle group of both hind limbs to measure the heat generated by skeletal muscle during activity. Care was taken to place the transponders so as not to disrupt locomotor function. Rats were allowed to recover for a week before the graded treadmill test was performed. Implant placement was examined during tissue harvest and data from inaccurately placed transponders were omitted from final analyses.

Body composition

Body composition was measured using EchoMRI-700 (Echo Medical Systems, Houston, TX) to determine the fat and lean mass (in grams) of each rat the day before test. This did not interfere with temperature transponder function.

Measurement of energy expenditure

After body composition determination, adult male Sprague-Dawley rats were measured for their EE and physical activity using small animal indirect calorimetry (4-chamber Oxymax FAST system, Columbus Instruments, Columbus, OH) with 24-48hrs of acclimation in their testing cage at thermoneutral conditions to avoid any novelty-induced alterations in calorimetric parameters, as previously reported (Gavini et.al,

2014). On the day of calorimetry, rats were weighed and injected either with a nonspecific MC receptor agonist MTII (Phoenix Pharmaceuticals, Mountain View, CA) (20pmoles/200nl) or vehicle (aCSF, 200nl) over a period of 30 seconds and holding in place for another 30 seconds to avoid back-flush, and then placed in the chamber with food and water; the chamber was then sealed. The calorimeter was calibrated using primary gas standards. Air was pumped into the chamber at 1.9-3.1 lpm, depending on the weight of the rat, and chamber air was sampled at 0.4 lpm. Measurement of gas exchange took place every 30 sec throughout the 4-hr period except for a 3.5-min room-air reference and settle period after each 60-sample interval. Physical activity data were collected using infrared beam-break counts, collected every 10 sec uninterrupted throughout the 4-hr period, in the X and Z axes; the first 15min of data were not included in the analysis. EE data (VO_2, VCO_2, RER, kcal/hr) were averaged, and physical activity data were expressed as mean beam breaks per minute. Four days after the first injection, the same was repeated with rats now receiving the other treatment (day1 MTII rats receiving vehicle on day5 and *vice versa*). This way each rat acted as its own control thereby nullifying the effects of body composition and other individual differences on calorimetric parameters (Schoeller & Jefford, 2002; Tschop et al., 2012).

As previously described (Gavini et al., 2014; Novak et al., 2010), physical activity EE were assessed by measuring gas exchange once every 10 sec during a treadmill activity test. At least one day after a 15-min treadmill acclimation period, rats were placed in the treadmill after weighing them and injecting with either MTII (20pmoles/200nl) or vehicle (aCSF) and allowed to acclimate without food for 2hrs.

After the 2-hr resting period, the treadmill was started at 7 m/min for 30 min, during which time physical activity EE data were collected. The same was repeated after 4 days with rats now receiving the counterbalanced injection. Because all rats received both injections, we compared EE between MTII and vehicle treatments using a 2-tailed paired *t*-test. A paired 2-tailed *t*-test was also used to compare treadmill gas exchange values between the treatments.

Home cage muscle temperature

To determine whether activation of MC receptors in VMH has any effect on the thermogenics of skeletal muscle, I measured skeletal muscle heat dissipation for 4hrs after intra-VMH MTII or vehicle microinjection. The activation of BAT thermogenesis was measured as a control process during this study. Rats were weighed and the injected either with MTII or vehicle, placed in their home cage and temperature data from the transponder implants on the gastroc and BAT were collected every 15min over a period of 4hrs and analyzed the data using a repeated-measures ANOVA. All rats received both injections.

Graded treadmill test

To determine skeletal muscle heat dissipation during controlled physical activity after MC receptor activation in VMH, I measured the temperatures of the gastroc muscle group using a graded treadmill test. The rats were acclimated to the treadmill for 10 minutes in the days prior to the test as well as immediately before the test. The rats received microinjection of either MTII or vehicle 1.5 hrs prior to the test, with the test

repeated after 4 days in order for each rat to receive each treatment. Gastroc temperatures in each leg were recorded at baseline (before injecting and right before start of the test) and at set intervals during a 5-level graded treadmill test as reported previously in chapter 2 (Gavini et al., 2014). The test was stopped at after 35 minutes and the data were analyzed using a 2-tailed paired *t*-test, with the time-course of temperature changes analyzed using a repeated-measures ANOVA.

Gene expression

Skeletal muscle (gastroc and quad), liver, WAT and BAT were collected from adult male Sprague-Dawley rats (N = 18, a different subset of above mentioned number) 4hrs after intra-VMH microinjection of either MTII or vehicle (N = 9/group) after euthanasia by rapid decapitation without anesthetic agents. Tissue samples were homogenized and total mRNA was extracted using an Ambion ribopure kit following manufacturer's instructions. The purity of mRNA was measured using NANODROP (ND-1000) (Nanodrop technologies) and A260/280 ratio to be ranging from 1.8 – 2.1.This mRNA was used to prepare cDNA using an Applied Biosystems kit and thermal cycling at 25^0C for 10 minutes, 48^0C for 30 minutes, 95^0 C for 5 minutes and holding at 4^0C. The cDNA was used for quantifying the expression of UCP1, UCP2, UCP, Kir6.1, Kir6.2, MED1, PPARα, PPARδ, PPARγ, PGC-1α, SERCA1, SERCA2, β_2-AR, β_3-AR, and GAPDH (used as a control). The relative expression was calculated using comparative Ct method (ΔCt). Data are expressed as a percent expression using the vehicle treated as the reference value (defined as 100%), and groups were compared using a 2-tialed t-test.

Western blotting

Tissues samples from adult Sprague-Dawley rats (same group of rats used for gene expression, N =18, 9/group), were homogenized with ice-cold RIPA buffer (Thermo Scientific) containing a protease inhibitor cocktail (Roche Diagnostics). The supernatant from the homogenization and subsequent centrifugation was used for the analysis. Equal quantities of supernatant and sample buffer (150mM tris-HCl pH 6.8, Trizma-base for pH, 6% SDS, 30% glycerol, 0.03% pyronin-Y, DTT) were mixed and tubes were heated at 90^0C for 3 minutes. Samples containing equal quantity of protein were loaded on to a gradient gel (4-15%) (Bio Rad) and electrophoresed using SDS running buffer (0.384M glycine, 0.05M Trizma bas, 0.1% SDS) at constant voltage (150V) for 30 minutes. The gel was blotted on to a PVDF membrane using semi-wet blotting apparatus and Otter et al. (1987) transfer buffer (49.6mM Trizma base, 384mM glycine, 17.5% methanol, 0.01% SDS) at constant current (400mAmp). The blot was incubated overnight in a blocking solution of 5% milk (Blotto) in 1xPBST (Phosphate buffered saline; 84mM sodium hydrogen phosphate, 16mM sodium dihydrogen phosphate, 100mM sodium chloride, tween20), then rinsed using 1xPBST. Primary antibodies were diluted in blocking solution at ratio recommended by manufacturer and incubated with the blot overnight. Secondary antibodies were diluted in blocking solution in the ratio 1:5000 and incubated for 1 hour at room temperature. After washing, the blots were developed using a chemiluminiscence detector using an Amersham kit (GE Healthcare, UK). The expression levels relative to actin were plotted as a percent of the reference value (with vehicle treatment as 100%), and groups were compared using 2-tailed t-tests.

Norepinephrine turnover (NETO)

Adult male Sprague-Dawley rats (N= 24, 8/group, a subset of above mentioned number) were used to assess sympathetic drive to peripheral tissues – liver, heart, BAT, skeletal muscle (including quad, lateral and medial gastroc, extensor digitorum longus (EDL) and soleus) and different WAT depots (mesenteric WAT (MWAT), gluteal WAT (GWAT), retroperitoneal WAT (RWAT), inguinal WAT (IWAT) and epididymal WAT (EWAT)) . Rats were individually housed on a 12:12 light:dark cycle with *ad libitum* access to standard rodent chow (5P00 MRH 3000, T.R. Last Co. Inc.) and water, and acclimated to daily handling for a week after stereotaxic surgery. Level of sympathetic drive to peripheral tissues was determined through the norepinephrine (NE) turnover (NETO) method using α-methyl-*p*-tyrosine (aMPT) as previously reported (Gavini et al., 2014; Shi et al., 2004). The rats were divided into 3 groups (aMPT/MT-II, aMPT/vehicle, control). On the day of study, rats receiving aMPT were injected with aMPT (125 mg aMPT/kg of body weight, 25 mg/ml) and with a second dose at same concentration 2 hours later. 30 minutes after first aMPT injection, rats received intra-VMH microinjection of either MTII (20pmoles/200nl) or vehicle (aCSF) depending on their group. All rats were euthanized by rapid decapitation between 1200 and 1500, 4 hours after first aMPT injection. Tissues were rapidly dissected and snap-frozen in liquid nitrogen.

Briefly, tissue was thawed and homogenized in a solution containing dihydroxybenzylamine (DHBA, internal standard) in 0.2M perchloric acid (PCA) with 1 mg/ml ascorbic acid (AA). Following centrifugation for 15 min at 7,500 *g* at 4°C,

catecholamines were extracted from the homogenate with alumina and were eluted into the PCA/AA. The catecholamines were assayed using an HPLC system with electrochemical detection (Coulochem III), MDTM mobile phase and reverse phase MD 150x3.2 column. NETO in peripheral tissues was calculated using the following formula (Gavini et al., 2014; Shi et al., 2004):

$k = (\lg[NE]0 - \lg[NE]4)/(0.434 \times 4)$

$K = k[NE]0$

k is the constant rate of NE efflux (also known as fractional turnover rate),

[NE]0 is the initial NE concentration or from 0-hr group (control),

[NE]4 is the final NE concentration or from 4-hr group (aMPT), and

K = NETO.

Difference in NETO of intra-VMH MTII-microinjected and vehicle-microinjected rat tissues were calculated with respect to control-group rats and compared using 1-tailed paired t-test for each tissue.

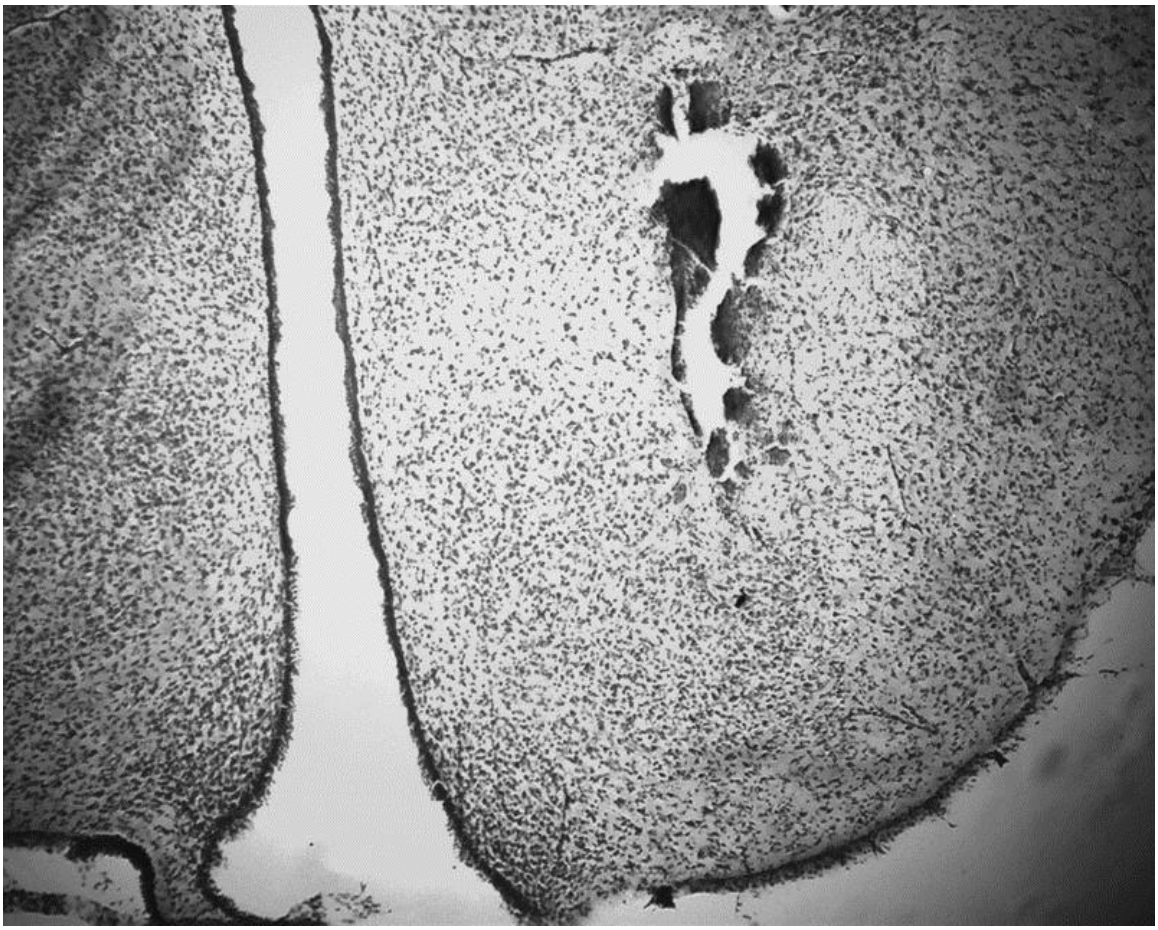

Figure 15: Cresyl violet stained brain section showing site specific injection into the ventromedial hypothalamus (VMH).

3.2 Results

Intra-VMH MTII induced a dose-dependent rise in energy expenditure and skeletal muscle and BAT heat dissipation (preliminary study)

A dose-response study using SD rats (N=8) to examine skeletal muscle heat dissipation after intra-VMH microinjections of the MCR agonist MTII showed a direct proportionality between dose and response. All rats received intra-VMH microinjections of MTII at increasing doses (10, 20, 50, 100pmoles/200nl) and vehicle (aCSF, 200nl) in random order. Based on my analysis, using only the rats that had cannulae successfully aimed at the VMH, the data showed a significant MTII-induced increase in muscle and BAT heat dissipation, compared to vehicle injection (Figures 16 and 17). The change in temperature was directly proportional to the dose of MTII used where higher doses induced a greater change in heat dissipation. Compared to vehicle-treated rats, temperatures of BAT of MTII-treated rats increased significantly between 30 - 105 minutes, and that of muscle starting around 120 minutes after MTII treatment to the end of study at 240 minutes. The temperatures of both BAT and skeletal muscle showed a clear dose-dependent pattern where higher doses (50 and 100pmoles) induced supraphysiological responses.

Next, I examined the changes in EE and physical activity upon activating MC receptors in the VMH. EE and physical activity were measured using an Oxymax FAST system in a calorimetry chamber for 4 hours post-injection. Compared to vehicle microinjection, both doses of intra-VMH MTII (20 and 50pmoles) induced a significant increase in EE, oxygen uptake (VO_2), and physical activity, and a significant decrease in

RER ($p<0.05$) (Figure 18), suggesting a shift in fuel preference to fat. At 50pmoles, the MTII-induced increases in EE, VO_2, and physical activity and decrease in RER were significantly higher than the 20pmoles dose of MTII.

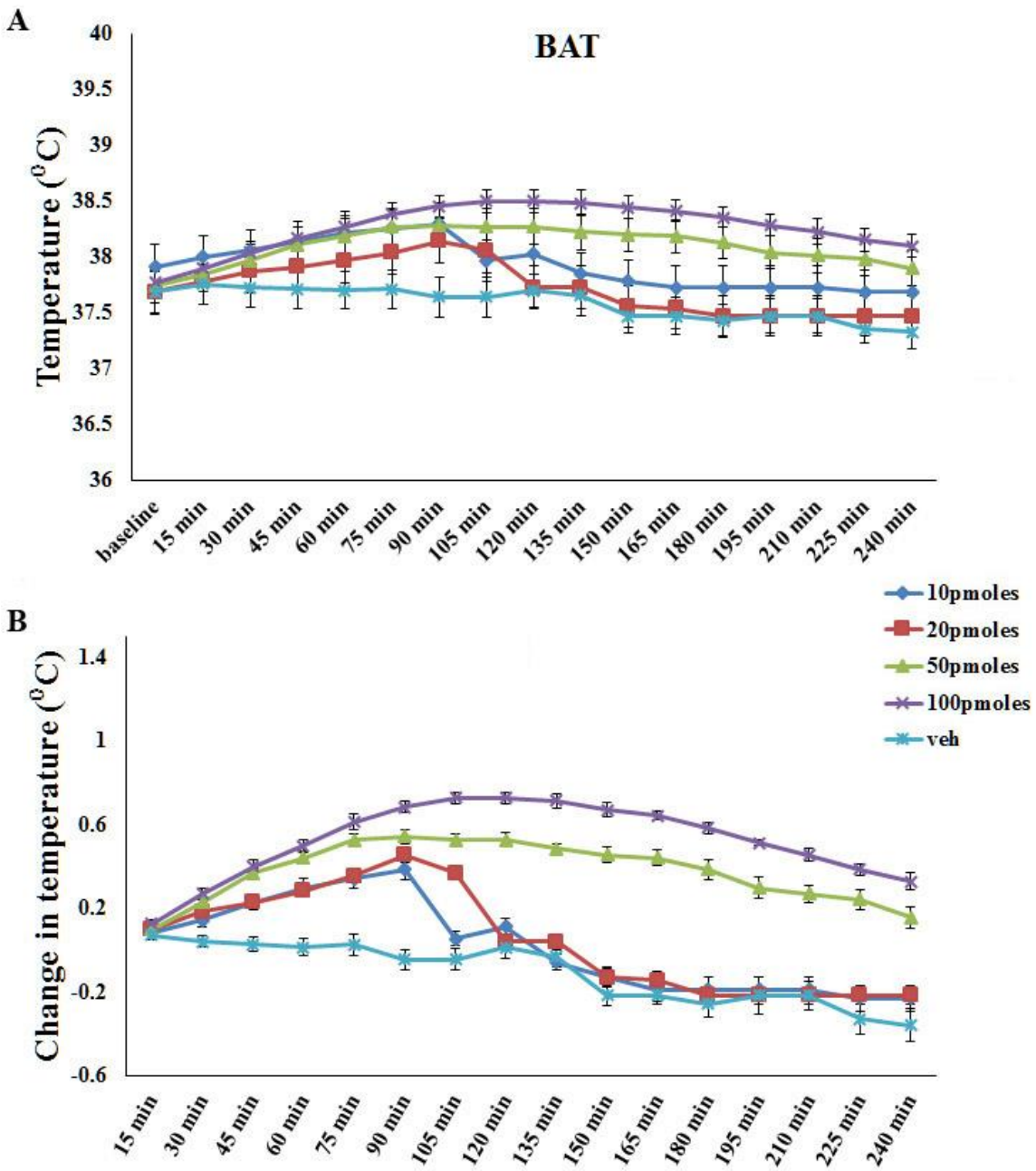
A
BAT
Temperature (°C)
40
39.5
39
38.5
38
37.5
37
36.5
36
baseline
15 min
30 min
45 min
60 min
75 min
90 min
105 min
120 min
135 min
150 min
165 min
180 min
195 min
210 min
225 min
240 min
B
Change in temperature (°C)
1.4
1
0.6
0.2
-0.2
-0.6
10pmoles
20pmoles
50pmoles
100pmoles
veh

Figure 16: Intra-VMH MTII induced a dose-dependent rise in brown adipose tissue thermogenesis. Brown adipose tissue (BAT) temperatures after intra-VMH microinjection of the mixed melanocortin receptor agonist MTII at increasing doses (10, 20, 50, 100pmoles, aCSF (vehicle)). Compared to vehicle administration, MTII injection induced a significant increase in the temperature of BAT. (A) BAT temperature, (B) change in BAT temperature from baseline after intra-VMH MTII microinjection. All values are means ± SEM for that particular time.

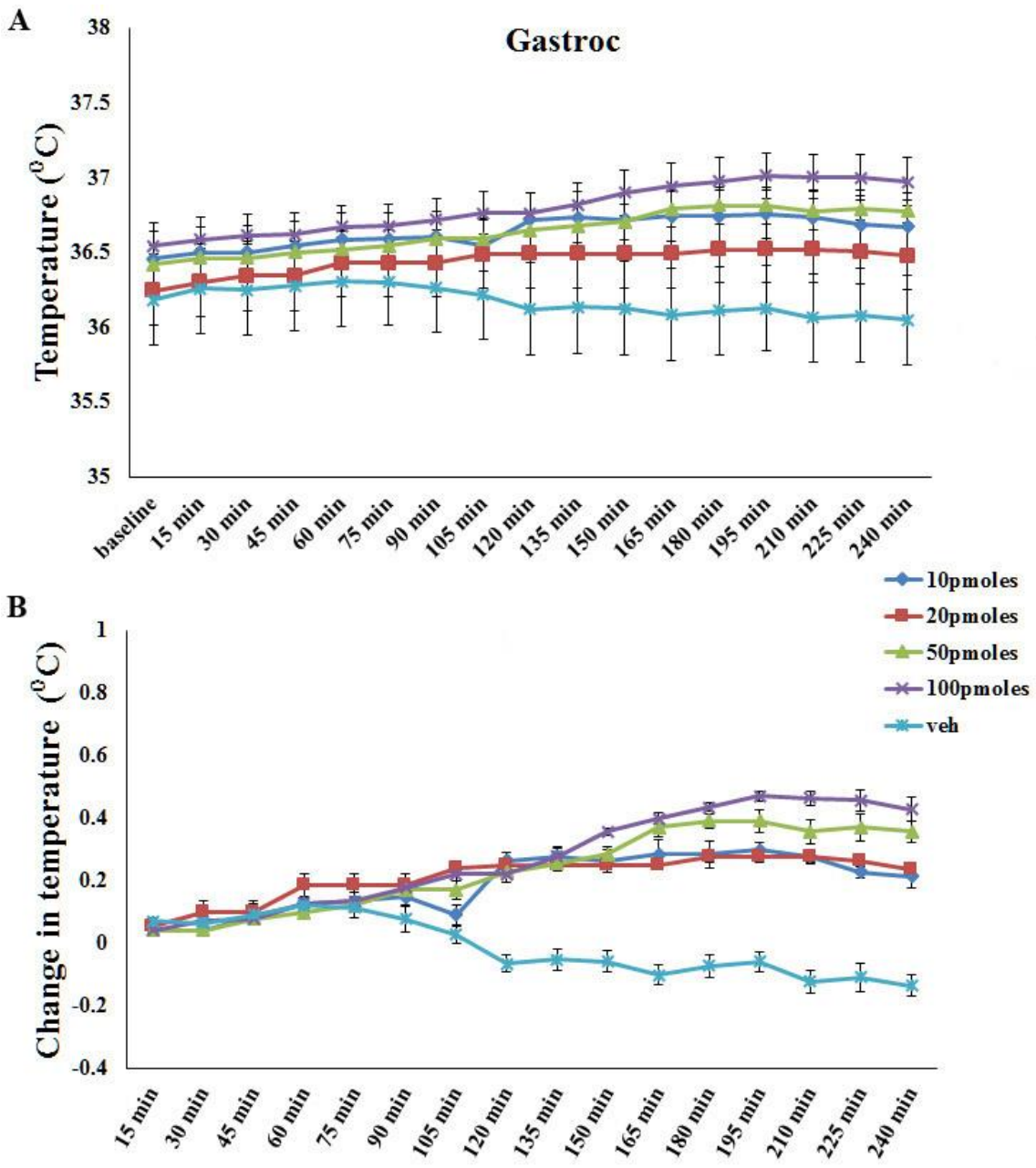
A
Gastroc
Temperature (°C)
38
37.5
37
36.5
36
35.5
35
baseline
15 min
30 min
45 min
60 min
75 min
90 min
105 min
120 min
135 min
150 min
165 min
180 min
195 min
210 min
225 min
240 min
B
Change in temperature (°C)
1
0.8
0.6
0.4
0.2
0
-0.2
-0.4
10pmoles
20pmoles
50pmoles
100pmoles
veh

Figure 17: Intra-VMH MTII induced a dose-dependent rise in skeletal muscle heat dissipation. Gastrocnemius (gastroc) temperatures after intra-VMH microinjection of the mixed melanocortin receptor agonist MTII at increasing doses (10, 20, 50, 100pmoles, aCSF (vehicle)). Compared to vehicle administration, MTII injection induced a significant increase in gastroc temperature. (A) Gastroc muscle temperature, (B) change in gastroc temperature from baseline after intra-VMH MTII microinjection. All values are means ± SEM for that particular time.

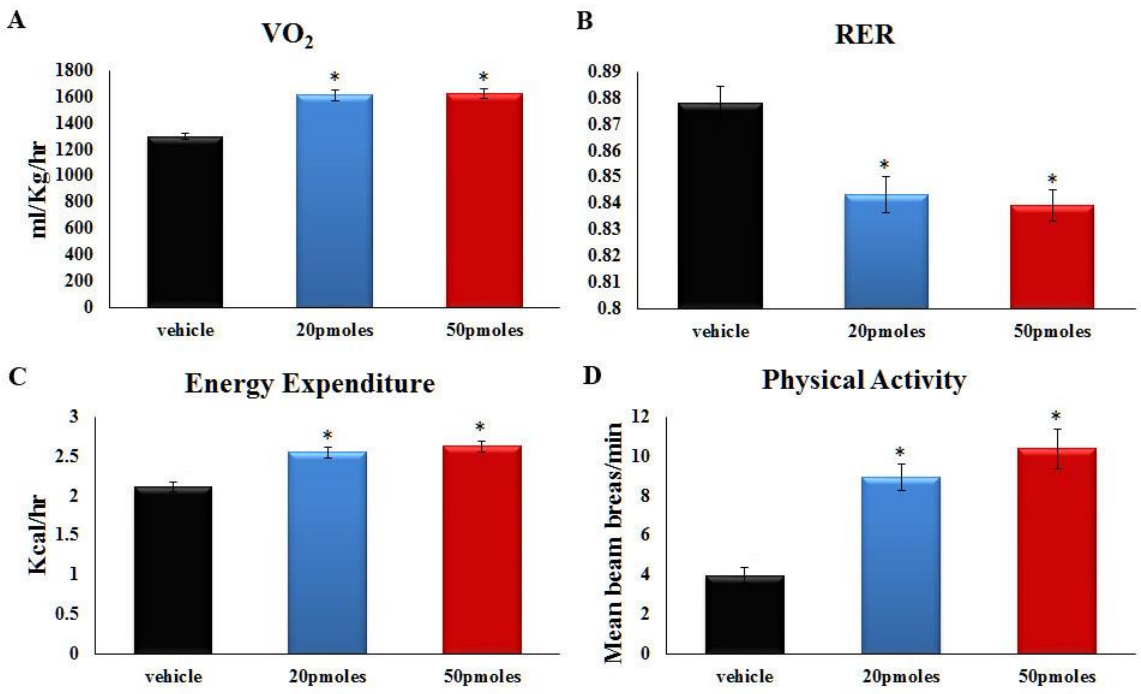

Figure 18: Calorimetric parameters after intra-VMH MTII microinjections. Rats with intra-VMH MTII microinjection (both 20 and 50pmoles) showed a significant increase in oxygen uptake (VO_2) (A), physical activity (D), and energy expenditure (C), with a significant decrease in RER (B). *significantly different from vehicle, $p<0.05$. All data are means ± SEM.

Rats with intra-VMH MTII microinjection have higher energy expenditure (Study 1a).

As shown in Figure 19, compared to vehicle microinjection, rats administered intra-VMH MTII have significantly higher EE, higher oxygen consumption (VO_2) and lower RER. All rats received microinjections of both vehicle and MTII thereby acting as their own controls during the study and eliminating the effects of body composition on calorimetric parameters (Schoeller & Jefford, 2002; Tschop et al., 2012). There was no significant difference in body weight, lean mass, or fat mass between the two sets of injections. Compared to vehicle, MTII-injection significantly increased rats' physical activity, both horizontal and ambulatory activity.

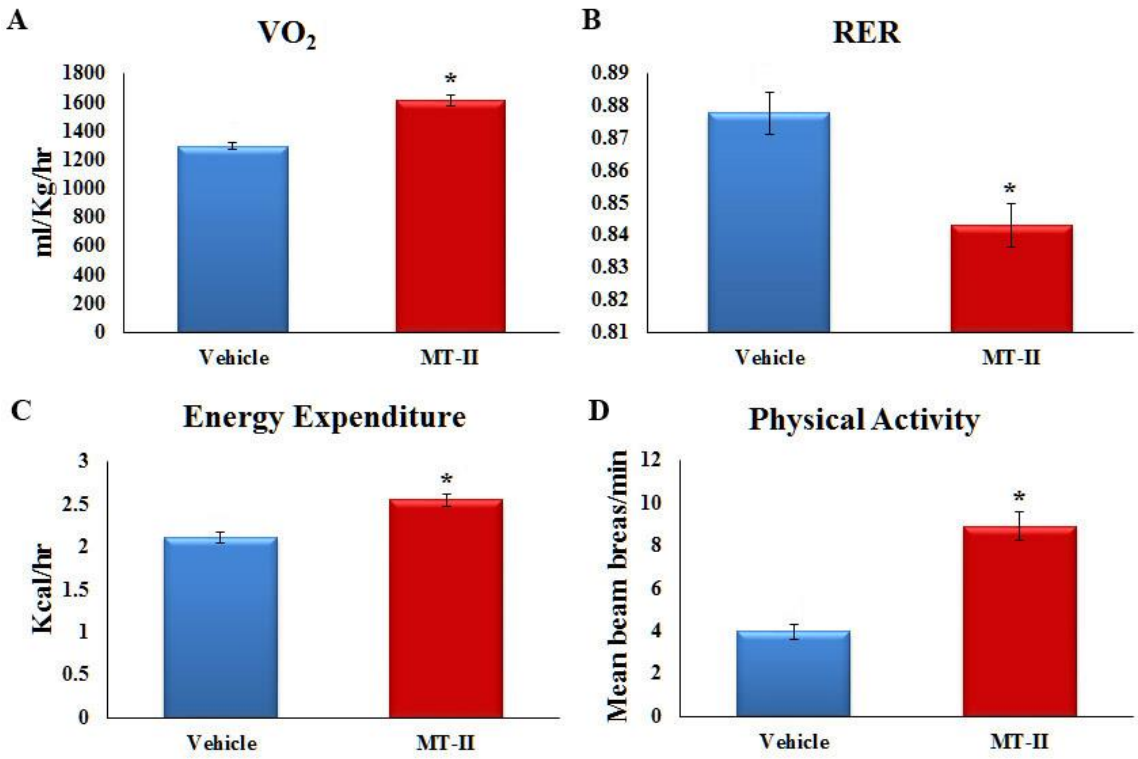

Figure 19: Intra-VMH MTII induced a significant increase in energy expenditure, oxygen uptake, and physical activity, with a significant decrease in respiratory exchange ratio. Oxygen uptake (VO_2), respiratory exchange ratio (RER), energy expenditure and physical activity 4hrs after intra-VMH MTII and vehicle administration. Compared to vehicle, MTII microinjections significantly increased VO_2 (A), energy expenditure (C) and physical activity (D) and decreased RER (B). (*significantly different from vehicle, $p<0.05$)

Intra-VMH MTII microinjection increases energy expenditure during controlled activity (Study 1a).

To demonstrate that increase in these calorimetric parameters is not dependent on the increase in physical activity after intra-VMH microinjection of MTII, a controlled treadmill activity study was performed. EE was measured during a low-grade treadmill exercise test to control for rats' workload. Again animals were compared to themselves – a within-animal design – to eliminate potentially confounding effects of individual differences, for example in body weight. As shown in Figure 20, compared to vehicle microinjection, rats receiving intra-VMH microinjection of MTII had higher EE, higher VO_2, and lower RER during a controlled treadmill activity. Therefore, the altered EE and calorimetric parameters after intra-VMH MTII treatment was not dependent on increased physical activity. As each rat acted as its own control and considering the lack of significant changes in body weight, lean mass, or fat mass between treatments, the potential confounding effect of differential workload during activity is negligible.

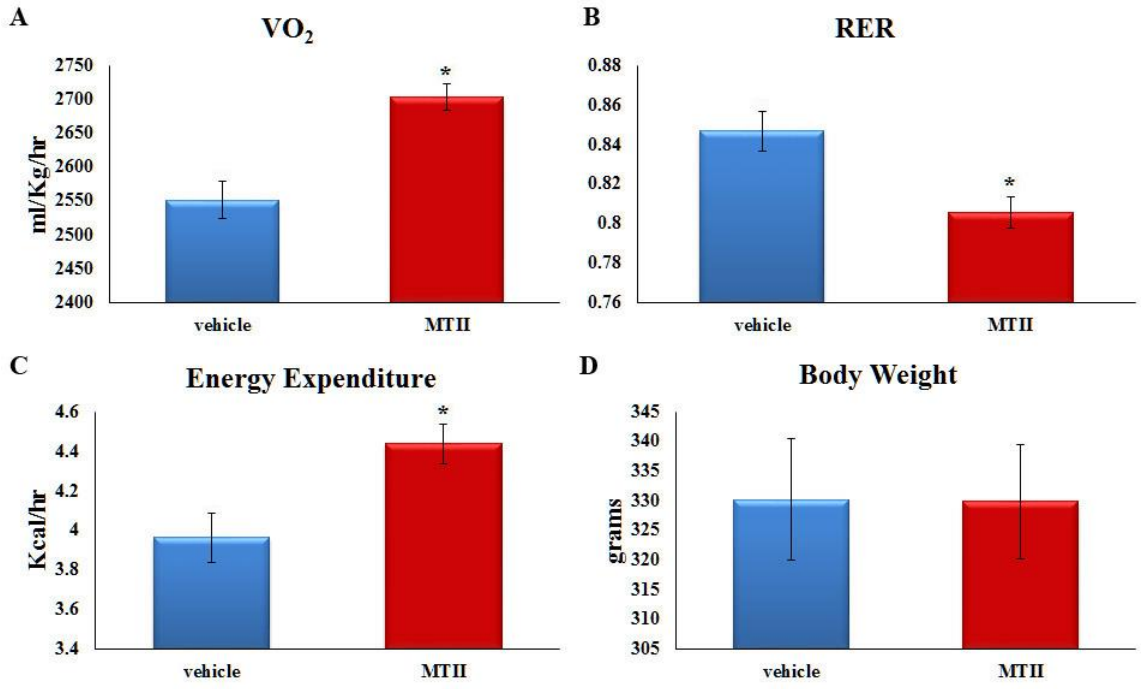

Figure 20: Intra-VMH MTII-induced alterations in energy expenditure and respiratory exchange ratio persisted during controlled treadmill activity. Oxygen uptake (VO_2), respiratory exchange ratio (RER), energy expenditure during controlled treadmill activity after intra-VMH MTII and vehicle administration. Compared to vehicle, MTII microinjections significantly increased VO_2 (A), energy expenditure (C) and decreased RER (B). No significant change was seen in body weight (D) between the treatments. (*significantly different from vehicle, $p<0.05$)

High activity energy expenditure after intra-VMH MTII microinjection is accompanied by skeletal muscle energy dissipation as heat (Study 1b).

Based on above results, intra-VMH MTII injection resulted in additional calories being used for the identical activity, indicating that intra-VMH MC receptor activation lowers economy of activity. Along with literature showing the association between VMH MC receptors and skeletal muscle fuel use and allocation, this implicates melanocortin-induced alteration of skeletal muscle energetics and thermogenesis as the underlying cause. To test this, I microinjected these rats with MTII or vehicle and measured BAT and gastroc temperatures under home-cage resting conditions as well as during a graded treadmill activity. During resting, compared to vehicle, MTII treatment induced higher BAT temperatures, and the rise in temperature from baseline was significantly higher after MTII treatment between 30min and 105min after injection (Figure 21). Compared to vehicle, intra-VMH MTII injection induced higher gastroc muscle temperatures and the rise in temperature from baseline was significantly higher compared to vehicle between 90min and 240min of the testing period (Figure 21).

Next, I tested the hypothesis that MTII injection decreases economy of activity as the rats expend calories through heat dissipation in skeletal muscle during activity. This was tested by measuring gastroc temperature during a graded exercise treadmill test. All rats received both sets of injections and there were no significant differences in body weight, lean mass, or fat mass observed between treatments. Compared to vehicle treatment, MTII injections induced a significant increase in gastroc temperature, and the maximal increase in temperature from baseline was also significantly higher after MTII

compared to vehicle (Figure 22), demonstrating overall that intra-VMH MC receptor activation lowers the economy of activity and that those surplus calories are dissipated as heat by skeletal muscle.

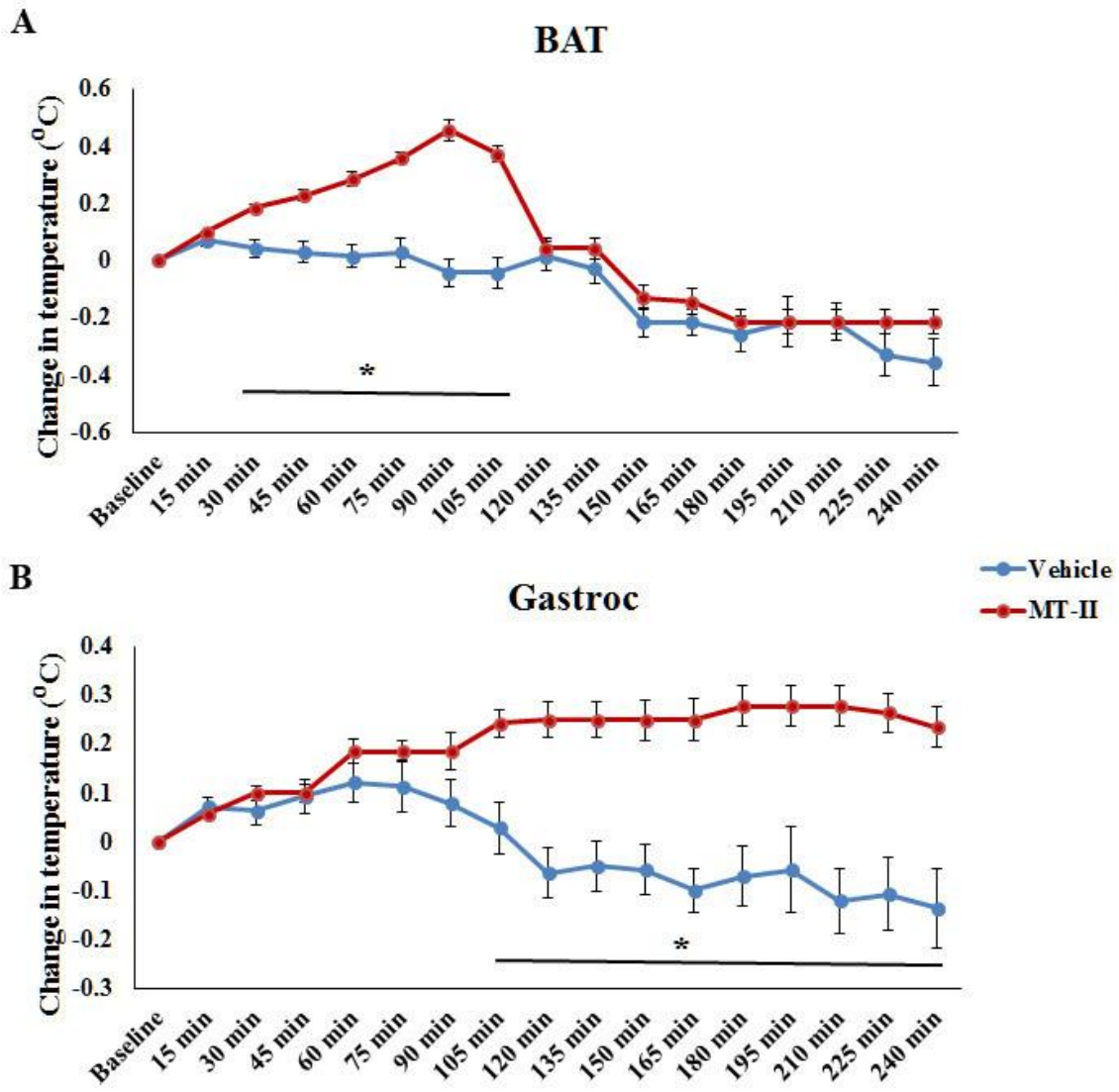

Figure 21: Intra-VMH MTII induced a significant increase in both brown adipose tissue and gastrocnemius temperatures compared to vehicle microinjection during the light phase. Change in temperature of gastrocnemius (gastroc) (B) and brown adipose tissue (BAT) (A) from baseline in rats after intra-VMH microinjections of MTII and vehicle. Change in temperature was significantly greater after MTII microinjection compared to vehicle between 105 min and 240 min for gastroc, and between 30 min and 105 min for BAT. (*MTII significantly higher than vehicle, $p<0.05$)

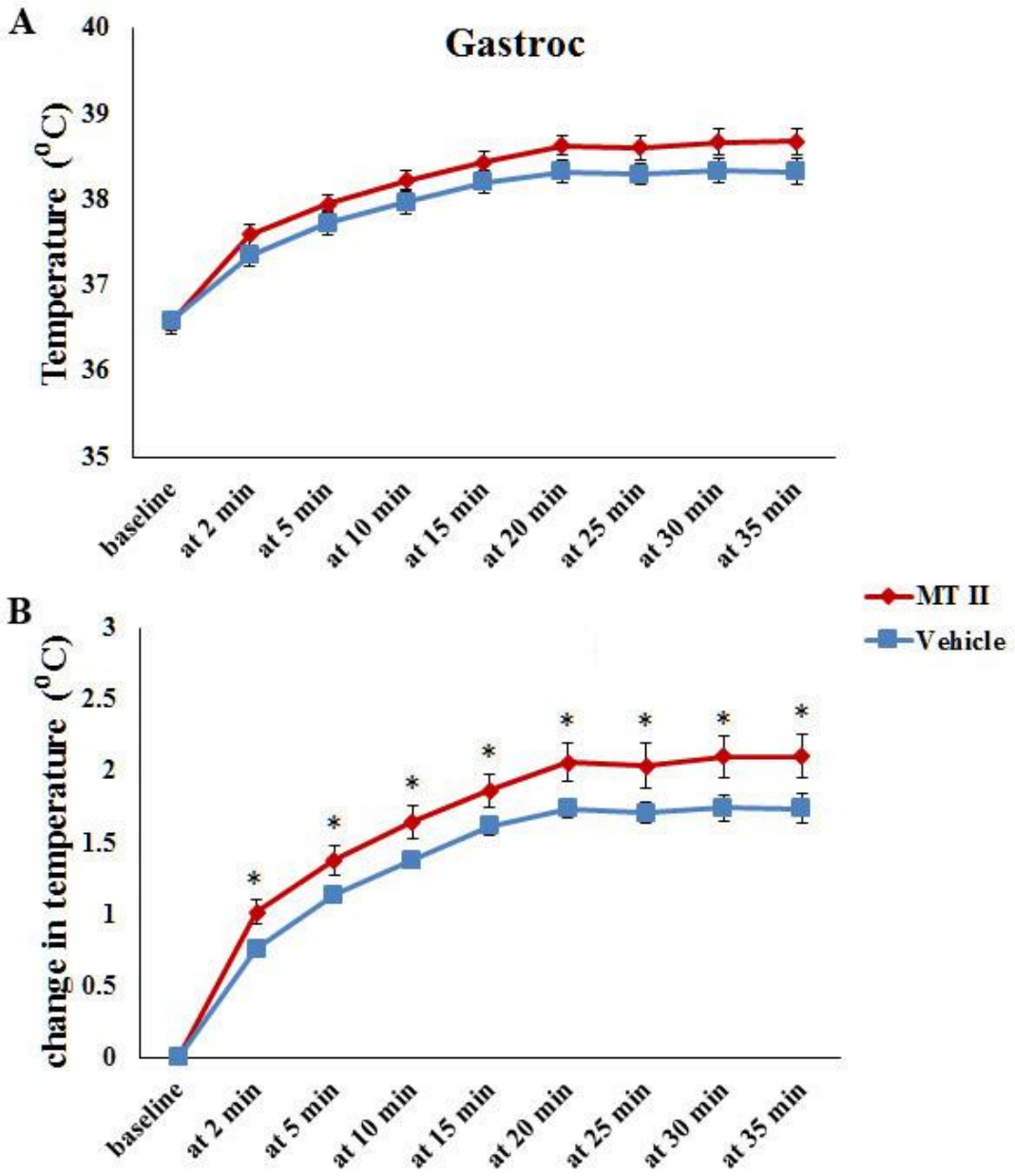

Figure 22: Intra-VMH MTII increased gastrocnemius temperature during a graded treadmill exercise test. Temperature (A) and change in temperature from baseline (B) of gastrocnemius (gastroc) in rats after intra-VMH microinjections of MTII and vehicle. Temperature was higher after MTII microinjection compared to. Change in temperature from baseline was significantly greater after MTII microinjection compared to vehicle. (*MTII significantly higher than vehicle, $p<0.05$)

Intra-VMH MT-II microinjection elevates sympathetic drive to metabolic tissues (Study 2a).

The SNS is likely to play a crucial role in the transmission of signals from hypothalamic nuclei downstream to peripheral metabolic tissues modulating fuel use and production. As illustrated in Figures 23, 24, and 25, compared to vehicle, intra-VMH MTII-microinjected rats had higher NETO in all tissues analyzed, indicating higher sympathetic drive to these tissues; this included skeletal muscle, different WAT depots, BAT, heart, and liver. This implicates a MC regulated pathway in the hypothalamus, particularly the VMH, in the regulation of SNS drive, potentially modulating muscle fuel storage and utilization.

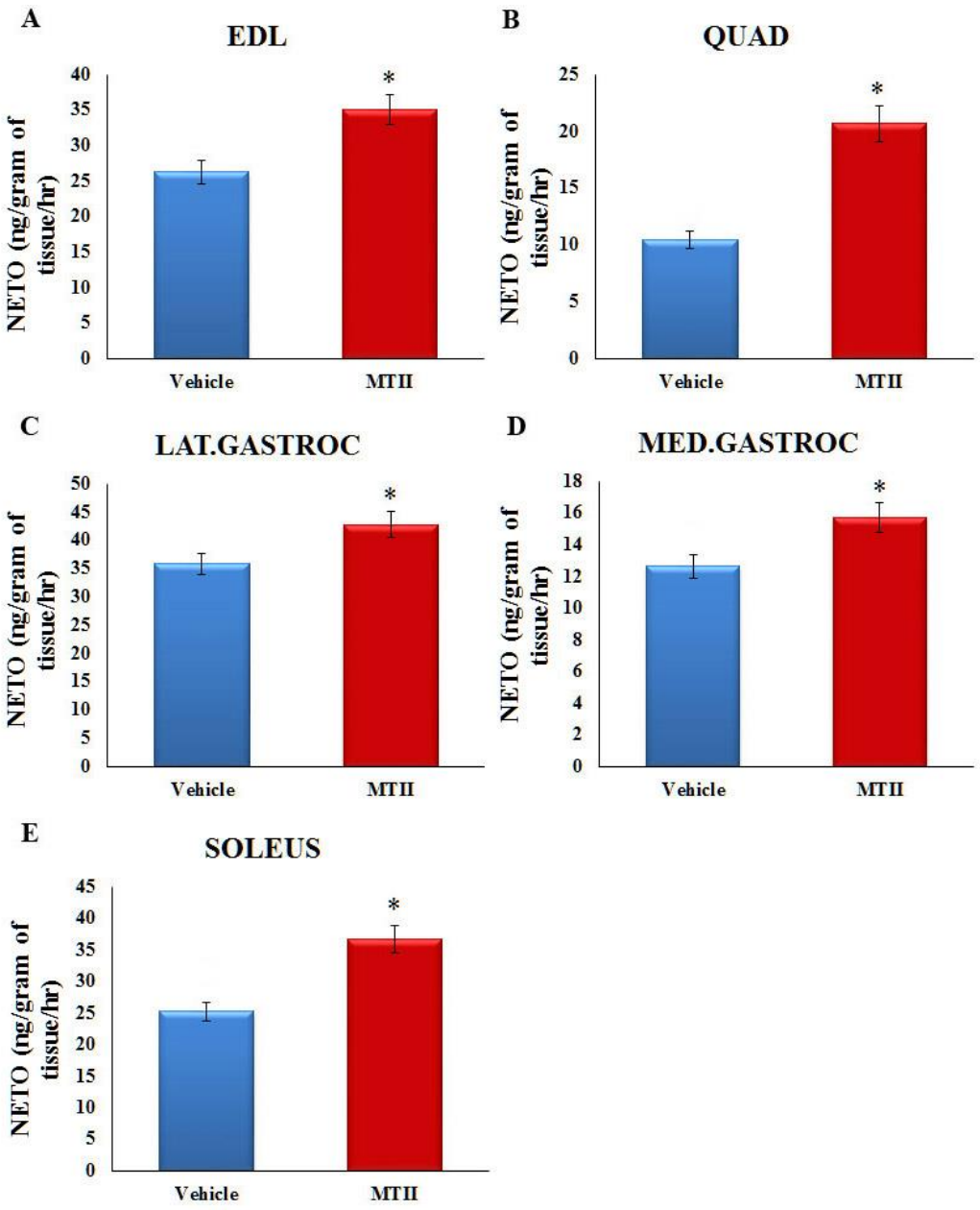

Figure 23: Intra-VMH MTII induced a significant increase in skeletal muscle NETO. Norepinephrine turnover (NETO) in skeletal muscle of intra-VMH MTII and vehicle microinjected rats in (A) extensor digitorum longus (EDL), (B) quadriceps (Quad), (C) lateral gastrocnemius (Lat.gastroc), (D) medial gastrocnemius (Med.gastroc), and (E) soleus. Compared to vehicle, intra-VMH MTII induced a significant increase in NETO (*MTII>vehicle, $p<0.05$).

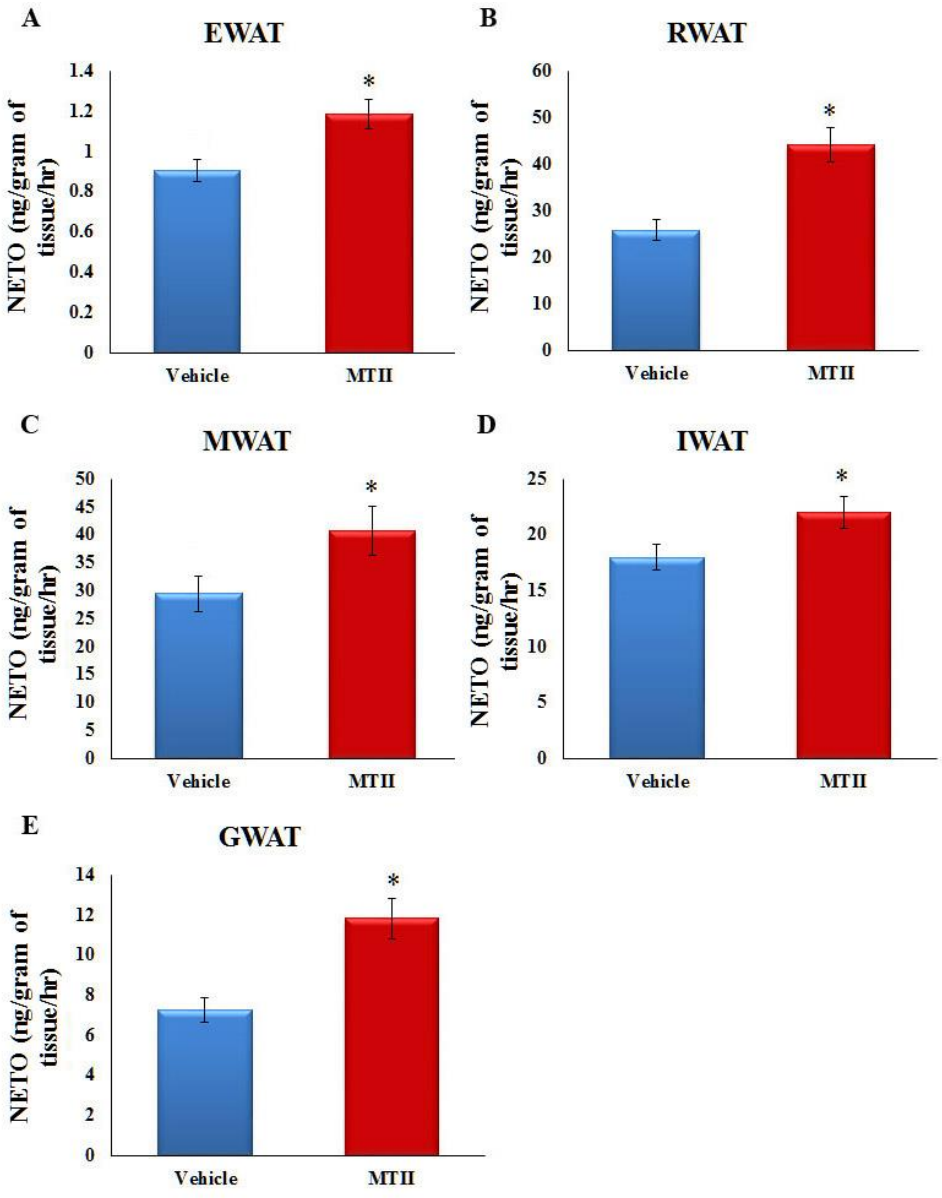

Figure 24: Intra-VMH MTII induced a significant increase in NETO of different white adipose depots. Norepinephrine turnover (NETO) of intra-VMH MTII- and vehicle-microinjected rats in different white adipose depots (WAT): (A) epididymal WAT (EWAT), (B) retroperitoneal WAT (RWAT), (C) mesenteric WAT (MWAT), (D) inguinal WAT (IWAT), and (E) gluteal WAT (GWAT). Compared to vehicle, intra-VMH MTII induced a significant increase in NETO in all WAT depots (*MTII>vehicle, $p<0.05$).

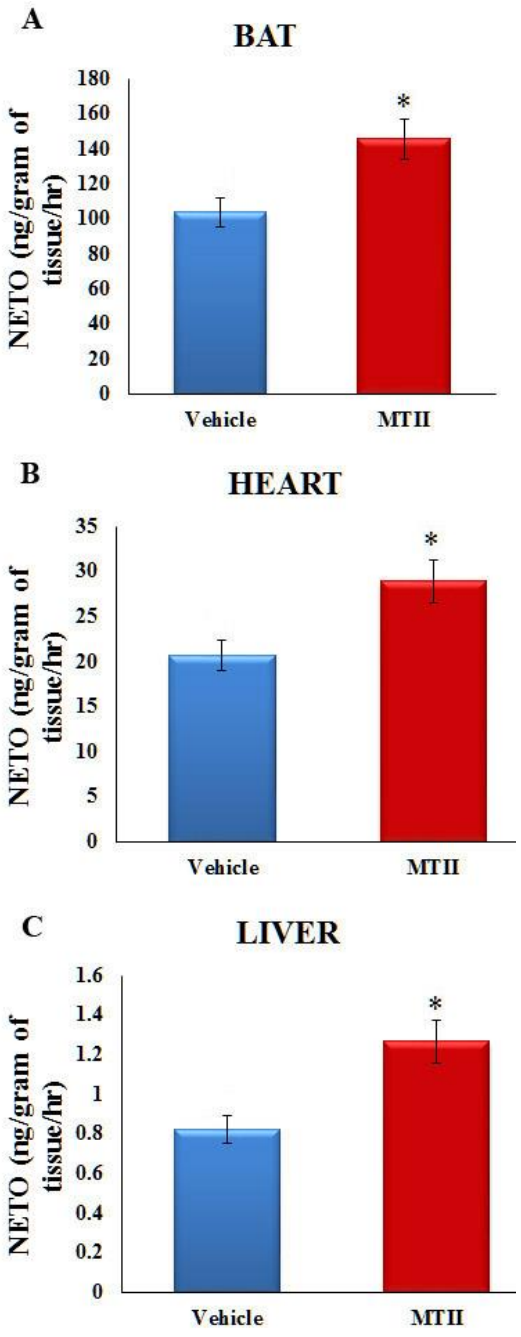

Figure 25: Intra-VMH MTII induced a significant increase in NETO of brown adipose tissue (BAT), heart, and liver. Norepinephrine turnover (NETO) of intra-VMH MTII and vehicle microinjected rats in (A) BAT, (B) heart, and (C) liver. Compared to vehicle, intra-VMH MTII induced a significant increase in NETO (*MTII>vehicle, $p<0.05$).

Intra-VMH MT-II microinjection elevates expression of mRNA of mediators of energy expenditure, with a trend towards lower expression of energy conserving processes in peripheral metabolic tissues, with some alteration in the protein content (Study 2b).

To determine the source of calorie use and heat dissipation in the muscle of MTII-treated rats, I examined the levels of mRNA expression of potential molecular mediators of energy balance – UCP1, UCP2, UCP3, Kir6.1, Kir6.2, MED1, PPARα, PPARδ, PPARγ, PGC-1α, Ca^{2+}-ATPase (SERCA), β_2-AR, and β_3-AR in the skeletal muscle including quad and gastroc, BAT, WAT, and liver. I found that, compared to vehicle administration, rats with intra-VMH MTII microinjections have elevated expression of UCP1, PGC-1α, PPARδ, PPARγ, and a trend ($1.0>p>0.05$) toward an increase in PPARα in their BAT (Figure 26). There were also trends toward an increase in intra-VMH MTII-treated rats in PPARγ, PPARα, and PPARδ in WAT (Figure 27). Intra-VMH MTII-treated rats showed a significant increase in mRNA expression of UCP2, PPARα, and PPARδ and a trend for PPARγ in the liver (Figure 28). Quadriceps of MTII-microinjected rats showed a significant increase in mRNA expression of UCP2, UCP3, PPARδ, SERCA1, and SERCA2 and a trend toward an increase in expression of PPARα, PPARγ, and β_2-AR (Figure 29). Quadriceps of intra-VMH MTII-treated rats also showed a reduction in mRNA expression of Kir6.1, Kir6.2, and MED1. Compared to vehicle, gastroc muscle of intra-VMH MTII rats had significantly higher mRNA expression of UCP2, UCP3, PGC-1α, PPARα, PPARδ, PPARγ, SERCA2, and β_2-AR (Figure 30). Gastroc muscle also showed a significant decrease in Kir6.2 and a trend toward a decrease in Kir6.1 and MED1 (Figure 30).

Protein expression of some mediators of EE were altered by intra-VMH MTII, but did not consistently change in accordance with mRNA expression. Compared to vehicle, BAT of intra-VMH MTII-treated rats showed significantly increased expression of UCP1, PGC-1α, pAMPK, and pACC, and trend toward increased expression of PPARγ, PPARα, β_3 AR, PPARδ, CPT1, and CD36/FAT (Figure 31). In WAT, no significant differences were observed except in expression of pAMPK, which was significantly elevated in MTII-treated rats (Figure 33). Similar to this was liver of MTII-microinjected rats, which showed a significant increase in pAMPK and a trend for increased expression of PPARγ, UCP2, β_2-AR, and PGC-1α (Figure 34). Compared to vehicle, quadriceps of MTII-treated rats showed a significant increase in pAMPK and pACC and a trend for increased expression of CD36/FAT, PPARα, PGC-1α, PPARδ, UCP3, UCP2, PPARγ, and SERCA1 (Figure 35). Compared to vehicle, gastroc muscle of intra-VMH MTII-microinjected rats showed a significant increase in expression of PGC-1α, PPARα, pAMPK, and pACC (Figure 37). Gastroc muscle also showed increasing trends in several proteins including SERCA1, SERCA2, β_2-AR, PPARγ, PPARδ, UCP2, UCP3, CPT1, and CD36/FAT (Figure 37).

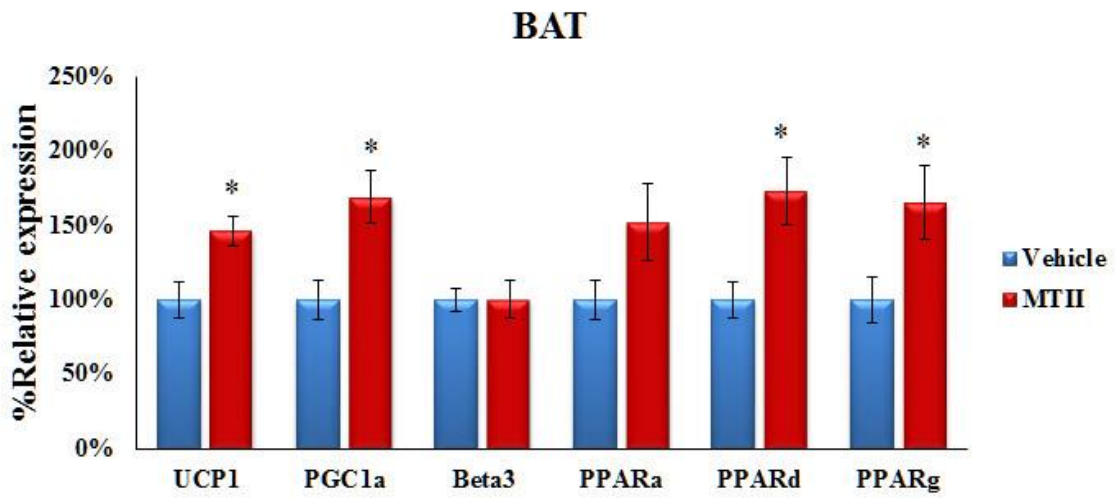

Figure 26: Intra-VMH MTII microinjection enhanced mRNA expression of mediators of energy expenditure in the brown adipose tissue (BAT). Compared to vehicle administration, rats with intra-VMH MTII microinjections have elevated expression of UCP1, PGC-1α, PPARδ, and PPARγ in BAT. (*significantly higher than vehicle, $p<0.05$)

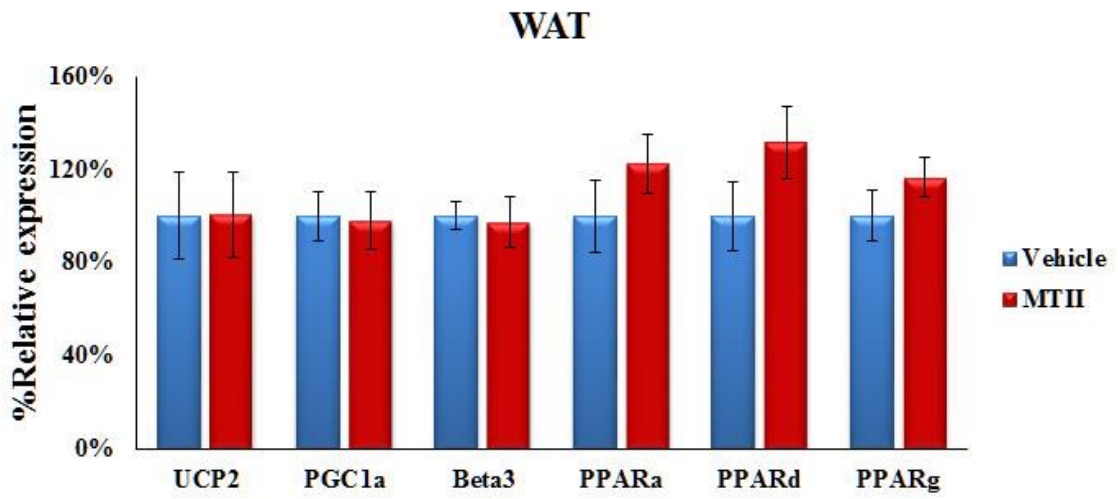

Figure 27: Intra-VMH MTII microinjection did not significantly alter mRNA expression of mediators of energy expenditure in the white adipose tissue (WAT). Compared to vehicle administration, rats with intra-VMH MTII microinjections showed a trend toward an increase in PPARγ, PPARα, and PPARδ.

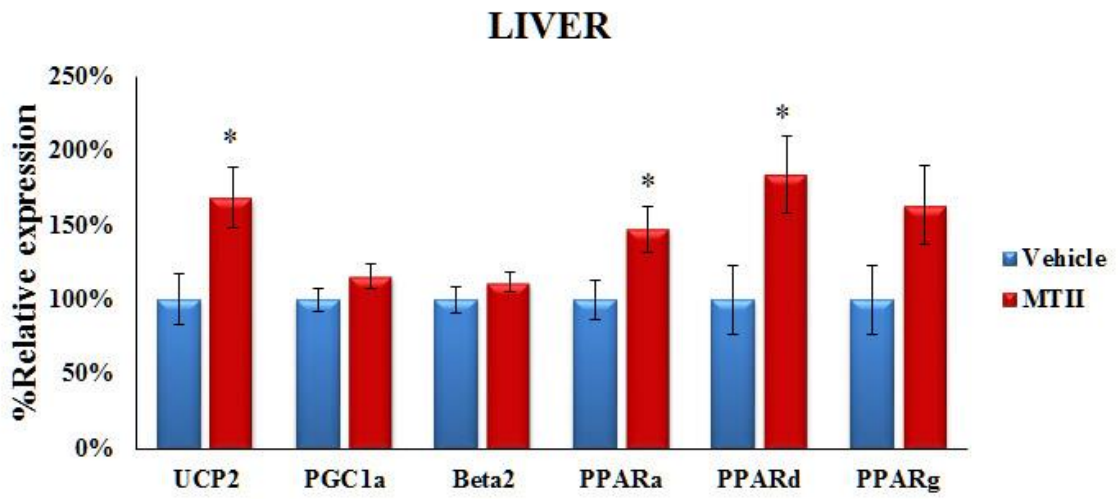

Figure 28: Intra-VMH MTII microinjection enhanced mRNA expression of mediators of energy expenditure in the liver. Compared to vehicle administration, rats with intra-VMH MTII microinjections have elevated expression of UCP2, PPARα, and PPARδ and a trend toward higher PPARγ in the liver. (*significantly higher than vehicle, $p<0.05$)

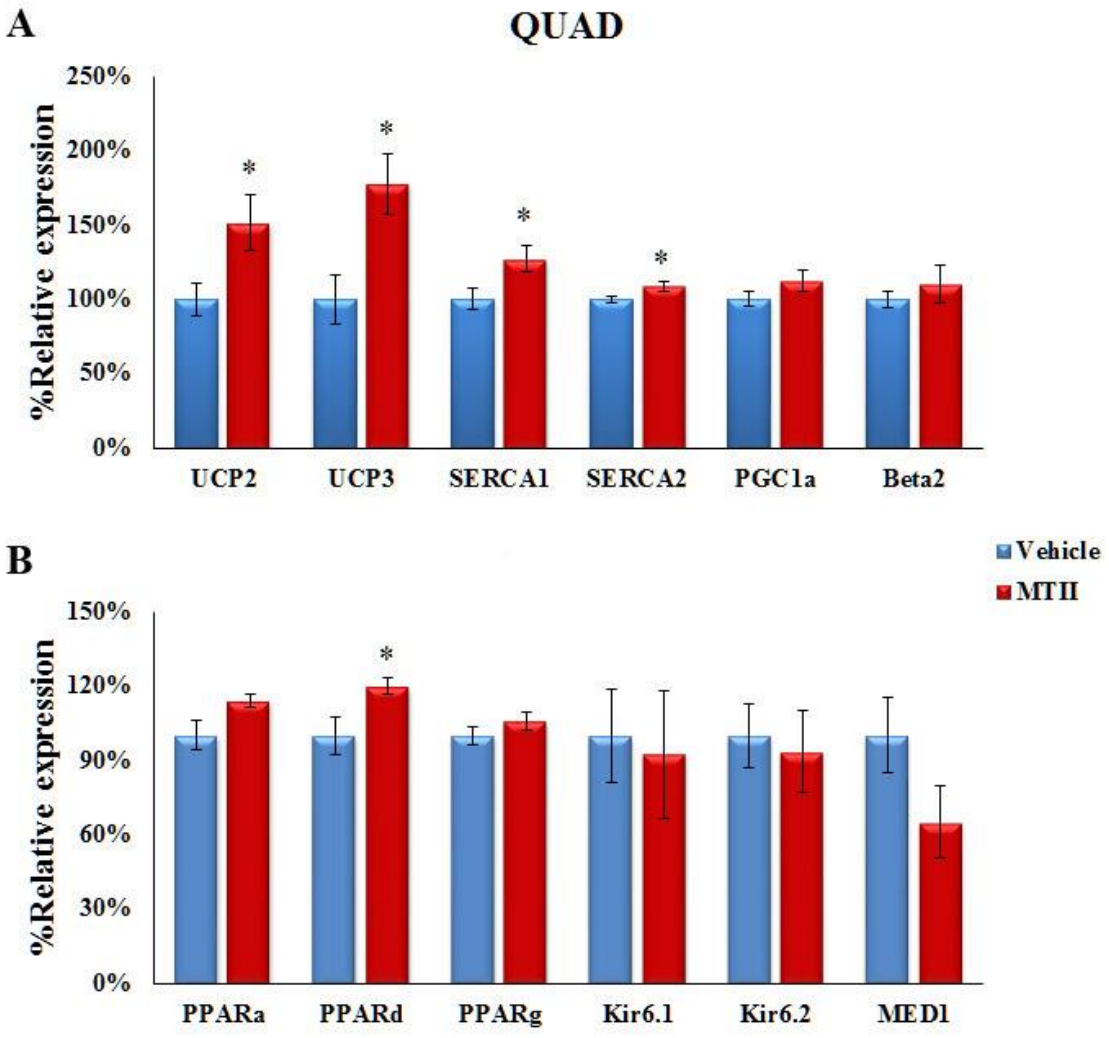

Figure 29: Intra-VMH MTII microinjection enhanced mRNA expression of mediators of energy expenditure in the quadriceps with a trend towards lower expression of energy conserving processes. Compared to vehicle administration, rats with intra-VMH MTII microinjections have elevated expression of UCP2, UCP3, SERCA1, SERCA2, and PPARδ and a trend toward higher PPARα in the quadriceps (quad). Quad of intra-VMH MTII-treated rats also showed a trend toward reduction in mRNA expression of MED1. (*significantly different from vehicle, $p<0.05$)

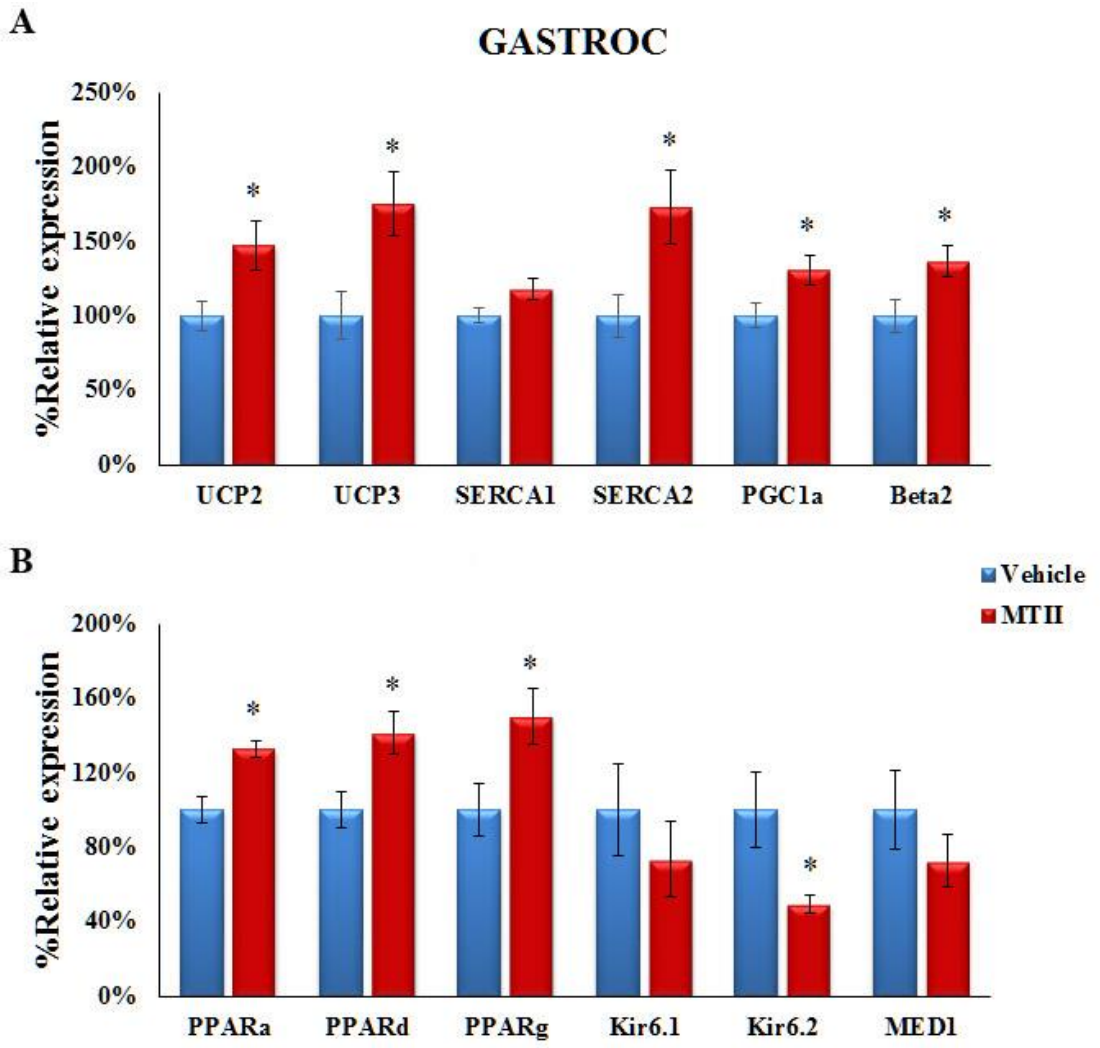

Figure 30: Intra-VMH MTII microinjection enhanced mRNA expression of mediators of energy expenditure in the gastrocnemius with a trend towards lower expression of energy conserving processes. Compared to vehicle administration, rats with intra-VMH MTII microinjections have elevated expression of UCP2, UCP3, SERCA2, PGC-1α, β_2-AR, PPARδ, PPARα, and PPARγ in the gastrocnemius (gastroc). Gastroc of intra-VMH MTII-treated rats also showed a significant reduction in mRNA expression of Kir6.2 and a trend toward decreased Kir6.1 and MED1. (*significantly different from vehicle, $p<0.05$)

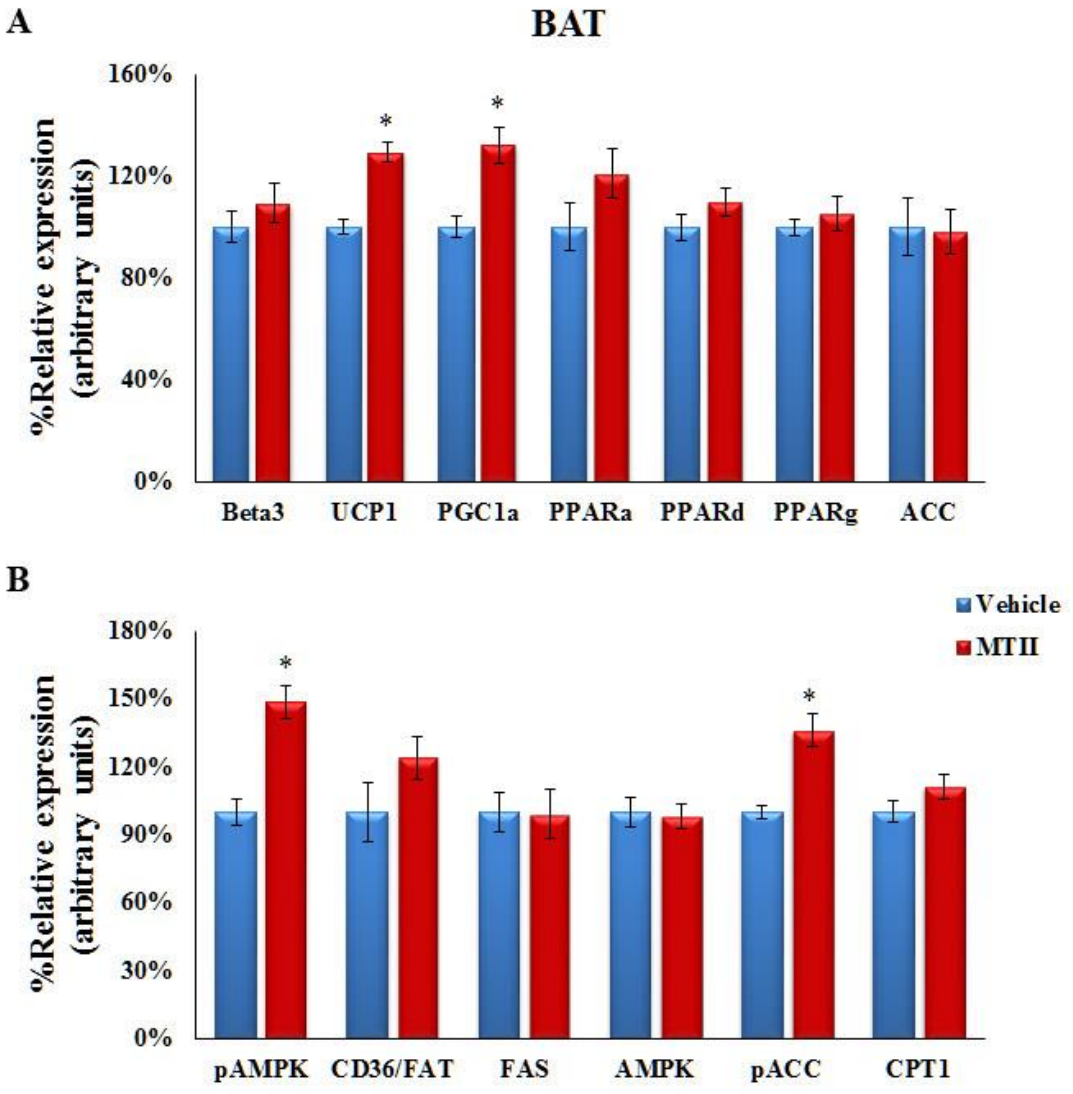

Figure 31: Intra-VMH MTII microinjection induced a trend toward an increase in protein expression of some mediators of energy expenditure in the brown adipose tissue (BAT). Compared to vehicle administration, rats with intra-VMH MTII microinjections have elevated expression of UCP1, PGC-1α, pAMPK, and pACC and a trend in PPARα, PPARδ, CD36/FAT and CPT1 in BAT. (*significantly greater than vehicle, $p<0.05$)

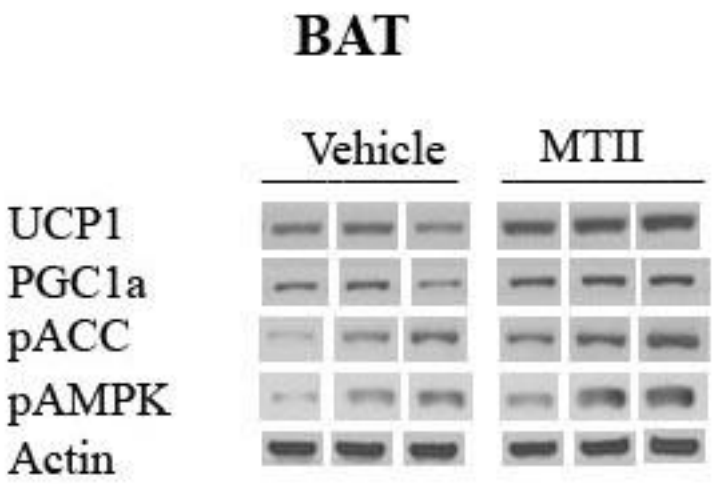

Figure 32: Representative western blot images showing the expression of molecular mediators of energy balance in brown adipose tissue (BAT). Uncoupling protein 1 (UCP1), peroxisomal proliferator activator γ coactivator 1α (PGC-1α), p-acetyl-CoA carboxylase (pACC), p-AMP-activated protein kinase (pAMPK), and actin as the loading control.

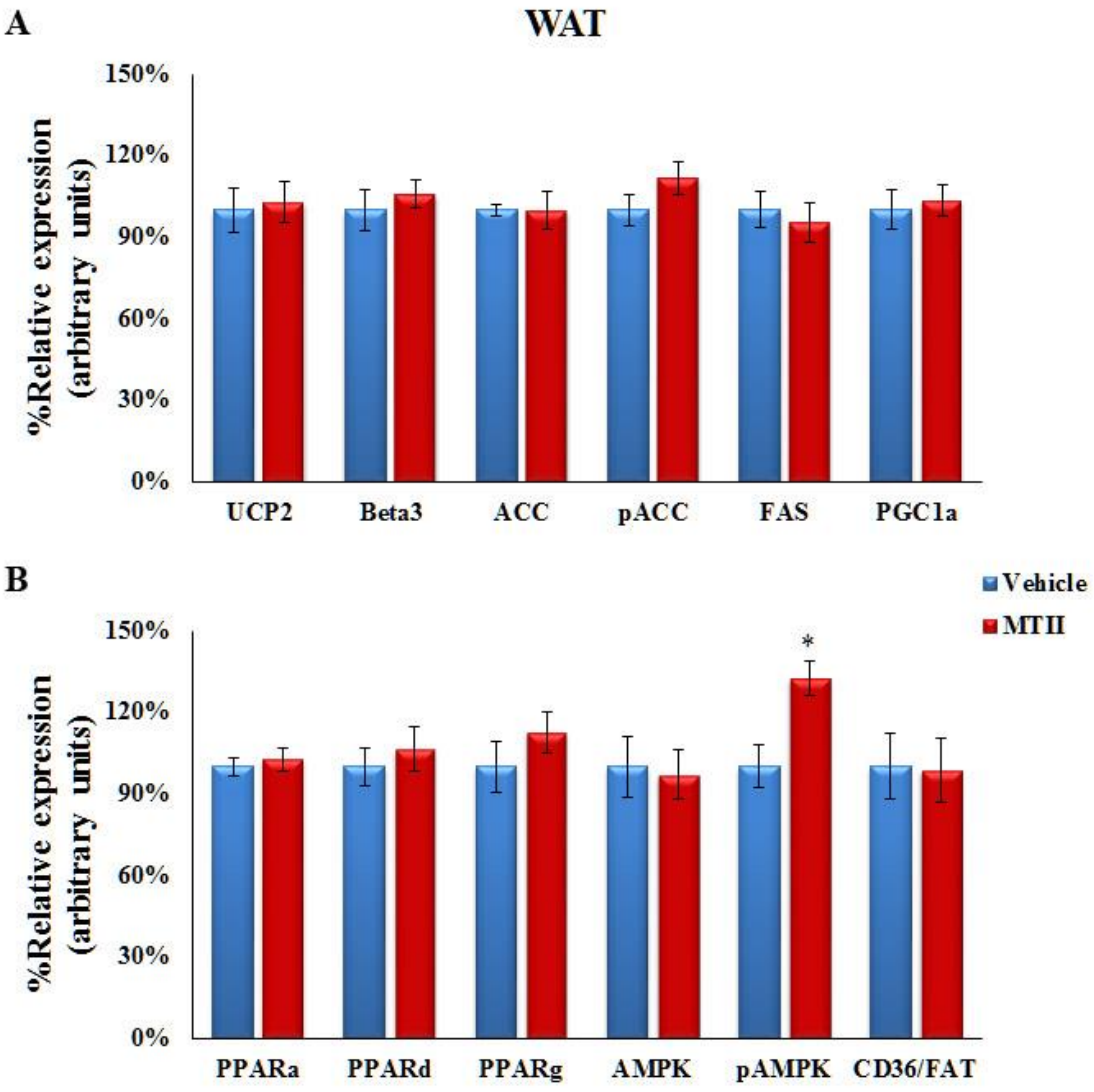

Figure 33: Intra-VMH MTII microinjection did not alter protein expression of mediators of energy expenditure in white adipose tissue (WAT). Compared to vehicle administration, rats with intra-VMH MTII microinjections had a significant increase in activation of AMPK (i.e., pAMPK) in WAT. (*significantly greater than vehicle, $p<0.05$)

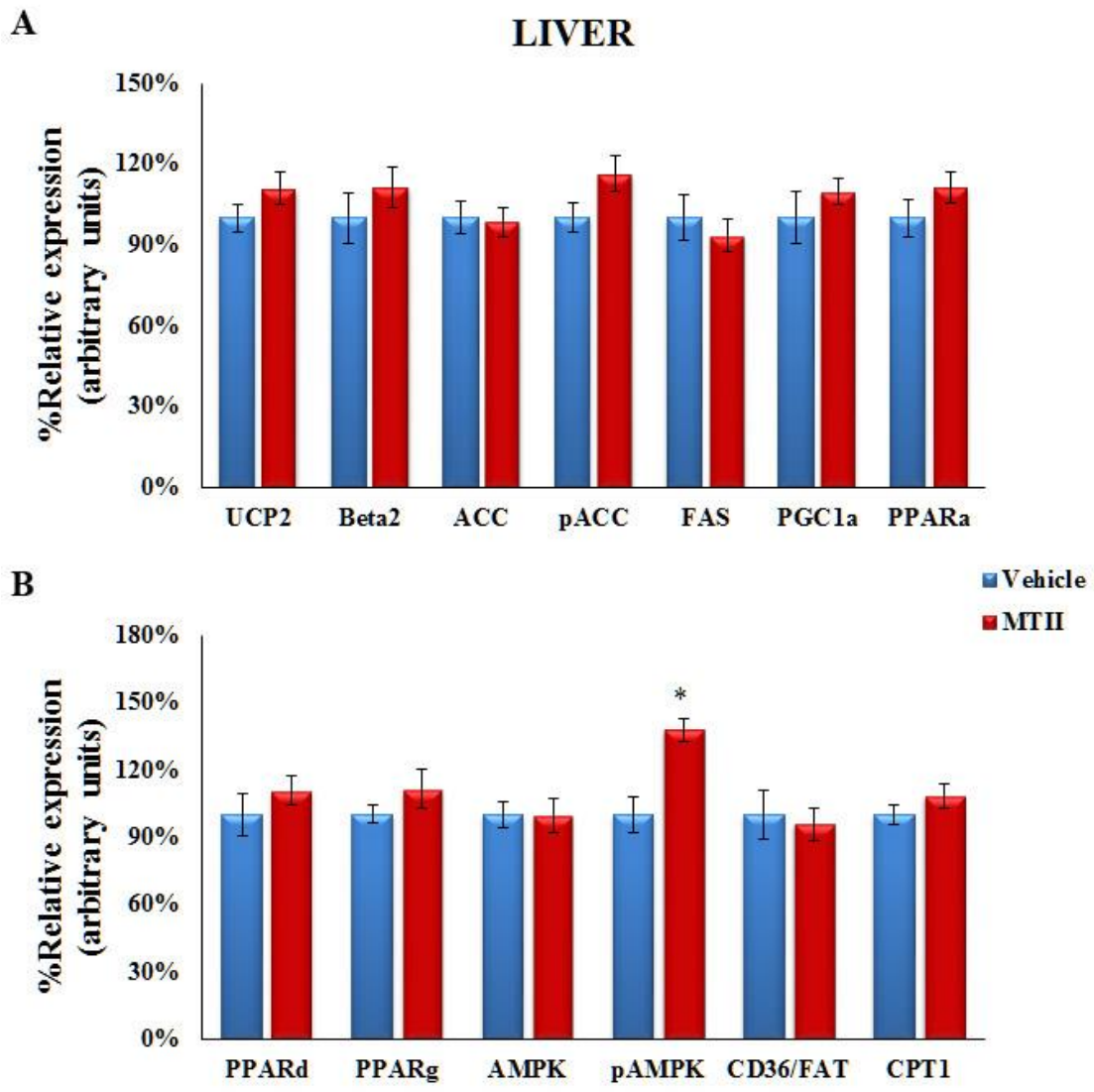

Figure 34: Intra-VMH MTII microinjection did not significantly alter protein expression of mediators of energy expenditure in the liver. Compared to vehicle administration, rats with intra-VMH MTII microinjections have elevated expression of pAMPK in the liver. (*significantly greater than vehicle, $p<0.05$)

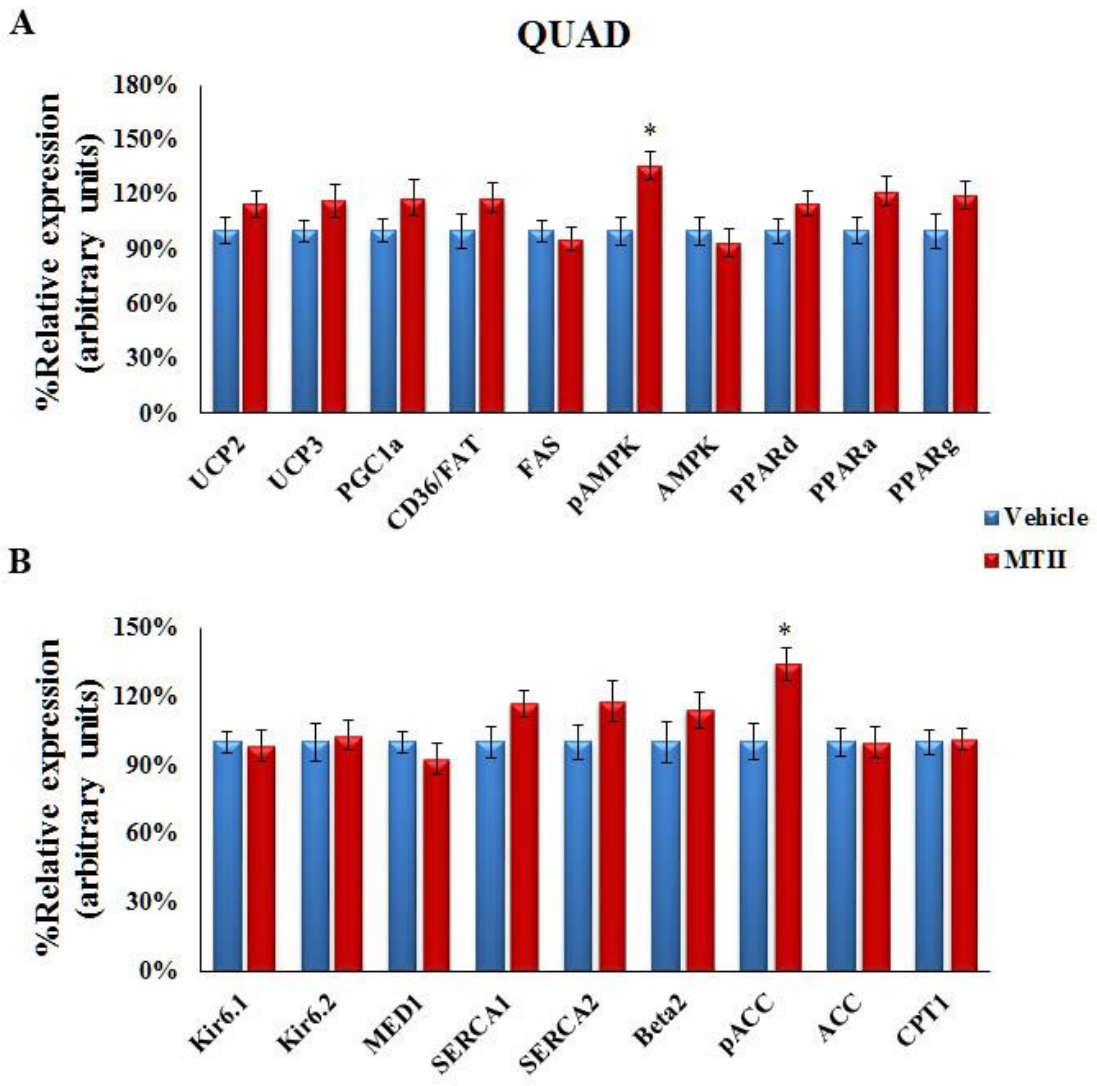

Figure 35: Intra-VMH MTII microinjection induced a trend toward an increase in protein expression of mediators of energy expenditure in the quadriceps. Compared to vehicle administration, rats with intra-VMH MTII microinjections have elevated expression of pAMPK and pACC in the quadriceps (quad). Quad of intra-VMH MTII-treated rats also showed a trend toward an increase in expression of UCP2, UCP3, PGC-1α, CD36/FAT, PPARα, PPARδ, PPARγ, SERCA1, SERCA2, and β_2-AR. (*significantly greater than vehicle, $p<0.05$)

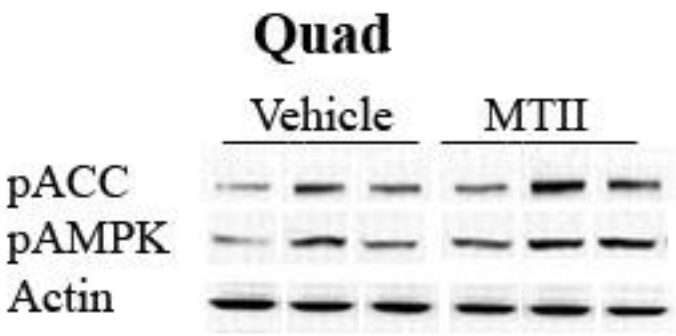

Figure 36: Representative western blot images showing the expression of molecular mediators of energy balance in the quadriceps (Quad). p-acetyl-CoA carboxylase (pACC), p-AMP-activated protein kinase (pAMPK), and actin as the loading control.

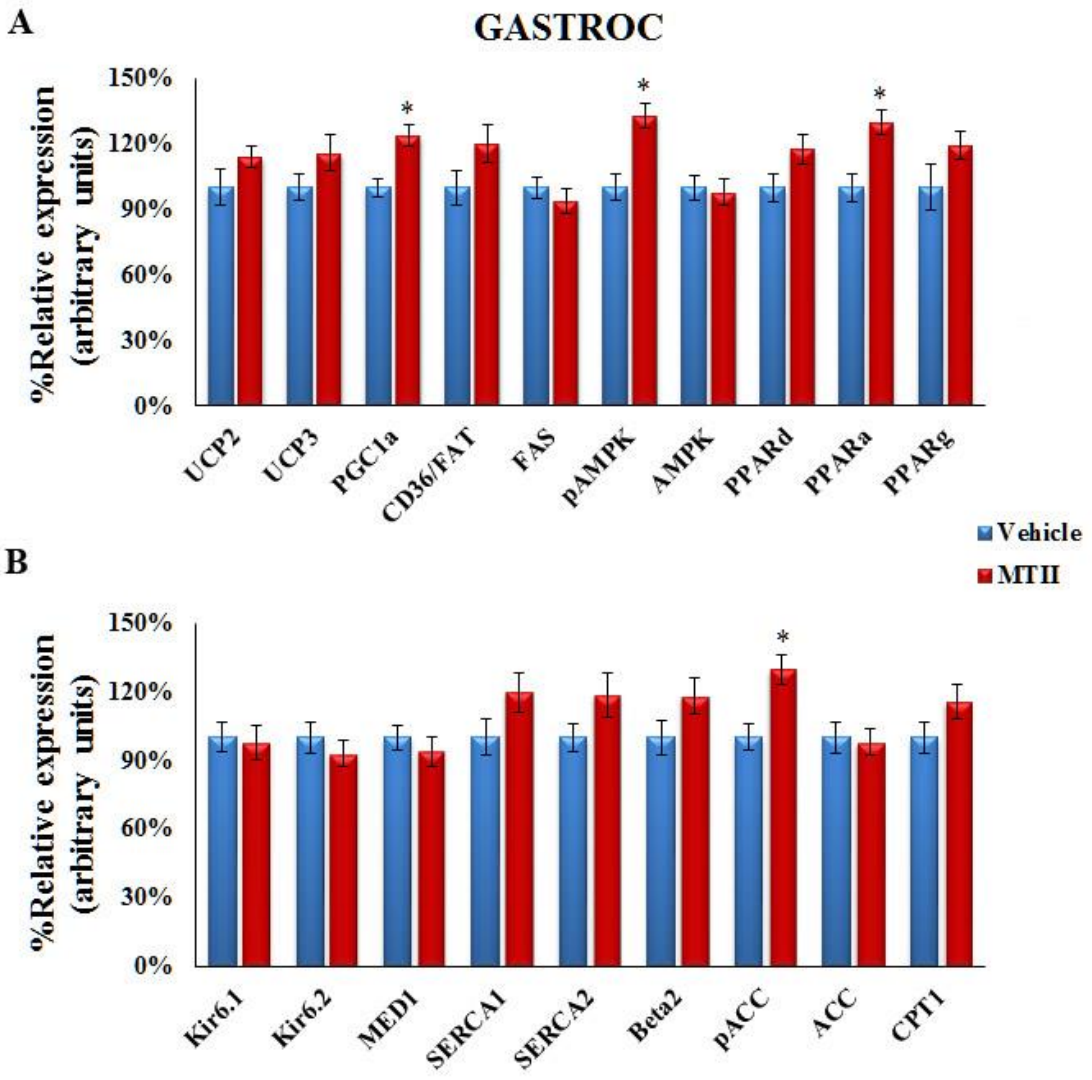

Figure 37: Intra-VMH MTII microinjection induced a significant increase in protein expression of some mediators and a trend toward an increase in other mediators of energy expenditure in the gastrocnemius. Compared to vehicle administration, rats with intra-VMH MTII microinjections have elevated expression of PGC-1α, pAMPK, PPARα, and pACC in the gastrocnemius (gastroc). Gastroc of intra-VMH MTII-treated rats also showed a trend toward an increase in expression of UCP2, UCP3, CD36/FAT, PPARδ, PPARγ, SERCA1, SERCA2, CPT1, and β_2-AR. (*significantly greater than vehicle, $p<0.05$)

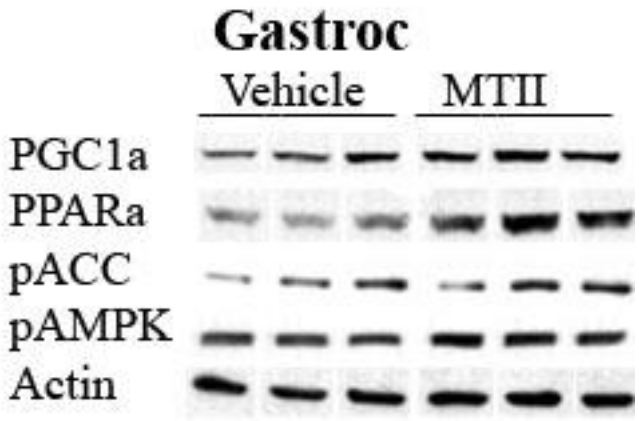

Figure 38: Representative western blot images showing the expression of molecular mediators of energy balance in the gastrocnemius (Gastroc). Peroxisomal proliferator activator γ coactivator 1α (PGC-1α), peroxisome proliferator activated receptor α (PPARα), p-acetyl-CoA carboxylase (pACC), p-AMP-activated protein kinase (pAMPK), and actin as the loading control.

3.3 Discussion

I found a dose-dependent increase in EE and decrease in RER after site-specific microinjections of MC3R/MC4R non-specific agonist MTII into the VMH. These changes in calorimetric parameters were seen even when activity level and workload were controlled for using a low-level treadmill activity test, suggesting that intra-VMH MC receptor activation lowers the economy of activity. Central MTII also induced an increase in skeletal muscle heat dissipation as well as BAT temperature values in freely moving animals (Figure 21), suggesting that part of increased EE is due to energy being dissipated as heat through these tissues. As with MTII-induced EE, the increase in muscle temperature persisted during controlled treadmill activity (Figure 22), ruling out differences in physical activity levels. Altogether, this supports the hypothesis that the activation of MC receptors in the VMH increases EE, lowers RER by switching fuel use to fatty acids, and at the same time lowers the economy by increasing heat production in peripheral tissues, particularly skeletal muscle. I also found that, compared to vehicle administration, intra-VMH MC receptor activation induced an increase in sympathetic drive to the peripheral metabolic tissues as indicated by increased NETO. This increased SNS stimulation of skeletal muscle is a likely mechanism through which EE and fuel utilization is altered as it known to modulate cellular energy mediators, including in muscle (Shiuchi et al., 2009). Altogether, these results support the function of a brain-muscle pathway where activation of MC receptors in the hypothalamus, particularly in the VMH, activate SNS outflow, increasing sympathetic drive to skeletal muscle, modulating fuel allocation and use through activation of molecular mediators of energy homeostasis potentially to enhance performance.

The central MC system plays a key role in the modulation of SNS outflow to peripheral tissues. Activation of MC receptors in the hypothalamus increases WAT lipolysis and thermogenesis at the level of BAT by modulating fuel allocation and uptake (Rossi et al., 2011; Shrestha et al., 2010). I considered the VMH and MC because of functional evidence supporting their role in modulating SNS outflow to muscle and altering metabolism. Stimulation of the VMH increases skeletal muscle fatty acid oxidation and glucose uptake, which is mediated by MC receptors (Miyaki et al., 2011; Shiuchi et al., 2009; Tanaka et al., 2007; Toda et al., 2009). This is consistent with my results where MC receptor activation in VMH increased total EE of the animal and this persisted even when activity was controlled. Even though functional studies show the importance of the VMH in the regulation of skeletal muscle metabolism, there were some unanswered questions regarding the neuroanatomical substrates underlying this. A limited number of VMH neurons were identified that innervate muscle through a multi-synaptic SNS pathway (Babic, Purpera, Banfield, Berthoud, & Morrison, 2010). More recently, however, it was found that SF-1 neurons of the VMH that impact metabolism project to the rostral ventrolateral medulla which controls SNS activity (Barnes & McDougal, 2014; Y. H. Choi, Fujikawa, Lee, Reuter, & Kim, 2013; Lindberg, Chen, & Li, 2013). Although results from immunostaining of the VMH show little presence of MC receptors, it has been shown to have high MC binding, and activity of the VMH but not the surrounding regions was found to be critical for the modulation of exercise-induced fatty acid oxidation (Haskell-Luevano et al., 1999; Miyaki et al., 2011; Mountjoy, Mortrud, Low, Simerly, & Cone, 1994; Trivedi et al., 2003). Taken together

with these studies, my findings support a role for an axis between the VMH and skeletal muscle via the SNS as a mediator of hypothalamic modulation of peripheral metabolism.

Evidence points to the assertion that skeletal muscle fatty acid metabolism is modulated by CNS, and that the signal is transmitted from CNS to muscle through the SNS via adrenergic receptors (Cha et al., 2005). Previous studies have shown that activation of hypothalamic MC receptors using MTII increases sympathetic drive to peripheral tissues including BAT and WAT (Brito, Brito, Baro, Song, & Bartness, 2007; Shi et al., 2004). Centrally administered MTII induced differential sympathetic drive to different WAT depots and BAT (Brito et al., 2007). Here, I found that, compared to vehicle treatment, activation of MC receptors through non-specific agonist MTII in the VMH, increased the sympathetic drive to peripheral metabolic tissues including muscle as well as WAT, BAT, and liver. This intra-VMH MC receptor-induced increase in sympathetic drive to peripheral tissues supports observed changes in calorimetric parameters like physical activity and EE, with the SNS promoting fatty acid uptake and use, and WAT providing fuel through lipolysis. Intra-VMH MC receptor activation also increased the activation of BAT thermogenesis, but was observed only for a limited duration signifying that the increase in EE and muscle temperatures are not entirely due to BAT thermogenesis.

As discussed before, the molecular pathways involved in EE and in energy conservation play an important role in determining an individual's propensity for obesity. Energetics at the level of metabolically active tissues like skeletal muscle help determine

the overall peripheral energy balance. I have shown that there is a significant increase in the expression of several of these mediators of EE at the level of both mRNA (Figures 26-30) and protein (Figures 31-37) in metabolically active tissues including muscle, and trends toward increases in several others. I have focused mainly on thermogenic proteins – UCP 1, 2, and 3, and calcium ATPase (SERCA1 and SERCA2). I analyzed proteins involved in fatty acid transport, metabolism, and activation – PPARα, δ, and γ, PGC1-α, acetyl-CoA carboxylase (ACC/pACC), fatty acid synthase (FAS), fatty acid transporter protein (CD36/FAT), and carnitine palmitoyltransferase 1 (CPT1). I also assessed indicators of cellular energy needs (AMPK/pAMPK), indicators of sympathetic regulation – beta adrenergic receptors (β_2 and β_3AR), and energy conserving proteins (K^+_{ATP} channel subunits and MED1). There was no significant change in mRNA or protein expression of mediators of conservation in all tissues analyzed. Compared to vehicle, intra-VMH MC receptor activation also induced a significant increase or an increasing trend in UCP1 in BAT (Figures 26 and 31), and UCP2 and UCP3 in oxidative gastroc muscle (Figures 30 and 37). UCP's have several hypothesized functions including thermogenesis in certain tissues, protection from ROS, mediation of insulin secretion, neuroprotection, and export of fatty acids (Fisler & Warden, 2006). Regulation of several of these functions is either directly or indirectly linked to metabolic disorders (see Chapter 1 section 1.7 for complete review). The increase in UCP after intra-VMH MC receptor activation and downstream SNS may account for some of the changes in the calorimetric parameters seen here such as increased EE partially through increased BAT thermogenesis and skeletal muscle heat dissipation, and may also be involved in fatty acid transport thereby affecting RER. Increased BAT thermogenesis was observed only

for a short duration (~for 1 hr after MC receptor activation) indicating alterations at the level of skeletal muscle are more likely to play a role in the observed changes in calorimetric parameters seen 1-4 hours after treatment.

Compared to vehicle, intra-VMH MC receptor activation induced a higher expression of PPAR's and co-activator PGC-1α, involved in regulation of metabolic pathways including lipid metabolism and mitochondrial biogenesis (Evans et al., 2004; Finck & Kelly, 2006). In metabolically active tissues like muscle, liver, and BAT, activation of PPARs leads to increased β-oxidation of fatty acids by switching muscle fibers to be oxidative, and also to adaptive thermogenesis (Y. X. Wang et al., 2003; Y. X. Wang et al., 2004). The expression and activity of these PPAR and co-activators like PGC-1α depends on the energy demands of the cell thereby affecting substrate uptake and utilization (Finck & Kelly, 2006). I found an increase in PPAR's and PGC-1α in BAT and skeletal muscle after intra-VMH MC receptor activation which likely contributed to the increased fatty acid oxidation as indicated by the low RER (Figure) and temporarily shutting down glucose oxidation. This is consistent with previous studies on PGC-1α altered tissue fuel selection (Finck & Kelly, 2006).

Compared to vehicle administration, gastroc muscle of intra-VMH MC receptor activated rats showed an increasing trend in SERCA1, SERCA2, and CD36/FAT (Figures 30 and 37). The expression of these proteins may explain to certain extent the reasons behind low economy of activity and negative energy balance in MTII-treated rats. CD36/FAT is involved in transport of fatty acids to heart and skeletal muscle for

oxidation in the mitochondria and its expression differs according to the metabolic challenges (Bonen et al., 2006). The SERCA pump regulates the cytosolic calcium level tightly and controls many cellular functions, from muscle contraction to cell signaling responsible for growth and differentiation (Periasamy & Kalyanasundaram, 2007). Increase in these calcium pumps involved in heat generation after intra-VMH MC receptor activation suggests their potential role in increased heat dissipation through muscle. In all tissues analyzed, intra-VMH MC receptor activation induced a trend toward increases in protein expression of mediators of EE, potentially because the relatively short amount of time after central MC receptor activation was insufficient for translation of proteins. Regardless, the significant increase in temperature at this time (4hrs after injection) indicates that there are functional differences in the cell.

Unlike the protein expression pattern observed above, intra-VMH MC receptor activation increased the expression of pAMPK and pACC in all tissues analyzed. In skeletal muscle, the degree of activation of AMPK is dependent of the metabolic stress caused by contraction. This MTII-induced increase in activation by phosphorylation of AMPK (pAMPK) may be responsible for increased expression of proteins involved in fuel allocation and utilization. Under basal conditions, leptin or adiponectin increases the expression of pAMPK in skeletal muscle and liver by increasing sympathetic drive to these tissues (Minokoshi et al., 2002; Tomas et al., 2002; Yamauchi et al., 2002). This increases energy expenditure in muscle by increasing fatty acid oxidation and up-regulating mitochondrial biogenesis (Minokoshi et al., 2002). pAMPK also inhibits ACC by phosphorylation (pACC) thereby inhibiting fatty acid synthesis (Corton et al., 1995;

Henin et al., 1995). MTII-induced activation of pAMPK would increase pACC, lowering malonyl-CoA concentration. This in turn, relieves the myocyte of inhibition for the uptake of fatty acids into mitochondria via the carnitine carrier system, thus stimulating fatty acid oxidation and also up-regulating mitochondrial biogenesis (Merrill et al., 1997; Winder et al., 2000).

The current results from my data demonstrate that melanocortins act in the VMH to activate SNS outflow, increasing sympathetic drive to skeletal muscle to modulate fuel allocation and use through differential activation of molecular mediators of energy homeostasis. One or more of these molecular pathways likely increases EE and lowers fuel economy during activity, dissipating wasted calories as heat while increasing free fatty acid uptake and use as fuel. Altogether, these results are consistent with the role of MC receptor activation in the VMH and their regulation of peripheral metabolism particularly in tissues like BAT and skeletal muscle via increased sympathetic drive (Shiuchi et al., 2009). These results suggest that the VMH is important for the regulation of peripheral metabolism, and that tissues like skeletal muscle can be a good target system to change EE to treat over-weight and obesity. Based on these studies on the VMH, central MC, and skeletal muscle, I proposed that functioning of this axis is heightened at every level in lean HCR compared to the obesity-prone LCR and may account for the individual differences in obesity propensity, which will be discussed in the next chapter.

CHAPTER 4

4.1 Introduction

As described before in Chapters 1 and 2, compared to LCR, HCR have elevated total EE, and this is predominantly due to heightened non-resting EE (rather than resting EE). This activity-related EE is not completely secondary to elevated physical activity as it persists even during controlled activity, indicating low economy of activity in these rats. Low economy of activity suggests wasting of calories to a greater extent in HCR than LCR, possibly through skeletal muscle thermogenic mechanisms. I found this wastage is in the form of heat, which is potentially regulated through molecular mediators of energy conservation and expenditure, and possibly a result of the enhanced sympathetic drive observed in these HCR. Under baseline conditions, compared to obese LCR, lean HCR rats showed heightened sympathetic drive to skeletal muscle and enhanced expression of mediators of energy expenditure and reduced expression of energy conservation processes, similar to what is seen after central activation of the brain-muscle pathway by MC receptors.

The alterations in the peripheral energy homeostatic mechanisms leading to phenotypic differences in muscle energetics may have a central origin. The hypothalamus, particularly the VMH, along with the central MC system, plays an important role in determining fuel partitioning and usage in peripheral tissues as

described in Chapter 1. I have shown that activation of MC receptors in the VMH increases EE and physical activity, and decreases RER, switching fuel preference to fats; it lowers fuel economy during activity, and 'wasted' calories are dissipated as heat; this process may engage molecular mediators of energy homeostasis. I have identified several potential molecular mediators of EE that showed heightened expression in skeletal muscle of the lean phenotype.

Based on previous studies in our lab (Shukla et al., 2012), we know that HCR and LCR show differences in central melanocortins, a system known to modulate sympathetic drive (Rahmouni et al., 2003; Shiuchi et al., 2009; Toda et al., 2009). Based on these observations, I proposed to examine the role of MC in the VMH in altering activity-related EE, heat dissipation, SNS drive, and molecular mediators of energy homeostasis in our lean and obesity-prone rats. I hypothesize that MC in the VMH is involved in altering skeletal muscle energetics through SNS and is responsible for the muscle work efficiency, contributing to the leanness that characterizes HCR. I predict that activation of MCR in the VMH will increase total EE, particularly activity-related EE, and lower fuel economy during activity, metabolizing fats in lieu of glucose. I also predict an increase in the expression of mediators involved in EE and fatty acid metabolism and decreased expression of energy conserving systems via the SNS to a greater extent in HCR than in LCR. Studies below were designed to investigate how VMH and downstream systems alter skeletal muscle EE, contributing to lean or obese phenotypes.

4.2 Methods

4.2.1 Study 1: Examine the effects of MC receptor activation in the VMH on skeletal muscle energetics, potentially explaining the differences in activity EE between lean rats (HCR) and obesity-prone rats (LCR). I predicted higher overall EE and increased energy use during physical activity in lean rats upon activation of MC receptors in VMH compared to obesity-prone LCR. Based on my results from previous studies, I also predicted that skeletal muscle heat generation will be higher in HCR compared to LCR after intra-VMH MC receptor activation.

Design

4.2.1.1 Study 1a: Measure skeletal muscle heat dissipation after VMH MC receptor activation with MTII in these rats during light phase in their regular cages and during a graded treadmill test. (N=24, 12/group)

Day -30 – 0: Arrival of animals, separation, housing and quarantine. (12/group)

Day 1 – 4: Stereotaxic surgeries to implant guide cannula aimed at VMH and transponder implants adjacent to gastroc in both hind limbs and adjacent to BAT.

Day 5 – 11: Recovery.

Day 12: Divided into MTII- and vehicle-treatment groups. Injected MTII or vehicle (aCSF) and measured heat dissipation at the level of skeletal muscle and BAT every 15 minutes for 4 hrs post-injection.

Day 17: Repeated day 12 by changing treatment (day 12 MTII group gets vehicle on day 17).

Day 21: Trained rats to walk on treadmill.

Day 22: Rats were divided into two cohorts (half of each group); cohort1 was subdivided into MTII- or vehicle-treatment groups. Rats were injected with MTII or aCSF; 105 - 120 minutes post injection, rats were allowed to walk on a treadmill at varying intensities for 30-35 minutes. Gastroc temperatures were measured at regular intervals.

Day 23: Repeated the same with cohort2.

Day 27: Repeated the process by changing the treatment.

Day 28: Repeated the same with cohort2.

4.2.1.2 Study 1b: Measure changes in EE and other calorimetric parameters (RER) upon VMH MC receptor activation with MTII in freely moving and activity-controlled rats. (N=24, 12/group)

Day -30 – 0: Arrival of animals, separation, housing and quarantine. (12/group)

Day 1 – 4: Stereotaxic surgeries to implant guide cannula aimed at VMH and transponder implants adjacent to gastroc in both hind legs and adjacent to BAT.

Day 5 – 11: Recovery

Day 11: Divided into 6 cohorts (4/cohort, 2 from each group) and each cohort into MTII and vehicle treatment groups.

Day 12: Acclimation of cohorts 1, 2, and 3 to calorimetry chamber and test cages.

Day 13: 0900 – 1300 - Measured EE and other calorimetric parameters using Oxymax FAST system (Columbus Instruments, Columbus, Ohio) for cohort 1 for 4 hrs post-injection with MTII or vehicle.

Day 13: 1400 – 1800 – Repeated for cohort 2. After completion removed cohorts 1 and 2 from chamber and placed in cohorts 4, 5, and 6.

Day 14: 0900 – 1300 – Repeated for cohort 3.

Day 14: 1400 – 1800 – Repeated for cohort 4.

Day 15: 0900 – 1300 – Repeated for cohort 5.

Day 15: 1400 – 1800 – Repeated for cohort 6. Removed the animals from calorimetry chamber and returned to the animal facility.

Day 17 - 20: Repeated day 12-15 by changing the treatment.

Day 22: Acclimated cohorts 1, 2, and 3 in calorimetry chamber for treadmill run (controlled activity). Trained rats to run on a treadmill.

Day 23: Each cohort was subdivided into MTII- or vehicle-treatment groups. Rats were injected with MTII or aCSF; at 105 – 120 minutes after injection, rats were allowed to walk on a treadmill for 30 minutes and changes in EE and other calorimetric parameters were measured. Removed cohorts 1 and 2 from the chamber and moved in cohorts 4, 5, and 6.

Day 24: Repeated the same with remaining rats. Removed the rats after completion of run.

Day 27 – 29: Repeated day 22 – 24 by changing treatment.

After completion of the studies, rats were euthanized, and brains were harvested and site checks were done for both cannula and transponder implants. Brains were fixed in formalin (10%) and then transferred to 10% formalin containing 30% sucrose. Only rats in which the dye injection site corresponds to the stereotaxic coordinates within (250μm) of the target (VMH) and transponder implants placed correctly adjacent to gastroc and BAT were used for data analysis in all studies.

4.2.2 Study 2: Examine the effects of VMH MC receptor activation on the SNS and how this pathway alters skeletal muscle energetics in our lean rats compared to obesity-prone rats. I predict that activation of MC receptors in the VMH will increase sympathetic drive to a greater extent in lean rats compared to obesity-prone rats.

Day -30 – 0: Arrival of animals, separation, housing and acclimate. (n=48, 24/group)

Day 1 – 4: Stereotaxic surgeries to implant guide cannula aimed at the VMH.

Day 5 – 11: Recovery.

Day 11: Divided into groups depending on treatment.

Day 12: Day of study

t hrs: Euthanized zero time point group from both HCR and LCR (to obtain baseline tissue NE content) (n=16, 8/group) and injected remaining with aMPT (125 mg aMPT/kg of body weight). (n=32, 16/group)

t+0.5hrs: Injected remaining HCR and LCR with either MTII (20pmoles/200nl) or aCSF (200nl) depending on the group (n=32, 16/group, 8/subgroup).

t+2hrs: Injected remaining animals with 2nd dose of aMPT (125 mg aMPT/kg of body weight). (n=32, 16/group)

t+4hrs: Euthanized rats by rapid decapitation and harvested tissue.

4.2.3 Study 3: Examine the effect of MC receptor activation in VMH on skeletal muscle mRNA and protein expression levels of molecular targets involved in EE, fuel utilization, and energy conservation between HCR and LCR. I predict that compared to LCR, HCR will have higher expression of proteins involved in EE and lower expression of proteins

of energy conservation at both mRNA and protein levels upon VMH MC receptor activation. I also predict that I will find higher expression of proteins involved in fat metabolism in HCR.

Day -30 – 0: Arrival of animals, separation, housing and acclimate. (n=24, 12/group)

Day 1 – 4: Stereotaxic surgeries to implant guide cannula aimed at the VMH.

Day 5 – 11: Recovery.

Day 11: Divided into groups depending on treatment.

Day 12: Day of study

t hrs: Injected with either MTII (20pmoles/200nl) or aCSF (200nl) depending on the group (n=12/group, 6/treatment) (each group was divided into either vehicle or MTII sub-groups)

t+4hrs: Euthanized the rats and harvested tissue.

Animals

Adult male HCR and LCR rats (N=96; 48/group) were obtained from the University of Michigan. Each rat was housed individually on a 12:12 light: dark cycle with lights on at 0700 EST. Rats received rodent chow (5P00 MRH 3000, T.R. Last Co. Inc.) and water *ad libitum*. All studies were conducted according to the Guide for the Care and Use of Laboratory Animals ("National Research Council (US) Committee for the Update of the Guide for the Care and Use of Laboratory Animals," 2011) and approval of the Kent State University IACUC.

Stereotaxic surgeries

Stereotaxic surgeries were performed on the rats once they are acclimated to the housing conditions as described above in Chapter 3. The rats were then allowed to recover with periodic monitoring before the start of the study.

Transponder implantation

A group of male HCR/LCR rats (N=24, 12/group, a subset of larger group mentioned above) received transponder implants during the stereotaxic surgery as described before in Chapter 3.

Body composition

Body composition was measured using EchoMRI-700 (Echo Medical Systems, Houston, TX) to determine the fat and lean mass (in grams) of each rat the day before test. This did not interfere with temperature transponder function.

Measurement of energy expenditure (EE)

After body composition determination, adult male HCR/LCR rats were measured for their EE, physical activity, and other calorimetry parameters after intra-VMH microinjections of MTII or vehicle under freely moving and activity-controlled conditions as described above in Chapter 3. Four days after the first injection, the same test was repeated with rats now receiving counterbalanced treatment (day1 MTII rats receiving vehicle on day5 and *vice versa*). All EE data from both studies were analyzed

using 2x2 mixed ANOVA, with treatment as the within-subjects independent variable and HCR vs. LCR as the between-subjects independent variable.

Home cage temperature and graded treadmill test

To determine whether activation of MC receptors in VMH has any differential effect on the thermogenesis of skeletal muscle of HCR and LCR, I measured the skeletal muscle heat dissipation after intra-VMH MT-II or vehicle microinjection in freely moving rats and during a low-level graded treadmill test as described before in Chapter 3. The activation of BAT thermogenesis is used as a control process during this study. A 3-way ANOVA was used to analyze the data (treatment as the within-subjects independent variable, HCR vs. LCR as the between-subjects independent variable, and with time as the other within-subjects independent variable).

mRNA and protein expression

Tissue samples were processed to evaluate mRNA and protein expression as described above in Chapter 2. The expression levels relative to GAPDH for mRNA and actin for protein were plotted as a percent of the reference value (with HCR-vehicle as 100%), and were analyzed using 2x2 mixed ANOVA, with treatment and HCR vs. LCR as between-subjects independent variable. As I was specifically interested in the magnitude of effect of MTII in HCR vs. LCR, I did planned (*a priori*) comparisons using t-tests with Bonferroni correction (2 t-tests, $0.05/2 = 0.025$, hence $p<0.025$).

Norepinephrine turnover (NETO)

Adult male HCR/LCR rats (N= 48, 24/group, a subset of above mentioned number) were used to assess sympathetic drive to peripheral tissues – liver, heart, BAT, skeletal muscle groups, and different WAT depots. After acclimation, stereotaxic surgeries were performed to implant guide cannulae aimed at VMH and allowed to recover for a week before conducting the experiment. VMH MC receptor activation was achieved through microinjection of the agonist MTII (20pmoles/200nl) with aCSF as a control. Both groups (HCR and LCR) were sub-divided into 3 groups according to the treatment (aMPT/MT-II, aMPT/vehicle, control; 8/treatment). On the day of study, rats receiving aMPT were injected with aMPT (125 mg aMPT/kg of BW, 25 mg/ml) and with a booster dose at same concentration 2 hours later. 30 minutes after first aMPT injection, rats received intra-VMH microinjection of either MT-II or vehicle depending on their group. All rats were euthanized by rapid decapitation between 1200 and 1500, 4 hours after first aMPT injection. Tissues were rapidly dissected and snap-frozen in liquid nitrogen and processed for NETO as described above in Chapter 2. Difference in NETO of intra-VMH MTII microinjected and vehicle microinjected rat tissues were calculated with respect to control group rats and was represented as NETO per gram of tissue in question and analyzed using a 2X2 mixed ANOVA, with treatment (MTII/aCSF) as paired and HCR vs. LCR as between-subjects independent variable.

4.3 Results

Lean HCR with intra-VMH MTII microinjection have higher energy expenditure compared to vehicle treated HCR and obese LCR.

As shown in Figure 39, compared to vehicle-microinjected HCR and MTII/vehicle treated LCR, HCR administered with intra-VMH MTII have significantly higher EE, higher oxygen consumption (VO_2), higher physical activity (horizontal and ambulatory activity), and lower RER. Compared to vehicle-treated LCR, LCR with microinjections of MTII, showed a higher EE, higher VO_2, higher physical activity, and lower RER. While both groups showed a significant response to MTII, the response was significantly greater in the HCR. All rats received microinjections of both vehicle and MTII thereby acting as their own controls during the study and eliminating the effects of body composition and other individual differences on calorimetric parameters. This increase in EE in lean HCR after intra-VMH MTII was significantly higher compared to all other groups even when body composition was taken into account. There was no significant difference in body weight, lean mass, or fat mass between the two sets of injections within the groups although HCR weighed significantly less than LCR and had significantly lower fat mass and lean mass (Table 3).

ANCOVA analyses of EE data from HCR/LCR revealed that body weight or lean mass were the dominant determinants of EE (Gavini et al., 2014), as EE was consistently higher in rats with greater body weight or lean mass (Figure 40). Intra-VMH MTII-induced EE also increased with higher body weight or lean mass, and intra-VMH MTII

treated HCR consistently had higher EE compared to the MTII-treated LCR or other groups after body weight or composition were considered using ANCOVA (Figure 40).

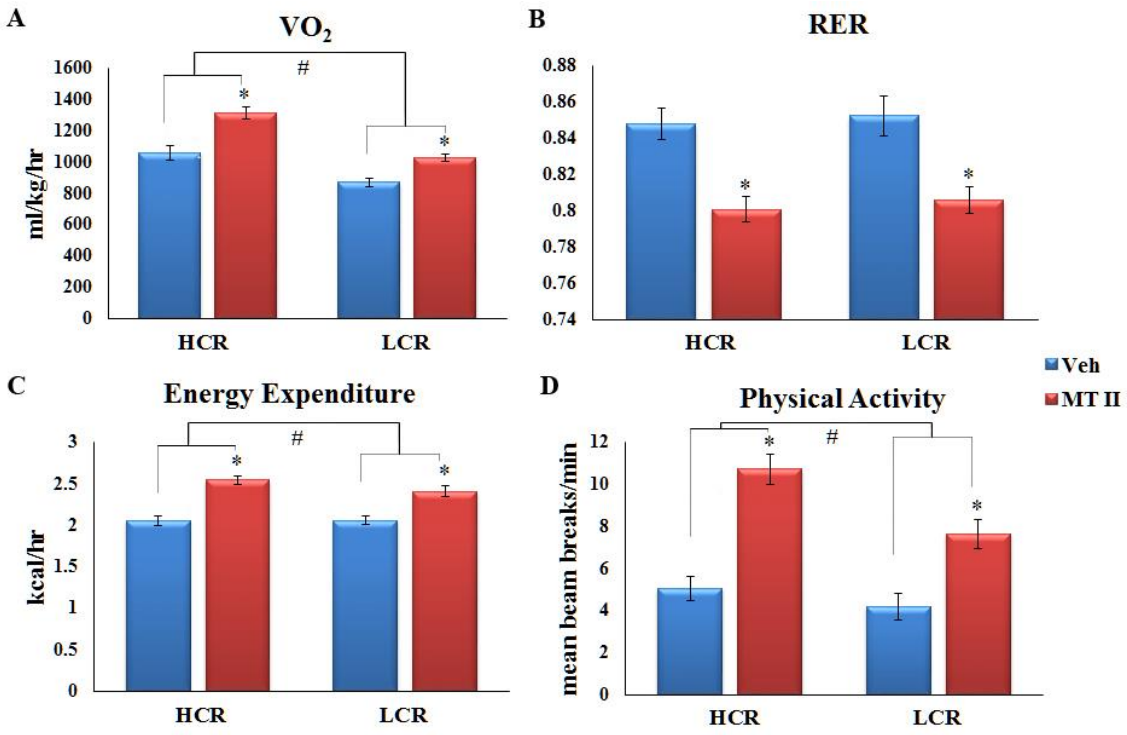

Figure 39: Intra-VMH MTII induced a significant increase in energy expenditure, oxygen uptake, and physical activity, and a significant decrease in respiratory exchange ratio in high- and low-capacity runners (HCR, LCR). HCR were significantly more affected than LCR. (A) Oxygen uptake (VO_2), (B) respiratory exchange ratio (RER), (C) energy expenditure, and (D) physical activity 4hrs after intra-VMH MTII and vehicle administration. Compared to vehicle, MTII microinjections significantly increased VO_2, energy expenditure and physical activity and decreased RER. MTII-induced changes in these parameters were significantly greater in HCR compared to LCR (*significantly greater than vehicle; # significantly greater elevation seen in HCR than in LCR, $p<0.05$).

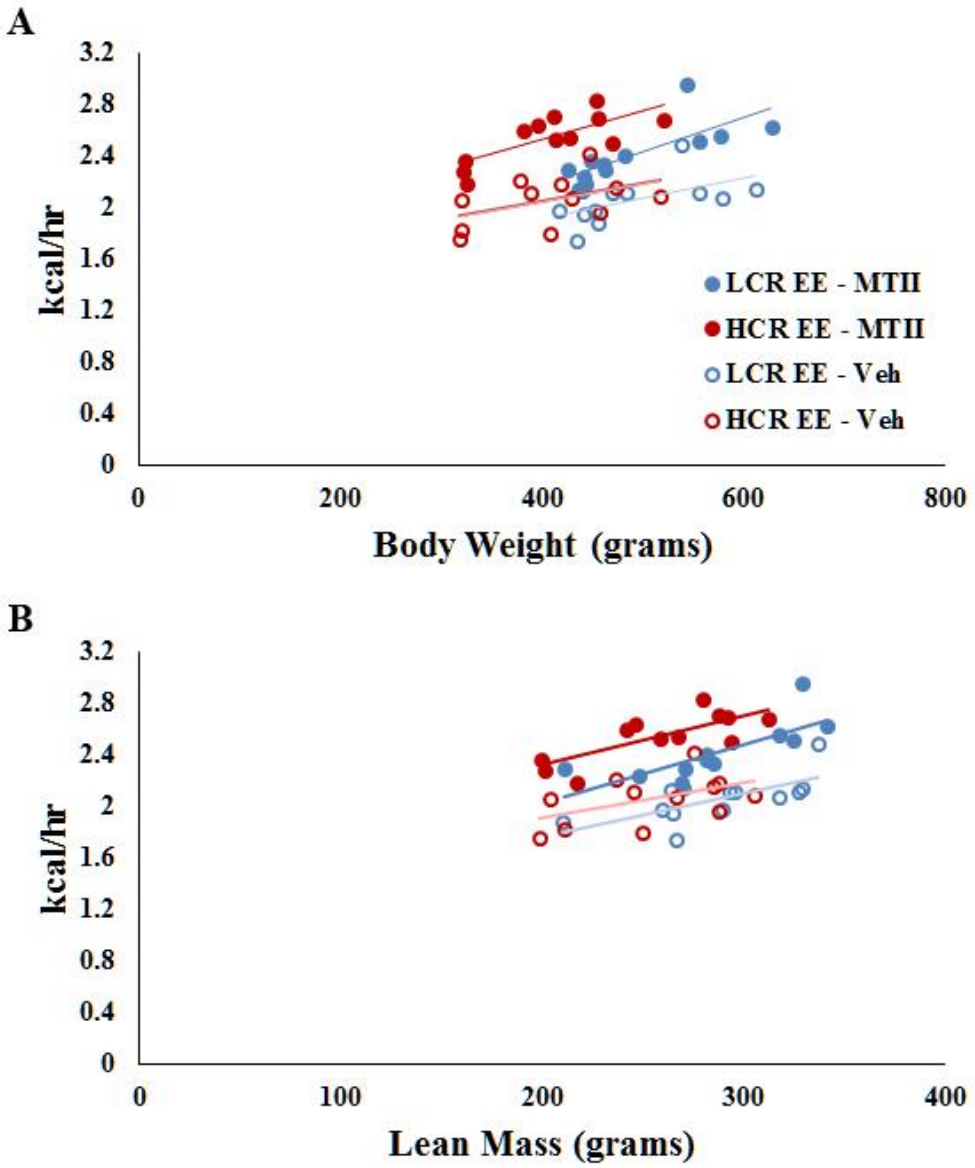

Figure 40: In both high- and low-capacity runners, energy expenditure increased along with body weight and lean mass. Energy expenditure (EE) was significantly higher in the lean phenotype (high-capacity runners, HCR) compared to low-capacity runners (LCR), even after lean mass and body weight were taken into account. MTII-induced EE also increased with body weight (A) and lean mass (B), and intra-VMH MTII-treated HCR had significantly higher EE compared to all other groups. (N=12/group)

4hr EE	HCR *#		LCR	
	Vehicle	MT-II	Vehicle	MT-II
Body Weight	405.925±18.491	408.152±18.131	489.587±18.625	491.722±19.193
Lean Mass	254.078±10.412	257.775±10.834	287.408±10.682	285.442±10.801
Fat Mass	68.016±7.012	68.309±6.642	104.904±10.825	107.759±10.554

Table 3: Body composition of lean high-capacity runners (HCR) and obesity-prone low-capacity runners (LCR). Within group, body weight, lean mass, and fat mass of HCR and LCR rats did not change between MTII and vehicle administration for tests of 4hr energy expenditure. (*$p<0.05$ compared to vehicle-injected LCR, #$p<0.05$ compared to MTII-injected LCR).

Lean HCR with intra-VMH MTII microinjections have higher energy expenditure compared to vehicle-treated HCR and obese LCR during controlled activity.

To ascertain that the increase in calorimetric parameters is not due to increase in physical activity after intra-VMH microinjection of MTII, a controlled treadmill activity study was performed. EE was measured during a low-grade treadmill exercise test controlling rats' workload, and animals were compared to themselves to rule out individual differences in body weight. As shown in Figure 41, compared to vehicle microinjection, rats receiving intra-VMH microinjection of MTII had significantly higher EE, higher VO_2, and lower RER in both HCR and LCR during controlled treadmill activity. The MTII-induced changes in treadmill EE and VO_2 were significantly greater in HCR than in LCR. Therefore, the MTII-induced alterations in calorimetric parameters were not secondary to increased physical activity. As each rat acted as its own control and considering the lack of significant change in body weight, lean mass, or fat mass between treatments, the impact of differential workload (body weight and composition combined with velocity and incline) during activity is negligible (Table 4). In all rats, EE during treadmill activity was consistently higher with greater body weight (Figure 42), which is not surprising as body weight is the main determinant of energy expenditure, especially during activity. Intra-VMH MTII-induced EE also increased with higher body weight and lean mass (Figure 42).

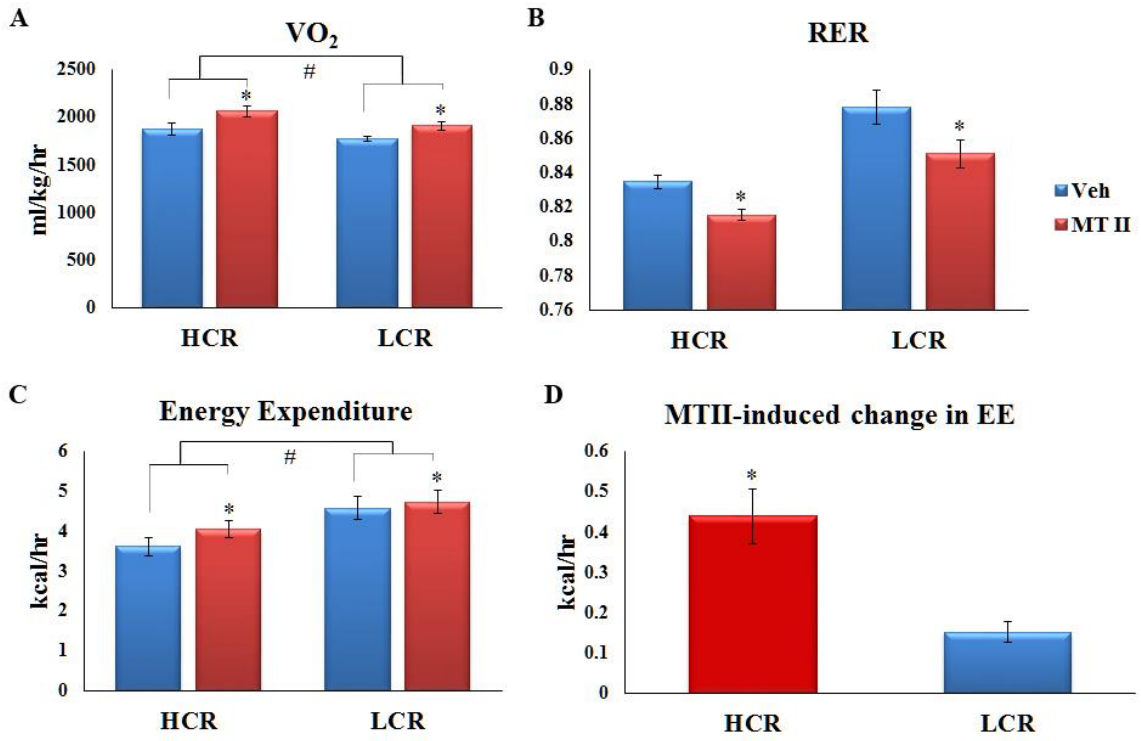

Figure 41: Intra-VMH MTII-induced alterations in energy expenditure and respiratory exchange ratio persisted during controlled treadmill activity, indicating that MTII-induced metabolic changes are not secondary to enhanced physical activity. (A) Oxygen uptake (VO_2), (B) respiratory exchange ratio (RER), and (C) energy expenditure (EE) during controlled treadmill activity after intra-VMH MTII and vehicle administration. Compared to vehicle, MTII microinjections significantly increased VO_2 and EE and decreased RER. (D) The MTII-induced change in EE was significantly higher in HCR compared to LCR. (*significantly greater than vehicle; # significantly greater elevation seen in HCR than in LCR, $p<0.05$).

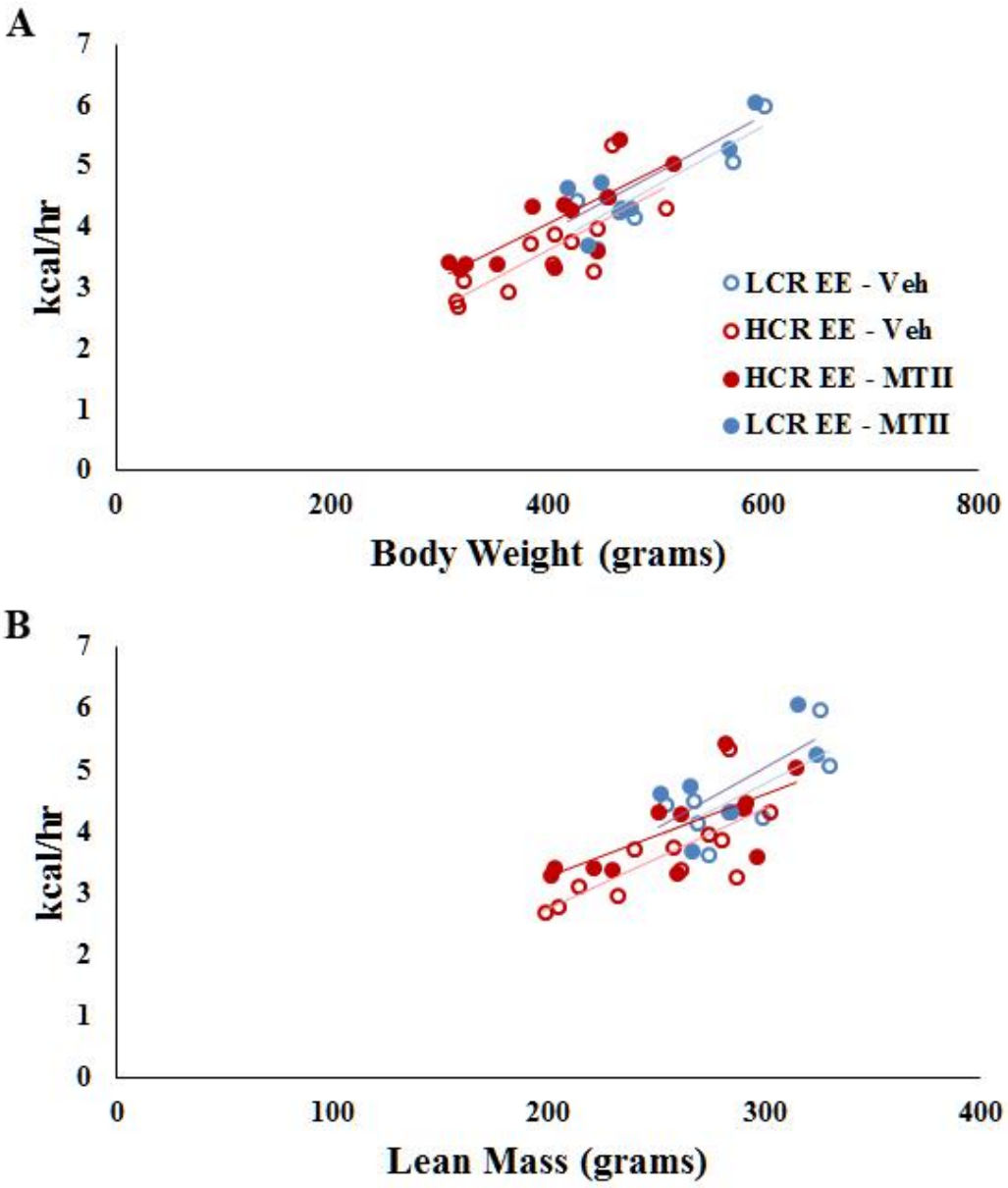

Figure 42: In both high- and low-capacity runners, activity-related energy expenditure increased along with body weight and lean mass. In all rats, activity-related energy expenditure increased along with body weight (A) and lean mass (B); MTII-induced activity-related energy expenditure also increased with body weight (A) and lean mass (B) (N = 12/group).

Treadmill EE	HCR*#		LCR	
	Vehicle	MT-II	Vehicle	MT-II
Body Weight	398.748±17.812	400.803±18.907	491.841±25.242	486.766±25.122
Lean Mass	252.463±10.048	258.017±10.997	288.826±11.401	283.826±10.092
Fat Mass	60.435±6.319	60.962±6.975	106.611±14.561	104.041±14.006

Table 4: Body composition of lean high-capacity runners (HCR) and obesity-prone low-capacity runners (LCR). Within-group body weight, lean mass, and fat mass of HCR and LCR rats did not differ between MTII and vehicle administration during controlled treadmill activity. (*$p<0.05$ compared to vehicle injected LCR, #$p<0.05$ compared to MTII injected LCR).

High activity energy expenditure after intra-VMH MTII microinjection is accompanied by skeletal muscle energy dissipation as heat.

The above study demonstrated that intra-VMH MTII microinjected rats utilized more calories to perform identical activity compared to after vehicle treatment, providing evidence to support the hypothesis that intra-VMH MC receptor activation lowers economy of activity in both the lean HCR and obesity-prone LCR, although this change is more prominent in HCR. This, along with my previous results and literature showing the association between VMH MC receptors and skeletal muscle fuel use and allocation, implicates alteration of skeletal muscle energetics possibly through thermogenic mechanisms as the underlying cause. To test this, I microinjected HCR and LCR rats with MTII or vehicle and measured their BAT and gastroc temperatures under resting conditions and during a graded treadmill activity test. During resting, compared to vehicle, MTII induced an increase in BAT temperature, and the change in temperature from baseline was significantly higher after MTII treatment (compared to vehicle) between 30min and 120min after injection (Figure 43). There was no difference either in temperature or change in temperature of BAT between HCR and LCR in response to MTII. In contrast to my prediction, compared to vehicle, intra-VMH MTII did not significantly increase gastroc muscle temperatures throughout the test duration; similarly, MTII did not induce a significant elevation in temperature when calculated as change from baseline temperature (Figure 44).

Next, I determined if the compromised economy of activity induced by central MC receptor activation is accompanied by energy dissipation through heat in skeletal

muscle. This was tested by measuring gastroc temperature during a graded exercise treadmill test. All rats received both sets of injections, and there were no significant changes in body weight, lean mass, or fat mass observed within groups between injections. Compared to vehicle injections, MTII injections induced higher gastroc temperatures in both HCR and LCR rats. This MTII-induced increase in maximal temperature was not significantly different between the groups, however (Figure 45). Consistent with my previous results (Chapter 2), lean HCR had higher skeletal muscle heat dissipation under both vehicle- and MTII-injected conditions compared to obesity-prone LCR whether treated with vehicle or MTII. These results demonstrate that intra-VMH MC receptor activation may lower the economy of activity where surplus calories are dissipated as heat by skeletal muscle as evident by higher gastroc temperatures, but there was no discernable difference in its effectiveness between lean and obese groups.

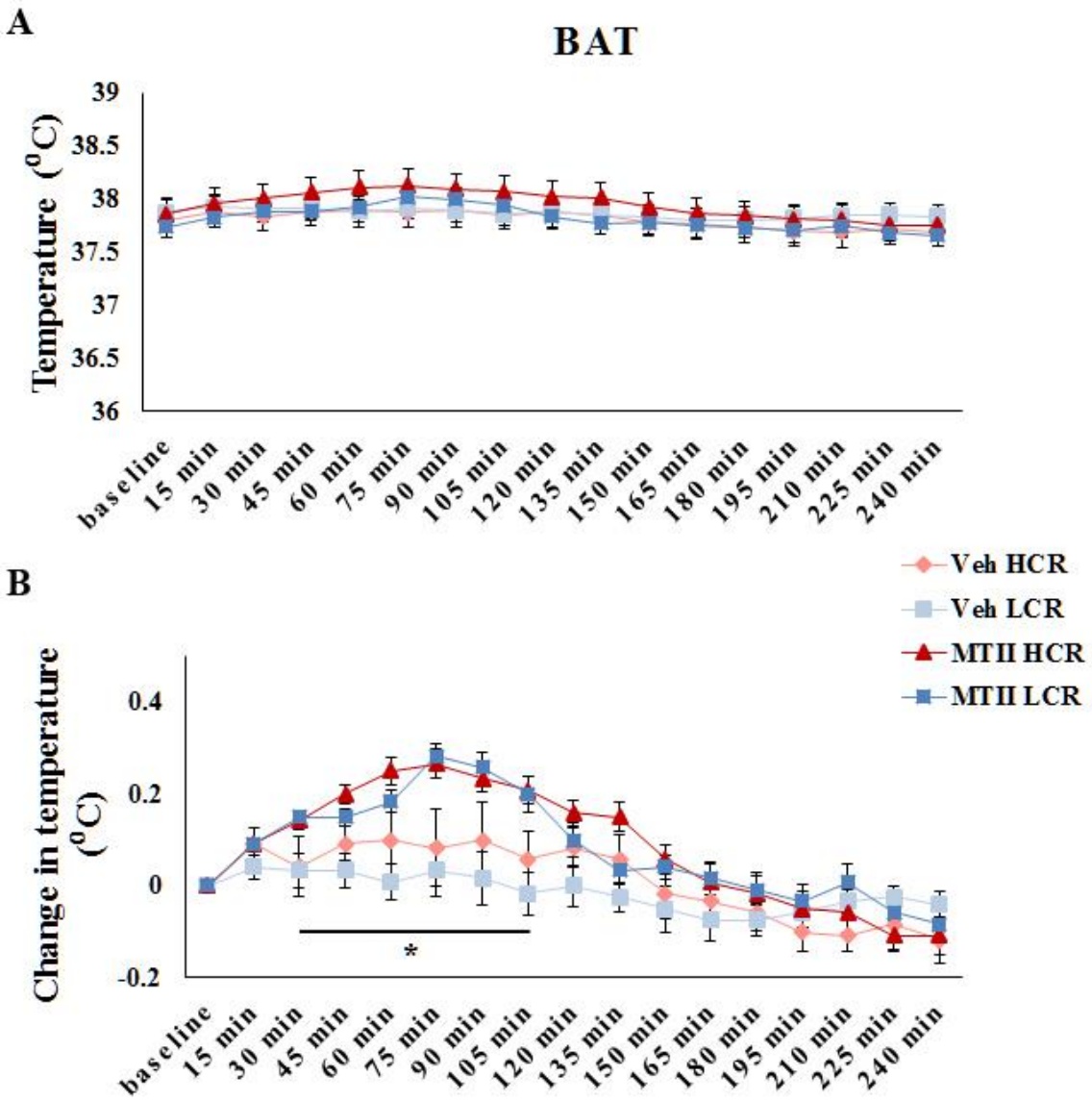

Figure 43: Intra-VMH MTII-induced increase in brown adipose tissue temperature in lean high-capacity runners (HCR) and obesity-prone low-capacity runners (LCR). (A) Compared to vehicle treatment, intra-VMH MTII induced a moderate but significant increase in brown adipose tissue (BAT) temperature in both lean HCR and obesity-prone LCR. (B) Change in BAT temperature was significantly greater after MTII treatment compared to vehicle between 30min and 120 min. (*significantly elevated over vehicle for both HCR and LCR, $p<0.05$)

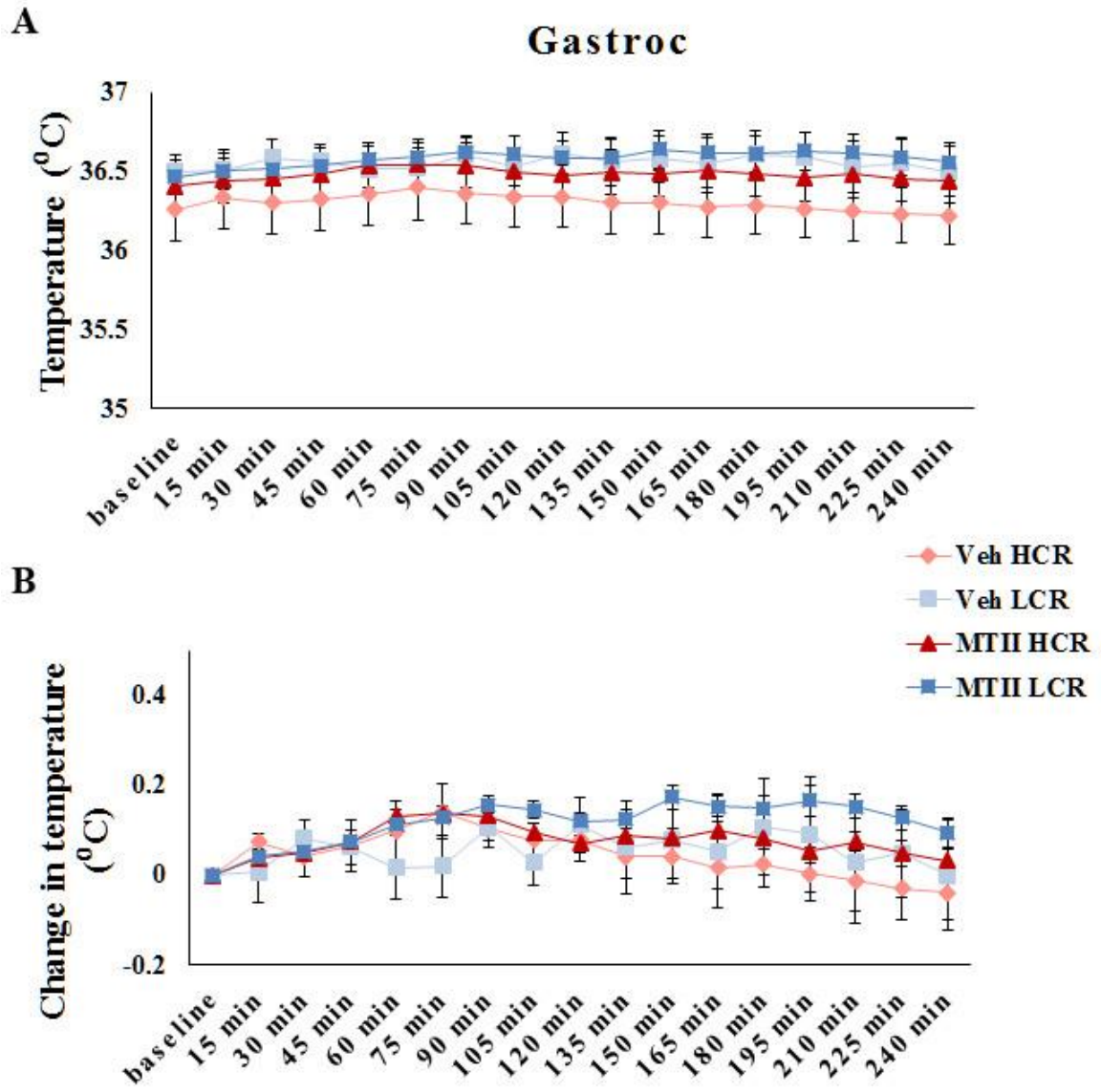

Figure 44: Gastrocnemius temperature after intra-VMH MTII in lean high-capacity runners and obesity-prone low-capacity runners. (A) Intra-VMH MTII-induced gastrocnemius (gastroc) temperature of lean HCR and obesity-prone LCR. (B) Change in temperature of gastroc from baseline after intra-VMH microinjections of MTII and vehicle.

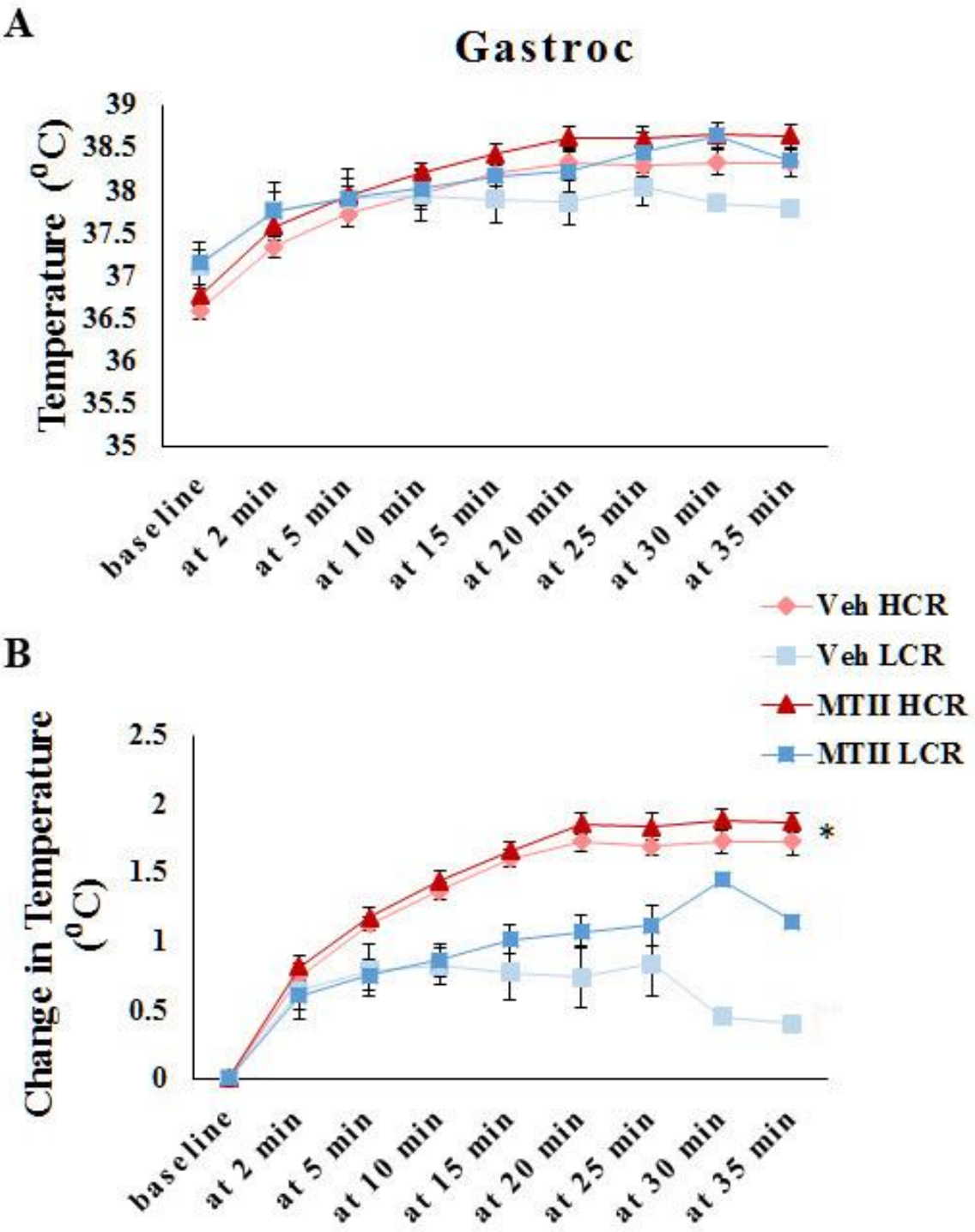
A
Gastroc
Temperature (°C)
39
38.5
38
37.5
37
36.5
36
35.5
35
baseline
at 2 min
at 5 min
at 10 min
at 15 min
at 20 min
at 25 min
at 30 min
at 35 min
Veh HCR
Veh LCR
MTII HCR
MTII LCR
B
Change in Temperature (°C)
2.5
2
1.5
1
0.5
0
*
baseline
at 2 min
at 5 min
at 10 min
at 15 min
at 20 min
at 25 min
at 30 min
at 35 min

Figure 45: Intra-VMH MTII increased activity-associated gastrocnemius temperature of high-capacity runners (HCR) and low-capacity runners (LCR) during graded treadmill exercise test. (A) Temperature and (B) change in temperature from baseline of gastrocnemius (gastroc) of lean HCR and obesity-prone LCR after intra-VMH MTII and vehicle treatments. Compared to vehicle treatment, gastroc temperature was higher after MTII treatment, although the increase in temperature from baseline was not significantly greater after MTII microinjection compared to vehicle. The increase in temperature from baseline was significantly higher in HCR (both vehicle and MTII groups) compared to LCR in either treatment condition (*HCR>LCR, $p<0.05$).

Intra-VMH MTII microinjection differentially elevated sympathetic drive to metabolic tissues in lean vs. obesity-prone rats.

Compared to vehicle microinjection, intra-VMH MT-II induced a significant increase in SNS drive to skeletal muscle of both lean HCR and obesity-prone LCR, although HCR were significantly more affected than LCR in some muscle subgroups (soleus, quadriceps, and gastrocnemius) (Figure 46). Intra-VMH MT-II also induced a significant increase in SNS drive to all white adipose depots studied, brown adipose tissue, heart, and liver (Figures 47 and 48). MTII-induced NETO was greater in HCR than in LCR for MWAT, GWAT, and IWAT (Figure 47), as well as for BAT and liver (Figure 48). Interestingly, both baseline and MTII-induced NETO of LCR was greater than that of HCR in heart (Figure 48), consistent with data suggestive of cardiovascular fitness associated with aerobic capacity. Compared to vehicle-treated LCR, vehicle-treated HCR had higher NETO in skeletal muscle, liver, BAT, and WAT depots. These are consistent with my previous findings in the HCR/LCR rats under baseline conditions for skeletal muscle and BAT (Chapter 2) (Gavini et al., 2014). These results support the hypothesis that the brain-muscle pathway, modulated by melanocortin receptors in the VMH, more effectively impacts metabolism in HCR compared to LCR, potentially due to differential activation of SNS, modulating muscle fuel storage and utilization.

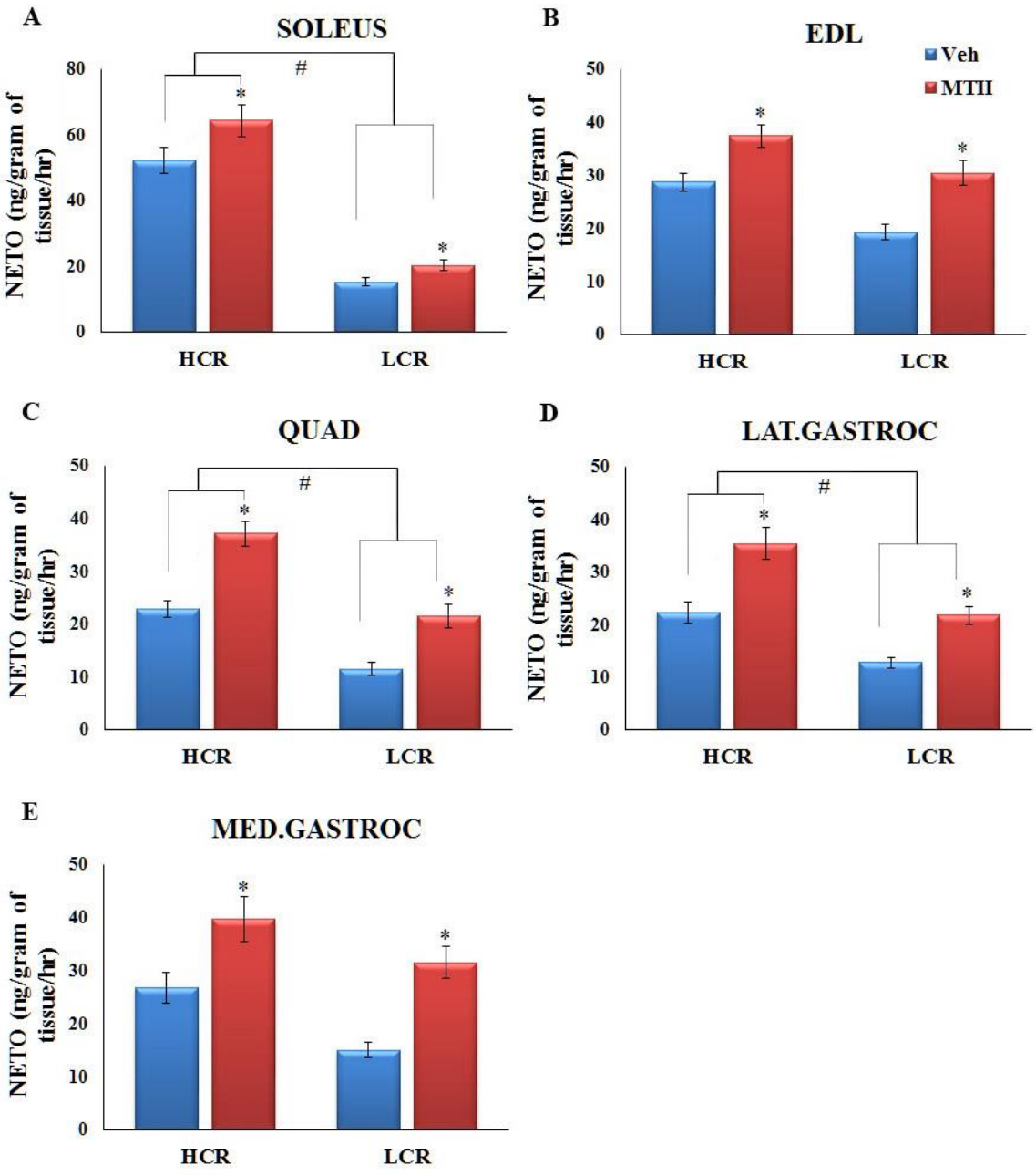
A
SOLEUS
NETO (ng/gram of tissue/hr)
80
60
40
20
0
#
*
*
HCR
LCR
B
EDL
Veh
MTII
NETO (ng/gram of tissue/hr)
50
40
30
20
10
0
*
*
HCR
LCR
C
QUAD
NETO (ng/gram of tissue/hr)
50
40
30
20
10
0
#
*
*
HCR
LCR
D
LAT.GASTROC
NETO (ng/gram of tissue/hr)
50
40
30
20
10
0
#
*
*
HCR
LCR
E
MED.GASTROC
NETO (ng/gram of tissue/hr)
50
40
30
20
10
0
*
*
HCR
LCR

Figure 46: Intra-VMH MTII induced a significant increase in skeletal muscle NETO. This effect was significantly greater in HCR than LCR in soleus, quadriceps, and gastrocnemius muscle groups. Norepinephrine turnover (NETO) in skeletal muscle of HCR and LCR in (A) soleus, (B) extensor digitorum longus (EDL), (C) quadriceps, (D) lateral gastrocnemius, and (E) medial gastrocnemius. Compared to vehicle, intra-VMH MTII induced a significant increase in NETO in both HCR and LCR. (*significant increase by MTII over vehicle; #significant interaction where the MTII-induced increase was greater in HCR than in LCR, $p<0.05$).

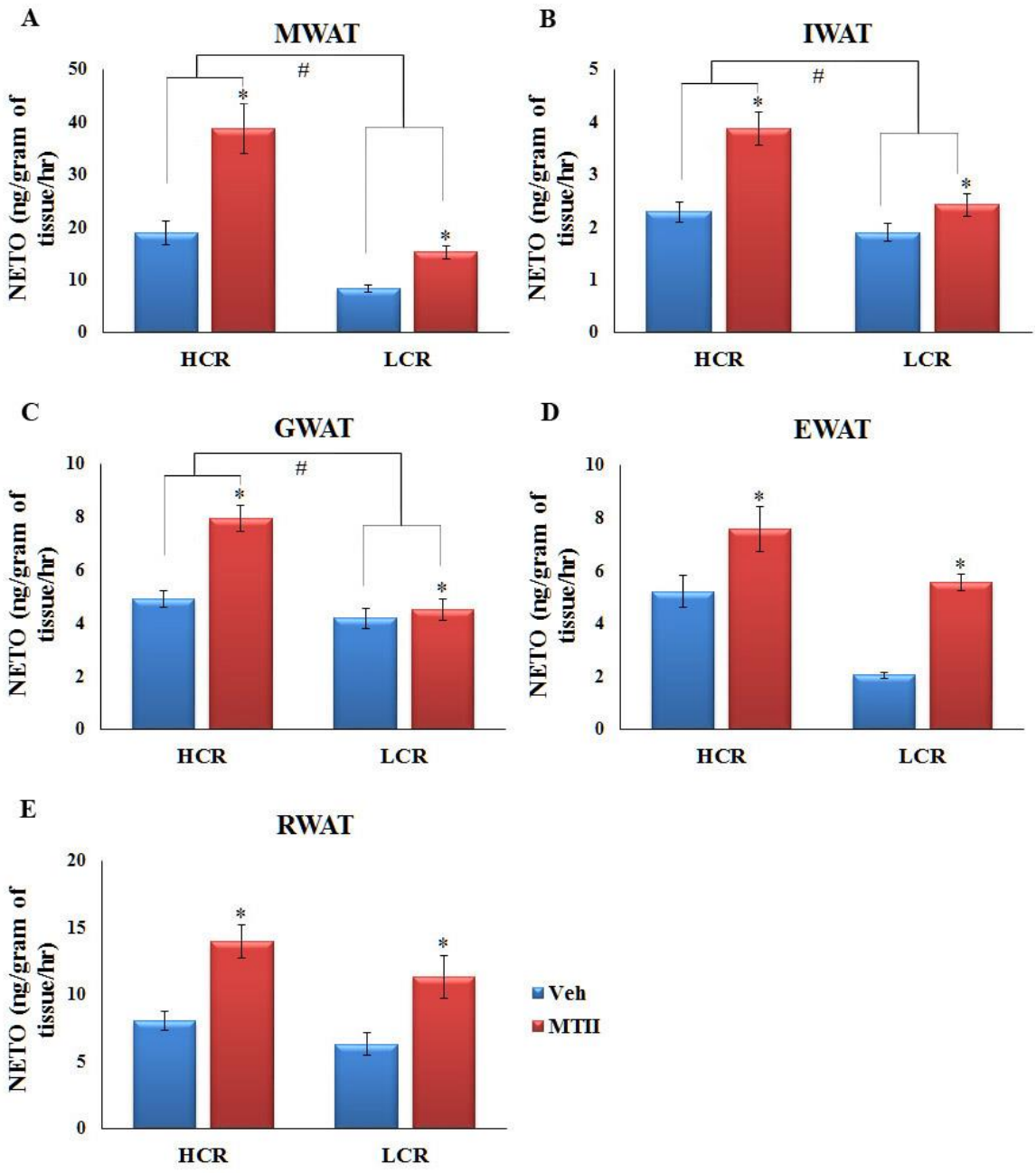
A
MWAT
NETO (ng/gram of tissue/hr)
50
40
30
20
10
0
#
*
*
HCR
LCR
B
IWAT
NETO (ng/gram of tissue/hr)
5
4
3
2
1
0
#
*
*
HCR
LCR
C
GWAT
NETO (ng/gram of tissue/hr)
10
8
6
4
2
0
#
*
*
HCR
LCR
D
EWAT
NETO (ng/gram of tissue/hr)
10
8
6
4
2
0
*
*
HCR
LCR
E
RWAT
NETO (ng/gram of tissue/hr)
20
15
10
5
0
*
*
HCR
LCR
Veh
MTII

Figure 47: Intra-VMH MTII induced a significant increase in NETO of different white adipose depots. Norepinephrine turnover (NETO) of HCR and LCR in white adipose depots (WAT): (A) mesenteric WAT (MWAT), (B) inguinal WAT (IWAT), (C) gluteal WAT (GWAT), (D) epididymal WAT (EWAT), and (E) retroperitoneal WAT (RWAT). Compared to vehicle, intra-VMH MTII induced a significant increase in NETO in both HCR and LCR. This effect was significantly greater in HCR than LCR in MWAT, GWAT, and IWAT. (*significant increase by MTII over vehicle; #significant interaction where the MTII-induced increase was greater in HCR than in LCR, $p<0.05$).

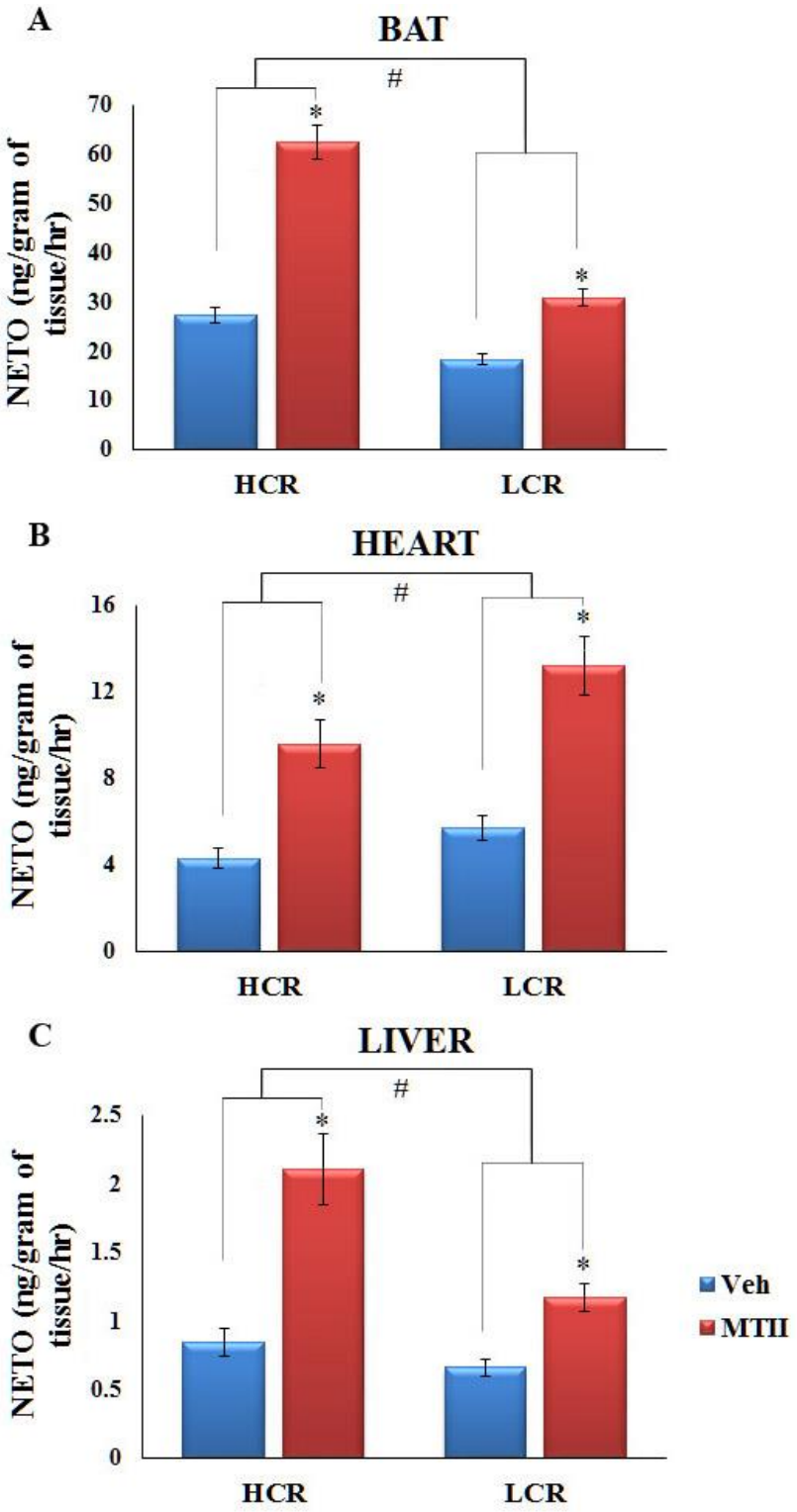
A
BAT
#
*
*
NETO (ng/gram of tissue/hr)
70
60
50
40
30
20
10
0
HCR
LCR
B
HEART
#
*
*
NETO (ng/gram of tissue/hr)
16
12
8
4
0
HCR
LCR
C
LIVER
#
*
*
NETO (ng/gram of tissue/hr)
2.5
2
1.5
1
0.5
0
HCR
LCR
Veh
MTII

Figure 48: Intra-VMH MTII induced a significant increase in NETO of brown adipose tissue, heart, and liver. Norepinephrine turnover (NETO) of HCR and LCR in (A) brown adipose tissue (BAT), (B) heart, and (C) liver. Compared to vehicle, intra-VMH MTII induced a significant increase in NETO in both HCR and LCR. Change in NETO was higher for HCR in BAT and liver and for LCR in heart. (*significant increase by MTII over vehicle; #significant interaction where the MTII-induced increase was greater in HCR than in LCR except for heart where LCR>HCR, $p<0.05$).

Intra-VMH MTII microinjection elevated expression of mRNA of mediators of energy expenditure, with a trend towards lowering expression of energy conserving processes in peripheral metabolism.

To determine the source of increased EE and heat dissipation in MTII-treated rats, I examined levels of mRNA expression of potential molecular mediators of energy balance in the skeletal muscle including quad and gastroc, as well as in BAT, WAT, and liver as described in Chapter 3. I found that, compared to vehicle-treated HCR, HCR with intra-VMH MTII microinjections had significantly elevated mRNA expression of UCP1, PGC-1α, PPARδ, PPARγ, and PPARα in BAT (Figure 49). Obesity-prone LCR with intra-VMH MTII did not show a significant increase the mRNA expression of above said proteins in BAT (Figure 49).

Intra-VMH MTII induced a significant increase in mRNA expression of PPARγ, PPARα, and PPARδ in WAT of intra-VMH MTII treated HCR compared to vehicle treatment in the same group (Figure 50). Compared to vehicle-treated LCR, intra-VMH MTII LCR did show significantly increased mRNA expression of PPARα and PPARδ in WAT with an increasing trend for UCP2, PPARγ, and β_3-AR (Figure 50). Intra-VMH MTII-treated HCR showed a significant increase in mRNA expression of UCP2, PPARα, PPARδ, PPARγ, and PGC-1α and an increasing trend for β_2 AR in the liver compared to vehicle-treated HCR (Figure 51). Compared to vehicle-treated LCR, intra-VMH MTII-treated LCR had a significant increase in mRNA expression of PPARα, PPARδ, PPARγ, and PGC-1α and an increasing trend for UCP2 and β_2 AR in the liver (Figure 51).

Quadriceps of MTII-microinjected HCR showed significantly higher mRNA expression of UCP2, UCP3, PPARα, PPARδ, SERCA1, and SERCA2 and an increasing trend in expression of PGC-1α, PPARγ, and β_2 AR (Figure 52). Quadriceps of intra-VMH MTII-treated rats also showed trend toward lower mRNA expression of Kir6.1, Kir6.2, and MED1 (Figure 52). Compared to vehicle-administered LCR, LCR with MTII showed significant higher mRNA expression of UCP2 and UCP3, and an increasing trend in expression of PPARα in the quad. LCR also showed trend toward lower expression of Kir6.1, Kir6.2, and MED1 after MTII microinjection (Figure 52).

Compared to vehicle, gastroc muscle of intra-VMH MTII HCR had significantly higher mRNA expression of UCP2, UCP3, PGC-1α, PPARα, PPARδ, PPARγ, SERCA1, SERCA2, and β_2 AR (Figure 53). Gastroc muscle also showed a significant decrease in Kir6.2 and a decreasing trend in Kir6.1 and MED1 (Figure 53). Gastroc of intra-VMH MTII-injected LCR showed a significant increase in expression of UCP2, UCP3, PPARα, PPARγ, and SERCA2. MTII-treated LCR also showed an increasing trend in mRNA expression of PGC-1α, and PPARδ (Figure 53), and a decreasing trend in Kir6.2 (Figure 53).

Protein expression of mediators of EE did not consistently change in accordance with mRNA expression. Compared to vehicle, BAT of intra-VMH MTII-treated HCR showed significantly higher expression of UCP1, PGC-1α, pAMPK, and pACC, and an increasing trend in expression of PPARα and CPT1 (Figure 54). No significant differences were observed in MTII-treated LCR, with trends toward higher PPARα,

pAMPK, PPARγ, and pACC (Figure 54). No significant differences were observed except in expression of pAMPK in WAT of MTII-treated HCR compared to vehicle-treated HCR (Figure 56). Compared to vehicle-injected HCR, liver of MTII-microinjected HCR showed significantly more pACC and pAMPK and an increasing trend in expression of PPARγ, UCP2, PPARδ, and PPARα (Figure 57). No significant differences were observed in LCR (Figure 57).

Compared to vehicle-injected HCR, quadriceps of MTII-treated HCR did not show any significant difference in protein expression of the proteins described above, but showed an increasing trend in expression of pAMPK, pACC, PPARγ, and SERCA1 (Figure 58). No significant differences or trends were found in protein expression of these energy mediators in MTII-injected LCR (Figure 58). Compared to vehicle-administered HCR, gastroc muscle of intra-VMH MTII-microinjected HCR showed a significant increase in the expression of PGC-1α, pAMPK, and pACC (Figure 59). Gastroc muscle of MTII-treated HCR also showed an increasing trend in PPARα, SERCA1, SERCA2, β_2 AR, PPARγ, PPARδ, UCP3, CPT1 and CD36/FAT (Figure 59). In LCR, no significant differences were observed in gastroc protein expression with MTII treatment (Figure 59).

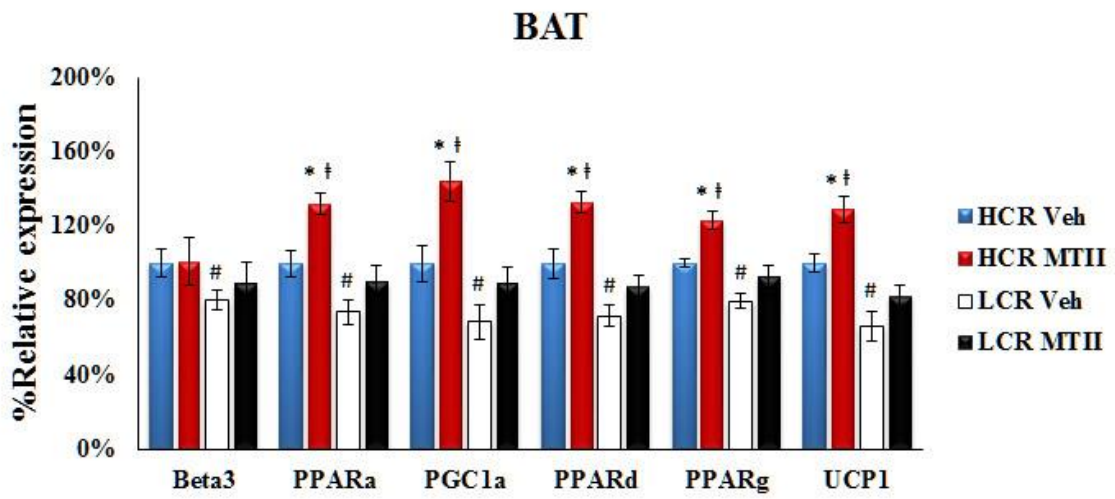

Figure 49: Intra-VMH MTII-induced mRNA expression of mediators of energy expenditure in the brown adipose tissue (BAT) of lean high-capacity runners (HCR) and obesity-prone low-capacity runners (LCR). Compared to vehicle-administered HCR, HCR with MTII microinjections have elevated expression of UCP1, PGC-1α, PPARα, PPARδ, and PPARγ in BAT. Compared to vehicle-treated LCR, LCR treated with MTII showed only trends toward increase in some mediators of energy expenditure in BAT. (*significantly greater than vehicle within group; łsignificantly greater than MTII-treated LCR; #significantly different from HCR vehicle, $p<0.05$).

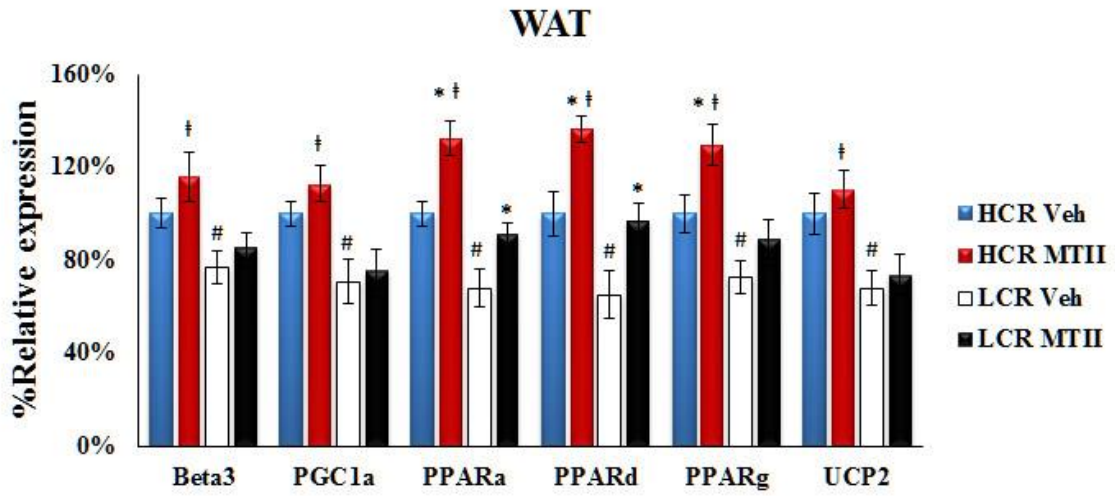

Figure 50: Intra-VMH MTII microinjection increased mRNA expression of mediators of energy expenditure in white adipose tissue (WAT) of HCR and LCR. Compared to vehicle treated HCR, HCR with intra-VMH MTII microinjections have enhanced expression of PPARγ, PPARα, and PPARδ and a trend toward increase in β_3-AR (Beta3) in WAT. MTII also enhanced the expression of PPARα and PPARδ with a trend toward increase in PPARγ in LCR. (*significantly greater than vehicle within group; łsignificantly greater than MTII-treated LCR; #significantly different from HCR vehicle, $p<0.05$).

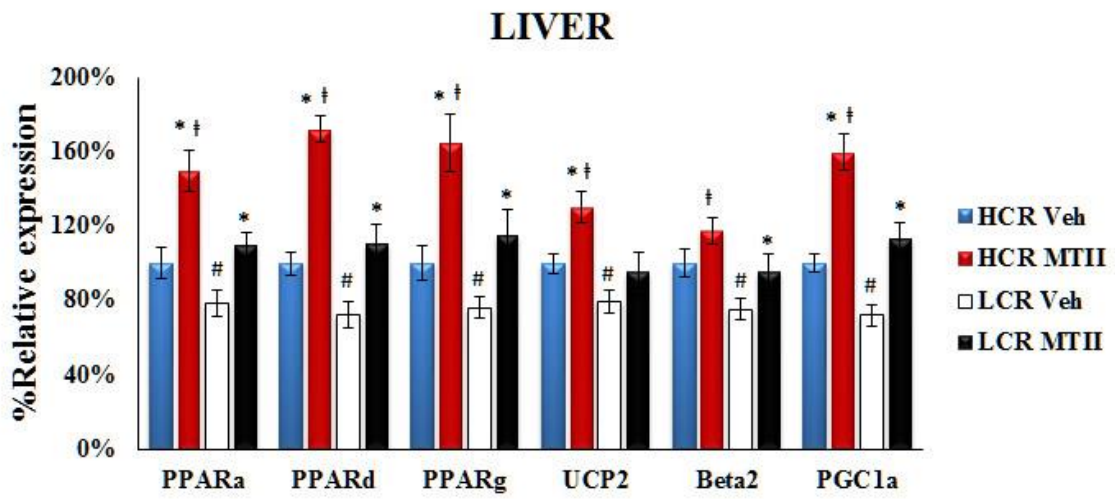

Figure 51: Intra-VMH MTII enhanced mRNA expression of mediators of energy expenditure in the liver of HCR and LCR. Compared to vehicle-treated HCR, HCR with intra-VMH MTII microinjections have elevated expression of UCP2, PPARα, PPARγ, PPARδ, and PGC-1α and a trend toward increase in β_2-AR in the liver. LCR treated with MTII also showed higher mRNA expression of PPARα, PPARδ, PPARγ, and PGC-1α and a trend toward higher β_2-AR in the liver. (*significantly greater than vehicle within group; łsignificantly greater than MTII-treated LCR; #significantly different from HCR vehicle, $p<0.05$).

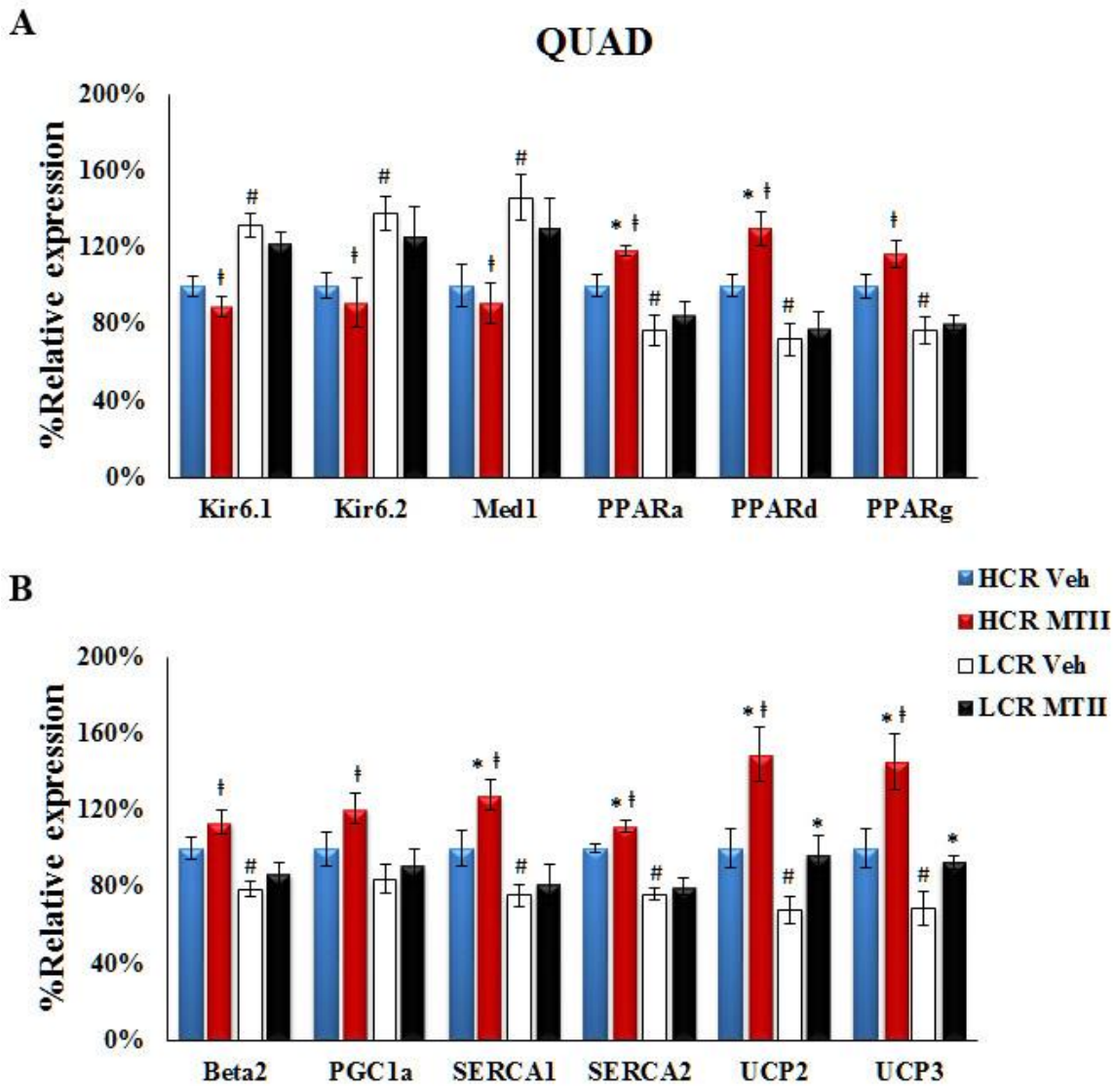
A
QUAD
%Relative expression
200%
160%
120%
80%
40%
0%
Kir6.1
Kir6.2
Med1
PPARa
PPARd
PPARg
B
HCR Veh
HCR MTII
LCR Veh
LCR MTII
%Relative expression
200%
160%
120%
80%
40%
0%
Beta2
PGC1a
SERCA1
SERCA2
UCP2
UCP3

Figure 52: Intra-VMH MTII microinjection enhanced mRNA expression of mediators of energy expenditure in the quadriceps of high- and low-capacity runners (HCR, LCR). Compared to vehicle-administered HCR, HCR with intra-VMH MTII microinjections have elevated expression of UCP2, UCP3, SERCA1, SERCA2, PPARα, and PPARδ and a trend toward increase in PGC-1α and PPARγ in the quadriceps (quad). Quad of intra-VMH MTII-treated LCR also showed enhanced mRNA expression of UCP2 and UCP3. (*significantly greater than vehicle within group; ŧsignificantly greater than MTII-treated LCR except for Kir6.1, Kir6.2, and MED1; #significantly different from HCR vehicle, $p<0.05$).

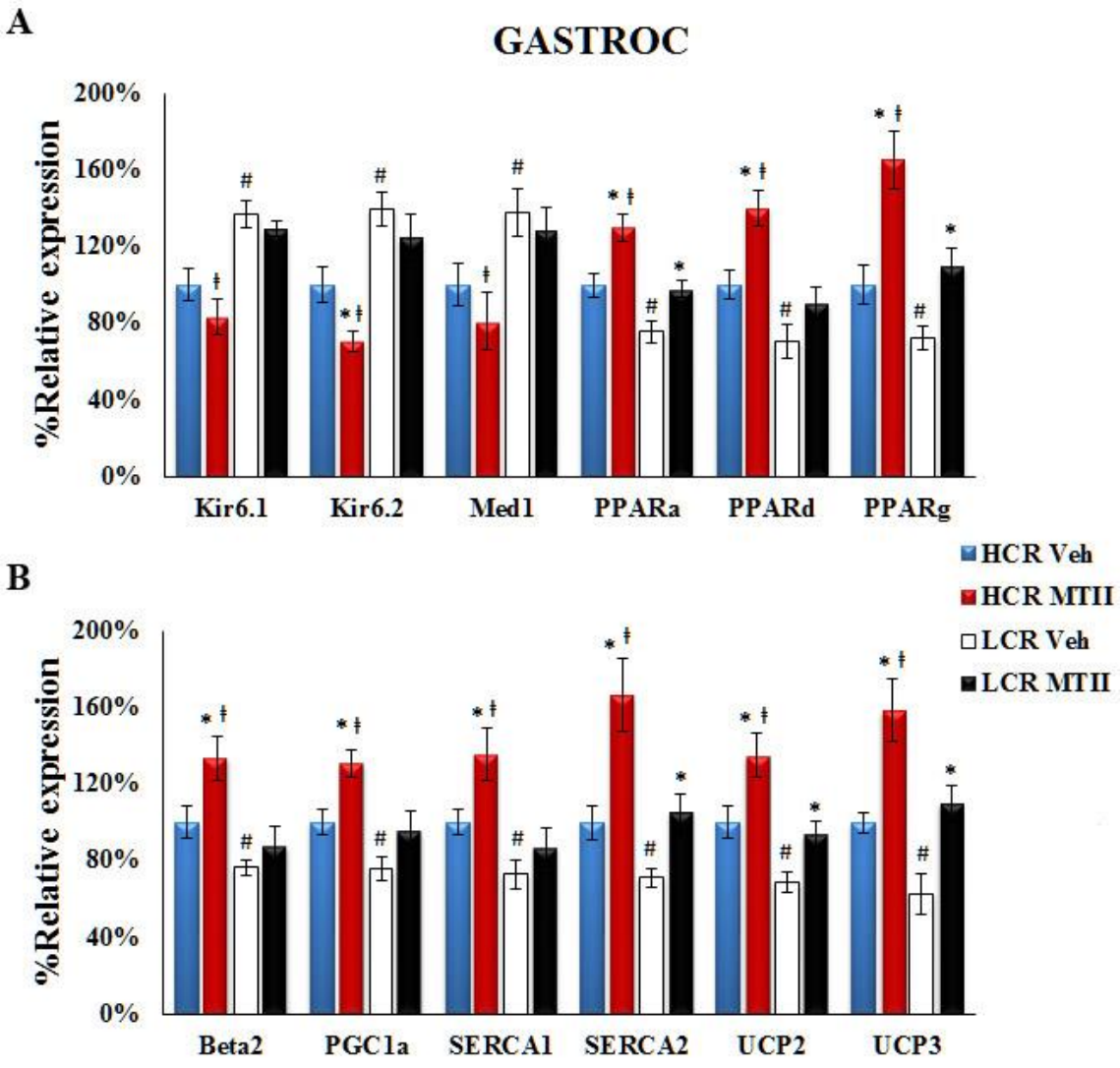
A
GASTROC
%Relative expression
200%
160%
120%
80%
40%
0%
Kir6.1
Kir6.2
Med1
PPARa
PPARd
PPARg
B
%Relative expression
200%
160%
120%
80%
40%
0%
Beta2
PGC1a
SERCA1
SERCA2
UCP2
UCP3
HCR Veh
HCR MTII
LCR Veh
LCR MTII

Figure 53: Intra-VMH MTII induced enhanced mRNA expression of mediators of energy expenditure in the gastrocnemius with a trend towards lower expression of energy conserving processes in high- and low-capacity runners (HCR, LCR). Compared to vehicle-treated HCR, HCR with MTII microinjections showed elevated expression of UCP2, UCP3, SERCA1, SERCA2, PGC-1α, β_2-AR, PPARδ, PPARα, and PPARγ in the gastrocnemius (gastroc). MTII-treated HCR also showed a reduction in expression of Kir6.2 and a trend toward a decrease in that of Kir6.1 and MED1. Gastroc of intra-VMH MTII-treated LCR also showed enhanced mRNA expression of PPARα, PPARγ, SERCA2, UCP2, and UCP3. (*significantly greater than vehicle within group; łsignificantly greater than MTII-treated LCR except for Kir6.1, Kir6.2, and MED1; #significantly different from HCR vehicle, $p<0.05$).

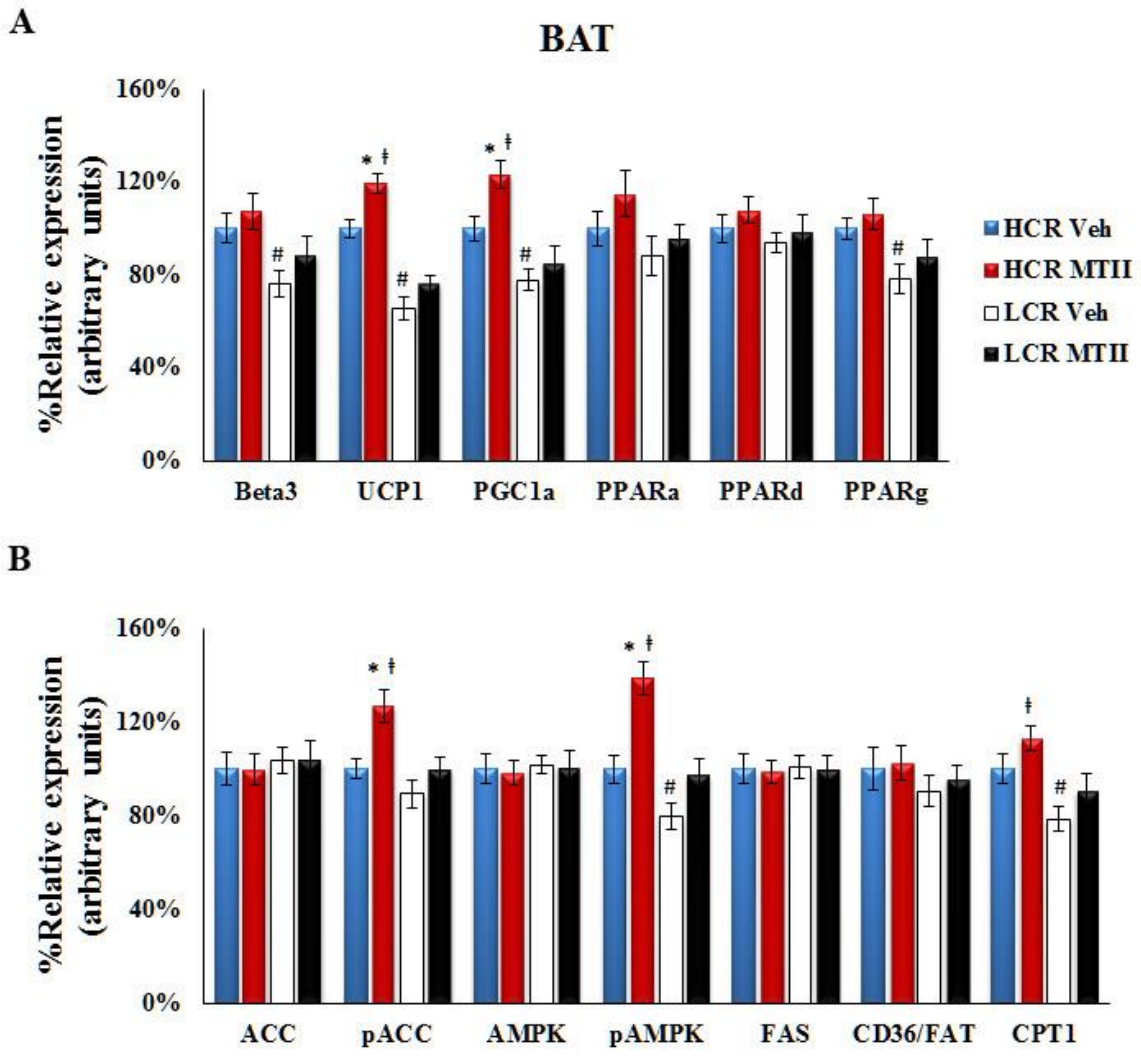

Figure 54: Intra-VMH MTII microinjection showed a trend toward an increase in protein expression of mediators of energy expenditure in the brown adipose tissue (BAT) of high- and low-capacity runners (HCR, LCR). Compared to vehicle treatment, HCR with intra-VMH MTII microinjections have elevated expression of UCP1, PGC-1α, pAMPK, and pACC and a trend toward increase in PPARα and CPT1 in BAT. Compared to vehicle injected LCR, MTII-treated LCR showed a trend toward increase in expression of pAMPK, pACC, and CPT1. (*significantly greater than vehicle within group; łsignificantly greater than MTII-treated LCR; #significantly different from HCR vehicle, $p<0.05$).

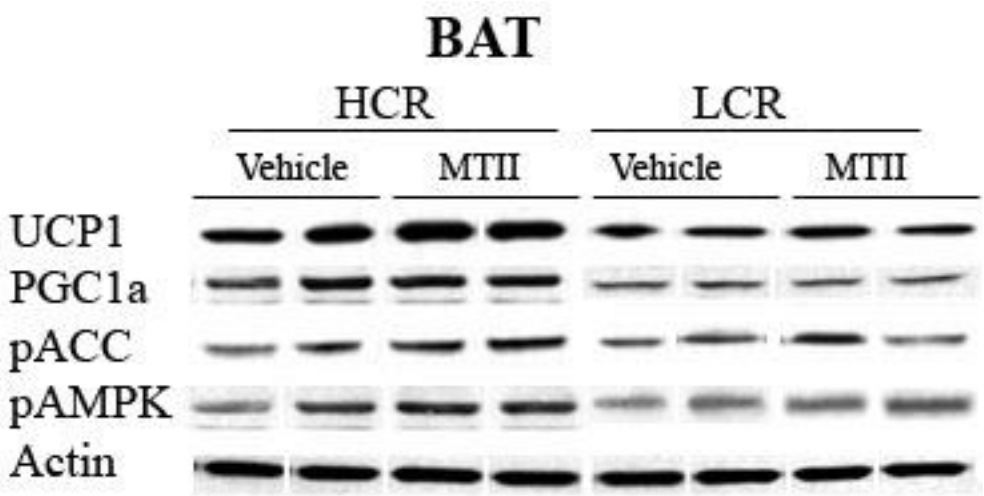

Figure 55: Representative western blot images showing the expression of molecular mediators of energy balance in the brown adipose tissue (BAT) of high- and low-capacity runners (HCR, LCR). Uncoupling protein 1 (UCP1), peroxisomal proliferator activator γ coactivator 1α (PGC-1α), p-acetyl-CoA carboxylase (pACC), p-AMP-activated protein kinase (pAMPK), and actin as the loading control.

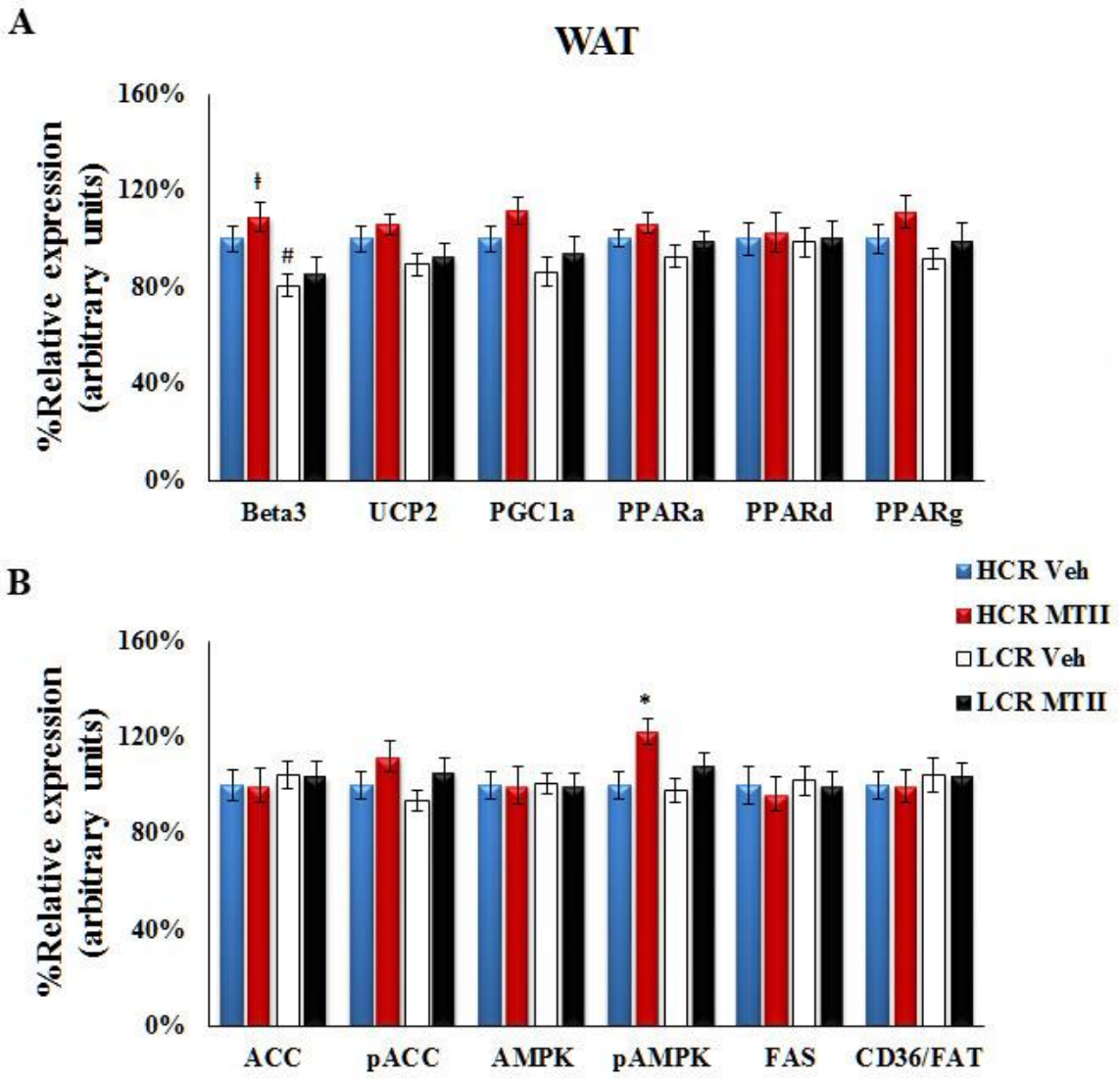

Figure 56: Intra-VMH MTII did not significantly alter protein expression of mediators of energy expenditure in white adipose tissue (WAT) of lean high- and obesity-prone low-capacity rats (HCR, LCR). Compared to vehicle-treated HCR, HCR with intra-VMH MTII microinjections had a significant increase in expression of pAMPK in WAT. (*significantly greater than vehicle within group; łsignificantly greater than MTII-treated LCR; #significantly different from HCR vehicle, $p<0.05$).

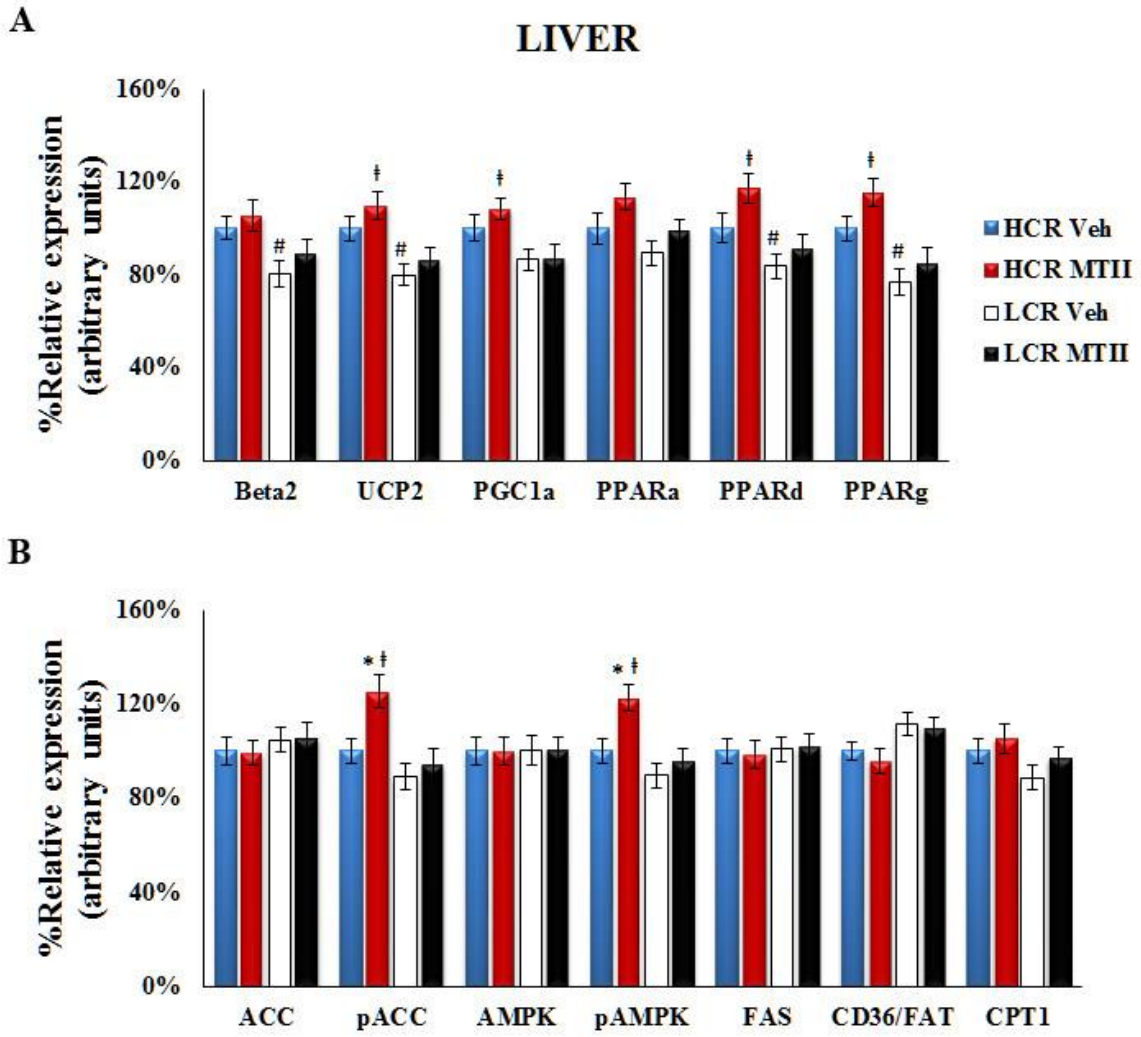

Figure 57: Intra-VMH MTII induced a trend toward increase in protein expression of mediators of energy expenditure in the liver of high- and low-capacity rats (HCR, LCR). Compared to vehicle-administered HCR, HCR with intra-VMH MTII microinjections have elevated expression of pAMPK and pACC and a trend toward an increase in PPARα, PPARδ, and PPARγ in the liver. (*significantly greater than vehicle within group; łsignificantly greater than MTII-treated LCR; #significantly different from HCR vehicle, $p<0.05$).

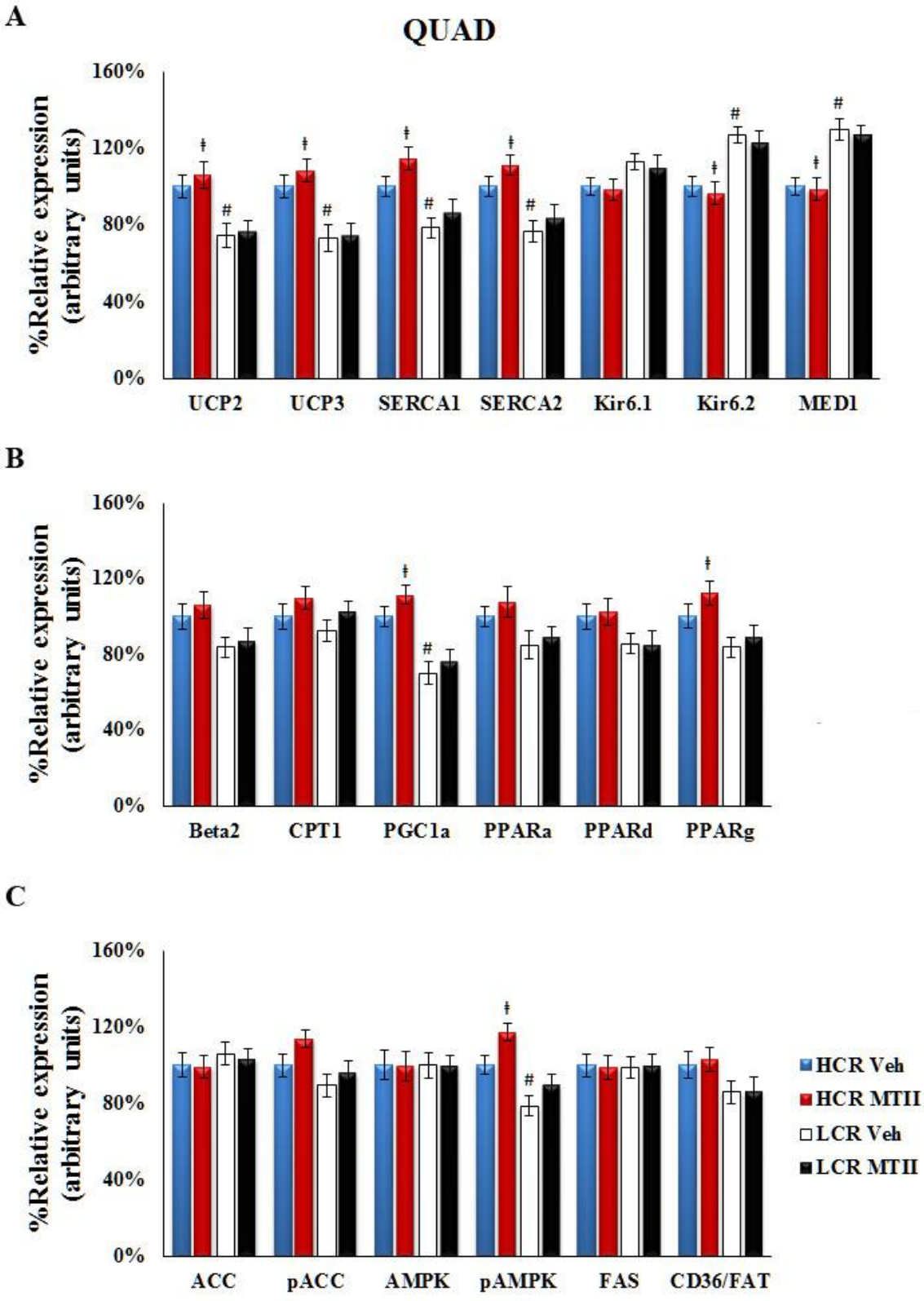
A
QUAD
%Relative expression (arbitrary units)
160%
120%
80%
40%
0%
UCP2
UCP3
SERCA1
SERCA2
Kir6.1
Kir6.2
MED1
B
%Relative expression (arbitrary units)
160%
120%
80%
40%
0%
Beta2
CPT1
PGC1a
PPARa
PPARd
PPARg
C
%Relative expression (arbitrary units)
160%
120%
80%
40%
0%
ACC
pACC
AMPK
pAMPK
FAS
CD36/FAT
HCR Veh
HCR MTII
LCR Veh
LCR MTII

Figure 58: Intra-VMH MTII microinjection induced a trend toward an increase in protein expression of mediators of energy expenditure in the quadriceps of high capacity rats (HCR). Compared to vehicle-treated HCR, HCR with MTII microinjections showed a trend toward increased expression of pAMPK, pACC, PGC-1α, PPARγ, and SERCA1 in the quadriceps (quad). (łsignificantly greater than MTII-treated LCR except for Kir6.2 and MED1; #significantly different from HCR vehicle, $p<0.05$).

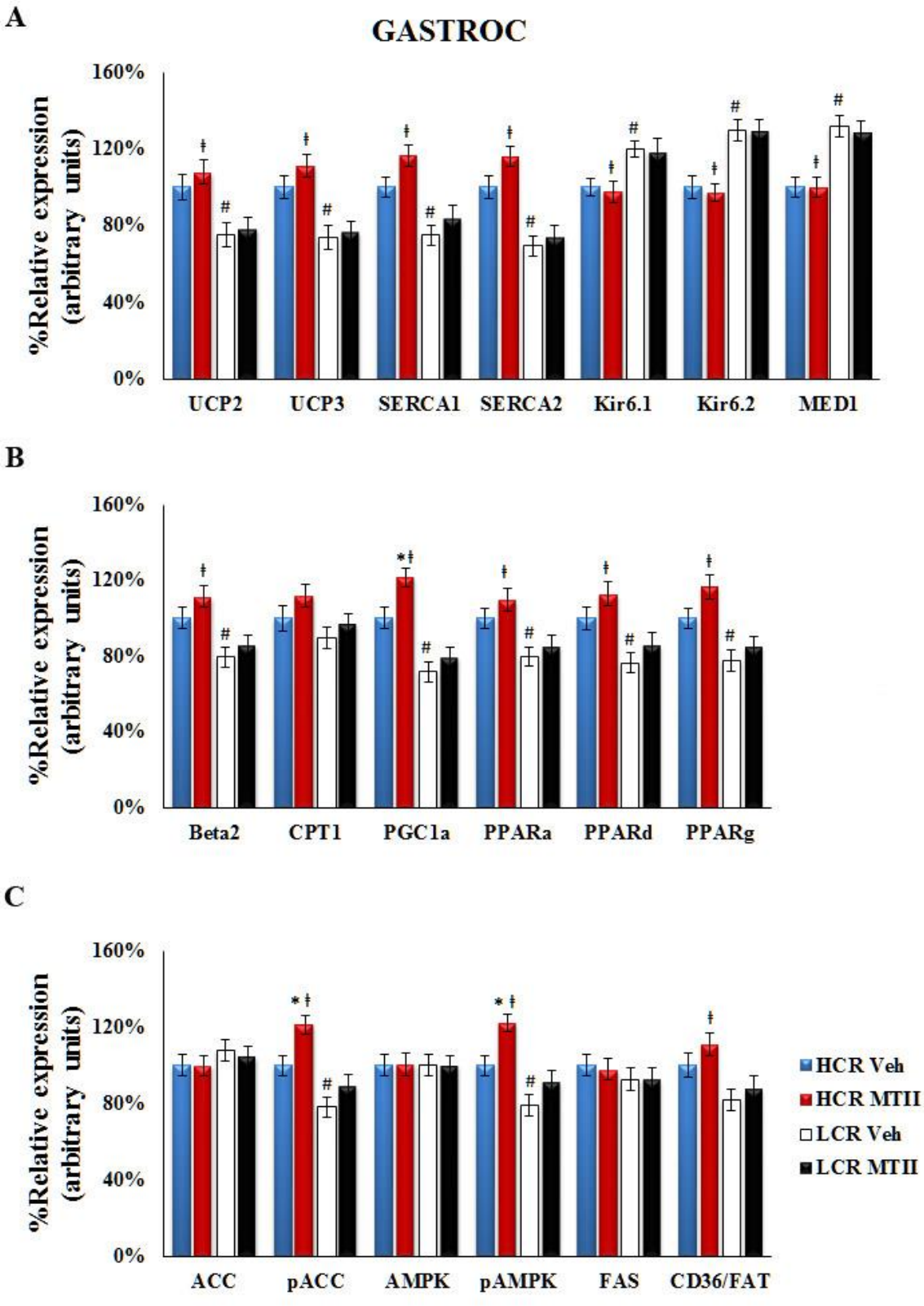
A
GASTROC
%Relative expression (arbitrary units)
160%
120%
80%
40%
0%
UCP2
UCP3
SERCA1
SERCA2
Kir6.1
Kir6.2
MED1
B
%Relative expression (arbitrary units)
160%
120%
80%
40%
0%
Beta2
CPT1
PGC1a
PPARa
PPARd
PPARg
C
%Relative expression (arbitrary units)
160%
120%
80%
40%
0%
ACC
pACC
AMPK
pAMPK
FAS
CD36/FAT
HCR Veh
HCR MTII
LCR Veh
LCR MTII

Figure 59: Intra-VMH MTII microinjection induced a trend toward an increase in protein expression of mediators of energy expenditure in the gastrocnemius of high- and low-capacity runners (HCR, LCR). Compared to vehicle-treated HCR, HCR with intra-VMH MTII microinjections have elevated expression of PGC-1α, pAMPK, and pACC in the gastrocnemius (gastroc). Gastroc of intra-VMH MTII-treated HCR also showed a trend toward an increase in expression of UCP3, CD36/FAT, PPARα, PPARδ, PPARγ, SERCA1, SERCA2, CPT1, and β_2-AR. (*significantly greater than vehicle within group; łsignificantly greater than MTII-treated LCR except for Kir6.1, Kir6.2, and MED1; #significantly different from HCR vehicle, $p<0.05$).

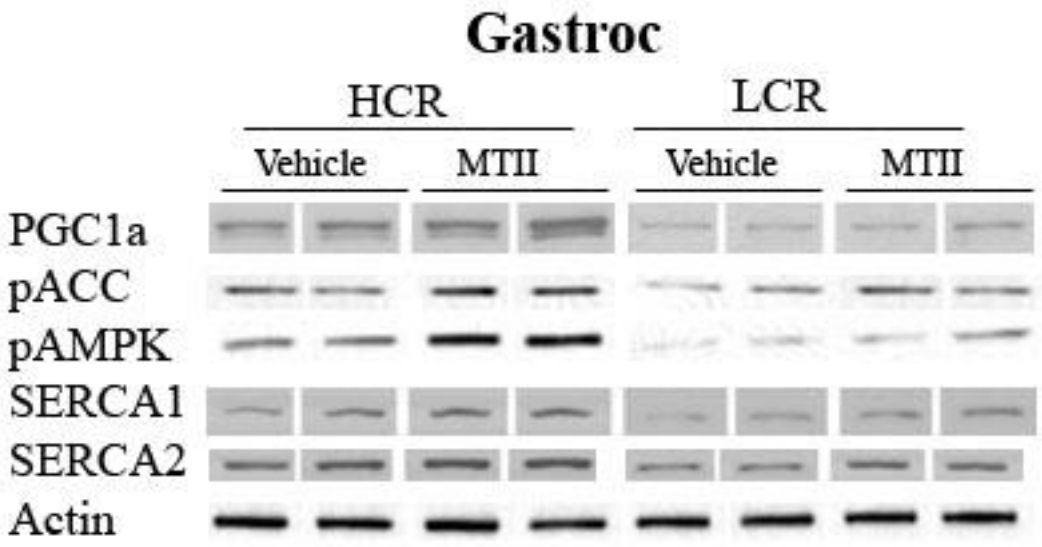

Figure 60: Representative western blot images showing the expression of molecular mediators of energy balance in the gastrocnemius (Gastroc). Peroxisomal proliferator activator γ coactivator 1α (PGC-1α), p-acetyl-CoA carboxylase (pACC), p-AMP-activated protein kinase (pAMPK), Sarcoplasmic/endoplasmic reticulum Ca^{2+}-ATPase (SERCA1 and 2) and actin as the loading control.

4.4 Discussion

In Chapter 2, I demonstrated that HCR have elevated total EE predominantly due to heightened activity-related EE. This activity-related EE is not completely secondary to elevated physical activity as it persists even during controlled activity, indicating low economy of activity in these rats. This low economy of activity suggests wasting of calories to a greater extent in HCR than LCR, potentially through elevated skeletal muscle thermogenesis, regulated through molecular mediators of energy conservation and expenditure, and in response to the enhanced sympathetic drive observed in these HCR. These phenotype-related differences were similar to those seen in response to intra-VMH MC receptor activation suggesting a difference in the response of VMH MC receptor-SNS-muscle axis in the lean HCR.

Indeed, I identified a phenotype-dependent increase in EE, physical activity, and VO_2, and a decrease in RER after site-specific microinjections of MC3R/MC4R non-specific agonist MTII into the VMH. In most cases, the changes in the calorimetric parameters were significantly higher in lean HCR compared to their obesity-prone LCR counterparts (Figure 39). Intra-VMH MC receptor activation induced greater changes in EE and VO_2 in HCR, and this persisted even during a controlled activity test (Figure 41). This holds true even when body weight or body composition was taken into consideration (Figures 40 and 42). These changes in calorimetric parameters remained even when controlled for activity using a low-level treadmill activity in both HCR and LCR, indicating that these changes are not secondary to elevated physical activity levels after

MTII microinjections. Altogether, this suggests that intra-VMH MC receptor activation lowers economy of activity and is more effective in lean HCR.

The increase in EE after central MC receptor activation is partially accompanied by increase in temperature of metabolically active tissues, as MTII induced an increase in skeletal muscle heat dissipation as well as BAT thermogenesis (Figures 43 and 44) in freely moving rats and an increase in gastroc muscle temperature during treadmill activity (Figure 45). These data support the function of the brain-muscle pathway proposed in Chapter 3. These findings also support the hypothesis that there may be a phenotypic variation in the effectiveness of intra-VMH MC receptor activation with lean HCR being more responsive.

While differential skeletal muscle activity thermogenesis and associated molecular mechanisms are important in maintaining leanness, it is not possible to propose a fully functional theoretical model unless we identify the driving force behind these adaptations. As explained in this and previous chapters, the CNS, particularly the hypothalamus, plays an important role in maintaining energy homeostasis and peripheral fuel metabolism (Braun & Marks, 2011; Shiuchi et al., 2009; Toda et al., 2009). Most of the actions of these energy-regulating nuclei are relayed to the peripheral tissues through the autonomic nervous system and are likely regulated through β adrenergic receptors (Shiuchi et al., 2009). In muscle, this pathway plays a critical role in altering muscle energetics through NE, increasing blood flow and fuel uptake and utilization. I found that, compared to vehicle administration, there was an increase in sympathetic outflow to

the peripheral metabolic tissues in both HCR and LCR, as shown by increased NETO in intra-VMH MTII-treated rats (Figures 46-48). This SNS outflow after intra-VMH MTII was significantly higher in the lean HCR compared to obesity-prone LCR in many of the tissues analyzed. This upregulation of the SNS relay to fuel-producing tissues like liver and WAT may underlie the greater responsiveness seen in HCR. One observation I find more interesting is the NETO in heart of the MTII-treated HCR and LCR. Unlike most of the tissues I looked at, baseline NETO in heart of LCR is higher than that of HCR. Compared to HCR, central MC receptor activation induced a greater NETO in the hearts of obese LCR (Figure 48). This fits with studies showing that HCR are protected against hypertension and is consistent with the data suggestive of cardiovascular fitness associated with aerobic capacity in rodents (Wisloff et al., 2005). This supports the idea that the effects of intra-VMH MC receptors are carried to the periphery through the SNS. This more effectively impacts metabolic processes in HCR compared to LCR and may be partially responsible for the lower fuel economy and the associated changes in cellular energy mediators in the periphery. These suggest that the observed differences in overall EE upon VMH MC receptor activation are partially due to differences in SNS modulation of skeletal muscle energetics in our lean and obesity-prone rats.

Both HCR and LCR showed a significantly increase in mRNA expression of proteins involved in EE and fatty acid metabolism and a trend in other energy balance mediators with central MC receptor activation. This applies not only to BAT and liver, but also to skeletal muscle which is the main focus of this work. While there were some instances of significant suppression of energy conserving processes, I found very little

effect on these processes. This may be due to the fact that the above said procedures were done in an acute fashion (3-4 hrs) which may not be adequate time to detect a significant inhibition in expression. This increase in proteins of fatty acid oxidation pathway and of that are involved in EE are also consistent with the observed phenotype-dependent changes in the activity, activity-related EE, and muscle energy use, supporting the proposed MC-activated VMH-SNS-muscle pathway. Although there was higher protein expression of mediators of EE, most of these changes were phosphorylation-related and did not require translation. Demonstrating protein concentration after increasing duration of central MC receptor activation may provide robust effects on protein expression. The above data affirmed my previous findings in Chapter 3, but also showed phenotype-dependent differences in HCR and LCR. I found that HCR show heightened expression of EE mechanisms in skeletal muscle compared to LCR under baseline conditions (Figures 52-53), consistent with results from Chapter 2. This lends further support to a theoretical model in which myocytes of the lean rats utilize more fuel through elevated EE along with reduced conservation mechanisms, resulting in low economy of activity and dissipating excess calories as heat. As described before, the alterations in the peripheral energy homeostatic mechanisms leading to observed phenotypic differences may have a central origin that may engage molecular mediators of energy homeostasis through an SNS relay. I have identified several potential molecular mediators of energy expenditure that showed heightened expression in skeletal muscle and other metabolically active tissues of the lean phenotype. Energetic mediators at the level of metabolically active tissues like skeletal muscle play an important role in determining the overall peripheral energy balance. I have shown that there is a significant increase or at

least an increasing trend in the expression of these mediators of EE at the level of both mRNA (Figures 49-53) and protein (Figures 54-59) in metabolically active tissues, while maintaining their baseline phenotypic differences.

Specifically, compared to vehicle, intra-VMH MTII-treated HCR showed a significant increase or an increasing trend in proteins involved in fatty acid oxidation pathway UCP1, UCP2, UCP3, PGC-1α, pAMPK, pACC PPARα, PPARγ, PPARδ, and CPT1 in BAT (Figure 54) and oxidative gastroc muscle (Figure 59). These changes may be responsible for the central MC receptor-induced increase in EE and decrease in RER. The increased EE and lowering RER after intra-VMH MC receptor activation can also be due to increased expression of the activated form of AMPK (pAMPK) in the metabolically active tissues, consistent with its role in upregulation of fatty acid oxidation and mitochondrial biogenesis through its regulation of ACC and CPT1 (Minokoshi et al., 2002). Although central MC receptor activation did increase EE and SNS drive to peripheral tissues in LCR, there were no significant changes in any mediators of energy balance except statistical trends in PPARα, pAMPK, PPARγ and pACC (Figures 49-59). This suggests phenotypic differences in myocyte responsiveness to adrenergic stimuli, consistent with the findings of Lessard, 2009. Compared to vehicle-administered HCR, gastroc muscle of intra-VMH MC receptor activated HCR showed an increasing trend in SERCA1, SERCA2, and CD36/FAT (Figure 59). SERCA are involved in skeletal muscle thermogenesis by regulating calcium homeostasis through ATP hydrolysis and generating heat in the process. Increased expression of these calcium pumps or stimulation of Ca^{2+} cycling increases heat dissipation through skeletal muscle which is both dependent and

independent of physical activity (muscular contraction for activity). The elevation of these proteins in HCR could contribute to leanness and low economy of activity in our animal model. This study will help identify potential mediators that can be targeted to alter energy balance equation towards negative energy balance.

Altogether, these findings support a role for differential activity-related skeletal muscle thermogenesis in maintaining leanness, recognize the importance of central homeostatic hypothalamic nuclei including the VMH, and identify potential molecular mechanisms underlying these differences. Activation of MC receptors in the VMH increases energy use in peripheral tissues in HCR and LCR similar to the observation in Chapter 2. It is likely that muscle fuel uptake and utilization is modulated through the SNS, affecting skeletal muscle or other metabolically active tissues. The central MC system, differentially expressed in the lean HCR and obese LCR is known to impact muscle lipid mobilization and glucose uptake in the periphery via SNS (Nogueiras et al., 2007; Shukla et al., 2012; Sohn et al., 2013; Tanaka et al., 2007; Toda et al., 2009). Put together, my data demonstrate that melanocortins in the VMH activate SNS outflow, increasing sympathetic drive to skeletal muscle, modulating fuel allocation and use through differential activation of molecular mediators of energy homeostasis. This increases EE and lowers fuel economy during activity, dissipating wasted calories as heat. I also demonstrated that functioning of this axis is heightened at every level in HCR compared to LCR. Activating MC receptors in the VMH increased sympathetic drive to skeletal muscle and other metabolically active tissues, altering the expression of mediators of EE, resulting in decreased fuel economy and increased activity-related EE in

a phenotype-dependent manner. These results implicate this pathway as a potential mechanism underlying high-endurance-associated low economy of activity and leanness.

CHAPTER 5

5.1 General discussion

Obesity is often considered to be a result of either excessive food intake or insufficient physical activity, or both. There is a great debate about which behavior deserves the most responsibility, an argument which has not yet produced effective solutions. Obesity can best be viewed in terms of energy balance. The basic components of energy balance include energy intake, energy expenditure, and energy storage (J. O. Hill, Wyatt, & Peters, 2012). Humans expend energy through resting metabolic rate, which is the amount of energy necessary to fuel the body at rest; the thermic effect of food, which is the energy cost of absorbing and metabolizing food consumed; and the energy expended through physical activity. Resting metabolic rate is proportional to body mass, particularly the amount of fat-free mass. The thermic effect of food is proportional to the total food consumed and, in a typical mixed diet, makes up 8% to 10% of total energy ingested. The energy expended through physical activity, the most variable component of energy expenditure, consists of the amount of physical activity performed multiplied by the energy cost of that activity (J. O. Hill et al., 2012). The mechanisms by which the body acts to achieve and maintain energy balance is not fully understood although available evidence points to a complex physiological control system. This system includes afferent signals from the periphery about the state of energy stores and efferent signals that affect energy intake and expenditure (J. O. Hill et al., 2012).

Factors that predispose an individual to be obese or resistant to obesity in an obesogenic environment are not fully explained. Sitting time and non-exercise activity (NEAT) have been linked through epidemiological studies to rates of metabolic syndrome, type 2 diabetes, obesity, and cardiovascular disease (George et al., 2013; Levine et al., 1999; Levine & Kotz, 2005; Moore et al., 2012) . This obviously raises the need for interventional studies to more conclusively test for the potential benefits of daily non-exercise physical activity. Even though NEAT plays an important role in overall EE, little is known about the molecular and neural mechanisms that are involved in the variance among individuals. Thus, there is a need to understand the mechanisms involved in the modulation of EE and the influence of this on weight gain and obesity propensity. A key trait that predicts NEAT or spontaneous physical activity is intrinsic aerobic capacity in both humans and rodents (Novak CM, 2009). High physical activity and aerobic capacity can be mechanistically linked and could be characteristics of the lean phenotype (Novak CM, 2009).

The CNS controls energy intake and EE, and the hypothalamus plays a critical role in this. Even though the hypothalamus has been the main focus of study for a long time, how hypothalamic nuclei interact with other homeostatic systems, such as hindbrain nuclei and non-homeostatic systems, to regulate food intake and EE remains to be elucidated in detail. I focus mainly on the VMH, part of a pathway regulating energy balance through its actions on peripheral glucose and lipid allocation, modulating RER and thermogenesis (Kim et al., 2011; Miyaki et al., 2011; Takahashi & Shimazu, 1981;

Toda et al., 2009). The central MC system also plays a vital role in controlling energy balance, increasing EE and physical activity, and decreasing appetite and modulating peripheral lipid metabolism (Butler, 2006; Nogueiras et al., 2007). Central MC modulates peripheral glucose and lipid metabolism and thermogenesis in BAT, demonstrating neuroendocrine control over peripheral cell metabolism, likely through regulation of the SNS (Nogueiras et al., 2007; Obici et al., 2001; Rahmouni et al., 2003; Voss-Andreae et al., 2007).

There has been a gradual shift in studies the on central regulation of metabolism from adipose and hepatic tissue towards regulation of muscle metabolism. Peripheral signals regarding the energy status of the individual alter the functioning of the hypothalamic nuclei which in turn regulate energy partitioning in muscle, possibly via a sympathetic relay (Belgardt & Bruning, 2010; Braun & Marks, 2011). Injection of leptin or orexin-A into the VMH increases glucose uptake and glycogen synthesis in skeletal muscle via the SNS, and this is dependent on MC signaling, as shown by studies using MTII (Shiuchi et al., 2009; Toda et al., 2009). To summarize, actions of central melanocortins in VMH could likely affect sympathetic drive to skeletal muscle, modulating energy use, potentially through molecular mediators of energy balance. The differences at each and every level of this pathway could be an underlying cause for the lean and obese phenotypes. Here, I investigate this pathway using an established rat model of leanness and obesity.

Based on my initial findings, lean HCR have higher total EE when rats were matched for body weight and/or lean mass. Partitioning total EE into its components clearly implicated the non-resting component (mostly activity-related EE) more than the resting component in this heightened total EE (Figures 7-9). This activity-related EE remained higher in HCR even when controlled for activity, showing decreased economy of activity in HCR (Gavini et al., 2014; Novak et al., 2010). This implicates differential skeletal muscle energy use as an underlying cause for differences in non-resting EE, which raises the question as to the fate of those 'surplus' calories being disposed by the HCR. HCR showed a significantly higher gastroc temperatures; the maximal rise in temperature was also significantly higher in HCR compared to LCR (Figure 11), demonstrating that HCR have heightened skeletal muscle heat dissipation compared to LCR.

To establish the source of this calorie use and heat production in HCR skeletal muscle, I examined mRNA and protein expression of molecular intermediates known to alter energy use in skeletal muscle. As predicted, HCR showed relatively lower levels of mRNA and protein content of energy conserving mechanisms (K^+_{ATP} channel subunits and MED1) and higher expression of mediators of EE in muscle (Figures 12-13), potentially explaining the compromised economy of activity in HCR muscle. This suggests a theoretical model in which myocytes of the lean rats utilize more fuel through elevated EE along with reduced conservation mechanisms resulting in low economy of activity, and dissipate excess calories as heat. These changes in EE mechanisms persisted between the two phenotypes after intra-VMH MC receptor activation (Figures 49-59).

Though differential skeletal muscle activity thermogenesis and associated molecular mechanisms are important in maintaining leanness, it is not possible to propose a fully functional theoretical model unless we know what the driving force behind these adaptations is. Most of the actions of energy-regulating nuclei are relayed to the peripheral tissues through the SNS and are likely regulated through β adrenergic receptors (Shiuchi et al., 2009). Compared to obesity-prone rats, lean rats have a significantly higher sympathetic drive at least to the two tissue types I examined (Figure 14). These data support a theoretical model in which the SNS modulates skeletal muscle metabolic fuel use, impacting fuel efficiency and increasing EE (mostly activity-related EE). Altogether, I have demonstrated that HCR and LCR differ in their total EE, particularly non-resting EE, and their activity-related EE is not completely secondary to physical activity or body weight. HCR have low economy of activity and possibly dispose of those 'surplus' calories in the form of heat through the regulation of mediators involved in energy balance; this may occur through higher sympathetic drive in HCR, altering their muscle energetics.

Effects of central MC receptor activation (with the agonist MTII) on calorimetric parameters were similar to the endogenous elevation seen in the HCR. This led me to hypothesize that activation of MC receptors in the VMH affects EE in a phenotype-dependent manner, with HCR being more responsive. I found that, intra-VMH MC receptor activation induced a significant increase in EE, VO_2, and physical activity, and a significant decrease in RER, suggesting a shift in fuel preference to fat. Intra-VMH MTII

induced changes in these parameters were significantly higher in HCR compared to LCR of the same treatment and irrespective of body weight or composition (Figures 39-40). Even when amount of physical activity was taken out of the equation, intra-VMH MC receptor-induced changes in these calorimetric parameters persisted, indicating that they were not completely attributable to heightened physical activity levels induced by central MC receptor activation (Figures 41). Compared to vehicle microinjection, intra-VMH MC receptor activation induced a significant increase in EE and VO_2 and a significant decrease in RER (Figures 19-20, 39, and 41) in both Sprague- Dawley and HCR/LCR rats, with HCR being more affected than LCR.

Based on these results and on the proposed model, activation of central MC receptors increases EE even when activity or body composition are controlled for, implicating lowered fuel economy of activity. Central MC peptides modulate fuel use in the periphery including skeletal muscle by altering muscle energetics. This was evident as shown by increased heat dissipation at the level of skeletal muscle in Sprague-Dawley rats but not in HCR/LCR (Figures 21 and 44). This is also the case with BAT, where in both Sprague- Dawley and HCR/LCR, activation of central MC receptors increased BAT thermogenesis (Figures 21 and 43). These data support the hypothesis that melanocortins act in the VMH to regulate skeletal muscle EE, dissipating calories as heat, analogous to VMH control of BAT. This strongly supports the hypothesized role of the VMH melanocortins in lowering economy of activity, potentially through alterations in fuel allocation and usage, resulting in enhanced skeletal muscle activity-related EE.

Central MC receptor-mediated effects in the periphery are relayed through the autonomic nervous system particularly the sympathetic division. Compared to vehicle, intra-VMH MC receptor activation induced significantly higher sympathetic drive to most of the tissues analyzed in both SD and HCR/LCR. This change in sympathetic outflow after MC receptor activation was significantly higher in HCR compared to LCR in every tissue analyzed except for heart. Heart of LCR had higher sympathetic drive compared to HCR during both baseline and central MC receptor activation, suggesting HCR are protected against hypertensive effects of MTII (da Silva et al., 2008; Haynes, Morgan, Djalali, Sivitz, & Mark, 1999; Rahmouni et al., 2003) which is in line with previous results from lean animals (do Carmo, Bassi, da Silva, & Hall, 2011).

These studies demonstrate that melanocortins in the VMH activate SNS outflow, increasing sympathetic drive to skeletal muscle, modulating fuel allocation and use through differential activation of molecular mediators of energy homeostasis. VMH MC receptor activation will also increase EE and lower fuel economy during activity, dissipating wasted calories as heat. The functioning of this VMH-skeletal muscle axis is heightened at every level in HCR compared to LCR possibly through increased sympathetic drive to skeletal muscle and other metabolic tissues excluding heart, altering the expression of mediators of EE and energy conservation. This results in decreased fuel economy and increased activity-related EE and heat dissipation, implicating this pathway as a potential mechanism underlying enhanced activity-related EE and leanness.

5.2 Future perspectives

I have shown that MC in the VMH is involved in altering skeletal muscle energetics through the SNS and likely contributes to the leanness that characterizes HCR by increasing total EE, particularly activity-related EE, and lower fuel economy during activity, metabolizing fats in lieu of glucose. I also show an increase in the expression of mediators involved in EE and fatty acid metabolism and decreased expression of energy conserving systems via the SNS to a greater extent in HCR than in LCR.

In addition to what I examined in these studies, the potential roles of other hypothalamic nuclei including the PVH and the DMH as well as other neuropeptides in the regulation of peripheral metabolism needs attention. As described earlier, the hypothalamus is comprised of interconnected yet anatomically distinct nuclei that respond to changes in energy status through hypothalamic peptides (Chari et al., 2010). Even though the hypothalamus has been the main target of studies in last few decades, the interactions of these hypothalamic nuclei with other homeostatic systems, such as hindbrain nuclei and other non-homeostatic systems in regulating whole body EE remains to be elucidated in detail. New methods like optogenetics and designer receptors exclusively activated by designer drugs (DREADDs) can be used to elucidate these pathways or a specific parts of the pathway, for example the role of VMH SF-1 neurons in metabolism (Y. H. Choi et al., 2013; Lindberg et al., 2013). These SF-1 neurons are involved in the regulation of energy balance by projecting both locally, within the VMH, as well as to other hypothalamic sites (Majdic et al., 2002). In particular, recent studies have shown that SF-1 positive neurons project to a number of autonomic centers, thus

regulating SNS outflow (Lindberg et al., 2013). Although my results implicate SNS as a mediator of central MC effects in the periphery, this needs further evaluation. Using pharmacological inhibitors for beta or alpha-adrenergic receptors or denervation studies may provide further evidence supporting this hypothesis. Understanding the signaling pathways involved in the regulation of mediators of energy balance (see Chapter 1) may present potential pharmacological targets to enhance activity EE to tackle overweight and obesity.

Present-day programs designed to increase EE are generating mixed results, suggesting the need for new strategies. In humans, in addition to the thermogenic tissue BAT, skeletal muscle has been demonstrated to significantly contribute thermogenesis (van den Berg et al., 2011). Although heat production from muscle has long been recognized as a thermogenic mechanism, whether muscle can produce heat independently of contraction remains controversial. Studies in birds and mammals suggest that skeletal muscle can be an important site of non-shivering thermogenesis (NST) and can be recruited during cold adaptation (Rowland, Bal, & Periasamy, 2014). Considerable research on thermogenesis during the last two decades has been focused on BAT. These studies clearly implicate BAT as an important site of NST in mammals, in particular in newborns and rodents. However, BAT is either absent, as in birds and pigs, or is only a minor component, as in adult large mammals including humans, bringing into question the BAT-centric view of thermogenesis (Rowland et al., 2014).

Skeletal muscle has a role as an elaborate energy production and consumption system that influences the whole body's energy metabolism (Iizuka, Machida, & Hirafuji, 2014). Skeletal muscle and exercise training have been known to bring about multiple benefits for human health maintenance and improvement by impacting glucose and lipid homeostasis and altering muscle fiber type composition, and much of this is centrally regulated (Braun & Marks, 2011; Iizuka et al., 2014). The mechanisms underlying the improvement of the human physical condition have been revealed to certain extent: skeletal muscle acts as an endocrine organ, synthesizing and secreting multiple factors, and these muscle-derived factors, so-called myokines, exert beneficial effects on peripheral and remote organs and skeletal muscle itself (Iizuka et al., 2014). Understanding the mechanisms of production and secretion of these myokines may lead to a new pharmacological approach for treatment of metabolic disorders.

Skeletal muscle is a unique tissue and adapts in response to both use and disuse. In response to an increased work-load (for example, high-resistance strength training), the muscle used will increase in both size and strength. In contrast, muscle disuse (such as injury-induced immobilization or bed rest) results in muscle weakness and atrophy (Ehrenborg & Krook, 2009). Exercise training also leads to changes in the metabolic phenotype of the muscle. In response to endurance exercise, the number of mitochondria in muscle increases, resulting in an increased capacity of the muscle to sustain aerobic metabolism and increased expression of the insulin-sensitive glucose transporter, GLUT4 (Ehrenborg & Krook, 2009). Trained muscle derives more of the energy required from fat and less from carbohydrate compared with untrained muscle during submaximal work

(work performed below the maximal oxygen utilization capacity) (Ehrenborg & Krook, 2009). A detailed understanding of the molecular regulation of skeletal muscle metabolism may reveal novel therapeutic targets in the treatment of metabolic disorders.

Appendix 4

Energy balance: role of hypothalamic fatty acids

Hypothalamic nuclei respond to metabolic fuels like glucose, lipids, and amino acids. Based on what we know, the brain is heavily dependent on glucose to meet its energy demands and it does not use fatty acids as a primary source of energy. It has been demonstrated, however, that certain enzymes and intermediates of fatty acid metabolism contribute to the ability of the hypothalamus to monitor energy status (Chari et al., 2010). For example, administration of long chain fatty acids (LCFA) into the third cerebral ventricle of rodents induces a significant decrease in plasma insulin and glucose levels within short time (Obici, Feng, et al., 2002; Obici, Zhang, Karkanias, & Rossetti, 2002). In the same study, central LCFAs decreased food intake and decreased hypothalamic NPY mRNA levels compared to control rats (Obici, Feng, et al., 2002; Obici, Zhang, et al., 2002); this is not surprising given that NPY leads to hunger in animals. This supports the proposition that hypothalamic actions on metabolism are nutritionally regulated, specifically by central LCFAs.

A possible explanation for the observed effects is that there might be an enhanced rate of LCFA-CoA metabolism in the hypothalamus of these overfed rats, or altered transport. Carnitine palmitoyltransferase-1 (CPT1) modulates the transportation of LCFAs into the mitochondria, where they undergo β-oxidation (Figure 61); the activity of this enzyme is likely a key factor in the level of cytosolic pool of LCFAs. Indeed, hypothalamic CPT1 activity was significantly increased in overfed rats (Chari et al.,

2010). Inhibiting hypothalamic lipid oxidation by inhibiting CPT1 activity was sufficient to restore fatty acid as well as glucose homeostasis in overfed rodents. Altogether, these studies highlight the importance of hypothalamic fatty acid metabolism in initiating the behavioral and metabolic responses necessary to regulate energy and glucose homeostasis.

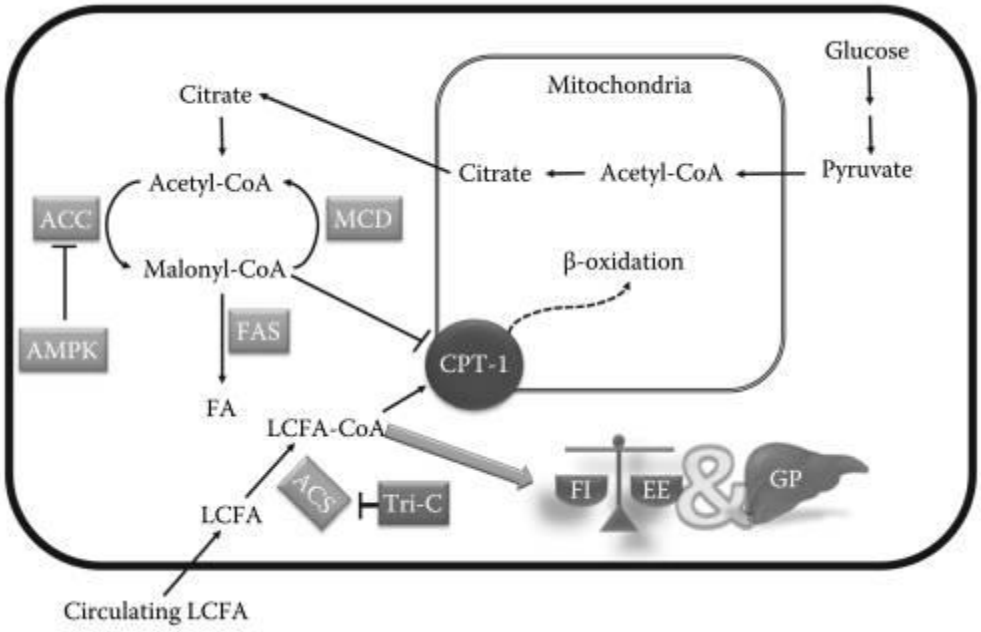

Figure 61: Generation of hypothalamic LCFA-CoA satiety signal. LCFA-CoAs gain access to the mitochondria to undergo β-oxidation via the acyltransferase CPT1, which is located on the outer mitochondrial membrane. Cellular fat oxidation is regulated by the availability of malonyl-CoA, which binds CPT1 and potently inhibits its activity. Malonyl-CoA, in turn, is mainly derived from acetyl-CoA—a glycolytic end-product—via the enzyme ACC; thus, the pathway is in a prime position to accurately monitor cellular energy status. Finally, ACC activity is allosterically inhibited by AMPK-mediated phosphorylation. LCFA-CoAs are also generated from LCFAs transported from the circulation via ACSs, the activity of which can be inhibited by triacsin C (Tri-C). FAS, fatty acid synthase; GP, glucose production; FI, food intake; EE, energy expenditure (Chari et al., 2010)

In the majority of tissues, cellular fat oxidation is regulated by malonyl-CoA, which is an end product of glycolysis by the enzyme acetyl-CoA carboxylase (ACC), and hence malonyl-CoA can precisely monitor cellular energy status. During fasting, the hypothalamic levels of malonyl-CoA rapidly decrease and act as a signal for hunger; during feeding, the level of malonyl-CoA in hypothalamus increases and acts as a signal to stop eating (Lopaschuk et al., 2010). The intracellular levels of malonyl-CoA determine the expression levels of AgRP/NPY and α-MSH in the ARC (Cha et al., 2005). This hypothesized mechanism of action is supported by studies demonstrating that administration of an inhibitor for FAS results in an increase in concentration of hypothalamic malonyl-CoA, which suppress expression of orexinergic neuropeptides (NYP and AgRP) and activates expression of anorexinergic neuropeptides (α-MSH) in the ARC. This leads to decrease in food intake and loss of body weight (Cha et al., 2005). The loss of body weight is not completely dependent on reduced food intake, but also involves increased EE (Cha et al., 2005). It is found that, within a short period after central administration of these inhibitors of FAS, CNS sends signals to peripheral tissues like skeletal muscle via the SNS to provoke increased fatty acid oxidation and expression of UCP3 and peroxisome proliferator activated receptor α (PPARα) in multiple peripheral tissues (Cha et al., 2005). To summarize, malonyl-CoA acts in hypothalamic neurons to control energy intake and expenditure (Figure 62) and alters the peripheral tissue metabolism by modulating the activity of SNS.

Although malonyl-CoA has been assumed to act as an intermediate in the hypothalamic signaling pathway that controls feeding behavior and energy expenditure,

the upstream molecular events that regulate its formation are less understood. Recent studies suggests that the changes in hypothalamic malonyl-CoA during feeding and fasting cycles result from changes in the phosphorylation state and activity of ACC, which is mediated by AMP kinase (AMPK) (figure) (Wolfgang & Lane, 2008). Both ACC1 and ACC2 are found in hypothalamic neurons and are known to be target for phosphorylation catalyzed by AMPK. Conditions that activate AMPK in the hypothalamus lead to phosphorylation/inactivation of ACC (Wolfgang & Lane, 2008). For example, leptin, an anorexigenic hormone produced primarily by white adipocytes, suppresses AMPK activity in the hypothalamus. This action inhibits ACC and thereby increases malonyl-CoA. Central administration of an AMPK activator lowers hypothalamic malonyl-CoA and promotes food intake (Wolfgang & Lane, 2008). These findings have led to the notion that fasting increases the [AMP]/[ATP] ratio in neurons in hypothalamic nuclei, leading to the activation of AMPK, the inactivation of ACC, thus decreasing malonyl-CoA (Wolfgang & Lane, 2008).

Within the hypothalamus, expression FAS and ACC is limited to specific populations of neurons. One possible molecular mechanism for a malonyl-CoA signal may be as an allosteric modifier of the neural enzyme CPT1. Specifically, CPT1a, the liver isoform, is found in the CNS and has been implicated in the malonyl-CoA signal (Obici, Feng, Arduini, Conti, & Rossetti, 2003). However, the CNS expresses a unique brain-specific CPT1 gene, CPT1c (Wolfgang & Lane, 2008). CPT1c is expressed in neurons throughout the CNS with concentrated localization in hypothalamic nuclei that are involved in energy homeostasis such as the ARC and the VMH (Wolfgang & Lane,

2008). CPT1c binds malonyl-CoA within the physiological range of malonyl-CoA in the hypothalamus (Wolfgang & Lane, 2008). CPT1c knockout mice showed decreased body weight resulting from decreased food intake, a phenotype consistent with a malonyl-CoA target enzyme CPT1 that controls body weight (Wolfgang & Lane, 2008). This phenotype is also consistent with the hypothalamic deletion of FAS, a condition in which mice are lean and exhibit lowered food intake and increased malonyl-CoA (Wolfgang & Lane, 2008). Altogether, these data support the model which states that the interaction between malonyl-CoA and CPT1c within the CNS is involved in nutrient sensing and alterations in energy intake likely affecting EE pathways.

The CNS uses mainly glucose during the fed state but will switch to the utilization of ketones during food deprivation (Wolfgang & Lane, 2008). It is widely accepted that the CNS does not efficiently use long-chain fatty acids for cellular energy purposes. The hypothalamus is unique in this regard because the regions involved in regulating energy homeostasis have more access to circulating fuels than do other regions of the CNS (Wolfgang & Lane, 2008). The hypothesis that fatty acids (or amino acids) act as satiety factors is contrary to traditional thought in animal physiology because free fatty acids and amino acid concentrations in the blood are high during food deprivation, a time of hunger (Wolfgang & Lane, 2008). Consistent with the rather small contribution of fatty acid oxidation to CNS metabolism in adult animals, CPT1c does not catalyze fatty acyl transfer from fatty acyl-CoAs to carnitine, nor does it promote fatty acid oxidation. The inability to catalyze fatty acyl transfer to carnitine is unexpected given the high degree of amino acid sequence similarity between CPT1c, CPT1a, and CPT1b. Indeed, CPT1c may

not act as an enzyme but may function through a regulatory protein-protein interaction that is altered by malonyl-CoA binding (Wolfgang & Lane, 2008). An alternative hypothesis for the effect of malonyl-CoA has been proposed whereby malonyl-CoA acts as an inhibitor of CPT1a and, therefore, fatty acid oxidation (Obici et al., 2003). Inhibition of fatty acid oxidation might promote an increase in the cellular long-chain acyl-CoA concentration to activate K^+_{ATP} channels independent of the sulfonylurea receptor-1 subunit (Wolfgang & Lane, 2008). Therefore, malonyl-CoA could integrate cellular nutrient signals provided by glucose flux and AMPK activity as well as the influx of free fatty acid from the cerebrospinal fluid (Wolfgang & Lane, 2008). In this way, neuronal fatty acyl-CoAs acting on K^+_{ATP} channels might play a role in hypothalamic nutrient sensing.

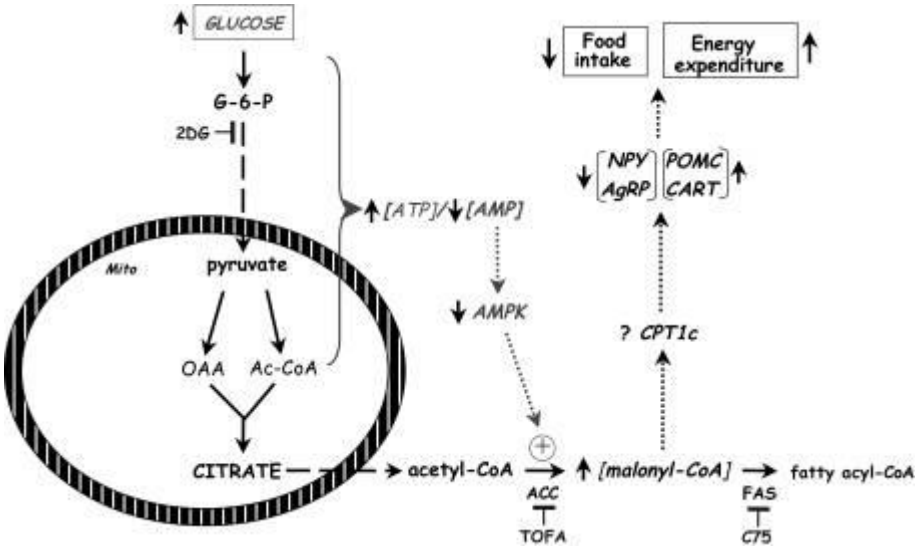

Figure 62: Role of malonyl-CoA in the hypothalamic control of feeding behavior and energy expenditure (Wolfgang & Lane, 2008Wolfgang & Lane, 2008).

REFERENCES

Aguilar-Bryan, L., Clement, J. P. t., Gonzalez, G., Kunjilwar, K., Babenko, A., & Bryan, J. (1998). Toward understanding the assembly and structure of KATP channels. [Review]. *Physiol Rev, 78*(1), 227-245.

Alekseev, A. E., Reyes, S., Yamada, S., Hodgson-Zingman, D. M., Sattiraju, S., Zhu, Z., . . . Zingman, L. V. (2010). Sarcolemmal ATP-sensitive K(+) channels control energy expenditure determining body weight. [Research Support, N.I.H., Extramural Research Support, Non-U.S. Gov't]. *Cell Metab, 11*(1), 58-69. doi: 10.1016/j.cmet.2009.11.009

Allison, D. B., Fontaine, K. R., Manson, J. E., Stevens, J., & VanItallie, T. B. (1999). Annual deaths attributable to obesity in the United States. [Research Support, U.S. Gov't, P.H.S.]. *JAMA, 282*(16), 1530-1538.

Anand, B. K., & Brobeck, J. R. (1951). Localization of a "feeding center" in the hypothalamus of the rat. *Proc Soc Exp Biol Med, 77*(2), 323-324.

Arsenijevic, D., Onuma, H., Pecqueur, C., Raimbault, S., Manning, B. S., Miroux, B., . . . Ricquier, D. (2000). Disruption of the uncoupling protein-2 gene in mice reveals a role in immunity and reactive oxygen species production. [Research Support,

Non-U.S. Gov't Research Support, U.S. Gov't, P.H.S.]. *Nat Genet, 26*(4), 435-439. doi: 10.1038/82565

Ashcroft, F. M., & Rorsman, P. (1989). Electrophysiology of the pancreatic beta-cell. [Research Support, Non-U.S. Gov't Review]. *Prog Biophys Mol Biol, 54*(2), 87-143.

Ashcroft, S. J., & Ashcroft, F. M. (1990). Properties and functions of ATP-sensitive K-channels. [Research Support, Non-U.S. Gov't Review]. *Cell Signal, 2*(3), 197-214.

Aspenes, S. T., Nilsen, T. I., Skaug, E. A., Bertheussen, G. F., Ellingsen, O., Vatten, L., & Wisloff, U. (2011). Peak oxygen uptake and cardiovascular risk factors in 4631 healthy women and men. [Research Support, Non-U.S. Gov't]. *Med Sci Sports Exerc, 43*(8), 1465-1473. doi: 10.1249/MSS.0b013e31820ca81c

Astrup, A., Bulow, J., Madsen, J., & Christensen, N. J. (1985). Contribution of BAT and skeletal muscle to thermogenesis induced by ephedrine in man. [Research Support, Non-U.S. Gov't]. *Am J Physiol, 248*(5 Pt 1), E507-515.

Aye, M. T., & Izaguirre, C. A. (1991). Erythroid lineage-specific activity in conditioned medium derived from cloned human marrow stromal cells (CFU-RF). [Research

Support, Non-U.S. Gov't]. *J Cell Physiol, 148*(3), 440-445. doi: 10.1002/jcp.1041480316

Azzu, V., Jastroch, M., Divakaruni, A. S., & Brand, M. D. (2010). The regulation and turnover of mitochondrial uncoupling proteins. [Research Support, N.I.H., Extramural Research Support, Non-U.S. Gov't Review]. *Biochim Biophys Acta, 1797*(6-7), 785-791. doi: 10.1016/j.bbabio.2010.02.035

Babic, T., Purpera, M. N., Banfield, B. W., Berthoud, H. R., & Morrison, C. D. (2010). Innervation of skeletal muscle by leptin receptor-containing neurons. [Research Support, N.I.H., Extramural]. *Brain Res, 1345*, 146-155. doi: 10.1016/j.brainres.2010.05.042

Bagnol, D., Lu, X. Y., Kaelin, C. B., Day, H. E., Ollmann, M., Gantz, I., . . . Watson, S. J. (1999). Anatomy of an endogenous antagonist: relationship between Agouti-related protein and proopiomelanocortin in brain. [Research Support, U.S. Gov't, P.H.S.]. *J Neurosci, 19*(18), RC26.

Bal, N. C., Maurya, S. K., Sopariwala, D. H., Sahoo, S. K., Gupta, S. C., Shaikh, S. A., . . . Periasamy, M. (2012). Sarcolipin is a newly identified regulator of muscle-based thermogenesis in mammals. [Research Support, N.I.H., Extramural Research Support, Non-U.S. Gov't]. *Nat Med, 18*(10), 1575-1579. doi: 10.1038/nm.2897

Barnes, M. J., & McDougal, D. H. (2014). Leptin into the rostral ventral lateral medulla (RVLM) augments renal sympathetic nerve activity and blood pressure. *Front Neurosci, 8*, 232. doi: 10.3389/fnins.2014.00232

Barsh, G. S., & Schwartz, M. W. (2002). Genetic approaches to studying energy balance: perception and integration. [Research Support, Non-U.S. Gov't Research Support, U.S. Gov't, P.H.S. Review]. *Nat Rev Genet, 3*(8), 589-600. doi: 10.1038/nrg862

Bartness, T. J., Vaughan, C. H., & Song, C. K. (2010). Sympathetic and sensory innervation of brown adipose tissue. [Research Support, N.I.H., Extramural Research Support, U.S. Gov't, Non-P.H.S. Review]. *Int J Obes (Lond), 34 Suppl 1*, S36-42. doi: 10.1038/ijo.2010.182

Baskin, K. K., Winders, B. R., & Olson, E. N. (2015). Muscle as a "mediator" of systemic metabolism. [Research Support, N.I.H., Extramural Research Support, Non-U.S. Gov't Review]. *Cell Metab, 21*(2), 237-248. doi: 10.1016/j.cmet.2014.12.021

Bassel-Duby, R., & Olson, E. N. (2006). Signaling pathways in skeletal muscle remodeling. [Review]. *Annu Rev Biochem, 75*, 19-37. doi: 10.1146/annurev.biochem.75.103004.142622

Beck, B., Kozak, R., Moar, K. M., & Mercer, J. G. (2006). Hypothalamic orexigenic peptides are overexpressed in young Long-Evans rats after early life exposure to fat-rich diets. [Research Support, Non-U.S. Gov't]. *Biochem Biophys Res Commun, 342*(2), 452-458. doi: 10.1016/j.bbrc.2006.01.158

Belgardt, B. F., & Bruning, J. C. (2010). CNS leptin and insulin action in the control of energy homeostasis. [Research Support, Non-U.S. Gov't Review]. *Ann N Y Acad Sci, 1212*, 97-113. doi: 10.1111/j.1749-6632.2010.05799.x

Berger, J. P., Akiyama, T. E., & Meinke, P. T. (2005). PPARs: therapeutic targets for metabolic disease. [Review]. *Trends Pharmacol Sci, 26*(5), 244-251. doi: 10.1016/j.tips.2005.03.003

Bernardis, L. L., & Bellinger, L. L. (1993). The lateral hypothalamic area revisited: neuroanatomy, body weight regulation, neuroendocrinology and metabolism. [Research Support, U.S. Gov't, Non-P.H.S. Review]. *Neurosci Biobehav Rev, 17*(2), 141-193.

Bernardis, L. L., & Bellinger, L. L. (1998). The dorsomedial hypothalamic nucleus revisited: 1998 update. [Review]. *Proc Soc Exp Biol Med, 218*(4), 284-306.

Berthoud, H. R. (2003). Neural systems controlling food intake and energy balance in the modern world. [Review]. *Curr Opin Clin Nutr Metab Care, 6*(6), 615-620. doi: 10.1097/01.mco.0000098084.40916.1f

Bonen, A., Tandon, N. N., Glatz, J. F., Luiken, J. J., & Heigenhauser, G. J. (2006). The fatty acid transporter FAT/CD36 is upregulated in subcutaneous and visceral adipose tissues in human obesity and type 2 diabetes. [Research Support, Non-U.S. Gov't]. *Int J Obes (Lond), 30*(6), 877-883. doi: 10.1038/sj.ijo.0803212

Boss, O., Samec, S., Paoloni-Giacobino, A., Rossier, C., Dulloo, A., Seydoux, J., . . . Giacobino, J. P. (1997). Uncoupling protein-3: a new member of the mitochondrial carrier family with tissue-specific expression. [Research Support, Non-U.S. Gov't]. *FEBS Lett, 408*(1), 39-42.

Braun, T. P., & Marks, D. L. (2011). Hypothalamic regulation of muscle metabolism. [Review]. *Curr Opin Clin Nutr Metab Care, 14*(3), 237-242. doi: 10.1097/MCO.0b013e328345bbcd

Bray, G. A., Ryan, D. H., & Harsha, D. W. (2003). Diet, Weight Loss, and Cardiovascular Disease Prevention. *Curr Treat Options Cardiovasc Med, 5*(4), 259-269.

Bray, M. S. (2000). Genomics, genes, and environmental interaction: the role of exercise. [Research Support, Non-U.S. Gov't Review]. *J Appl Physiol (1985), 88*(2), 788-792.

Brito, M. N., Brito, N. A., Baro, D. J., Song, C. K., & Bartness, T. J. (2007). Differential activation of the sympathetic innervation of adipose tissues by melanocortin receptor stimulation. [Research Support, N.I.H., Extramural Research Support, Non-U.S. Gov't]. *Endocrinology, 148*(11), 5339-5347. doi: 10.1210/en.2007-0621

Butler, A. A. (2006). The melanocortin system and energy balance. [Research Support, N.I.H., Extramural Research Support, Non-U.S. Gov't Review]. *Peptides, 27*(2), 281-290. doi: 10.1016/j.peptides.2005.02.029

Cadenas S, B. J., Samec S, Seydoux J, Din N, Dulloo AG, Brand MD. (1999). UCP2 and UCP3 rise in starved rat skeletal muscle but mitochondrial proton conductance is unchanged. *FEBS Lett, 462*(3), 257-260.

Cannon, B., & Nedergaard, J. (2004). Brown adipose tissue: function and physiological significance. [Research Support, Non-U.S. Gov't Review]. *Physiol Rev, 84*(1), 277-359. doi: 10.1152/physrev.00015.2003

Cauchi, S., Stutzmann, F., Cavalcanti-Proenca, C., Durand, E., Pouta, A., Hartikainen, A. L., . . . Froguel, P. (2009). Combined effects of MC4R and FTO common genetic variants on obesity in European general populations. [Multicenter Study Research Support, Non-U.S. Gov't]. *J Mol Med (Berl), 87*(5), 537-546. doi: 10.1007/s00109-009-0451-6

Cha, S. H., Hu, Z., Chohnan, S., & Lane, M. D. (2005). Inhibition of hypothalamic fatty acid synthase triggers rapid activation of fatty acid oxidation in skeletal muscle. [Comparative Study Research Support, Non-U.S. Gov't]. *Proc Natl Acad Sci U S A, 102*(41), 14557-14562. doi: 10.1073/pnas.0507300102

Cha, S. H., Rodgers, J. T., Puigserver, P., Chohnan, S., & Lane, M. D. (2006). Hypothalamic malonyl-CoA triggers mitochondrial biogenesis and oxidative gene expression in skeletal muscle: Role of PGC-1alpha. [Research Support, N.I.H., Extramural Research Support, Non-U.S. Gov't]. *Proc Natl Acad Sci U S A, 103*(42), 15410-15415. doi: 10.1073/pnas.0607334103

Chagnon, Y. C., Chen, W. J., Perusse, L., Chagnon, M., Nadeau, A., Wilkison, W. O., & Bouchard, C. (1997). Linkage and association studies between the melanocortin receptors 4 and 5 genes and obesity-related phenotypes in the Quebec Family Study. [Research Support, Non-U.S. Gov't Research Support, U.S. Gov't, P.H.S.]. *Mol Med, 3*(10), 663-673.

Chakravarthy, M. V., Pan, Z., Zhu, Y., Tordjman, K., Schneider, J. G., Coleman, T., . . . Semenkovich, C. F. (2005). "New" hepatic fat activates PPARalpha to maintain glucose, lipid, and cholesterol homeostasis. [Comparative Study Research Support, N.I.H., Extramural Research Support, U.S. Gov't, P.H.S.]. *Cell Metab, 1*(5), 309-322. doi: 10.1016/j.cmet.2005.04.002

Chari, M., Lam, C. K. L., & Lam, T. K. T. (2010). Hypothalamic Fatty Acid Sensing in the Normal and Disease States. In J. P. Montmayeur & J. le Coutre (Eds.), *Fat Detection: Taste, Texture, and Post Ingestive Effects*. Boca Raton (FL).

Chen, A. S., Marsh, D. J., Trumbauer, M. E., Frazier, E. G., Guan, X. M., Yu, H., . . . Van der Ploeg, L. H. (2000). Inactivation of the mouse melanocortin-3 receptor results in increased fat mass and reduced lean body mass. *Nat Genet, 26*(1), 97-102. doi: 10.1038/79254

Chen, W., & Roeder, R. G. (2011). Mediator-dependent nuclear receptor function. [Research Support, N.I.H., Extramural Review]. *Semin Cell Dev Biol, 22*(7), 749-758. doi: 10.1016/j.semcdb.2011.07.026

Chen, W., Zhang, X., Birsoy, K., & Roeder, R. G. (2010). A muscle-specific knockout implicates nuclear receptor coactivator MED1 in the regulation of glucose and

energy metabolism. [Research Support, N.I.H., Extramural Research Support, Non-U.S. Gov't]. *Proc Natl Acad Sci U S A, 107*(22), 10196-10201. doi: 10.1073/pnas.1005626107

Choi, C. S., Fillmore, J. J., Kim, J. K., Liu, Z. X., Kim, S., Collier, E. F., . . . Shulman, G. I. (2007). Overexpression of uncoupling protein 3 in skeletal muscle protects against fat-induced insulin resistance. [Research Support, N.I.H., Extramural]. *J Clin Invest, 117*(7), 1995-2003. doi: 10.1172/JCI13579

Choi, Y. H., Fujikawa, T., Lee, J., Reuter, A., & Kim, K. W. (2013). Revisiting the Ventral Medial Nucleus of the Hypothalamus: The Roles of SF-1 Neurons in Energy Homeostasis. *Front Neurosci, 7*, 71. doi: 10.3389/fnins.2013.00071

Church, T. S., Thomas, D. M., Tudor-Locke, C., Katzmarzyk, P. T., Earnest, C. P., Rodarte, R. Q., . . . Bouchard, C. (2011). Trends over 5 decades in U.S. occupation-related physical activity and their associations with obesity. *PLoS One, 6*(5), e19657. doi: 10.1371/journal.pone.0019657

Clapham, J. C., Arch, J. R., Chapman, H., Haynes, A., Lister, C., Moore, G. B., . . . Abuin, A. (2000). Mice overexpressing human uncoupling protein-3 in skeletal muscle are hyperphagic and lean. [Research Support, Non-U.S. Gov't]. *Nature, 406*(6794), 415-418. doi: 10.1038/35019082

Conley, K. E., Jubrias, S. A., Amara, C. E., & Marcinek, D. J. (2007). Mitochondrial dysfunction: impact on exercise performance and cellular aging. [Research Support, N.I.H., Extramural Review]. *Exerc Sport Sci Rev, 35*(2), 43-49. doi: 10.1249/JES.0b013e31803e88e9

Corton, J. M., Gillespie, J. G., Hawley, S. A., & Hardie, D. G. (1995). 5-aminoimidazole-4-carboxamide ribonucleoside. A specific method for activating AMP-activated protein kinase in intact cells? [Research Support, Non-U.S. Gov't]. *Eur J Biochem, 229*(2), 558-565.

Cowley, M. A., Pronchuk, N., Fan, W., Dinulescu, D. M., Colmers, W. F., & Cone, R. D. (1999). Integration of NPY, AGRP, and melanocortin signals in the hypothalamic paraventricular nucleus: evidence of a cellular basis for the adipostat. [Research Support, Non-U.S. Gov't Research Support, U.S. Gov't, P.H.S.]. *Neuron, 24*(1), 155-163.

D.W. Brown, D. R. B., G.W. Heath, L. Balluz, W.H. Giles, E.S. Ford and A.H. Mokdad. (2004). Associations between physical activity dose and health-related quality of life. *Med Sci Sports Exerc, 36*, 890-896.

da Silva, A. A., do Carmo, J. M., Kanyicska, B., Dubinion, J., Brandon, E., & Hall, J. E. (2008). Endogenous melanocortin system activity contributes to the elevated

arterial pressure in spontaneously hypertensive rats. [Research Support, N.I.H., Extramural Research Support, Non-U.S. Gov't]. *Hypertension, 51*(4), 884-890. doi: 10.1161/HYPERTENSIONAHA.107.100636

Desvergne, B., Michalik, L., & Wahli, W. (2006). Transcriptional regulation of metabolism. [Review]. *Physiol Rev, 86*(2), 465-514. doi: 10.1152/physrev.00025.2005

do Carmo, J. M., Bassi, M., da Silva, A. A., & Hall, J. E. (2011). Systemic but not central nervous system nitric oxide synthase inhibition exacerbates the hypertensive effects of chronic melanocortin-3/4 receptor activation. [Research Support, N.I.H., Extramural]. *Hypertension, 57*(3), 428-434. doi: 10.1161/HYPERTENSIONAHA.110.163931

Dube, M. G., Kalra, S. P., & Kalra, P. S. (1999). Food intake elicited by central administration of orexins/hypocretins: identification of hypothalamic sites of action. [Research Support, U.S. Gov't, P.H.S.]. *Brain Res, 842*(2), 473-477.

Dukes, I. D., & Philipson, L. H. (1996). K+ channels: generating excitement in pancreatic beta-cells. [Research Support, Non-U.S. Gov't Research Support, U.S. Gov't, P.H.S. Review]. *Diabetes, 45*(7), 845-853.

Ehrenborg, E., & Krook, A. (2009). Regulation of skeletal muscle physiology and metabolism by peroxisome proliferator-activated receptor delta. [Research Support, Non-U.S. Gov't Review]. *Pharmacol Rev, 61*(3), 373-393. doi: 10.1124/pr.109.001560

Ekelund, U., Brage, S., Franks, P. W., Hennings, S., Emms, S., & Wareham, N. J. (2005). Physical activity energy expenditure predicts progression toward the metabolic syndrome independently of aerobic fitness in middle-aged healthy Caucasians: the Medical Research Council Ely Study. [Research Support, Non-U.S. Gov't]. *Diabetes Care, 28*(5), 1195-1200.

Elias, C. F., Saper, C. B., Maratos-Flier, E., Tritos, N. A., Lee, C., Kelly, J., . . . Elmquist, J. K. (1998). Chemically defined projections linking the mediobasal hypothalamus and the lateral hypothalamic area. [Research Support, Non-U.S. Gov't Research Support, U.S. Gov't, P.H.S.]. *J Comp Neurol, 402*(4), 442-459.

Elmquist, J. K., Elias, C. F., & Saper, C. B. (1999). From lesions to leptin: hypothalamic control of food intake and body weight. [Review]. *Neuron, 22*(2), 221-232.

Enkvetchakul, D., Loussouarn, G., Makhina, E., & Nichols, C. G. (2001). ATP interaction with the open state of the K(ATP) channel. *Biophys J, 80*(2), 719-728. doi: 10.1016/S0006-3495(01)76051-1

Esterbauer, H., Schneitler, C., Oberkofler, H., Ebenbichler, C., Paulweber, B., Sandhofer, F., . . . Patsch, W. (2001). A common polymorphism in the promoter of UCP2 is associated with decreased risk of obesity in middle-aged humans. [Research Support, Non-U.S. Gov't]. *Nat Genet, 28*(2), 178-183. doi: 10.1038/88911

Evans, R. M., Barish, G. D., & Wang, Y. X. (2004). PPARs and the complex journey to obesity. [Review]. *Nat Med, 10*(4), 355-361. doi: 10.1038/nm1025

Fan, W., Boston, B. A., Kesterson, R. A., Hruby, V. J., & Cone, R. D. (1997). Role of melanocortinergic neurons in feeding and the agouti obesity syndrome. [Research Support, Non-U.S. Gov't Research Support, U.S. Gov't, P.H.S.]. *Nature, 385*(6612), 165-168. doi: 10.1038/385165a0

Fathi, Z., Iben, L. G., & Parker, E. M. (1995). Cloning, expression, and tissue distribution of a fifth melanocortin receptor subtype. *Neurochem Res, 20*(1), 107-113.

Feige, J. N., & Auwerx, J. (2007). Transcriptional coregulators in the control of energy homeostasis. [Review]. *Trends Cell Biol, 17*(6), 292-301. doi: 10.1016/j.tcb.2007.04.001

Finck, B. N., & Kelly, D. P. (2006). PGC-1 coactivators: inducible regulators of energy metabolism in health and disease. [Research Support, N.I.H., Extramural Review]. *J Clin Invest, 116*(3), 615-622. doi: 10.1172/JCI27794

Fisler, J. S., & Warden, C. H. (2006). Uncoupling proteins, dietary fat and the metabolic syndrome. *Nutr Metab (Lond), 3*, 38. doi: 10.1186/1743-7075-3-38

Fleury, C., Neverova, M., Collins, S., Raimbault, S., Champigny, O., Levi-Meyrueis, C., . . . Warden, C. H. (1997). Uncoupling protein-2: a novel gene linked to obesity and hyperinsulinemia. [Comparative Study Research Support, Non-U.S. Gov't Research Support, U.S. Gov't, P.H.S.]. *Nat Genet, 15*(3), 269-272. doi: 10.1038/ng0397-269

Fuller, P. M., Warden, C. H., Barry, S. J., & Fuller, C. A. (2000). Effects of 2-G exposure on temperature regulation, circadian rhythms, and adiposity in UCP2/3 transgenic mice. [Research Support, U.S. Gov't, Non-P.H.S. Research Support, U.S. Gov't, P.H.S.]. *J Appl Physiol (1985), 89*(4), 1491-1498.

Galgani, J., & Ravussin, E. (2008). Energy metabolism, fuel selection and body weight regulation. [Research Support, N.I.H., Extramural Research Support, Non-U.S. Gov't Review]. *Int J Obes (Lond), 32 Suppl 7*, S109-119. doi: 10.1038/ijo.2008.246

Gallagher, D., Belmonte, D., Deurenberg, P., Wang, Z., Krasnow, N., Pi-Sunyer, F. X., & Heymsfield, S. B. (1998). Organ-tissue mass measurement allows modeling of REE and metabolically active tissue mass. [Research Support, U.S. Gov't, P.H.S.]. *Am J Physiol, 275*(2 Pt 1), E249-258.

Gantz, I., Miwa, H., Konda, Y., Shimoto, Y., Tashiro, T., Watson, S. J., . . . Yamada, T. (1993). Molecular cloning, expression, and gene localization of a fourth melanocortin receptor. [Research Support, U.S. Gov't, Non-P.H.S. Research Support, U.S. Gov't, P.H.S.]. *J Biol Chem, 268*(20), 15174-15179.

Garland, T., Jr., Schutz, H., Chappell, M. A., Keeney, B. K., Meek, T. H., Copes, L. E., . . . Eisenmann, J. C. (2011). The biological control of voluntary exercise, spontaneous physical activity and daily energy expenditure in relation to obesity: human and rodent perspectives. [Research Support, N.I.H., Extramural Research Support, U.S. Gov't, Non-P.H.S. Review]. *J Exp Biol, 214*(Pt 2), 206-229. doi: 10.1242/jeb.048397

Garlid, K. D. (2000). Opening mitochondrial K(ATP) in the heart--what happens, and what does not happen. [Research Support, U.S. Gov't, P.H.S. Review]. *Basic Res Cardiol, 95*(4), 275-279.

Garlid, K. D., Orosz, D. E., Modriansky, M., Vassanelli, S., & Jezek, P. (1996). On the mechanism of fatty acid-induced proton transport by mitochondrial uncoupling protein. [Research Support, Non-U.S. Gov't Research Support, U.S. Gov't, P.H.S.]. *J Biol Chem, 271*(5), 2615-2620.

Gavini, C. K., Mukherjee, S., Shukla, C., Britton, S. L., Koch, L. G., Shi, H., & Novak, C. M. (2014). Leanness and heightened nonresting energy expenditure: role of skeletal muscle activity thermogenesis. [Comparative Study Research Support, N.I.H., Extramural Research Support, Non-U.S. Gov't]. *Am J Physiol Endocrinol Metab, 306*(6), E635-647. doi: 10.1152/ajpendo.00555.2013

Ge, K., Guermah, M., Yuan, C. X., Ito, M., Wallberg, A. E., Spiegelman, B. M., & Roeder, R. G. (2002). Transcription coactivator TRAP220 is required for PPAR gamma 2-stimulated adipogenesis. [Research Support, Non-U.S. Gov't Research Support, U.S. Gov't, P.H.S.]. *Nature, 417*(6888), 563-567. doi: 10.1038/417563a

George, E. S., Rosenkranz, R. R., & Kolt, G. S. (2013). Chronic disease and sitting time in middle-aged Australian males: findings from the 45 and Up Study. *Int J Behav Nutr Phys Act, 10*, 20. doi: 10.1186/1479-5868-10-20

Ghanassia, E., Brun, J. F., Mercier, J., & Raynaud, E. (2007). Oxidative mechanisms at rest and during exercise. [Review]. *Clin Chim Acta, 383*(1-2), 1-20. doi: 10.1016/j.cca.2007.04.006

Gold, R. M. (1973). Hypothalamic obesity: the myth of the ventromedial nucleus. *Science, 182*(4111), 488-490.

Gong, D. W., He, Y., & Reitman, M. L. (1999). Genomic organization and regulation by dietary fat of the uncoupling protein 3 and 2 genes. *Biochem Biophys Res Commun, 256*(1), 27-32. doi: 10.1006/bbrc.1999.0239

Gong, D. W., Monemdjou, S., Gavrilova, O., Leon, L. R., Marcus-Samuels, B., Chou, C. J., . . . Reitman, M. L. (2000). Lack of obesity and normal response to fasting and thyroid hormone in mice lacking uncoupling protein-3. *J Biol Chem, 275*(21), 16251-16257. doi: 10.1074/jbc.M910177199

Griffon, N., Mignon, V., Facchinetti, P., Diaz, J., Schwartz, J. C., & Sokoloff, P. (1994). Molecular cloning and characterization of the rat fifth melanocortin receptor. *Biochem Biophys Res Commun, 200*(2), 1007-1014.

Grill, H. J. (2006). Distributed neural control of energy balance: contributions from hindbrain and hypothalamus. [Research Support, N.I.H., Extramural Review]. *Obesity (Silver Spring), 14 Suppl 5*, 216S-221S. doi: 10.1038/oby.2006.312

Hakansson, M. L., Brown, H., Ghilardi, N., Skoda, R. C., & Meister, B. (1998). Leptin receptor immunoreactivity in chemically defined target neurons of the hypothalamus. [Research Support, Non-U.S. Gov't]. *J Neurosci, 18*(1), 559-572.

Halestrap, A. P. (1989). The regulation of the matrix volume of mammalian mitochondria in vivo and in vitro and its role in the control of mitochondrial metabolism. [Research Support, Non-U.S. Gov't Review]. *Biochim Biophys Acta, 973*(3), 355-382.

Hamilton, M. T., Healy, G.N., Dunstan, D.W., Zderic, T.W., and Owen, N. (2008). Too little exercise and too much sitting: inactivity physiology and the need for new recommendations on sedentary behavior *Curr. Cardiovasc. Risk Rep.*, 292–298. doi: 10.1007/s12170-008-0054-8

Hardie, D. G., Hawley, S. A., & Scott, J. W. (2006). AMP-activated protein kinase--development of the energy sensor concept. [Research Support, Non-U.S. Gov't Review]. *J Physiol, 574*(Pt 1), 7-15. doi: 10.1113/jphysiol.2006.108944

Harper, M. E., Dent, R. M., Bezaire, V., Antoniou, A., Gauthier, A., Monemdjou, S., & McPherson, R. (2001). UCP3 and its putative function: consistencies and controversies. [Review]. *Biochem Soc Trans, 29*(Pt 6), 768-773.

Haskell-Luevano, C., Chen, P., Li, C., Chang, K., Smith, M. S., Cameron, J. L., & Cone, R. D. (1999). Characterization of the neuroanatomical distribution of agouti-related protein immunoreactivity in the rhesus monkey and the rat. [Research Support, U.S. Gov't, P.H.S.]. *Endocrinology, 140*(3), 1408-1415. doi: 10.1210/endo.140.3.6544

Haslam, D. W., & James, W. P. (2005). Obesity. *Lancet Diabetes Endocrinol*. doi: 10.1016/S0140-6736(05)67483-1

Haynes, W. G., Morgan, D. A., Djalali, A., Sivitz, W. I., & Mark, A. L. (1999). Interactions between the melanocortin system and leptin in control of sympathetic nerve traffic. [Research Support, Non-U.S. Gov't Research Support, U.S. Gov't, Non-P.H.S. Research Support, U.S. Gov't, P.H.S.]. *Hypertension, 33*(1 Pt 2), 542-547.

Henin, N., Vincent, M. F., Gruber, H. E., & Van den Berghe, G. (1995). Inhibition of fatty acid and cholesterol synthesis by stimulation of AMP-activated protein kinase. [Research Support, Non-U.S. Gov't]. *FASEB J, 9*(7), 541-546.

Heo, M., Allison, D. B., Faith, M. S., Zhu, S., & Fontaine, K. R. (2003). Obesity and quality of life: mediating effects of pain and comorbidities. [Research Support, Non-U.S. Gov't Research Support, U.S. Gov't, P.H.S.]. *Obes Res, 11*(2), 209-216. doi: 10.1038/oby.2003.33

Hernandez-Sanchez, C., Ito, Y., Ferrer, J., Reitman, M., & LeRoith, D. (1999). Characterization of the mouse sulfonylurea receptor 1 promoter and its regulation. *J Biol Chem, 274*(26), 18261-18270.

Hesselink, M. K., Greenhaff, P. L., Constantin-Teodosiu, D., Hultman, E., Saris, W. H., Nieuwlaat, R., . . . Schrauwen, P. (2003). Increased uncoupling protein 3 content does not affect mitochondrial function in human skeletal muscle in vivo. [Research Support, Non-U.S. Gov't]. *J Clin Invest, 111*(4), 479-486. doi: 10.1172/JCI16653

Hetherington AW, R. S. (1940). Hypothalamic lesions and adiposity in the rat. *Anat Rec, 78*, 149-172.

Hill, J. O., Wyatt, H. R., & Peters, J. C. (2012). Energy balance and obesity. [Research Support, N.I.H., Extramural Review]. *Circulation, 126*(1), 126-132. doi: 10.1161/CIRCULATIONAHA.111.087213

Hill, J. W. (2012). PVN pathways controlling energy homeostasis. *Indian J Endocrinol Metab, 16*(Suppl 3), S627-636. doi: 10.4103/2230-8210.105581

Himms-Hagen, J., & Harper, M. E. (2001). Physiological role of UCP3 may be export of fatty acids from mitochondria when fatty acid oxidation predominates: an hypothesis. [Research Support, Non-U.S. Gov't Review]. *Exp Biol Med (Maywood), 226*(2), 78-84.

Holloway, G. P., Bonen, A., & Spriet, L. L. (2009). Regulation of skeletal muscle mitochondrial fatty acid metabolism in lean and obese individuals. [Research Support, Non-U.S. Gov't Review]. *Am J Clin Nutr, 89*(1), 455S-462S. doi: 10.3945/ajcn.2008.26717B

Holmes, B. F., Kurth-Kraczek, E. J., & Winder, W. W. (1999). Chronic activation of 5'-AMP-activated protein kinase increases GLUT-4, hexokinase, and glycogen in muscle. [Research Support, U.S. Gov't, P.H.S.]. *J Appl Physiol (1985), 87*(5), 1990-1995.

Horvath, T. L., Diano, S., & Barnstable, C. (2003). Mitochondrial uncoupling protein 2 in the central nervous system: neuromodulator and neuroprotector. [Research Support, U.S. Gov't, P.H.S. Review]. *Biochem Pharmacol, 65*(12), 1917-1921.

Horvath, T. L., Diano, S., Miyamoto, S., Barry, S., Gatti, S., Alberati, D., . . . Warden, C. H. (2003). Uncoupling proteins-2 and 3 influence obesity and inflammation in transgenic mice. [Research Support, Non-U.S. Gov't Research Support, U.S. Gov't, P.H.S.]. *Int J Obes Relat Metab Disord, 27*(4), 433-442. doi: 10.1038/sj.ijo.0802257

Horvath, T. L., Warden, C. H., Hajos, M., Lombardi, A., Goglia, F., & Diano, S. (1999). Brain uncoupling protein 2: uncoupled neuronal mitochondria predict thermal synapses in homeostatic centers. [Research Support, Non-U.S. Gov't Research Support, U.S. Gov't, P.H.S.]. *J Neurosci, 19*(23), 10417-10427.

Hu, F. B., Leitzmann, M. F., Stampfer, M. J., Colditz, G. A., Willett, W. C., & Rimm, E. B. (2001). Physical activity and television watching in relation to risk for type 2 diabetes mellitus in men. *Arch Intern Med, 161(12)*, 1542-1548.

Huszar, D., Lynch, C. A., Fairchild-Huntress, V., Dunmore, J. H., Fang, Q., Berkemeier, L. R., . . . Lee, F. (1997). Targeted disruption of the melanocortin-4 receptor results in obesity in mice. [Research Support, Non-U.S. Gov't]. *Cell, 88*(1), 131-141.

Iizuka, K., Machida, T., & Hirafuji, M. (2014). Skeletal muscle is an endocrine organ. [Review]. *J Pharmacol Sci, 125*(2), 125-131.

Inagaki, N., Gonoi, T., Clement, J. P. t., Namba, N., Inazawa, J., Gonzalez, G., . . . Bryan, J. (1995). Reconstitution of IKATP: an inward rectifier subunit plus the sulfonylurea receptor. [Research Support, Non-U.S. Gov't Research Support, U.S. Gov't, P.H.S.]. *Science, 270*(5239), 1166-1170.

Jensen, M. T. S. a. M. D. (2000). Metabolic complications of obesity. Pathophysiologic considerations. *Med Clin North Am*, *84*, 363-385.

Jia, Y., Qi, C., Kashireddi, P., Surapureddi, S., Zhu, Y. J., Rao, M. S., . . . Reddy, J. K. (2004). Transcription coactivator PBP, the peroxisome proliferator-activated receptor (PPAR)-binding protein, is required for PPARalpha-regulated gene expression in liver. [Research Support, U.S. Gov't, P.H.S.]. *J Biol Chem, 279*(23), 24427-24434. doi: 10.1074/jbc.M402391200

Johannsen, D. L., Welk, G. J., Sharp, R. L., & Flakoll, P. J. (2008). Differences in daily energy expenditure in lean and obese women: the role of posture allocation. [Comparative Study]. *Obesity (Silver Spring), 16*(1), 34-39. doi: 10.1038/oby.2007.15

Joosen, A. M., Gielen, M., Vlietinck, R., & Westerterp, K. R. (2005). Genetic analysis of physical activity in twins. [Twin Study]. *Am J Clin Nutr, 82*(6), 1253-1259.

Jorgensen, S. B., Nielsen, J. N., Birk, J. B., Olsen, G. S., Viollet, B., Andreelli, F., . . . Wojtaszewski, J. F. (2004). The alpha2-5'AMP-activated protein kinase is a site 2 glycogen synthase kinase in skeletal muscle and is responsive to glucose loading. [Research Support, Non-U.S. Gov't]. *Diabetes, 53*(12), 3074-3081.

Joseph, J. W., Koshkin, V., Zhang, C. Y., Wang, J., Lowell, B. B., Chan, C. B., & Wheeler, M. B. (2002). Uncoupling protein 2 knockout mice have enhanced insulin secretory capacity after a high-fat diet. [Research Support, Non-U.S. Gov't Research Support, U.S. Gov't, P.H.S.]. *Diabetes, 51*(11), 3211-3219.

K.M. Flegal, M. D. C., C.L. Ogden and C.L. Johnson. (2002). Prevalence and trends in obesity among US adults, 1999-2000. *JAMA, 1723-7*.

K.R. Fontaine, D. T. R., C. Wang, A.O. Westfall and D.B. Allison. (2003). Years of life lost due to obesity. *JAMA, 187-93*.

Kalsbeek, A., Drijfhout, W. J., Westerink, B. H., van Heerikhuize, J. J., van der Woude, T. P., van der Vliet, J., & Buijs, R. M. (1996). GABA receptors in the region of the dorsomedial hypothalamus of rats are implicated in the control of melatonin and corticosterone release. [Research Support, Non-U.S. Gov't]. *Neuroendocrinology, 63*(1), 69-78.

Kelley, D. E., He, J., Menshikova, E. V., & Ritov, V. B. (2002). Dysfunction of mitochondria in human skeletal muscle in type 2 diabetes. [Research Support, Non-U.S. Gov't Research Support, U.S. Gov't, P.H.S.]. *Diabetes, 51*(10), 2944-2950.

Kersten, S., Seydoux, J., Peters, J. M., Gonzalez, F. J., Desvergne, B., & Wahli, W. (1999). Peroxisome proliferator-activated receptor alpha mediates the adaptive response to fasting. [Research Support, Non-U.S. Gov't]. *J Clin Invest, 103*(11), 1489-1498. doi: 10.1172/JCI6223

Kim, K. W., Zhao, L., Donato, J., Jr., Kohno, D., Xu, Y., Elias, C. F., . . . Elmquist, J. K. (2011). Steroidogenic factor 1 directs programs regulating diet-induced thermogenesis and leptin action in the ventral medial hypothalamic nucleus. [Research Support, N.I.H., Extramural Research Support, Non-U.S. Gov't]. *Proc Natl Acad Sci U S A, 108*(26), 10673-10678. doi: 10.1073/pnas.1102364108

King, B. M. (2006). The rise, fall, and resurrection of the ventromedial hypothalamus in the regulation of feeding behavior and body weight. [Review]. *Physiol Behav, 87*(2), 221-244. doi: 10.1016/j.physbeh.2005.10.007

Klein, S. (2004). The national obesity crisis: a call for action. [Editorial]. *Gastroenterology, 126*(1), 6.

Kliewer, S. A., Xu, H. E., Lambert, M. H., & Willson, T. M. (2001). Peroxisome proliferator-activated receptors: from genes to physiology. [Review]. *Recent Prog Horm Res, 56*, 239-263.

Koch LG, a. B. S. (2008). Development of animal models to test the fundamental basis of geneenvironment interactions. *Obesity (Silver Spring), 16 Suppl 3*, S28-32.

Koch, L. G., & Britton, S. L. (2001). Artificial selection for intrinsic aerobic endurance running capacity in rats. [Research Support, U.S. Gov't, P.H.S.]. *Physiol Genomics, 5*(1), 45-52.

Koch, L. G., Britton, S. L., & Wisloff, U. (2012). A rat model system to study complex disease risks, fitness, aging, and longevity. [Research Support, N.I.H., Extramural Research Support, Non-U.S. Gov't Review]. *Trends Cardiovasc Med, 22*(2), 29-34. doi: 10.1016/j.tcm.2012.06.007

Koch, L. G., Kemi, O. J., Qi, N., Leng, S. X., Bijma, P., Gilligan, L. J., . . . Wisloff, U. (2011). Intrinsic aerobic capacity sets a divide for aging and longevity. [Research Support, N.I.H., Extramural Research Support, Non-U.S. Gov't]. *Circ Res, 109*(10), 1162-1172. doi: 10.1161/CIRCRESAHA.111.253807

Kodama, S., Saito, K., Tanaka, S., Maki, M., Yachi, Y., Asumi, M., . . . Sone, H. (2009). Cardiorespiratory fitness as a quantitative predictor of all-cause mortality and cardiovascular events in healthy men and women: a meta-analysis. [Meta-Analysis Research Support, Non-U.S. Gov't]. *JAMA, 301*(19), 2024-2035. doi: 10.1001/jama.2009.681

Kodera, Y., Takeyama, K., Murayama, A., Suzawa, M., Masuhiro, Y., & Kato, S. (2000). Ligand type-specific interactions of peroxisome proliferator-activated receptor gamma with transcriptional coactivators. [Research Support, Non-U.S. Gov't Retracted Publication]. *J Biol Chem, 275*(43), 33201-33204. doi: 10.1074/jbc.C000517200

Kokkinos P, M. J., Kokkinos JP, Pittaras A, Narayan P, Manolis A, Karasik P, Greenberg M, Papademetriou V, Singh S. (2008). Exercise capacity and mortality in black and white men. *Circulation, 117*, 614-622.

Kotz, C. M., Teske, J. A., & Billington, C. J. (2008). Neuroregulation of nonexercise activity thermogenesis and obesity resistance. [Review]. *Am J Physiol Regul Integr Comp Physiol, 294*(3), R699-710. doi: 10.1152/ajpregu.00095.2007

Kotz, C. M., Teske, J. A., Levine, J. A., & Wang, C. (2002). Feeding and activity induced by orexin A in the lateral hypothalamus in rats. [Research Support, U.S. Gov't, Non-P.H.S. Research Support, U.S. Gov't, P.H.S.]. *Regul Pept, 104*(1-3), 27-32.

Kotz, C. M., Wang, C., Levine, A. S., & Billington, C. J. (2002). Urocortin in the hypothalamic PVN increases leptin and affects uncoupling proteins-1 and -3 in rats. [Research Support, U.S. Gov't, Non-P.H.S. Research Support, U.S. Gov't, P.H.S.]. *Am J Physiol Regul Integr Comp Physiol, 282*(2), R546-551. doi: 10.1152/ajpregu.00436.2001

Kotz, C. M., Wang, C. F., Briggs, J. E., Levine, A. S., & Billington, C. J. (2000). Effect of NPY in the hypothalamic paraventricular nucleus on uncoupling proteins 1, 2, and 3 in the rat. [Research Support, Non-U.S. Gov't Research Support, U.S. Gov't, Non-P.H.S. Research Support, U.S. Gov't, P.H.S.]. *Am J Physiol Regul Integr Comp Physiol, 278*(2), R494-498.

Kozak, L. P. (2010). Brown fat and the myth of diet-induced thermogenesis. [Research Support, N.I.H., Extramural Review]. *Cell Metab, 11*(4), 263-267. doi: 10.1016/j.cmet.2010.03.009

Kozak, L. P., & Young, M. E. (2012). Heat from calcium cycling melts fat. [Comment News]. *Nat Med, 18*(10), 1458-1459. doi: 10.1038/nm.2956

Krauss, S., Zhang, C. Y., & Lowell, B. B. (2005). The mitochondrial uncoupling-protein homologues. [Research Support, Non-U.S. Gov't Research Support, U.S. Gov't, P.H.S. Review]. *Nat Rev Mol Cell Biol, 6*(3), 248-261. doi: 10.1038/nrm1572

Krempler, F., Esterbauer, H., Weitgasser, R., Ebenbichler, C., Patsch, J. R., Miller, K., . . . Patsch, W. (2002). A functional polymorphism in the promoter of UCP2 enhances obesity risk but reduces type 2 diabetes risk in obese middle-aged humans. [Research Support, Non-U.S. Gov't]. *Diabetes, 51*(11), 3331-3335.

Kurth-Kraczek, E. J., Hirshman, M. F., Goodyear, L. J., & Winder, W. W. (1999). 5' AMP-activated protein kinase activation causes GLUT4 translocation in skeletal muscle. [Research Support, U.S. Gov't, P.H.S.]. *Diabetes, 48*(8), 1667-1671.

Kusunoki, M., Tsutsumi, K., Iwata, K., Yin, W., Nakamura, T., Ogawa, H., . . . Miyata, T. (2005). NO-1886 (ibrolipim), a lipoprotein lipase activator, increases the expression of uncoupling protein 3 in skeletal muscle and suppresses fat accumulation in high-fat diet-induced obesity in rats. *Metabolism, 54*(12), 1587-1592. doi: 10.1016/j.metabol.2005.06.005

LaMonte, M. J., Blair, S. N., & Church, T. S. (2005). Physical activity and diabetes prevention. [Review]. *J Appl Physiol (1985), 99*(3), 1205-1213. doi: 10.1152/japplphysiol.00193.2005

LeBrasseur, N. K., Walsh, K., & Arany, Z. (2011). Metabolic benefits of resistance training and fast glycolytic skeletal muscle. [Research Support, N.I.H., Extramural Research Support, Non-U.S. Gov't Review]. *Am J Physiol Endocrinol Metab, 300*(1), E3-10. doi: 10.1152/ajpendo.00512.2010

Lehrke, M., & Lazar, M. A. (2005). The many faces of PPARgamma. [Review]. *Cell, 123*(6), 993-999. doi: 10.1016/j.cell.2005.11.026

Lessard, S. J., Rivas, D. A., Chen, Z. P., van Denderen, B. J., Watt, M. J., Koch, L. G., . . . Hawley, J. A. (2009). Impaired skeletal muscle beta-adrenergic activation and lipolysis are associated with whole-body insulin resistance in rats bred for low intrinsic exercise capacity. [Research Support, N.I.H., Extramural Research Support, Non-U.S. Gov't]. *Endocrinology, 150*(11), 4883-4891. doi: 10.1210/en.2009-0158

Lessard, S. J., Rivas, D. A., Stephenson, E. J., Yaspelkis, B. B., 3rd, Koch, L. G., Britton, S. L., & Hawley, J. A. (2011). Exercise training reverses impaired skeletal muscle metabolism induced by artificial selection for low aerobic capacity. [Research

Support, Non-U.S. Gov't Research Support, U.S. Gov't, Non-P.H.S.]. *Am J Physiol Regul Integr Comp Physiol, 300*(1), R175-182. doi: 10.1152/ajpregu.00338.2010

Levine, J. A. (2002). Non-exercise activity thermogenesis (NEAT). [Review]. *Best Pract Res Clin Endocrinol Metab, 16*(4), 679-702.

Levine, J. A., Eberhardt, N. L., & Jensen, M. D. (1999). Role of nonexercise activity thermogenesis in resistance to fat gain in humans. [Clinical Trial Research Support, Non-U.S. Gov't Research Support, U.S. Gov't, P.H.S.]. *Science, 283*(5399), 212-214.

Levine, J. A., & Kotz, C. M. (2005). NEAT--non-exercise activity thermogenesis--egocentric & geocentric environmental factors vs. biological regulation. [Research Support, N.I.H., Extramural Research Support, Non-U.S. Gov't Research Support, U.S. Gov't, P.H.S. Review]. *Acta Physiol Scand, 184*(4), 309-318. doi: 10.1111/j.1365-201X.2005.01467.x

Levine, J. A., Lanningham-Foster, L. M., McCrady, S. K., Krizan, A. C., Olson, L. R., Kane, P. H., . . . Clark, M. M. (2005). Interindividual variation in posture allocation: possible role in human obesity. [Comparative Study Research Support,

Non-U.S. Gov't Research Support, U.S. Gov't, P.H.S.]. *Science, 307*(5709), 584-586. doi: 10.1126/science.1106561

Li, B., Nolte, L. A., Ju, J. S., Han, D. H., Coleman, T., Holloszy, J. O., & Semenkovich, C. F. (2000). Skeletal muscle respiratory uncoupling prevents diet-induced obesity and insulin resistance in mice. [Research Support, U.S. Gov't, P.H.S.]. *Nat Med, 6*(10), 1115-1120. doi: 10.1038/80450

Lin, B., Coughlin, S., & Pilch, P. F. (1998). Bidirectional regulation of uncoupling protein-3 and GLUT-4 mRNA in skeletal muscle by cold. [Research Support, U.S. Gov't, P.H.S.]. *Am J Physiol, 275*(3 Pt 1), E386-391.

Lin, J., Handschin, C., & Spiegelman, B. M. (2005). Metabolic control through the PGC-1 family of transcription coactivators. [Research Support, N.I.H., Extramural Research Support, U.S. Gov't, P.H.S. Review]. *Cell Metab, 1*(6), 361-370. doi: 10.1016/j.cmet.2005.05.004

Lin, J., Wu, H., Tarr, P. T., Zhang, C. Y., Wu, Z., Boss, O., . . . Spiegelman, B. M. (2002). Transcriptional co-activator PGC-1 alpha drives the formation of slow-twitch muscle fibres. [Research Support, Non-U.S. Gov't Research Support, U.S. Gov't, P.H.S.]. *Nature, 418*(6899), 797-801. doi: 10.1038/nature00904

Lindberg, D., Chen, P., & Li, C. (2013). Conditional viral tracing reveals that steroidogenic factor 1-positive neurons of the dorsomedial subdivision of the ventromedial hypothalamus project to autonomic centers of the hypothalamus and hindbrain. [Research Support, N.I.H., Extramural]. *J Comp Neurol, 521*(14), 3167-3190. doi: 10.1002/cne.23338

Lopaschuk, G. D., Ussher, J. R., & Jaswal, J. S. (2010). Targeting intermediary metabolism in the hypothalamus as a mechanism to regulate appetite. [Research Support, Non-U.S. Gov't Review]. *Pharmacol Rev, 62*(2), 237-264. doi: 10.1124/pr.109.002428

Love-Gregory, L., & Abumrad, N. A. (2011). CD36 genetics and the metabolic complications of obesity. [Research Support, N.I.H., Extramural Research Support, Non-U.S. Gov't Review]. *Curr Opin Clin Nutr Metab Care, 14*(6), 527-534. doi: 10.1097/MCO.0b013e32834bbac9

Lucia, A., Hoyos, J., Perez, M., Santalla, A., & Chicharro, J. L. (2002). Inverse relationship between VO2max and economy/efficiency in world-class cyclists. [Evaluation Studies]. *Med Sci Sports Exerc, 34*(12), 2079-2084. doi: 10.1249/01.MSS.0000039306.92778.DF

Lutz, T. A., & Woods, S. C. (2012). Overview of animal models of obesity. [Review]. *Curr Protoc Pharmacol, Chapter 5*, Unit5 61. doi: 10.1002/0471141755.ph0561s58

MacLellan, J. D., Gerrits, M. F., Gowing, A., Smith, P. J., Wheeler, M. B., & Harper, M. E. (2005). Physiological increases in uncoupling protein 3 augment fatty acid oxidation and decrease reactive oxygen species production without uncoupling respiration in muscle cells. [Research Support, N.I.H., Extramural Research Support, Non-U.S. Gov't Research Support, U.S. Gov't, P.H.S.]. *Diabetes, 54*(8), 2343-2350.

Majdic, G., Young, M., Gomez-Sanchez, E., Anderson, P., Szczepaniak, L. S., Dobbins, R. L., . . . Parker, K. L. (2002). Knockout mice lacking steroidogenic factor 1 are a novel genetic model of hypothalamic obesity. [Research Support, Non-U.S. Gov't Research Support, U.S. Gov't, P.H.S.]. *Endocrinology, 143*(2), 607-614. doi: 10.1210/endo.143.2.8652

Marx, J. (2002). Unraveling the causes of diabetes. [News]. *Science, 296*(5568), 686-689. doi: 10.1126/science.296.5568.686

Merrill, G. F., Kurth, E. J., Hardie, D. G., & Winder, W. W. (1997). AICA riboside increases AMP-activated protein kinase, fatty acid oxidation, and glucose uptake

in rat muscle. [Research Support, Non-U.S. Gov't Research Support, U.S. Gov't, P.H.S.]. *Am J Physiol, 273*(6 Pt 1), E1107-1112.

Michael, L. F., Wu, Z., Cheatham, R. B., Puigserver, P., Adelmant, G., Lehman, J. J., . . . Spiegelman, B. M. (2001). Restoration of insulin-sensitive glucose transporter (GLUT4) gene expression in muscle cells by the transcriptional coactivator PGC-1. [Research Support, U.S. Gov't, P.H.S.]. *Proc Natl Acad Sci U S A, 98*(7), 3820-3825. doi: 10.1073/pnas.061035098

Mills, E. M., Banks, M. L., Sprague, J. E., & Finkel, T. (2003). Pharmacology: uncoupling the agony from ecstasy. *Nature, 426*(6965), 403-404. doi: 10.1038/426403a

Minokoshi, Y., Kim, Y. B., Peroni, O. D., Fryer, L. G., Muller, C., Carling, D., & Kahn, B. B. (2002). Leptin stimulates fatty-acid oxidation by activating AMP-activated protein kinase. [Research Support, Non-U.S. Gov't Research Support, U.S. Gov't, P.H.S.]. *Nature, 415*(6869), 339-343. doi: 10.1038/415339a

Miyaki, T., Fujikawa, T., Kitaoka, R., Hirano, N., Matsumura, S., Fushiki, T., & Inoue, K. (2011). Noradrenergic projections to the ventromedial hypothalamus regulate fat metabolism during endurance exercise. *Neuroscience, 190*, 239-250. doi: 10.1016/j.neuroscience.2011.05.051

Moore, S. C., Patel, A. V., Matthews, C. E., Berrington de Gonzalez, A., Park, Y., Katki, H. A., . . . Lee, I. M. (2012). Leisure time physical activity of moderate to vigorous intensity and mortality: a large pooled cohort analysis. [Research Support, N.I.H., Extramural Research Support, N.I.H., Intramural Research Support, Non-U.S. Gov't]. *PLoS Med, 9*(11), e1001335. doi: 10.1371/journal.pmed.1001335

Mootha, V. K., Lindgren, C. M., Eriksson, K. F., Subramanian, A., Sihag, S., Lehar, J., . . . Groop, L. C. (2003). PGC-1alpha-responsive genes involved in oxidative phosphorylation are coordinately downregulated in human diabetes. [Research Support, Non-U.S. Gov't]. *Nat Genet, 34*(3), 267-273. doi: 10.1038/ng1180

Moritz, W., Leech, C. A., Ferrer, J., & Habener, J. F. (2001). Regulated expression of adenosine triphosphate-sensitive potassium channel subunits in pancreatic beta-cells. [Research Support, U.S. Gov't, P.H.S.]. *Endocrinology, 142*(1), 129-138. doi: 10.1210/endo.142.1.7885

Mountjoy, K. G., Mortrud, M. T., Low, M. J., Simerly, R. B., & Cone, R. D. (1994). Localization of the melanocortin-4 receptor (MC4-R) in neuroendocrine and autonomic control circuits in the brain. [Research Support, U.S. Gov't, P.H.S.]. *Mol Endocrinol, 8*(10), 1298-1308. doi: 10.1210/mend.8.10.7854347

Mul, J. D., van Boxtel, R., Bergen, D. J., Brans, M. A., Brakkee, J. H., Toonen, P. W., . . . Cuppen, E. (2012). Melanocortin receptor 4 deficiency affects body weight regulation, grooming behavior, and substrate preference in the rat. *Obesity (Silver Spring), 20*(3), 612-621. doi: 10.1038/oby.2011.81

Muroya, S., Funahashi, H., Yamanaka, A., Kohno, D., Uramura, K., Nambu, T., . . . Yada, T. (2004). Orexins (hypocretins) directly interact with neuropeptide Y, POMC and glucose-responsive neurons to regulate Ca 2+ signaling in a reciprocal manner to leptin: orexigenic neuronal pathways in the mediobasal hypothalamus. [Comparative Study Research Support, Non-U.S. Gov't]. *Eur J Neurosci, 19*(6), 1524-1534. doi: 10.1111/j.1460-9568.2004.03255.x

Myers J, P. M., Froelicher V, Do D, Partington S, Atwood JE. (2002). Exercise capacity and mortality among men referred for exercise testing. *N Engl J Med, 346*, 793-801.

Naples, S. P., Borengasser, S. J., Rector, R. S., Uptergrove, G. M., Morris, E. M., Mikus, C. R., . . . Thyfault, J. P. (2010). Skeletal muscle mitochondrial and metabolic responses to a high-fat diet in female rats bred for high and low aerobic capacity. [Research Support, N.I.H., Extramural Research Support, U.S. Gov't, Non-P.H.S.]. *Appl Physiol Nutr Metab, 35*(2), 151-162. doi: 10.1139/H09-139

. National Research Council (US) Committee for the Update of the Guide for the Care and Use of Laboratory Animals. (2011) *Guide for the Care and Use of Laboratory Animals* (8th ed.). Washington (DC).

Nicholls, D. G. (2001). A history of UCP1. [Review]. *Biochem Soc Trans, 29*(Pt 6), 751-755.

Nichols, C. G. (2006). KATP channels as molecular sensors of cellular metabolism. [Review]. *Nature, 440*(7083), 470-476. doi: 10.1038/nature04711

Nogueiras, R., Wiedmer, P., Perez-Tilve, D., Veyrat-Durebex, C., Keogh, J. M., Sutton, G. M., . . . Tschop, M. H. (2007). The central melanocortin system directly controls peripheral lipid metabolism. [Research Support, Non-U.S. Gov't]. *J Clin Invest, 117*(11), 3475-3488. doi: 10.1172/JCI31743

Noland RC, T. J., Henes ST, Whitfield BR, Woodlief TL, Evans JR, Lust JA, Britton SL, Koch LG, Dudek RW, Dohm GL, Cortright RN, and Lust RM. (2007). Artificial selection for high-capacity endurance running is protective against high-fat diet-induced insulin resistance. *Am J Physiol Endocrinol Metab, 293*, E31-41.

Novak CM, E. C., Gerber SM, Chini EN, Zhang M, Britton SL, Koch LG, and Levine JA. (2009). Endurance capacity, not body size, determines physical activity levels: role of skeletal muscle PEPCK. *PLoSONE, 4*(e5869).

Novak, C. M., Escande, C., Burghardt, P. R., Zhang, M., Barbosa, M. T., Chini, E. N., . . . Levine, J. A. (2010). Spontaneous activity, economy of activity, and resistance to diet-induced obesity in rats bred for high intrinsic aerobic capacity. [Research Support, N.I.H., Extramural Research Support, Non-U.S. Gov't Research Support, U.S. Gov't, Non-P.H.S.]. *Horm Behav, 58*(3), 355-367. doi: 10.1016/j.yhbeh.2010.03.013

Novak, C. M., & Levine, J. A. (2007). Central neural and endocrine mechanisms of non-exercise activity thermogenesis and their potential impact on obesity. [Review]. *J Neuroendocrinol, 19*(12), 923-940. doi: 10.1111/j.1365-2826.2007.01606.x

Novak, C. M., & Levine, J. A. (2009). Daily intraparaventricular orexin-A treatment induces weight loss in rats. [Research Support, N.I.H., Extramural Research Support, Non-U.S. Gov't]. *Obesity (Silver Spring), 17*(8), 1493-1498. doi: 10.1038/oby.2009.91

Obici, S., Feng, Z., Arduini, A., Conti, R., & Rossetti, L. (2003). Inhibition of hypothalamic carnitine palmitoyltransferase-1 decreases food intake and glucose production. [Research Support, Non-U.S. Gov't Research Support, U.S. Gov't, P.H.S.]. *Nat Med, 9*(6), 756-761. doi: 10.1038/nm873

Obici, S., Feng, Z., Morgan, K., Stein, D., Karkanias, G., & Rossetti, L. (2002). Central administration of oleic acid inhibits glucose production and food intake. [Research Support, Non-U.S. Gov't Research Support, U.S. Gov't, P.H.S.]. *Diabetes, 51*(2), 271-275.

Obici, S., Feng, Z., Tan, J., Liu, L., Karkanias, G., & Rossetti, L. (2001). Central melanocortin receptors regulate insulin action. [Research Support, Non-U.S. Gov't Research Support, U.S. Gov't, P.H.S.]. *J Clin Invest, 108*(7), 1079-1085. doi: 10.1172/JCI12954

Obici, S., Zhang, B. B., Karkanias, G., & Rossetti, L. (2002). Hypothalamic insulin signaling is required for inhibition of glucose production. [Research Support, Non-U.S. Gov't Research Support, U.S. Gov't, P.H.S.]. *Nat Med, 8*(12), 1376-1382. doi: 10.1038/nm798

Ogden, C. L., Carroll, M. D., Kit, B. K., & Flegal, K. M. (2014). Prevalence of childhood and adult obesity in the United States, 2011-2012. *JAMA, 311*(8), 806-814. doi: 10.1001/jama.2014.732

Ollmann, M. M., Wilson, B. D., Yang, Y. K., Kerns, J. A., Chen, Y., Gantz, I., & Barsh, G. S. (1997). Antagonism of central melanocortin receptors in vitro and in vivo by agouti-related protein. [Research Support, Non-U.S. Gov't Research Support, U.S.

Gov't, Non-P.H.S. Research Support, U.S. Gov't, P.H.S.]. *Science, 278*(5335), 135-138.

Otter, T., King, S. M., & Witman, G. B. (1987). A two-step procedure for efficient electrotransfer of both high-molecular-weight (greater than 400,000) and low-molecular-weight (less than 20,000) proteins. [Research Support, U.S. Gov't, P.H.S.]. *Anal Biochem, 162*(2), 370-377.

Pedersen, B. K. (2011). Muscles and their myokines. [Research Support, Non-U.S. Gov't]. *J Exp Biol, 214*(Pt 2), 337-346. doi: 10.1242/jeb.048074

Pedersen, B. K. ((2009b)). The Diseasome of Physical Inactivity and the role of myokines in muscle-fat cross talk. *J. Physiol, 587*, 5559-5568.

Periasamy, M., & Kalyanasundaram, A. (2007). SERCA pump isoforms: their role in calcium transport and disease. [Research Support, N.I.H., Extramural Review]. *Muscle Nerve, 35*(4), 430-442. doi: 10.1002/mus.20745

Rahmouni, K., Haynes, W. G., Morgan, D. A., & Mark, A. L. (2003). Role of melanocortin-4 receptors in mediating renal sympathoactivation to leptin and insulin. [Research Support, Non-U.S. Gov't Research Support, U.S. Gov't, Non-P.H.S. Research Support, U.S. Gov't, P.H.S.]. *J Neurosci, 23*(14), 5998-6004.

Ranadive, S. A., & Vaisse, C. (2008). Lessons from extreme human obesity: monogenic disorders. [Research Support, N.I.H., Extramural Research Support, Non-U.S. Gov't Review]. *Endocrinol Metab Clin North Am, 37*(3), 733-751, x. doi: 10.1016/j.ecl.2008.07.003

Ranki, H. J., Budas, G. R., Crawford, R. M., & Jovanovic, A. (2001). Gender-specific difference in cardiac ATP-sensitive K(+) channels. [Research Support, Non-U.S. Gov't]. *J Am Coll Cardiol, 38*(3), 906-915.

Razquin, C., Marti, A., & Martinez, J. A. (2011). Evidences on three relevant obesogenes: MC4R, FTO and PPARgamma. Approaches for personalized nutrition. [Review]. *Mol Nutr Food Res, 55*(1), 136-149. doi: 10.1002/mnfr.201000445

Ren, Y., Xu, X., & Wang, X. (2003). Altered mRNA expression of ATP-sensitive and inward rectifier potassium channel subunits in streptozotocin-induced diabetic rat heart and aorta. [Comparative Study Research Support, Non-U.S. Gov't]. *J Pharmacol Sci, 93*(4), 478-483.

Ribeiro MO, B. S., Kaneshige M, et al. (2010). Expression of uncoupling protein 1 in mouse brown adipose tissue is thyroid hormone receptor-beta isoform specific and required for adaptive thermogenesis. *Endocrinology, 151*, 432-440.

Rivas, D. A., Lessard, S. J., Saito, M., Friedhuber, A. M., Koch, L. G., Britton, S. L., . . . Hawley, J. A. (2011). Low intrinsic running capacity is associated with reduced skeletal muscle substrate oxidation and lower mitochondrial content in white skeletal muscle. [Research Support, N.I.H., Extramural Research Support, Non-U.S. Gov't]. *Am J Physiol Regul Integr Comp Physiol, 300*(4), R835-843. doi: 10.1152/ajpregu.00659.2010

Rolfe, D. F., & Brown, G. C. (1997). Cellular energy utilization and molecular origin of standard metabolic rate in mammals. [Review]. *Physiol Rev, 77*(3), 731-758.

Rossi, J., Balthasar, N., Olson, D., Scott, M., Berglund, E., Lee, C. E., . . . Elmquist, J. K. (2011). Melanocortin-4 receptors expressed by cholinergic neurons regulate energy balance and glucose homeostasis. [Research Support, N.I.H., Extramural Research Support, Non-U.S. Gov't]. *Cell Metab, 13*(2), 195-204. doi: 10.1016/j.cmet.2011.01.010

Rothwell, N. J., & Stock, M. J. (1979). A role for brown adipose tissue in diet-induced thermogenesis. [Comparative Study]. *Nature, 281*(5726), 31-35.

Rousset, S., Alves-Guerra, M. C., Mozo, J., Miroux, B., Cassard-Doulcier, A. M., Bouillaud, F., & Ricquier, D. (2004). The biology of mitochondrial uncoupling proteins. [Research Support, Non-U.S. Gov't Review]. *Diabetes, 53 Suppl 1*, S130-135.

Rowland, L. A., Bal, N. C., & Periasamy, M. (2014). The role of skeletal-muscle-based thermogenic mechanisms in vertebrate endothermy. *Biol Rev Camb Philos Soc*. doi: 10.1111/brv.12157

Samec, S., Seydoux, J., & Dulloo, A. G. (1998). Interorgan signaling between adipose tissue metabolism and skeletal muscle uncoupling protein homologs: is there a role for circulating free fatty acids? [Research Support, Non-U.S. Gov't]. *Diabetes, 47*(11), 1693-1698.

Samec, S., Seydoux, J., & Dulloo, A. G. (1999). Post-starvation gene expression of skeletal muscle uncoupling protein 2 and uncoupling protein 3 in response to dietary fat levels and fatty acid composition: a link with insulin resistance. [Research Support, Non-U.S. Gov't]. *Diabetes, 48*(2), 436-441.

Santini, F., Maffei, M., Pelosini, C., Salvetti, G., Scartabelli, G., & Pinchera, A. (2009). Melanocortin-4 receptor mutations in obesity. [Review]. *Adv Clin Chem, 48*, 95-109.

Sawyer, B. J., Blessinger, J. R., Irving, B. A., Weltman, A., Patrie, J. T., & Gaesser, G. A. (2010). Walking and running economy: inverse association with peak oxygen uptake. [Research Support, N.I.H., Extramural]. *Med Sci Sports Exerc, 42*(11), 2122-2127. doi: 10.1249/MSS.0b013e3181de2da7

Schiaffino, S., & Reggiani, C. (2011). Fiber types in mammalian skeletal muscles. [Comparative Study Research Support, Non-U.S. Gov't Review]. *Physiol Rev, 91*(4), 1447-1531. doi: 10.1152/physrev.00031.2010

Schoeller, D. A., & Jefford, G. (2002). Determinants of the energy costs of light activities: inferences for interpreting doubly labeled water data. [Research Support, U.S. Gov't, P.H.S. Validation Studies]. *Int J Obes Relat Metab Disord, 26*(1), 97-101. doi: 10.1038/sj.ijo.0801851

Schonfeld-Warden, N. A., & Warden, C. H. (2001). Physiological effects of variants in human uncoupling proteins: UCP2 influences body-mass index. [Review]. *Biochem Soc Trans, 29*(Pt 6), 777-784.

Schrauwen, P., & Hesselink, M. (2002). UCP2 and UCP3 in muscle controlling body metabolism. [Research Support, Non-U.S. Gov't Review]. *J Exp Biol, 205*(Pt 15), 2275-2285.

Schrauwen, P., & Hesselink, M. K. (2004). The role of uncoupling protein 3 in fatty acid metabolism: protection against lipotoxicity? [Research Support, Non-U.S. Gov't Review]. *Proc Nutr Soc, 63*(2), 287-292. doi: 10.1079/PNS2003336

Schrauwen, P., Hoeks, J., Schaart, G., Kornips, E., Binas, B., Van De Vusse, G. J., . . . Hesselink, M. K. (2003). Uncoupling protein 3 as a mitochondrial fatty acid anion exporter. *FASEB J, 17*(15), 2272-2274. doi: 10.1096/fj.03-0515fje

Schrauwen, P., Schaart, G., Saris, W. H., Slieker, L. J., Glatz, J. F., Vidal, H., & Blaak, E. E. (2000). The effect of weight reduction on skeletal muscle UCP2 and UCP3 mRNA expression and UCP3 protein content in Type II diabetic subjects. [Research Support, Non-U.S. Gov't]. *Diabetologia, 43*(11), 1408-1416. doi: 10.1007/s001250051547

Sedentary Behaviour Research, N. (2012). Letter to the editor: standardized use of the terms "sedentary" and "sedentary behaviours". [Letter]. *Appl Physiol Nutr Metab, 37*(3), 540-542. doi: 10.1139/h2012-024

Seeley, R. J., & Woods, S. C. (2003). Monitoring of stored and available fuel by the CNS: implications for obesity. [Research Support, Non-U.S. Gov't Research Support, U.S. Gov't, P.H.S. Review]. *Nat Rev Neurosci, 4*(11), 901-909. doi: 10.1038/nrn1245

Seino, S. (1999). ATP-sensitive potassium channels: a model of heteromultimeric potassium channel/receptor assemblies. [Research Support, Non-U.S. Gov't Review]. *Annu Rev Physiol, 61*, 337-362. doi: 10.1146/annurev.physiol.61.1.337

Seino, S., & Miki, T. (2003). Physiological and pathophysiological roles of ATP-sensitive K+ channels. [Research Support, Non-U.S. Gov't]. *Prog Biophys Mol Biol, 81*(2), 133-176.

Sheehan, M. T., & Jensen, M. D. (2000). Metabolic complications of obesity. Pathophysiologic considerations. [Research Support, Non-U.S. Gov't Research Support, U.S. Gov't, P.H.S. Review]. *Med Clin North Am, 84*(2), 363-385, vi.

Shi, H., Bowers, R. R., & Bartness, T. J. (2004). Norepinephrine turnover in brown and white adipose tissue after partial lipectomy. [Research Support, Non-U.S. Gov't Research Support, U.S. Gov't, P.H.S.]. *Physiol Behav, 81*(3), 535-542. doi: 10.1016/j.physbeh.2004.02.023

Shieh, C. C., Coghlan, M., Sullivan, J. P., & Gopalakrishnan, M. (2000). Potassium channels: molecular defects, diseases, and therapeutic opportunities. [Review]. *Pharmacol Rev, 52*(4), 557-594.

Shiuchi, T., Haque, M. S., Okamoto, S., Inoue, T., Kageyama, H., Lee, S., . . . Minokoshi, Y. (2009). Hypothalamic orexin stimulates feeding-associated glucose utilization in skeletal muscle via sympathetic nervous system. [Research Support, Non-U.S. Gov't]. *Cell Metab, 10*(6), 466-480. doi: 10.1016/j.cmet.2009.09.013

Shrestha, Y. B., Vaughan, C. H., Smith, B. J., Jr., Song, C. K., Baro, D. J., & Bartness, T. J. (2010). Central melanocortin stimulation increases phosphorylated perilipin A and hormone-sensitive lipase in adipose tissues. [Research Support, N.I.H., Extramural]. *Am J Physiol Regul Integr Comp Physiol, 299*(1), R140-149. doi: 10.1152/ajpregu.00535.2009

Shukla, C., Britton, S. L., Koch, L. G., & Novak, C. M. (2012). Region-specific differences in brain melanocortin receptors in rats of the lean phenotype. [Research Support, N.I.H., Extramural Research Support, Non-U.S. Gov't]. *Neuroreport, 23*(10), 596-600. doi: 10.1097/WNR.0b013e328354f5c1

Simmons, R. K., Griffin, S. J., Steele, R., Wareham, N. J., Ekelund, U., & ProActive Research, T. (2008). Increasing overall physical activity and aerobic fitness is associated with improvements in metabolic risk: cohort analysis of the ProActive trial. [Multicenter Study Research Support, Non-U.S. Gov't]. *Diabetologia, 51*(5), 787-794. doi: 10.1007/s00125-008-0949-4

Simoneau, J. A., Colberg, S. R., Thaete, F. L., & Kelley, D. E. (1995). Skeletal muscle glycolytic and oxidative enzyme capacities are determinants of insulin sensitivity and muscle composition in obese women. [Research Support, Non-U.S. Gov't Research Support, U.S. Gov't, Non-P.H.S. Research Support, U.S. Gov't, P.H.S.]. *FASEB J, 9*(2), 273-278.

Smith, A. G., & Muscat, G. E. (2005). Skeletal muscle and nuclear hormone receptors: implications for cardiovascular and metabolic disease. [Review]. *Int J Biochem Cell Biol, 37*(10), 2047-2063. doi: 10.1016/j.biocel.2005.03.002

Sohn, J. W., Harris, L. E., Berglund, E. D., Liu, T., Vong, L., Lowell, B. B., . . . Elmquist, J. K. (2013). Melanocortin 4 receptors reciprocally regulate sympathetic and parasympathetic preganglionic neurons. [Research Support, N.I.H., Extramural Research Support, Non-U.S. Gov't]. *Cell, 152*(3), 612-619. doi: 10.1016/j.cell.2012.12.022

Spiegelman, B. M., Hu, E., Kim, J. B., & Brun, R. (1997). PPAR gamma and the control of adipogenesis. [Review]. *Biochimie, 79*(2-3), 111-112.

Stephenson, E. J., Stepto, N. K., Koch, L. G., Britton, S. L., & Hawley, J. A. (2012a). Divergent skeletal muscle respiratory capacities in rats artificially selected for high and low running ability: a role for Nor1? [Research Support, N.I.H.,

Extramural Research Support, Non-U.S. Gov't]. *J Appl Physiol, 113*(9), 1403-1412. doi: 10.1152/japplphysiol.00788.2012

Stephenson, E. J., Stepto, N. K., Koch, L. G., Britton, S. L., & Hawley, J. A. (2012b). Divergent skeletal muscle respiratory capacities in rats artificially selected for high and low running ability: a role for Nor1? [Research Support, N.I.H., Extramural Research Support, Non-U.S. Gov't]. *J Appl Physiol (1985), 113*(9), 1403-1412. doi: 10.1152/japplphysiol.00788.2012

Sullivan, P. G., Dube, C., Dorenbos, K., Steward, O., & Baram, T. Z. (2003). Mitochondrial uncoupling protein-2 protects the immature brain from excitotoxic neuronal death. [Research Support, Non-U.S. Gov't Research Support, U.S. Gov't, P.H.S.]. *Ann Neurol, 53*(6), 711-717. doi: 10.1002/ana.10543

Sullivan, P. G., Rippy, N. A., Dorenbos, K., Concepcion, R. C., Agarwal, A. K., & Rho, J. M. (2004). The ketogenic diet increases mitochondrial uncoupling protein levels and activity. [Comparative Study Research Support, Non-U.S. Gov't Research Support, U.S. Gov't, P.H.S.]. *Ann Neurol, 55*(4), 576-580. doi: 10.1002/ana.20062

Sullivan, P. G., Springer, J. E., Hall, E. D., & Scheff, S. W. (2004). Mitochondrial uncoupling as a therapeutic target following neuronal injury. [Review]. *J Bioenerg Biomembr, 36*(4), 353-356. doi: 10.1023/B:JOBB.0000041767.30992.19

Sutton, R. E., Koob, G. F., Le Moal, M., Rivier, J., & Vale, W. (1982). Corticotropin releasing factor produces behavioural activation in rats. [Research Support, Non-U.S. Gov't Research Support, U.S. Gov't, P.H.S.]. *Nature, 297*(5864), 331-333.

Suzuki, M., Li, R. A., Miki, T., Uemura, H., Sakamoto, N., Ohmoto-Sekine, Y., . . . Nakaya, H. (2001). Functional roles of cardiac and vascular ATP-sensitive potassium channels clarified by Kir6.2-knockout mice. [Research Support, Non-U.S. Gov't Research Support, U.S. Gov't, P.H.S.]. *Circ Res, 88*(6), 570-577.

Szewczyk, A. (1996). The ATP-regulated K+ channel in mitochondria: five years after its discovery. [Research Support, Non-U.S. Gov't Review]. *Acta Biochim Pol, 43*(4), 713-719.

Taegtmeyer, S. H. a. H. (2003). Epidemic obesity and the metabolic syndrome. *Circulation, 108*, 1541-1545.

Takahashi, A., & Shimazu, T. (1981). Hypothalamic regulation of lipid metabolism in the rat: effect of hypothalamic stimulation on lipolysis. *J Auton Nerv Syst, 4*(3), 195-205.

Tanaka, T., Masuzaki, H., Yasue, S., Ebihara, K., Shiuchi, T., Ishii, T., . . . Nakao, K. (2007). Central melanocortin signaling restores skeletal muscle AMP-activated protein kinase phosphorylation in mice fed a high-fat diet. [Comparative Study Research Support, Non-U.S. Gov't]. *Cell Metab, 5*(5), 395-402. doi: 10.1016/j.cmet.2007.04.004

Teske, J. A., Billington, C. J., Kuskowski, M. A., & Kotz, C. M. (2012). Spontaneous physical activity protects against fat mass gain. [Research Support, N.I.H., Extramural Research Support, Non-U.S. Gov't Research Support, U.S. Gov't, Non-P.H.S.]. *Int J Obes (Lond), 36*(4), 603-613. doi: 10.1038/ijo.2011.108

Toda, C., Shiuchi, T., Lee, S., Yamato-Esaki, M., Fujino, Y., Suzuki, A., . . . Minokoshi, Y. (2009). Distinct effects of leptin and a melanocortin receptor agonist injected into medial hypothalamic nuclei on glucose uptake in peripheral tissues. [Research Support, Non-U.S. Gov't]. *Diabetes, 58*(12), 2757-2765. doi: 10.2337/db09-0638

Tomas, E., Tsao, T. S., Saha, A. K., Murrey, H. E., Zhang Cc, C., Itani, S. I., . . . Ruderman, N. B. (2002). Enhanced muscle fat oxidation and glucose transport by ACRP30 globular domain: acetyl-CoA carboxylase inhibition and AMP-activated protein kinase activation. [Research Support, Non-U.S. Gov't Research Support, U.S. Gov't, P.H.S.]. *Proc Natl Acad Sci U S A, 99*(25), 16309-16313. doi: 10.1073/pnas.222657499

Trivedi, P., Jiang, M., Tamvakopoulos, C. C., Shen, X., Yu, H., Mock, S., . . . Guan, X. M. (2003). Exploring the site of anorectic action of peripherally administered synthetic melanocortin peptide MT-II in rats. [Comparative Study]. *Brain Res, 977*(2), 221-230.

Tsai, A. G., Williamson, D. F., & Glick, H. A. (2011). Direct medical cost of overweight and obesity in the USA: a quantitative systematic review. [Research Support, N.I.H., Extramural Research Support, Non-U.S. Gov't Review]. *Obes Rev, 12*(1), 50-61. doi: 10.1111/j.1467-789X.2009.00708.x

Tschop, M. H., Speakman, J. R., Arch, J. R., Auwerx, J., Bruning, J. C., Chan, L., . . . Ravussin, E. (2012). A guide to analysis of mouse energy metabolism. *Nat Methods, 9*(1), 57-63. doi: 10.1038/nmeth.1806

Tweedie, C., Romestaing, C., Burelle, Y., Safdar, A., Tarnopolsky, M. A., Seadon, S., . . . Hepple, R. T. (2011). Lower oxidative DNA damage despite greater ROS production in muscles from rats selectively bred for high running capacity. [Research Support, N.I.H., Extramural Research Support, Non-U.S. Gov't]. *Am J Physiol Regul Integr Comp Physiol, 300*(3), R544-553. doi: 10.1152/ajpregu.00250.2010

Valassi, E., Scacchi, M., & Cavagnini, F. (2008). Neuroendocrine control of food intake. [Review]. *Nutr Metab Cardiovasc Dis, 18*(2), 158-168. doi: 10.1016/j.numecd.2007.06.004

van Baak, M. A. (2008). Meal-induced activation of the sympathetic nervous system and its cardiovascular and thermogenic effects in man. [Review]. *Physiol Behav, 94*(2), 178-186. doi: 10.1016/j.physbeh.2007.12.020

van den Berg, S. A., van Marken Lichtenbelt, W., Willems van Dijk, K., & Schrauwen, P. (2011). Skeletal muscle mitochondrial uncoupling, adaptive thermogenesis and energy expenditure. [Research Support, Non-U.S. Gov't Review]. *Curr Opin Clin Nutr Metab Care, 14*(3), 243-249. doi: 10.1097/MCO.0b013e3283455d7a

Vidal-Puig, A., Solanes, G., Grujic, D., Flier, J. S., & Lowell, B. B. (1997). UCP3: an uncoupling protein homologue expressed preferentially and abundantly in skeletal

muscle and brown adipose tissue. [Research Support, Non-U.S. Gov't Research Support, U.S. Gov't, P.H.S.]. *Biochem Biophys Res Commun, 235*(1), 79-82. doi: 10.1006/bbrc.1997.6740

Voss-Andreae, A., Murphy, J. G., Ellacott, K. L., Stuart, R. C., Nillni, E. A., Cone, R. D., & Fan, W. (2007). Role of the central melanocortin circuitry in adaptive thermogenesis of brown adipose tissue. [Research Support, N.I.H., Extramural Research Support, Non-U.S. Gov't]. *Endocrinology, 148*(4), 1550-1560. doi: 10.1210/en.2006-1389

Wang, C., Billington, C. J., Levine, A. S., & Kotz, C. M. (2000). Effect of CART in the hypothalamic paraventricular nucleus on feeding and uncoupling protein gene expression. *Neuroreport, 11*(14), 3251-3255.

Wang, Y., & Ashraf, M. (1999). Role of protein kinase C in mitochondrial KATP channel-mediated protection against Ca2+ overload injury in rat myocardium. [Research Support, U.S. Gov't, P.H.S.]. *Circ Res, 84*(10), 1156-1165.

Wang, Y. X., Lee, C. H., Tiep, S., Yu, R. T., Ham, J., Kang, H., & Evans, R. M. (2003). Peroxisome-proliferator-activated receptor delta activates fat metabolism to prevent obesity. [Research Support, Non-U.S. Gov't]. *Cell, 113*(2), 159-170.

Wang, Y. X., Zhang, C. L., Yu, R. T., Cho, H. K., Nelson, M. C., Bayuga-Ocampo, C. R., . . . Evans, R. M. (2004). Regulation of muscle fiber type and running endurance by PPARdelta. [Research Support, Non-U.S. Gov't]. *PLoS Biol, 2*(10), e294. doi: 10.1371/journal.pbio.0020294

Warren, T. Y., Barry, V., Hooker, S. P., Sui, X., Church, T. S., & Blair, S. N. (2010). Sedentary behaviors increase risk of cardiovascular disease mortality in men. [Research Support, N.I.H., Extramural Research Support, Non-U.S. Gov't]. *Med Sci Sports Exerc, 42*(5), 879-885. doi: 10.1249/MSS.0b013e3181c3aa7e

Weingarten, H. P., Chang, P. K., & McDonald, T. J. (1985). Comparison of the metabolic and behavioral disturbances following paraventricular- and ventromedial-hypothalamic lesions. [Research Support, Non-U.S. Gov't]. *Brain Res Bull, 14*(6), 551-559.

Weiss, L., Hoffmann, G. E., Schreiber, R., Andres, H., Fuchs, E., Korber, E., & Kolb, H. J. (1986). Fatty-acid biosynthesis in man, a pathway of minor importance. Purification, optimal assay conditions, and organ distribution of fatty-acid synthase. [Research Support, Non-U.S. Gov't]. *Biol Chem Hoppe Seyler, 367*(9), 905-912.

Wende, A. R., Huss, J. M., Schaeffer, P. J., Giguere, V., & Kelly, D. P. (2005). PGC-1alpha coactivates PDK4 gene expression via the orphan nuclear receptor

ERRalpha: a mechanism for transcriptional control of muscle glucose metabolism. [Research Support, N.I.H., Extramural]. *Mol Cell Biol, 25*(24), 10684-10694. doi: 10.1128/MCB.25.24.10684-10694.2005

Willis, L. H., Slentz, C.A., Bateman, L.A., Shields, A.T., Piner, L.W., Bales, C.W.,, & Houmard, J. A., and Kraus, W.E. (2012). Effects of aerobic and/or resistance training on body mass and fat mass in overweight or obese adults. *J. Appl. Physiol., 113,* 1831-1837.

Winder, W. W., Holmes, B. F., Rubink, D. S., Jensen, E. B., Chen, M., & Holloszy, J. O. (2000). Activation of AMP-activated protein kinase increases mitochondrial enzymes in skeletal muscle. [Research Support, U.S. Gov't, P.H.S.]. *J Appl Physiol (1985), 88*(6), 2219-2226.

Wisloff, U., Najjar, S. M., Ellingsen, O., Haram, P. M., Swoap, S., Al-Share, Q., . . . Britton, S. L. (2005). Cardiovascular risk factors emerge after artificial selection for low aerobic capacity. [Research Support, Non-U.S. Gov't Research Support, U.S. Gov't, Non-P.H.S. Research Support, U.S. Gov't, P.H.S.]. *Science, 307*(5708), 418-420. doi: 10.1126/science.1108177

Wolfgang, M. J., & Lane, M. D. (2008). Hypothalamic malonyl-coenzyme A and the control of energy balance. [Review]. *Mol Endocrinol, 22*(9), 2012-2020. doi: 10.1210/me.2007-0538

Xu, M., Wang, Y., Ayub, A., & Ashraf, M. (2001). Mitochondrial K(ATP) channel activation reduces anoxic injury by restoring mitochondrial membrane potential. [Research Support, U.S. Gov't, P.H.S.]. *Am J Physiol Heart Circ Physiol, 281*(3), H1295-1303.

Yamauchi, T., Kamon, J., Minokoshi, Y., Ito, Y., Waki, H., Uchida, S., . . . Kadowaki, T. (2002). Adiponectin stimulates glucose utilization and fatty-acid oxidation by activating AMP-activated protein kinase. [Research Support, Non-U.S. Gov't Research Support, U.S. Gov't, P.H.S.]. *Nat Med, 8*(11), 1288-1295. doi: 10.1038/nm788

York, D., & Bouchard, C. (2000). How obesity develops: insights from the new biology. [Review]. *Endocrine, 13*(2), 143-154. doi: 10.1385/ENDO:13:2:143

Yuan, C. X., Ito, M., Fondell, J. D., Fu, Z. Y., & Roeder, R. G. (1998). The TRAP220 component of a thyroid hormone receptor- associated protein (TRAP) coactivator complex interacts directly with nuclear receptors in a ligand-dependent fashion. [Research Support, U.S. Gov't, P.H.S.]. *Proc Natl Acad Sci U S A, 95*(14), 7939-7944.

Zanuso, S., Jimenez, A., Pugliese, G., Corigliano, G., & Balducci, S. (2010). Exercise for the management of type 2 diabetes: a review of the evidence. [Review]. *Acta Diabetol, 47*(1), 15-22. doi: 10.1007/s00592-009-0126-3

Zhan, W. Z., Swallow, J. G., Garland, T., Jr., Proctor, D. N., Carter, P. A., & Sieck, G. C. (1999). Effects of genetic selection and voluntary activity on the medial gastrocnemius muscle in house mice. [Research Support, U.S. Gov't, Non-P.H.S. Research Support, U.S. Gov't, P.H.S.]. *J Appl Physiol (1985), 87*(6), 2326-2333.

Zhuo, M. L., Huang, Y., Liu, D. P., & Liang, C. C. (2005). KATP channel: relation with cell metabolism and role in the cardiovascular system. [Research Support, Non-U.S. Gov't Review]. *Int J Biochem Cell Biol, 37*(4), 751-764. doi: 10.1016/j.biocel.2004.10.008

Zurlo F, L. K., Bogardus C, Ravussin E. (1990). Skeletal muscle metabolism is a major determinant of resting energy expenditure. *J Clin Invest, 86*, 1423– 1427.